

http://researchcommons.waikato.ac.nz/

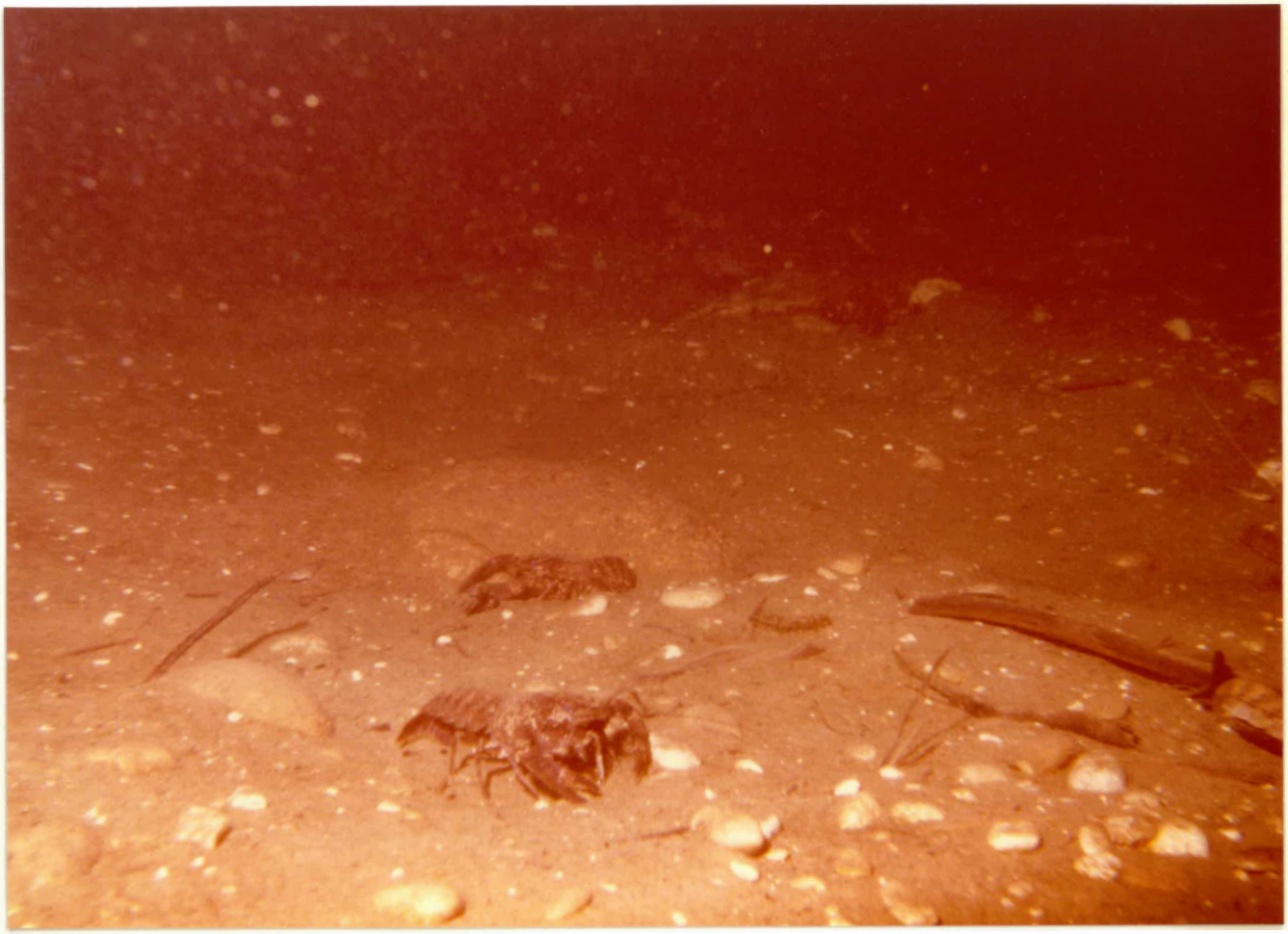
Research Commons at the University of Waikato

Copyright Statement:

The digital copy of this thesis is protected by the Copyright Act 1994 (New Zealand).

The thesis may be consulted by you, provided you comply with the provisions of the Act and the following conditions of use:

- Any use you make of these documents or images must be for research or private study purposes only, and you may not make them available to any other person.
- Authors control the copyright of their thesis. You will recognise the author's right to be identified as the author of the thesis, and due acknowledgement will be made to the author where appropriate.
- You will obtain the author's permission before publishing any material from the thesis.



"If the kura could only speak ..."

Sediments in Lake Taupo at 30 m depth near Kuratau.
Pumice fragments and twigs lie partly buried in mud.
Freshwater crayfish (<15 cm) are common. Photo - A Devcich)

SEDIMENTOLOGY
OF
LAKE TAUPO,
CENTRAL NORTH ISLAND,
NEW ZEALAND

A thesis

submitted in partial fulfilment

of the requirements for the Degree

of

Master of Science in Earth Sciences

at the

University of Waikato

by

GUY STAFFORD LISTER

University of Waikato

1978

ABSTRACT

Lake Taupo, with an area of 616 km^2, is the largest of several lakes of volcano-tectonic origin in the Central Volcanic Region, North Island, New Zealand. In the past the lake has been affected by catastrophic volcanic events, the last being the Taupo Pumice eruptions of about 131 A.D. Since then the catchment has restabilised and sedimentation in the lake has diminished.

A number of depositional environments in Lake Taupo are characterised on the basis of surficial sediment texture and depositional processes. These environments include: shelf (sands, gravels, sand-gravel mixtures); slope (silty sands, sandy silts); rise (sandy silts, silts); basin (silts); sub-lacustrine talus slope and sub-lacustrine hill (gravel-sand-mud mixtures).

Close to existing or pre-existing river mouths, and on sub-lacustrine talus slopes, gravels typically include one or more types of catchment-derived rock fragments (andesite, rhyolite, ignimbrite, greywacke). In other parts of the lake, gravels are almost entirely pumice fragments derived from pumice tephras and breccias within the catchment. Shelf and slope sands consist of rock fragments, volcanic glass, quartz and plagioclase feldspar. Slope and rise sediments may also contain sand-sized benthic and aufwuch diatom tests (e.g. *Synedra* sp., *Nitzschia* sp., *Surirella* sp.). Basinal sediments include a minor, very fine-fine sand fraction of andesitic Ngauruhoe Ash. Silt in basinal sediments comprises planktic diatom tests (*Melosira* sp. >> *Cyclotella* sp. ≃ *Epithemia* sp.) and terrigenous grains (volcanic glass, rock fragments, quartz, plagioclase

feldspar). Subordinate clay-sized material is dominated by diatomaceous and authigenic silica, detrital illite and kaolinite, and montmorillonite of probable hydrothermal origin.

The distribution and provenance of sediment components in the lake indicate that terrigenous material is derived mainly from southern catchment regions (greywacke and andesite lithologies) and to a lesser extent from the northeastern catchment (rhyolitic volcanics). Gravels and sands are deposited in shallow water where they may be re-worked by coastal processes; suspended silts and clays are transported offshore by surface or inter-flow currents, and deposited in basinal regions of the lake.

An extensive sub-bottom surface of sedimentary pumice, deposited in Lake Taupo during and soon after the Taupo Pumice eruptions, has been identified from sediment cores and seismic profiles of the lake bottom. Mud-layer thicknesses overlying this pumice surface indicate average basinal sedimentation rates of less than 30 mm/yr for central and northern lake regions, to more than 140 mm/yr in southern lake regions.

Areal distribution patterns of sediment texture and composition, together with depositional rates, form the basis for a proposed model of sedimentation in Lake Taupo.

ACKNOWLEDGEMENTS

I wish to thank the Earth Sciences Department staff of the University of Waikato, particularly my supervisor Dr Cam Nelson, who spent considerable time in the field, provided academic guidance, and moments of respite on the squash court.

I am particularly grateful to Mr Jack Irwin and Dr Dick Pickrill, of the New Zealand Oceanographic Institute, for providing assistance and equipment which enabled the seismic-profiling of Lake Taupo to be carried out, and to the staff of Ecology Division, D.S.I.R., Taupo, for considerable logistic support.

A number of people, including Messrs. Laurie Gaylor, Mike Vennard and Peter King are thanked for their assistance in the field, as is Mr Harold Larsen for provision of his boat.

Dr Vivienne Cassie, of Botany Division, D.S.I.R., Auckland, is sincerely thanked for her assistance with the identification of diatom species, as is Dr Carolyn Beltz of the University of Waikato, for her help with scanning electron microscopy.

I thank Mrs M. McLean for producing an excellent typescript, the University photographers Messrs. Rex Julian and Brian Fargher for their assistance, and Messrs. J. Clayton and A. Devcich for provision of underwater photo negatives.

Finally, I acknowledge a grant (No. 200/12973) from the Lottery Profits, Scientific Research Distribution Committee, Wellington, which assisted logistic support during field-work.

TABLE OF CONTENTS

		Page
ABSTRACT		i
ACKNOWLEDGEMENTS		iii
CONTENTS		iv
LIST OF FIGURES		viii
LIST OF TABLES		xvii
CHAPTER 1:	INTRODUCTION	
1.1	Location	1
1.2	Objectives	1
1.3	Relevance of lake sediment research	3
CHAPTER 2:	PHYSICAL CHARACTERISTICS OF LAKE TAUPO CATCHMENT	5
2.1	Climate	5
2.2	Topography	9
2.3	Geology	21
2.4	Soils	25
	Yellow-brown pumice soils	25
	Central recent soils from volcanic ash	27
	Recent soils from alluvium	27
2.5	Vegetation	29
	Taupo lowlands	29
	Kaimanawa Ranges	29
	Hauhungaroa Range	31
	Tongariro mountains	31
2.6	Hydrology	32
2.7	Catchment erosion	38
CHAPTER 3:	MORPHOMETRY, HYDRODYNAMICS AND AQUATIC FLORA OF LAKE TAUPO	44
3.1	Morphometry	44
3.2	Lake hydrodynamics	48
	Thermal structure	48
	Lake circulation and inflow currents	51
3.3	Aquatic flora	56
	Macrophytes	56
	Algal flora	60

		Page
CHAPTER 4:	FIELDWORK AND PRELIMINARY INVESTIGATION	62
4.1	Outline of fieldwork	62
4.2	Sampling network	62
4.3	Position fixing	63
4.4	Sampling techniques and equipment	64
	Surficial sediments	64
	Core samples	64
	River sediment samples	64
4.5	Sediment field characteristics	65
4.6	Unusual deep-water samples	69
4.7	Sediment hydrogen ion concentration (pH) and redox potentials (Eh)	72
4.8	Lake water temperature and clarity	76
4.9	Preliminary investigation	78
4.10	Sediment colour and water content	81
CHAPTER 5:	TEXTURAL ANALYSIS	84
5.1	Method	84
5.2	Textural character	85
5.3	Shelf sediments	90
5.4	Slope, rise and basinal sediments	90
5.5	Mixed sediments	90
5.6	Gravel and sand trends	92
5.7	Silt and clay trends	92
5.8	Silt modes	97
CHAPTER 6:	SEDIMENT COMPOSITION	102
6.1	Organic matter	102
6.2	X.R.D. of bulk samples	104
	Method	104
	Standard intensity-concentration curves	104
	Sample preparation	105
	Results	105
6.3	X.R.D. of oriented mounts	111
	Method	111
	Results - silt fraction	111
	- clay fraction	113
6.4	Differential thermal analysis (D.T.A.)	117
	Method	117
	Results	123
6.5	Infra-red absorption (I.R.A.)	123
	Sample preparation	123
	Results	125
6.6	Scanning Electron microscopy	130
	Method	130
	Silt sample preparation	131
	Results	131
	Identification of diatom frustules	139
	Clay sample preparation	139
	Results	154

		Page
CHAPTER 7:	DISCUSSION AND INTERPRETATION OF EXPERIMENTAL RESULTS	172
7.1	Introduction	172
7.2	Sediment textural implications	172
	Sub-lacustrine talus environment	173
	Shelf environment	173
	Slope and rise environments	177
	Basinal environment	179
	Sub-lacustrine hilltop environment	188
7.3	Feldspar and quartz trends	191
7.4	Clay-sized material	195
	Crystalline clay mineral content	197
	Crystalline clay mineral trends	197
	Sources of clay minerals	198
	Absence of allophane	206
7.5	Organic matter content	209
CHAPTER 8:	STRATIGRAPHY OF SEDIMENT DEPOSITED IN LAKE TAUPO SINCE THE 131 A.D. TAUPO PUMICE ERUPTIONS	214
8.1	Seismic-profile chart referencing and methodology	214
8.2	Basis of profile interpretation	216
8.3	Seismic profile descriptions and interpretations	219
	General features of profiles	219
	Run 6 from Waihi towards Taupo	220
	Runs 1 and 2 from the Stump Bay shelf to the Kuratau shelf	231
	Run 11 from the Oruatua shelf to the Poukura shelf	236
	Run 10 from the Waihaha shelf to the Hatepe shelf	239
	Run 7 from Motutaiko Island to Hatepe	245
	Run 3 from Motawhara Island to central Western Bay	245
	Run 4 from Kawakawa Bay	245
	Run 5 from Whangamata Bay	248
	Run 8 from Tapaueharuru Bay	250
	Run 9 into Rotongaio Bay	252
8.4	Sedimentation rates	255
CHAPTER 9:	SUMMARY AND CONCLUSIONS	261
9.1	Summary	261
	Catchment characteristics	261
	Lake characteristics	264
	Sediment characteristics	265
9.2	Conclusions	269
	Sedimentation model	270

Page

APPENDICES

Appendix I	Sub-catchments within Taupo catchment	275
Appendix II	Hydrogen ion concentrations (pH) and redox potentials for Lake Taupo sediment samples.	277
Appendix III	Textural data, classification, statistics and terminology for Lake Taupo sediment samples.	278
Appendix IV	Quartz and plagioclase feldspar intensity-concentration curves for X.R.D. analyses.	282
Appendix V	Bulk sediment X.R.D. analyses	283
Appendix VI	X.R.D. analyses of crystalline clay minerals in Lake Taupo sediments.	284
Appendix VII	Lake Taupo sediment core number 1	285
Appendix VIII	Grid references for Lake Taupo sample sites, and University of Waikato reference numbers for sediment samples stored in the University rock store.	286

BIBLIOGRAPHY 288

LIST OF FIGURES

		Page
Fig. 1.1	Location of Lake Taupo catchment in the North Island of New Zealand.	2
1.2	Population trends in the Lake Taupo area	4
2.1	Annual rainfall distribution over the Taupo catchment and wind rose for Lake Taupo.	6
2.2	Rainfall data from stations at Taupo and Chateau Tongariro.	7
2.3	Air temperature data from stations at Taupo and Chateau Tongariro.	8
2.4	Humidity data from stations at Taupo and Chateau Tongariro.	8
2.5	Average seasonal distribution of wind calms for Taupo catchment.	9
2.6	Topographic map of Lake Taupo catchment	10
2.7	Catchment topography to the northeast of Tapaueharuru Bay.	12
2.8	Catchment topography to the east of Lake Taupo	12
2.9	Hydrothermal activity near Waihi village	13
2.10	Waihaha River valley and ignimbrite cliffs	13
2.11	Catchment topography to the south of Lake Taupo	14
2.12	Old lake-level terraces (a) around Mine Bay and (b) to the north of Hatepe.	17
2.13	An aerial view of the Tongariro River delta (a) in 1965 and (b) in 1976.	18
2.14	An aerial view of the Stump Bay-Motuoapa coastal region in (a) 1958, (b) in 1965, and (c) in 1976.	19-20
2.16	Location of the Tongariro, Taupo, Maroa, Rotorua and Okataina Volcanic Centres within the Taupo Volcanic Zone.	23
2.17	Soil parent-rock map for Taupo catchment	24
2.18	Soil map for Taupo catchment	26
2.19	Soil classes for potential pastoral use in the Taupo catchment.	28
2.20	Land use map for Taupo catchment	30

		Page
Fig. 2.21 -	Sub-catchments within Taupo catchment	33
2.22 -	Specific discharge map of runoff from Taupo catchment.	35
2.23 -	Water balance estimations for stations at Taupo and Chateau Tongariro.	36
2.24 -	Borrowed catchment and water diversion system resulting from the Tongariro hydro-electricity scheme.	37
2.25 -	Erosion of coastal pumice-breccia cliffs to the north of Hatepe.	43
3.1 -	An idealised cross-section of lake bathymetry showing the terminology used to describe regions of the lake bed.	46
3.2 -	Bathymetric cross-sections of Lake Taupo: (a) Waihi to Waipahihi (b) Kawakawa Point to Hatepe (c) Te Koromiko Point to Oruatua	47
3.3 -	(a) Summer water-temperature profile for Lake Taupo in 1955-56. (b) Seasonal thermocline depths in Lake Taupo during 1955-56.	49
3.4 -	Annual temperature range of surface and bottom waters in Lake Taupo during 1955-56.	49
3.5 -	Idealised bathymetric cross-section of a nearshore-offshore region showing types of continuous density currents that may arise from river inflow into (a) a stratified lake or (b) a homothermous lake.	53
3.6 -	Turbid Tongariro River water flowing below the less dense surface waters of Lake Taupo.	55
3.7 -	Colonisation of shelf sediment by *Glossostigma* sp.	57
3.8 -	An underwater mound of sediment entrapped by mainly *Myriophyllum elatinoides* and *Isoetes kirkii*.	57
3.9 -	*Potamogeton crispus* growing on the lake bed in Waihi Bay.	58
3.10 -	Dense stands of *Lagarosiphon major* (a) near Kuratau and (b) in Stump Bay.	58,59
3.11	*Elodea canadensis* growing just below the shelf-break near Kuratau.	59
4.1 -	Surface ripples formed on weed-free shelf sediments	66
4.2 -	A cobble/gravel lag in shallow water near Oruatua	66

		Page
Fig. 4.3 -	Slope-rise sediments in Lake Taupo at about 40 m water depth near Kuratau.	67
4.4 -	Sediment sample 66 immediately after recovery from the bottom of Lake Taupo.	67
4.5 -	Sediment sample 67 immediately after recovery from the lake bed.	68
4.6 -	Sinter crust and embedded pumice fragments from the surface of sediment sample 76.	70
4.7 -	Sediment sample 115 immediately after recovery from the lake bed.	71
4.8 -	Freshwater mussel shells (a) from live specimens and (b) from dead specimens.	71
4.9 -	(a) Redox potentials (Eh) in the surficial sediments of Lake Taupo. (b) Hydrogen ion concentrations (pH) in the surficial sediments of Lake Taupo.	73
4.10 -	(a) Sediment Eh vs. water depth (b) Sediment pH vs. water depth (c) Sediment Eh vs. pH	74
4.11 -	Lake temperature profiles and water clarity at some sediment core sites in Lake Taupo.	77
4.12 -	Flow chart for laboratory procedures used on Lake Taupo sediment samples.	79
4.13 -	Sediment water content map	80
4.14 -	Sediment colour map	83
5.1 -	Ternarydiagram plots of sediment texture for (a) gravel-bearing sediment and (b) gravel-free sediment from Lake Taupo.	86
5.2 -	Sediment texture vs. water depth for (a) shelf sediment and (b) slope, rise, and basinal sediments from Lake Taupo.	87
5.3 -	Distribution of sediment textural types in Lake Taupo.	88
5.4 -	Sediment gravel content map for Lake Taupo	91
5.5 -	Sediment sand content map for Lake Taupo	93
5.6 -	Sediment silt content map for Lake Taupo	94
5.7 -	Sediment clay content map for Lake Taupo	95

		Page
Fig. 5.8 -	Clay:silt ratio in Lake Taupo	96
5.9 -	Frequency grain-size curves of selected sediment samples.	98
5.10 -	5.5-6.0ϕ:7.0-7.5ϕ grain-size ratio in the silt fraction of Lake Taupo sediments.	99
5.11 -	Mean grain size of surficial sediments in Lake Taupo.	101
6.1 -	Sediment organic matter content map for Lake Taupo.	103
6.2 -	X-ray diffractogram of sediment sample 30.	107
6.3 -	Weight-percent plagioclase feldspar in organic-free sediments from Lake Taupo.	108
6.4 -	Weight-percent quartz in organic-free sediments from Lake Taupo.	109
6.5 -	Feldspar:quartz ratio in the surficial sediments of Lake Taupo.	110
6.6 -	X-ray diffractograms showing the effects of glycol and heat treatments on oriented clay sample 1.	115
6.7 -	X-ray diffractograms showing the effects of glycol and heat treatments on oriented clay sample 99.	116
6.8 -	Relative heights of 7Å kaolinite X.R.D. peaks from the clay fraction of Lake Taupo sediments.	118
6.9 -	Relative heights of 10Å illite X.R.D. peaks from the clay fraction of Lake Taupo sediments.	119
6.10 -	Relative heights of 15Å montmorillonite X.R.D. peaks from the clay fraction of Lake Taupo sediments.	120
6.11 -	Relative abundance of montmorillonite in the surficial sediments of Lake Taupo.	121
6.12 -	Differential thermographs of (a) sediment sample 46 and (b) the clay fraction from sample 46.	122
6.13 -	Infra-red absorption spectra of clay-sized material in Lake Taupo sediments.	124
6.14 -	Infra-red absorption spectra of clay-sized rhyolitic glass, micaceous minerals, silica gel, allophane, illite, montmorillonite and vermiculite.	126

Page

Fig. 6.15 - Infra-red absorption spectra of (a) coarse silt 113, (b) medium silt 113 and (c) clay 114. 128

6.16 - Infra-red absorption spectra of a typical basinal sand fraction (sample 54) and coarse silt fraction (sample 113) from Lake Taupo. 129

6.17 - Total dry sediment from (a) sample 74 and (b) sample 103. 132

6.18 - (a) Coarse silt, (b) medium silt and (c) fine-very fine silt from sample 2. 134

6.19 - (a) Coarse-medium silt and (b) fine-very fine silt from sample 4. 135

6.20 - (a) Coarse-medium silt and (b) fine-very fine silt from sample 54. 136

6.21 - (a) Coarse silt, (b) medium silt and (c) fine-very fine silt from sample 103. 137

6.22 - (a) A silt-sized, vesiculated, pumice fragment, (b1) glass shards and (b2) terrigenous silt particles lacking distinct morphology. 138

6.23 - *Melosira* sp. diatom tests 142

6.24 - *Cyclotella stelligera* diatom test (tilted specimen) 142

6.25 - (a) *Cyclotella stelligera* diatom test (valve interior) 143
(b) *Cyclotella stelligera* diatom test (valve exterior)

6.26 - *Rhopalodia gibba* diatom test (valve interior) 144

6.27 - *Epithemia* sp. diatom test (valve interior) 144

6.28 - *Synedra ulna* diatom test 145

6.29 - *Cocconeis placentulata* diatom test (pseudoraphe valve) 145

6.30 - (a) and (b) *Fragillaria* sp. diatom tests 146

6.31 - *Coscinodiscus* sp. ad *lacustris* diatom test 147

6.32 - (a) and (b) Valvocopula (diatom girdle-band) 148

6.33 - *Surirella* sp. diatom test (with girdle) 149

6.34 - *Surirella* sp. diatom test (asymmetrical valve) 149

		Page
Fig. 6.35 -	(a) *Surirella tenera* diatom test (b) Siliceous sponge spicule	150
6.36 -	*Surirella tenera* diatom test	150
6.37 -	(a) *Cymatopleura solea* diatom test (b) *Cymbella* sp. diatom test (c) *Synedra ulna* diatom test	151
6.38 -	*Nitzschia* sp. diatom test	151
6.39 -	L.R.G.T. (ultraplankter)	152
6.40 -	Unidentified biological structure from sediment sample 14.	153
6.41 -	Diatomite sample collected from Scenic Bay, Lake Taupo.	153
6.42 -	Coarse clay fraction from sediment sample 12	155
6.43 -	Layers formed by differential settling of sample 55 coarse clay through a 15 cm water column.	155
6.44 -	(a) and (b) Top-layer components from sample 55 clay	156
6.45 -	(a), (b) and (c) Middle-layer components from sample 55 clay.	157
6.46 -	(a) and (b) Bottom-layer components from sample 55 clay.	158
6.47 -	(a) and (b) Authigenic siliceous microspherulites	161
6.48 -	(a) and (b) Very fine silt and clay sized bio-capsules.	163
6.49 -	(a) and (b) Sulphur-rich, sub-spherical particles in the very fine silt-clay fraction of Lake Taupo sediments.	165
6.50 -	S.E.M. X-ray energy dispersive spectrum of a sulphur-rich particle illustrated in Fig. 6.49.	166
6.51 -	(a) Clay-sized volcanic glass fragments (b) Clay-sized diatom test fragments	168
6.52 -	(a) Sample 34 "fine clay" (b) Sample 104 "fine clay"	170
6.53 -	Sample 104 "fine clay" (broken edge of aggregate)	171

		Page
Fig. 6.54 -	S.E.M. X-ray energy dispersive spectrum from sample 104 "fine clay".	171
7.1 -	Idealised cross-section of a sub-lacustrine talus facies showing types of sediment input.	174
7.2 -	Idealised cross-section of wave motion in deep water.	174
7.3 -	A comparison of selected shelf sediment textures and their exposure to prevailing wind-wave action.	176
7.4 -	Approximate distribution of sand-sized diatom tests in the surficial sediments of Lake Taupo.	178
7.5 -	Terrigenous silt as a percentage of total silt content in the surficial sediments of Lake Taupo.	180
7.6 -	(a) Flow directions of suspended-sediment laden currents in Lake Taupo. (b) Band 4 Landsat image showing a plume of suspended sediment in Lake Taupo on 22 December, 1975. (c) Relative density of suspended sediment illustrated in Fig. 7.6(b).	182 184
7.7 -	(a) Sediment cores obtained from Lake Taupo in 1973. (b) Areal extent of Ngauruhoe Ash as a soil parent material	186
7.8 -	Idealised cross-section of a shelf-slope-rise-basin area showing types and extent of various sediment inputs and transport mechanisms.	187
7.9 -	Positions in Lake Taupo of deep-water sediments containing redeposited sand and pumice gravel, and of sub-lacustrine hilltop sediments enriched in sand and pumice gravel.	190
7.10 -	Approximate content of amorphous, terrigenous silt in the silt fraction of basinal sediments in central and northern Lake Taupo.	196
7.11 -	Relationships between absolute and relative clay mineral contents in (a,b) the clay fraction, and (c) in the total sediment.	200
7.12 -	Rates of clay deposition with distance from lake-shore source area.	201
7.13 -	Suspended sediment load vs. discharge for some rivers and streams flowing into Lake Taupo.	203
7.14 -	(a) and (b) Distribution of clay minerals in South Pacific deep-marine sediments. (c) Composition of dust found in New Zealand snow fields.	207

		Page
Fig. 8.1 -	Lake Taupo sediment core number 5	218
8.2 -	Run 6 seismic profile (Waihi towards Taupo)	221, 227, 230
8.3 -	Lake Taupo sediment core number 2	222
8.4 -	Lake Taupo sediment core number 4	225
8.5 -	Lake Taupo sediment core number 3	228
8.6 -	Runs 1 and 2 seismic profiles (Stump Bay to Kuratau.	232-233
8.7 -	A cross-section of the shelf-rise area in Stump Bay, showing probable direction of sediment slump movement.	234
8.8 -	Idealised cross-sections of coastal and shelf-slope modifications resulting from the post-131 A.D. drop in lake level of 34 m.	235
8.9 -	Run 11 seismic profile (Oruatua to Poukura)	237
8.10 -	Run 10 seismic profile (Waihaha River mouth to Hatepe).	242-244
8.11 -	Run 7 seismic profile (Motutaiko Island to Hatepe).	246
8.12 -	Run 3 seismic profile (Motawhara Island to central Western Bay).	247
8.13 -	Run 4 seismic profile (from Kawakawa Bay)	247
8.14 -	Run 5 seismic profile (from Whangamata Bay)	249
8.15 -	Run 8 seismic profile (from Tapaueharuru Bay)	251
8.16 -	Run 9 seismic profile (into Rotongaio Bay)	253
8.17 -	Lake Taupo sediment core number 6	254
8.18 -	Shallow, sub-bottom sediment stratigraphy in Lake Taupo.	256
8.19 -	A comparison of sedimentation trends indicated by seismic profiles and terrigenous silt contents in the surficial sediments of Lake Taupo.	257
9.1 -	A possible sequence of events in Lake Taupo since 130 A.D.	271

Page

Fig. 9.2 - Interrelated catchment characteristics responsible for the major sediment influxes into the southern end of Lake Taupo. 272

9.3 - A proposed sedimentation model for Lake Taupo 273

Lift out maps in back pocket:

Map 1 - Geology of Lake Taupo catchment

2 - Lake Taupo catchment erosion

3 - Lake Taupo bathymetry and sediment sample sites.

LIST OF TABLES

		Page
Table 2.1	(a) Discharge ranges for some rivers and streams flowing into Lake Taupo. (b) Calculated mean discharges for some rivers and streams flowing into Lake Taupo.	34
3.1	Morphometric data for Lake Taupo	45
3.2	Estimated average annual water budget for Lake Taupo.	45
3.3	Past observations of diatom species in Lake Taupo.	61
5.1	Shelf-sediment textures	89
6.1	Quartz and feldspar content variations through the silt fractions of selected sediment samples.	112
6.2	Identification characteristics of crystalline clay minerals (oriented mounts) using X-ray diffraction.	114
6.3	Diatom species identified in Lake Taupo sediments.	140
6.4	Further diatom species identified by V. Cassie.	141
6.5	Coarse-clay components in sample 55 from Lake Taupo.	160
6.6	Approximate abundance of morphologically distinct components in the coarse clay fraction of sample 55.	160
7.1	Textural character of deep-water sediments containing redeposited pumice gravel and/or sand, and of sediments on sub-lacustrine hills.	189
7.2	Approximate contents of some minerals in yellow-brown pumice soils, recent soils from andesitic ash and different soil parent rocks.	193
8.1	Average sedimentation rates for deep-water regions of Lake Taupo over the last 1800 years.	260

CHAPTER 1

INTRODUCTION

1.1 LOCATION

Lake Taupo is one of several lakes of volcano-tectonic origin in the Central Volcanic Region of the North Island of New Zealand. It occupies a natural land catchment of 286,515 ha. which ranges in altitude from 357 m to 2800 m above sea level. A further 67,110 ha. of artificially diverted catchment, resulting from the Tongariro hydro-electricity scheme, increases the total catchment area to 353,625 ha. Lake Taupo is drained by the Waikato River (Fig. 1.1).

1.2 OBJECTIVES

This study is concerned primarily with documenting the characteristics of the surficial sediments of Lake Taupo. Specific aims are:

1. To establish the texture, composition and provenance of bottom sediments.
2. To identify sedimented diatom species.
3. To identify and establish the relative importance of agents currently transporting sediment to, and within, the lake.
4. To determine average sedimentation rates in the lake and explain any areal trends.
5. To propose a sedimentation model for Lake Taupo.

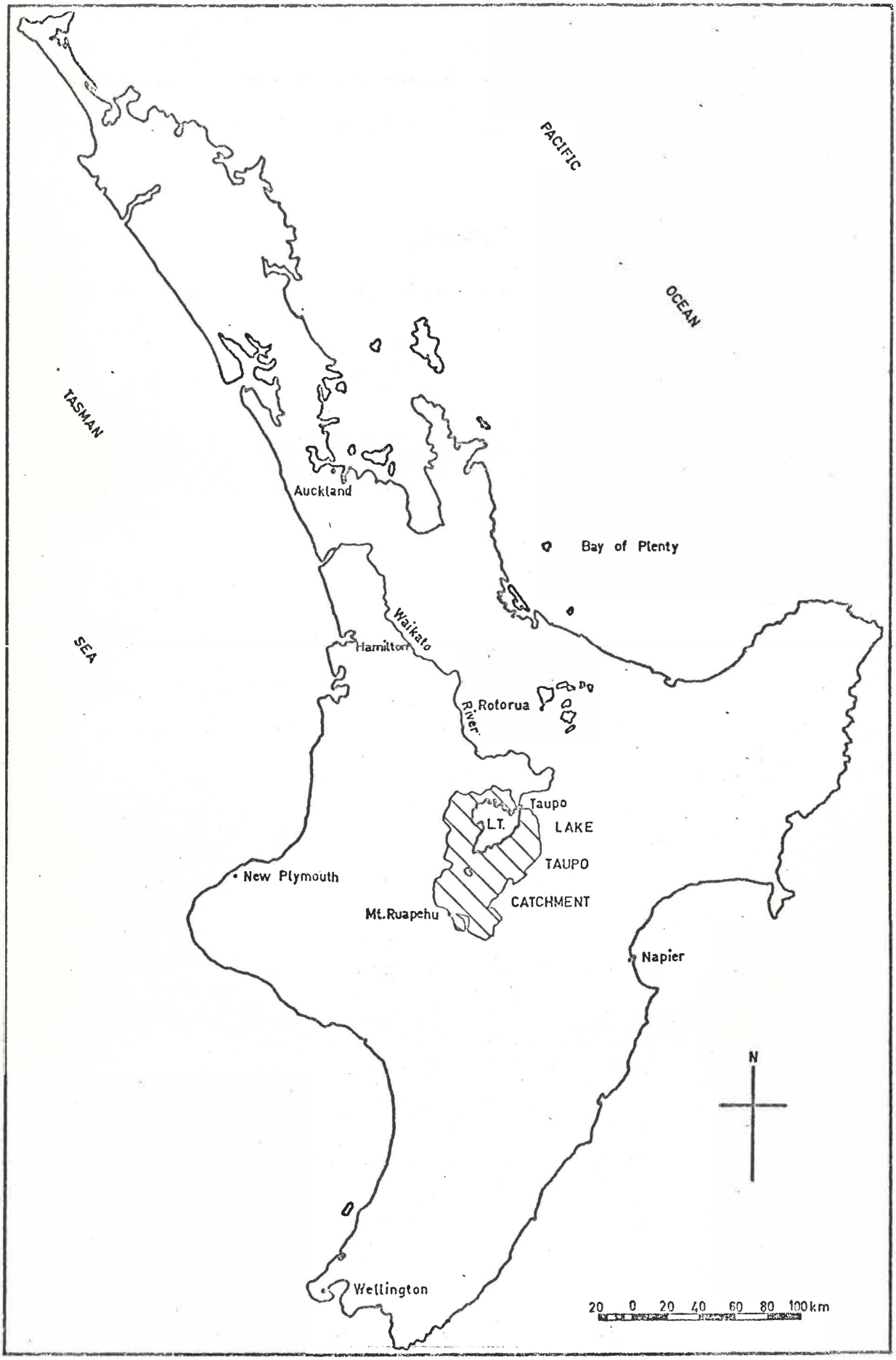


Fig. 1.1. Location of Lake Taupo catchment in the North Island of New Zealand.

It is hoped that the data resulting from this study will provide a base-line against which the effects of future catchment use may be measured.

1.3 RELEVANCE OF LAKE SEDIMENT RESEARCH

A need exists for qualitative and quantitative information on lake sediments in New Zealand. Fresh water is one of the country's major natural resources and lakes are natural reservoirs for this resource.

Lake Taupo, with an area of 616 km^2, is Australasia's largest lake and an important resource both for recreation (e.g. trout fishing, boating and tourism) and the supply of unspoiled water. Outflow waters in the Waikato River are used for domestic, agricultural and industrial purposes, including the generation of electricity at eight hydro-electricity stations (1045 mW). Thus management of this resource has effects well beyond Lake Taupo itself.

Lake management requires planning and policies which take into account the various competing pressures for development of catchment lands. It is necessary to balance these requirements against the need to preserve the quality of the lake and its waters. Lake management clearly requires fundamental data on the lake and in particular its response to various uses and changes within the catchment. Ideally the whole lake system should be considered if valid cause-and-effect relationships are to be established.

Sediments are an intimate part of the lake system. They influence especially the nutrient budget, and hence the ecology,

trophic status and evolution rate of the lake, yet little detailed work on New Zealand lake sediments is available (Glasby, 1975; Chittenden *et al.* 1976; McColl, 1977). Sediments provide a record of catchment evolution. Vertical changes in sediment character may indicate short- and/or long-term changes in climate; catchment hydrology, vegetation and erosion; lake plankton, trophic status, and hydrologic regime. Tectonic and volcanic events may also be recorded. Areal changes in the sediment character may indicate areal changes in the lakes hydrologic regime, and the proximity and relative importance of sediment sources.

Knowledge of surficial sediment character provides a base-line against which future sedimentary data may be compared. Such knowledge is particularly desirable for Lake Taupo which is still in almost pristine condition despite farming, forestry, residential and recreational pressures in the area. It is inevitable that the demand on this resource will increase in the future (Fig. 1.2).

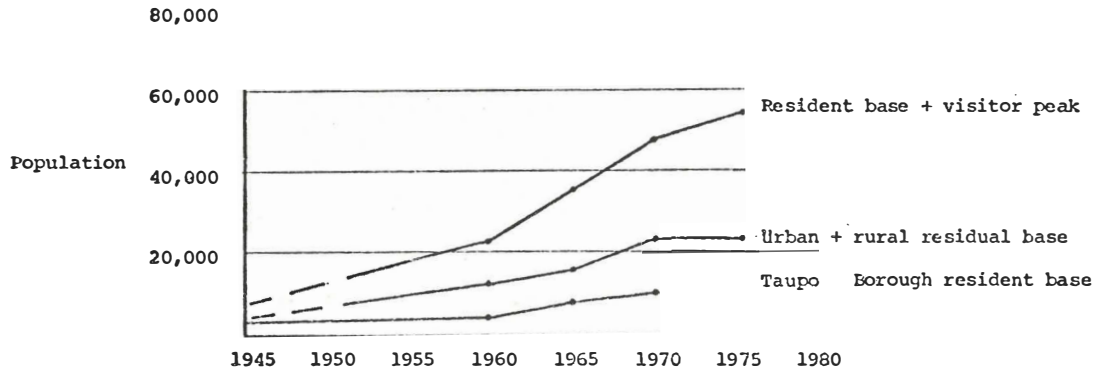


Fig. 1.2 Population trends in the Lake Taupo area (W.V.A. 1973)

CHAPTER 2

PHYSICAL CHARACTERISTICS OF LAKE TAUPO CATCHMENT

2.1 CLIMATE

The geographic position, altitude and surrounding topography (Figs. 1.1, 2.6) of the Taupo catchment produces an 'interior' rather than an 'oceanic' climate, described as cool and superhumid, or microthermal, by de Lisle and Kerr (1963). Bounding ranges to the east and west help create a wind tunnel through which the prevailing winds flow (Fig. 2.1). West and northwest winds flowing over the National Park volcanoes and ranges to the west are largely responsible for the high rainfalls in the southern catchment and a rainshadow effect to the northeast (Fig. 2.1). Rainfall, temperature and humidity data from two extreme stations, Taupo and Chateau Tongariro, illustrate the climatic diversity within the catchment (Figs. 2.2 to 2.4).

Rainfall is fairly evenly distributed throughout the year, although a summer minimum occurs which periodically leads to drought conditions in low rainfall areas. Total annual rainfalls may vary by up to 50% from the yearly average. High intensity rainfalls are especially characteristic in the southern catchment.

The overall elevation of the catchment causes considerable surface cooling by night radiation, giving a fairly large diurnal temperature range. As a result the lower catchment area accumulates relatively dense air at the surface giving night and early morning calms, especially in autumn and winter (Fig. 2.5).

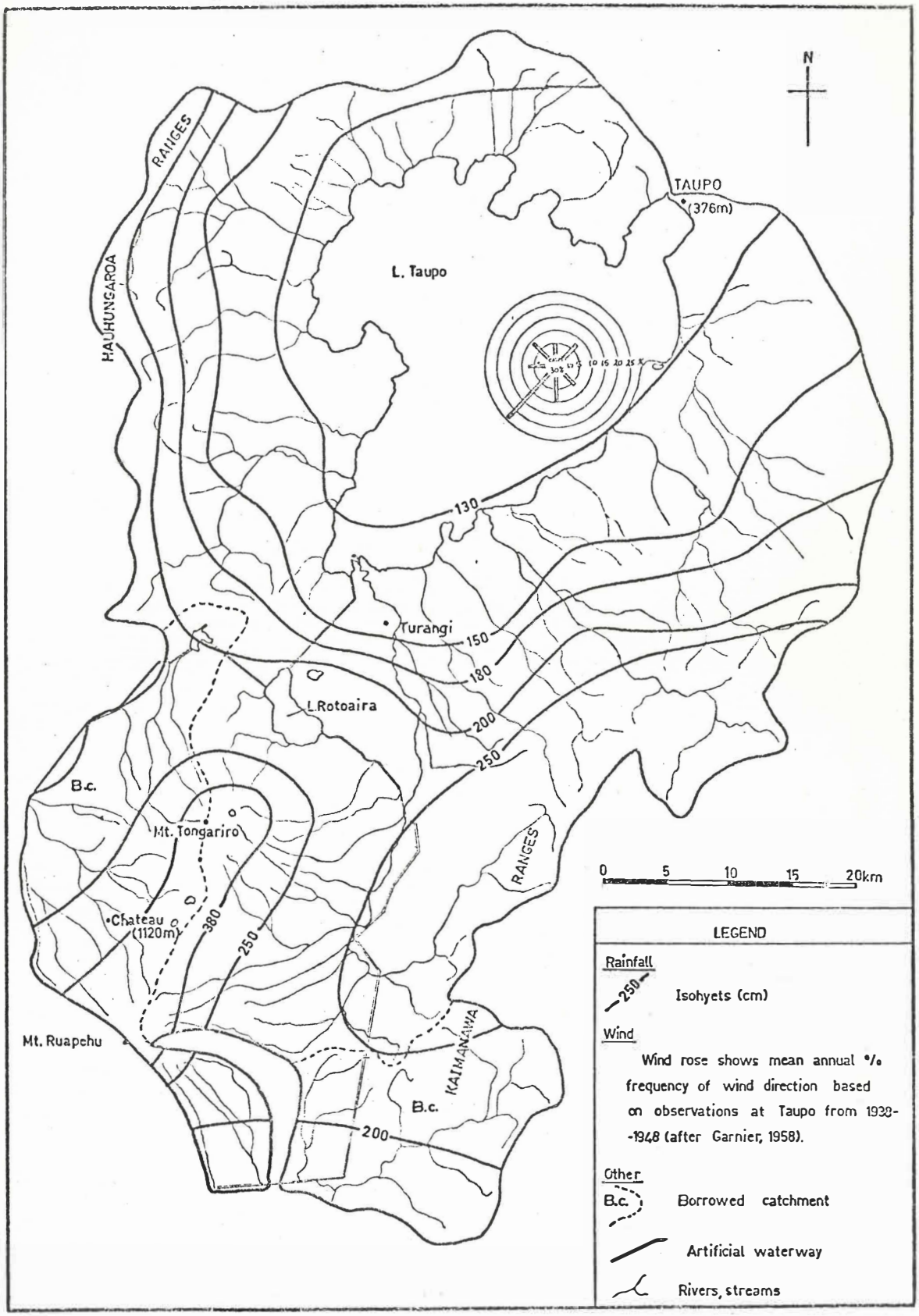
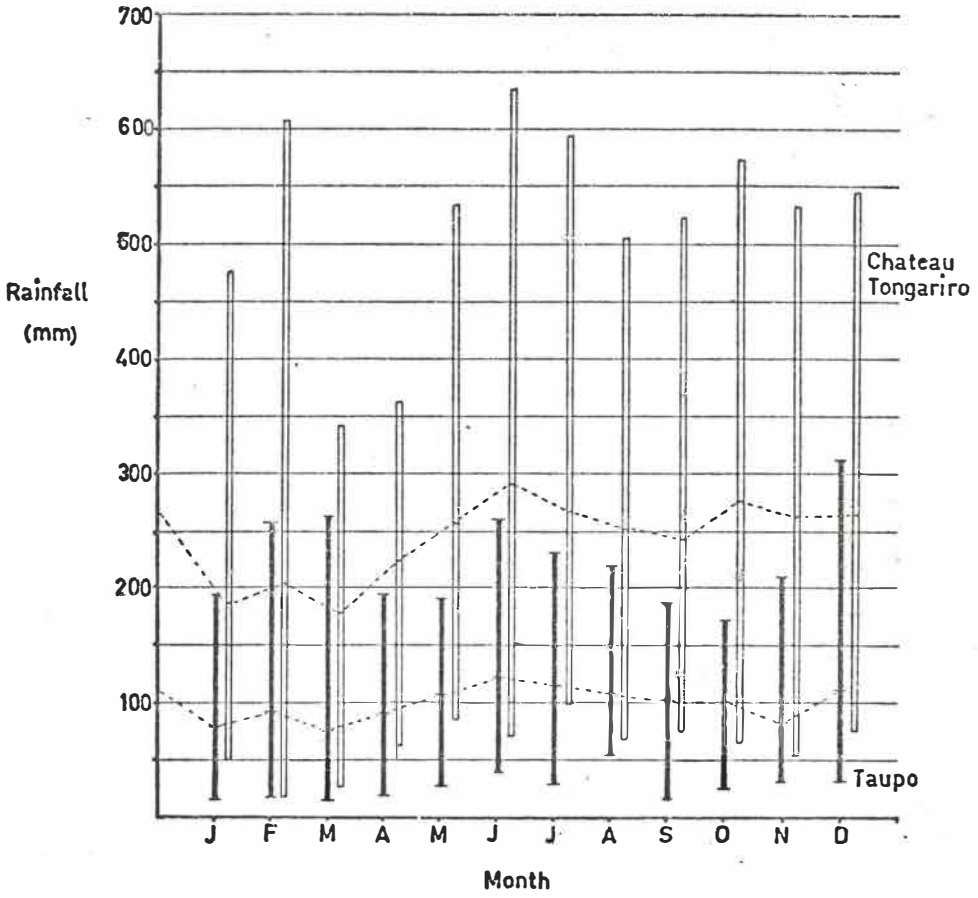


Fig. 2.1. Lake Taupo catchment mean annual rainfall distribution (based on de Lisle and Kerr, 1963; Maunder and Browne, 1972; Maunder, 1974) and mean annual percent frequency of wind direction (after Garnier, 1958).



(a) Mean monthly maximum, normal and minimum rainfalls for Taupo (1941-1970) and Chateau Tongariro (1940-1970)

(b)

Annual rainfall (m.m.)	Mean Maximum	Mean Normal	Mean Minimum
Taupo (1941-1970)	1720	1199	922
Chateau Tongariro (1949-1970)	3695	2914	1873

(c)

Average number of days >1 mm rainfall													per year
Taupo (1949-1970)	8	8	8	9	11	12	12	12	10	12	11	11	123
Chateau Tongariro (1940-1970)	12	11	12	14	16	17	17	17	16	18	17	16	187
Month	J	F	M	A	M	J	J	A	S	O	N	D	

(d)

Maximum 1 day rainfall (mm)													
Taupo (1949-1970)	85	130	85	75	60	55	70	95	70	90	75	100	
Chateau Tongariro (1940-1970)	110	145	120	80	120	85	80	95	90	135	95	120	

Fig. 2.2. Rainfall data from stations at Taupo and Chateau Tongariri (based on N.Z. Meteorological Service, 1973).

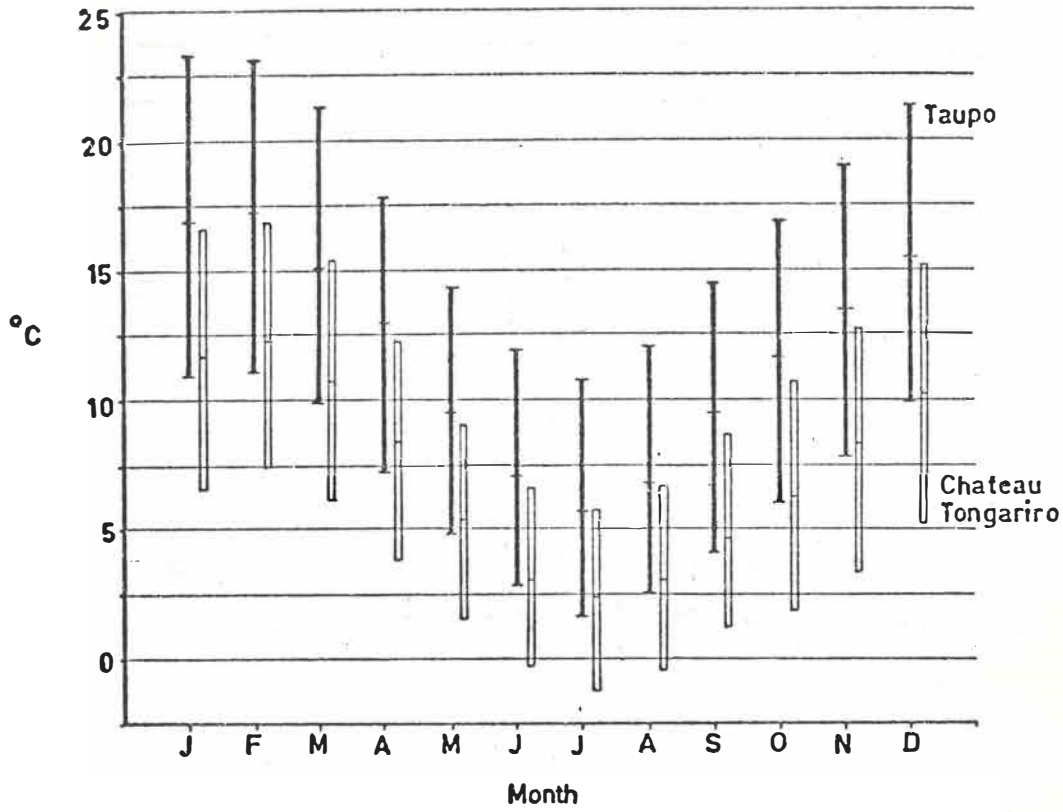


Fig. 2.3. Mean daily maximum, normal and minimum temperatures for Taupo (1949-1970) and Chateau Tongariro (1930-1970); based on N.Z. Meteorological Service (1973).

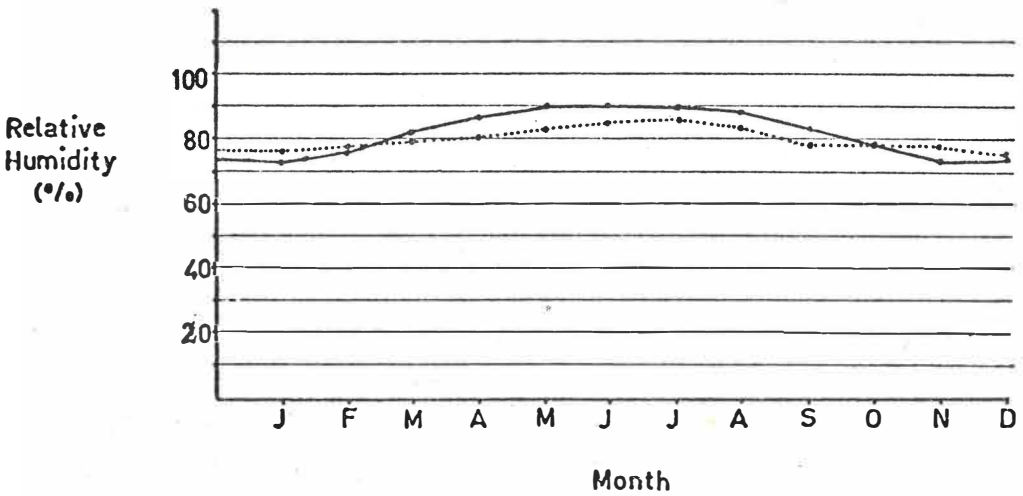


Fig. 2.4. Average relative humidity (9 a.m.) for Taupo (1949-1970) and Chateau Tongariro (1930-1970); based on N.Z. Meteorological Service (1973).

WINTER	SPRING	SUMMER	AUTUMN
34%	21%	20%	25%

Fig. 2.5. Average seasonal distribution of wind calms for Lake Taupo catchment (1938-1948), based on Garnier (1958).

A small permanent snow field exists on Mt Ruapehu above 2500 m and rarely descends to below 500 m. During spring and winter snow persists above 1500 m. The frequency and amount of snow varies considerably from winter to winter.

2.2 TOPOGRAPHY

The topography of Lake Taupo catchment is summarised in Fig. 2.6. The depression occupied by Lake Taupo consists of two structural entities. The Western Bay area is thought to be a cauldera resulting from collapse following the eruptions of the Whakamaru Ignimbrite (Briggs, 1976) dated at 330,000 yrs B.P. (Kohn, 1973). The rest of the lake occupies part of a long, broad, fault-bounded depression extending roughly northeast from Turangi to Reporoa.

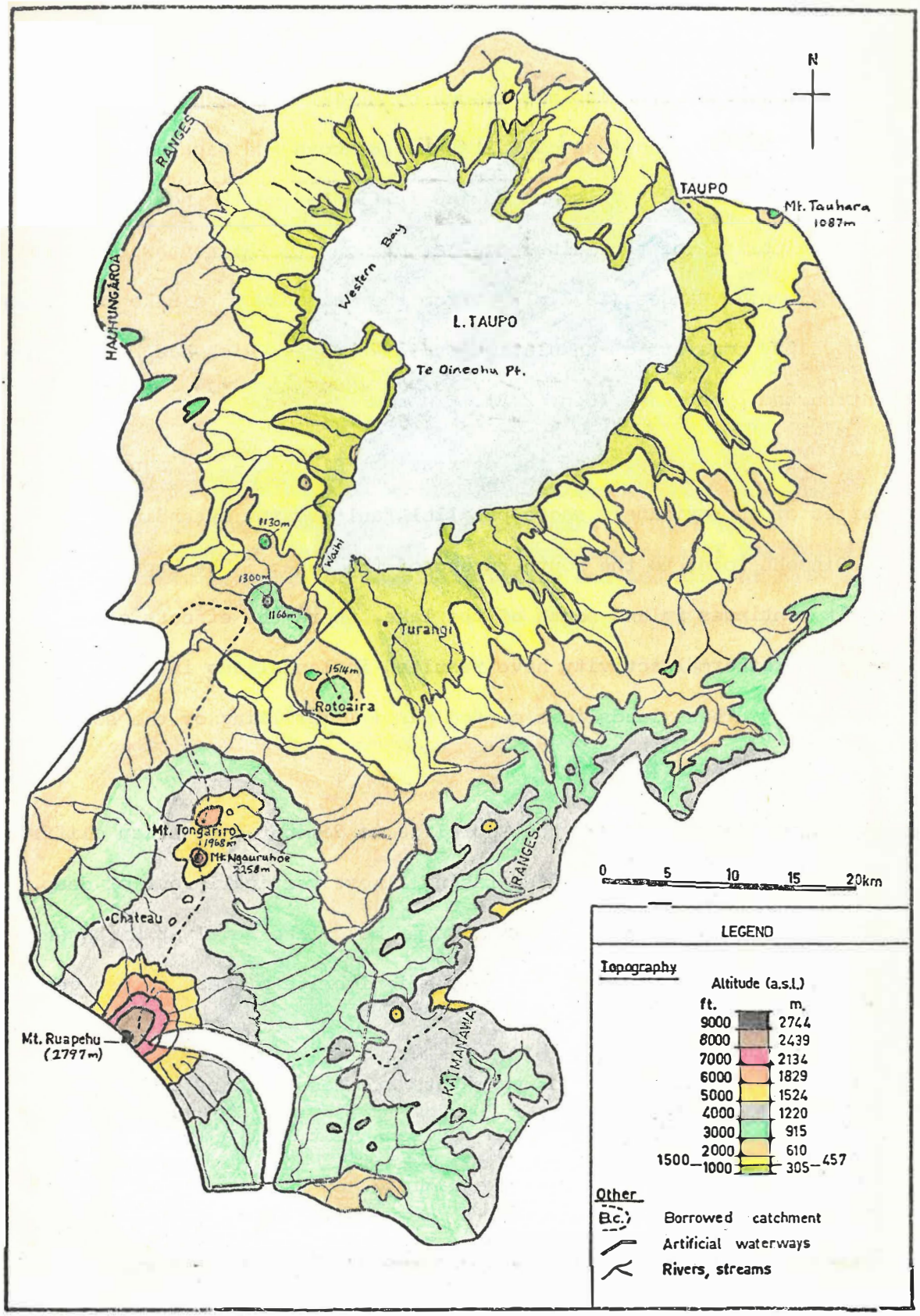


Fig. 2.6. Lake Taupo catchment topography (after Lands and Survey, 1975a).

The lake is contained in this trough by Mt Tauhara (1087 m), a dacite cone, and coalescing fans of Waitahanui Breccia and Haparangi Rhyolitic Pumice (Fig. 2.7). This depression is flanked to the northeast by the ignimbrites of the Kaingaroa Plateau, and to the southwest by the Kaimanawa Ranges (1372 m). From the Kaimanawas to Lake Taupo the topography consists of undulating pumice breccia which has been deeply entrenched by streams (Fig. 2.8).

The western side of the depression is bordered by a prominent series of approximately shore-parallel fault scarps extending from Te Oineohu Point to the southern end of the lake. The Hipaua Ridge Fault continues inland south of the lake, where the effects of continuing hydrothermal activity have resulted in landslides in 1834, 1846 and 1910. These landslides caused partial infilling of the southern end of the lake (Fig. 2.9).

Around Western Bay the shoreline is dominated by steep cliffs of Whakamaru Ignimbrite, often rising almost vertically out of deep water and reaching heights up to 300 m above lake level at Karangahape Cliffs. To the west of the lake the ignimbrite plateau slopes gently up towards the Hauhungaroa Range (914 m) which forms the western catchment boundary. The ignimbrite sheets are dissected by pumiceous ash-filled valleys (Fig. 2.10). To the southwest of the lake the rhyolitic domes of Rangitukua (729 m), Pukekaikiore and Kuharua (1130 m) rise above the plateau.

To the south of the lake, beyond a plain of pumice alluvium and the andesitic cones of Kakaramea (1300 m), Tihia (1166 m), and



Fig. 2.7. Catchment topography to the northeast of Lake Taupo: Mt Tauhara (dacite 1087 m), surrounding fans of Waitahanui Breccia/Haparangi Rhyolitic Pumice and the distant Kaingaroa ignimbrite plateau.



Fig. 2.8. Catchment topography to the east of central Stump Bay: Rolling lowlands of pumice breccia lie behind a plain of pumice alluvium. The Kaimanawa Ranges can be seen in the distance.



Fig. 2.9. Hydrothermal activity on Hipaua Ridge and along the edge of Lake Taupo at Waihi village.



Fig. 2.10. Cliffs of Whakamaru Ignimbrite along the northern side of the Waihaha River valley, Western Bay, Lake Taupo. Similar cliffs surround much of Western Bay.



Fig. 2.11. View from Whangamata Bay across Lake Taupo to the snow-capped volcanoes of Tongariro National Park. Beyond the Karangahape Cliffs (right foreground) lie the peaks of (right to left) Kuharua (1130 m), Kakaramea (1300 m), Tihia (1166 m) and Pihanga (1514 m).

Pihanga (1514 m), the landscape is dominated by the andesitic cones of Mt Tongariro (1968 m), Mt Ngauruhoe (2258 m), and Mt Ruapehu (2797 m) (Fig. 2.11).

At the northern end of the lake northeast trending fault blocks project into the lake, the downthrown blocks forming a series of small bays separated by prominent peninsulas formed by the uplifted blocks. Movement occurred on some of these faults in 1922 resulting in shore subsidence of up to 3.7 m (Ward, 1922).

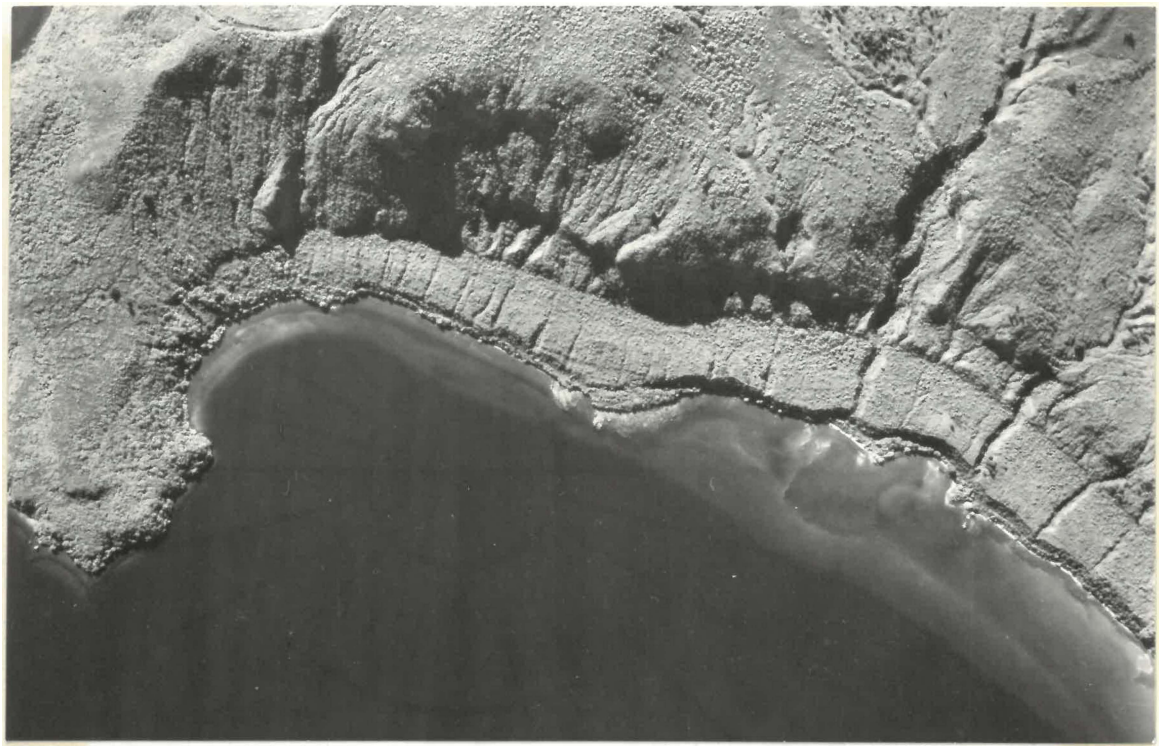
The present shape of Lake Taupo is a relatively recently developed one. Pumiceous tuffs overlying lake sediments in the Reporoa Valley, the north end of Lake Taupo, and the valley of the Hinemaiaia Stream all indicate the existence of a more extensive lake during the Pleistocene prior to volcanic activity in the Maroa and Taupo Volcanic Centres (100,000-50,000 yrs B.P.). The lake has since been further modified by pumice air-fall and ash-flow deposits. Eruptions of the Oruanui Formation (Vucetich and Pullar, 1969) about 20,000 years ago resulted in a westward shift of the eastern shoreline and a rise in lake level to 55 m above its present level. The lake level gradually subsided as outflow incised a new channel.

The lake was further reduced in size, principally along the eastern side, by the widespread and thick ash-fall and ash-flow pumice deposits of the 3000-3400 year old Waimahia Formation, and the Taupo Ash eruptions of 131 A.D. (Baumgart, 1954; Baumgart and Healy, 1956; Healy, 1964; Vucetich and Pullar, 1964). The huge amounts of pumice both directly deposited and washed into the lake after the Taupo

eruptions blocked the outlet. The lake rose to about 34 m above its present level where it remained long enough to cut a well defined terrace that is visible around much of the present coastline (Fig. 2.12a and b). Eventually overflow cut the present Waikato River outlet and the lake level subsided again. The amount of pumice being eroded and transported into the lake gradually decreased as water courses re-opened and vegetation became re-established in the catchment.

Most recently, coastal processes have shaped the lake shoreline, particularly on the eastern side of the lake. Formation of a classic birdfoot delta by the Tongariro River, and the flanking swamp areas to the south and east of the delta (Fig. 2.13) illustrate the inability of coastal processes in these areas to cope with sediment influx. Further eastwards along the coast, at the Waimarino River mouth, more exposed conditions and a smaller sediment influx have resulted in beach accretion by ridge formation rather than by delta formation. These beach ridges, together with ridges in southwest Motuoapa Bay which were probably constructed of sediments deposited by pre-existing Tauranga-Taupo River courses, have formed a tombolo, the Motuoapa Headland (Fig. 2.14). Beach-ridge accretion has also occurred along the lake shoreline to the north of Te Kohaiakahu Point, probably from pumice eroded from cliffs to the south.

(a)

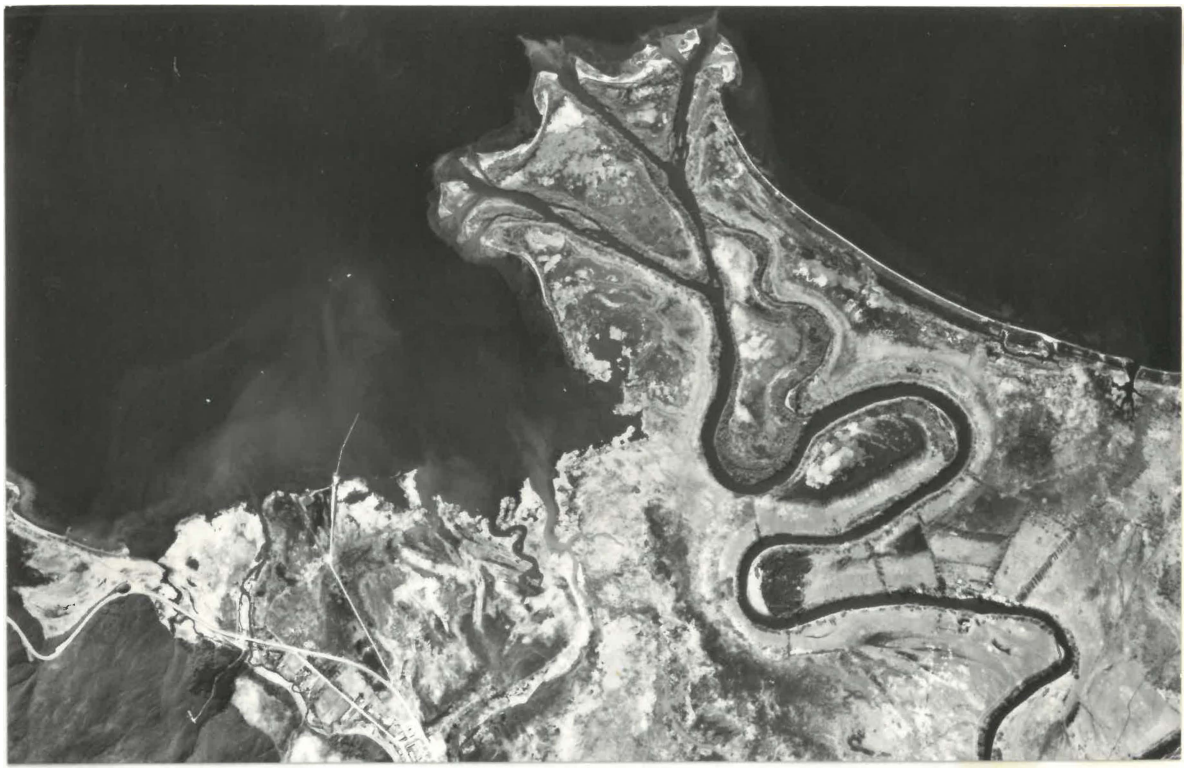


(b)



Fig. 2.12. Old lake-level terraces around the shores of Lake Taupo. (a) Mine Bay. Remnants of a +55 m terrace (∿20,000 yr.B.P.) remain above a wider +34 m terrace (∿1800 yr.B.P.). Below the +34 m terrace there is evidence of minor still-stands during the last major drop in lake level (Photo- N.Z. Lands and Survey). (b) East Coast of Lake Taupo to the north of Hatepe. A wide +34 m terrace, fans of alluvium at valley mouths (centre). and cliff erosion (left) are evidence of the erodible nature of the pumice breccia lithology (Photo C. Nelson).

(a)



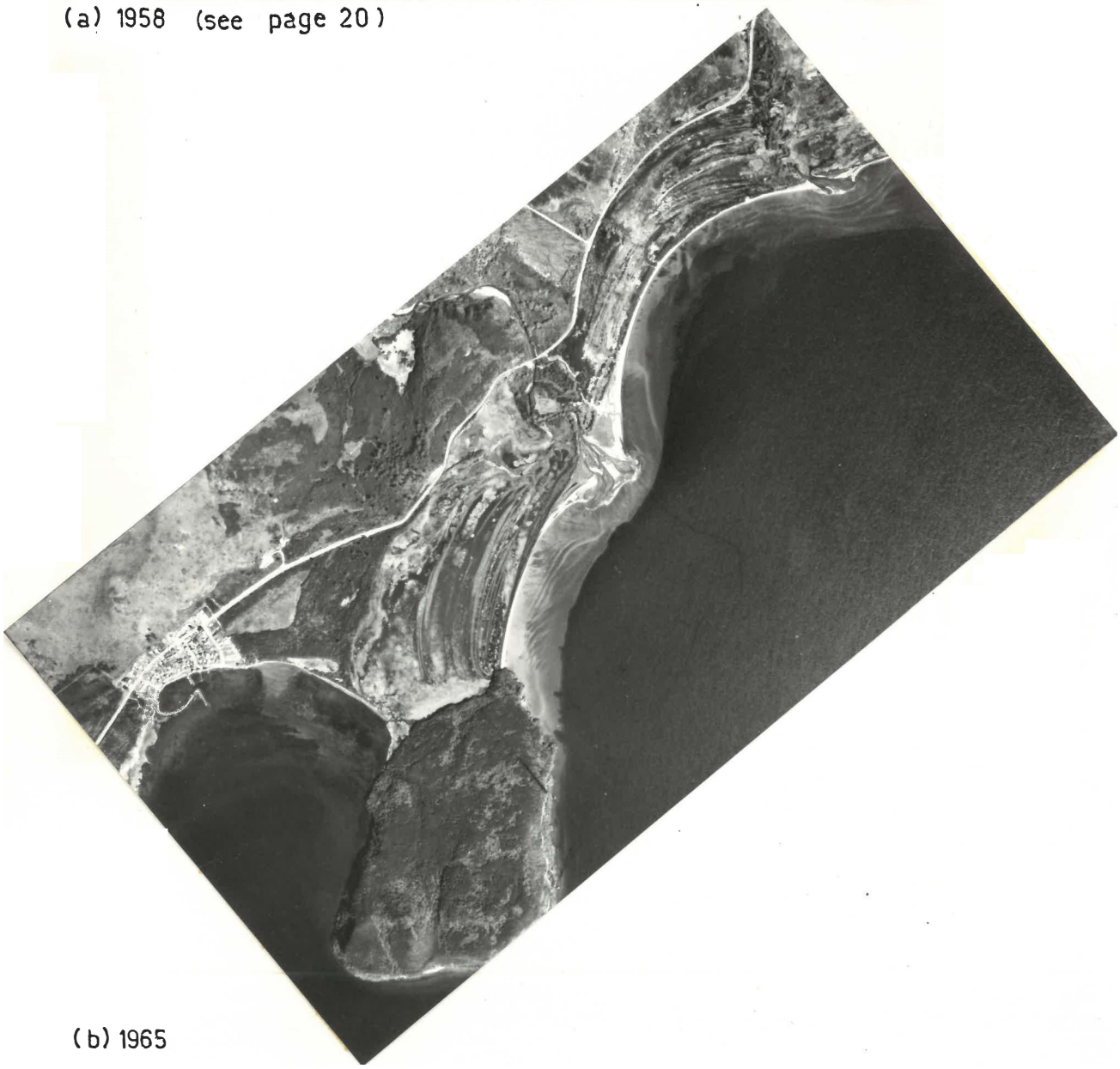
(b)



Fig. 2.13. Tongariro River delta-Waihi Bay region. (a) 1965. Sediment-laden water from the middle and main mouths of the Tongariro River appear to extend into the lake and submerge over the shelf edge (cf. Fig. 3.6). Discoloured water (? suspended sediment, ?organic leachates) enter Waihi Bay from swampy regions to the south of the delta. (b) 1976. Minor modifications to the delta since 1965 are evident, particularly around the middle and main mouths. South of the delta, the Tokaanu tailrace (Tongariro hydro-electricity scheme) discharges into Waihi Bay. An aquatic weed-bed has developed in the vicinity of the boat jetty. (Photos - N.Z. Lands and Survey).



(a) 1958 (see page 20)



(b) 1965



(c) 1976

Fig. 2.14. Stump Bay-Motuoapa region showing lake-shelf morphology, coastal accretion of beach ridges, and Motuoapa tombolo.
(a) 1958. Recent catchment floods have deposited sediment at the Waimarino and Waiotaka River mouths (centre, bottom left), and along the course followed by an over-bank flow from the Waimarino River (lower centre). 'Notches' along the shelf-break may indicate past slumping of outer-shelf sediments.
(b) 1965. Some growth and re-shaping of the Waimarino 'delta' has occurred since 1958. Swell-wave action and/or longshore currents have modified the shelf-sediment topography and sealed the temporary flood-flow mouths of 1958. Aquatic weed growth is evident in the sheltered waters of Motuoapa Bay.
(c) 1976. Sediment deposits around the Waimarino and Waiotaka River mouths appear stable and support some vegetation. (Photos - N.Z. Lands and Survey).

2.3 GEOLOGY

A geological map of Lake Taupo catchment is included in the map pocket of this thesis (Map 1).

Details of the origin and geological history of the Lake Taupo area are complex and not fully understood. Most development occurred in the middle to Late Pleistocene, with modifications during the Holocene. The distribution and possible origin of Quaternary volcanic rocks have been described by Grindley (1960), Healy (1962, 1964), Healy *et al.* (1964), Grindley and Mathews (1965), Mathews (1967) and Ewart and Stipp (1968).

The oldest rocks within the catchment are the Early Mesozoic greywackes of the Kaimanawa and Hauhungaroa Ranges. A schist core of possible Permian age is exposed in the Kaimanawas.

Small areas of Tertiary marine sediments outcrop within the catchment including Middle-Late Miocene siltstones and sandstones in the southern Hauhungaroas, and Pliocene fossiliferous sandstones, siltstones and limestones in the Moawhango Basin (borrowed catchment).

SUMMARY OF VOLCANIC HISTORY

During the Early Quaternary, elevation of the Kaimanawa and Hauhungaroa Ranges and downfaulting of the area between these ranges occurred. Laharic material in the Hauhungaroas and ignimbrite in the Kaimanawas is evidence of volcanic activity prior to these movements. Dominantly acidic volcanism has continued through to the present day. Reworked material from the early eruptions of

ignimbrite and pumice breccia was deposited in a lacustrine environment in the Lake Taupo region and forms the Huka Group. Rhyolite occurs in lavas, domes, pumice breccias, large volumes of welded ignimbrites and as airfall tephra. Andesitic lavas, lahars, and ash have dominated the southern part of the catchment since the Early Quaternary (Grindley, 1960; Grindley and Mathews, 1965; Mathews, 1967).

Lake Taupo catchment includes the Taupo and Tongariro Volcanic Centres, two of the five volcanic centres of the Taupo Volcanic Zone (Fig. 2.16; Healy, 1962, 1964). The Tongariro Volcanic Centre is andesitic; the others are rhyolitic. The rhyolitic centres are marked by rhyolitic domes and are flanked to the east and west by extensive ignimbrite plateaux. A general volcanic succession for the rhyolitic centres has been outlined by Ewart and Stipp (1968) and includes chronologically:

1. Extensive ignimbrite deposits.
2. First phase of viscous rhyolite lava dome formation (e.g. North Taupo region, Karangahape, Rangitukua).
3. Pumice breccia deposits from localised glowing avalanche deposits.
4. Second phase of rhyolite domes and flows, usually occurring within the central parts of the volcanic centres (e.g. the domes around the southern end of Lake Taupo.
5. Violent eruptions of rhyolitic tephra, which blanketed much of the central and southern North Island.

The stratigraphy and chronology of Late Quaternary volcanic ashes in the Central North Island are fully described by Healy *et al.* (1964), and their distribution is presented in a series of isopach maps by Pullar and Birrell (1973).

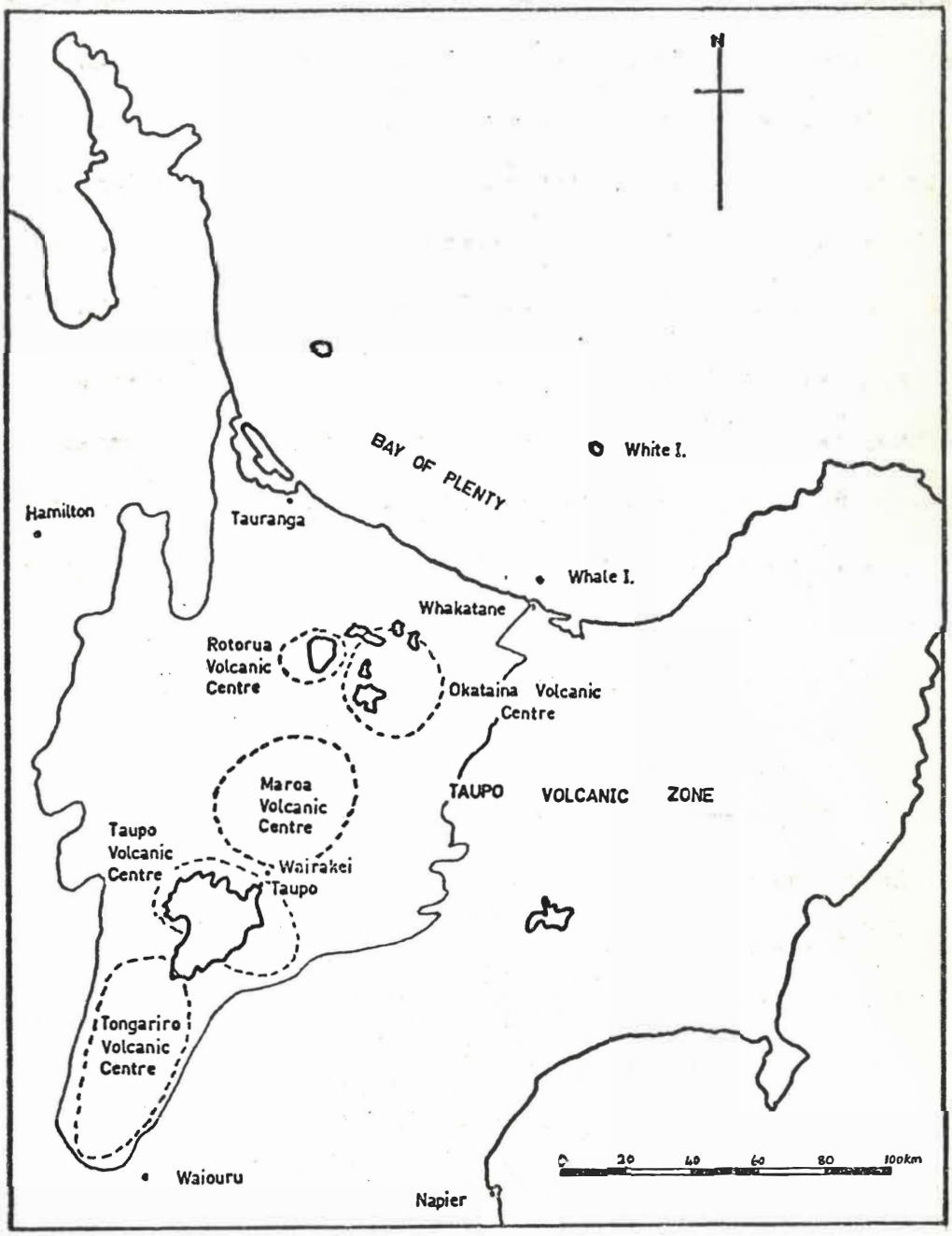


Fig. 2.16. Location of the Tongariro, Taupo, Maroa, Rotorua and Okataina Volcanic Centres within the Taupo Volcanic Zone in the North Island of New Zealand.

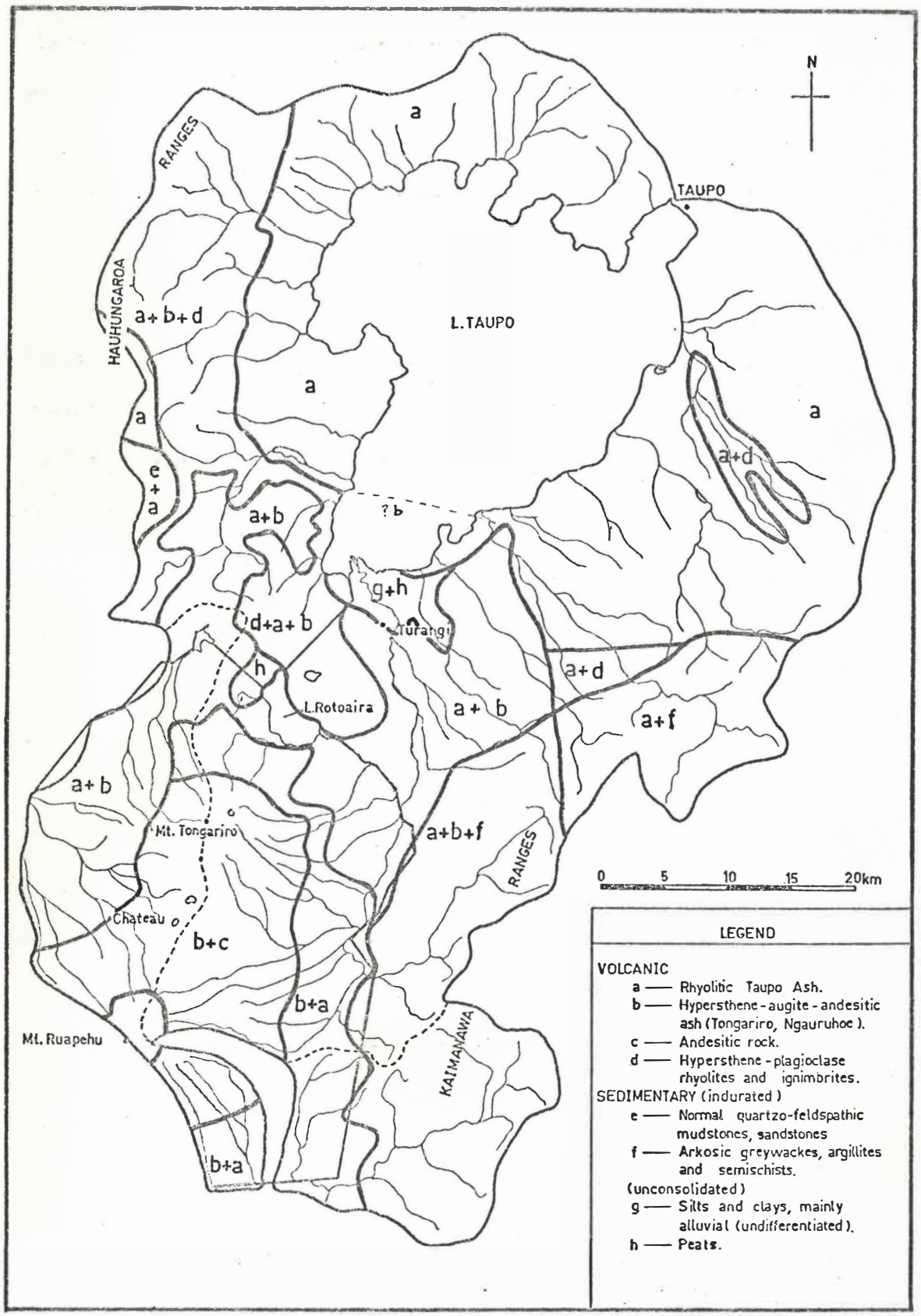


Fig. 2.17. Parent rock of Taupo catchment soils (based on New Zealand Soil Bureau, 1973).

Although all the rhyolites of the Taupo Centre may be correlated mineralogically and are treated as one group, they tend to become more basic towards the southern end of Lake Taupo (lower quartz content, absence of biotite, higher overall hypersthene percentages, and augite in some; Ewart, 1968).

As a result of the loss of these vast quantities of magma, warping, faulting, collapse and subsidence has occurred, creating the depression now occupied by Lake Taupo. Wells drilled at the Wairakei geothermal field (Fig. 2.16) show alternating lake sediments and volcanic rocks to a depth of more than 2000 m, indicative of subsidence over a long period. Subsidence is still occurring (Ward, 1922) and the volcanoes of the Tongariro Volcanic Centre are still active.

2.4 SOILS

Catchment soils are almost entirely derived from volcanic materials (Fig. 2.17; Gibbs *et al.* 1968). The two main soil types are yellow-brown pumice soils and central recent soils from volcanic ash (Fig. 2.18). A small area of central yellow-brown earth and central yellow-brown loam occurs against the western catchment boundary, and a small area of recent soils from alluvium occurs at the southern end of Lake Taupo. The volcanic parent materials largely determine soil properties and so influence the erosion rates and derived sediment properties.

Yellow-brown pumice soils

Yellow-brown pumice soils are the most extensive within the catchment and are partly or wholly formed on Taupo Ash. "- the soil-forming deposits consist of silty ash over sandy ash over gravelly sand

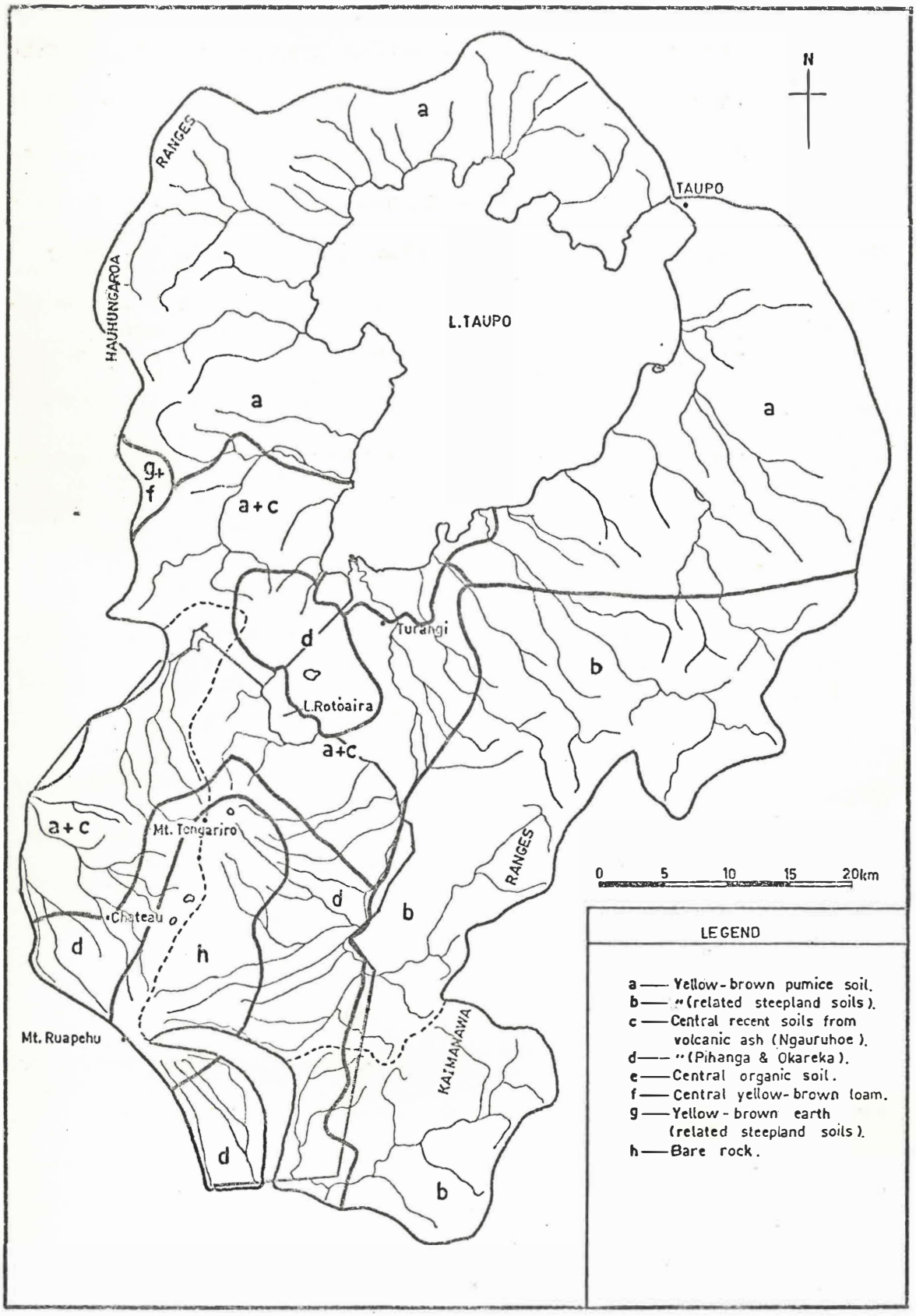


Fig. 2.18, Lake Taupo catchment soils (based on New Zealand Soil Bureau, 1962).

or gravel. Around Lake Taupo - the surface layer is a sand; -" (Gibbs *et al.* 1968, p.50). They are coarse textured, friable, porous and weakly weathered, containing vesicular pumice fragments throughout the profile. The clay content (5-15%) is dominated by allophane together with some amorphous hydrous iron and aluminium oxides and silicates (Fieldes, 1968). The allophane forms a stable mineral-organic complex with humic material which inhibits the decomposition of organic matter, particularly in the topsoil (Fieldes, 1955). Yellow-brown pumice soils may be influenced by subordinate amounts of greywacke, Ngauruhoe Ash, and andesitic Mangatawai Ash (Fig. 2.17; Pullar *et al.* 1973).

Central Recent Soils from Volcanic Ash

Within the catchment these soils are derived wholly or predominantly from andesitic ash erupted intermittently from Mt Ngauruhoe and Mt Ruapehu since the 131 A.D. Taupo Pumice eruptions. The soils are friable and have a high organic matter content in the subsoil due to gradual burial of topsoils by successive eruptions, 60 of which have occurred in the last 100 years. The clay fraction composition is similar to that of yellow-brown pumice soils.

Recent Soils from Alluvium

These soils are derived from undifferentiated alluvium eroded from inland catchment areas. They occur in drainage valley bottoms at the southern end of Lake Taupo, where they mark an area of Holocene sediment accumulation that has partly infilled the lake. Close to the lake shore these soils become more peaty, water-logged and swampy.

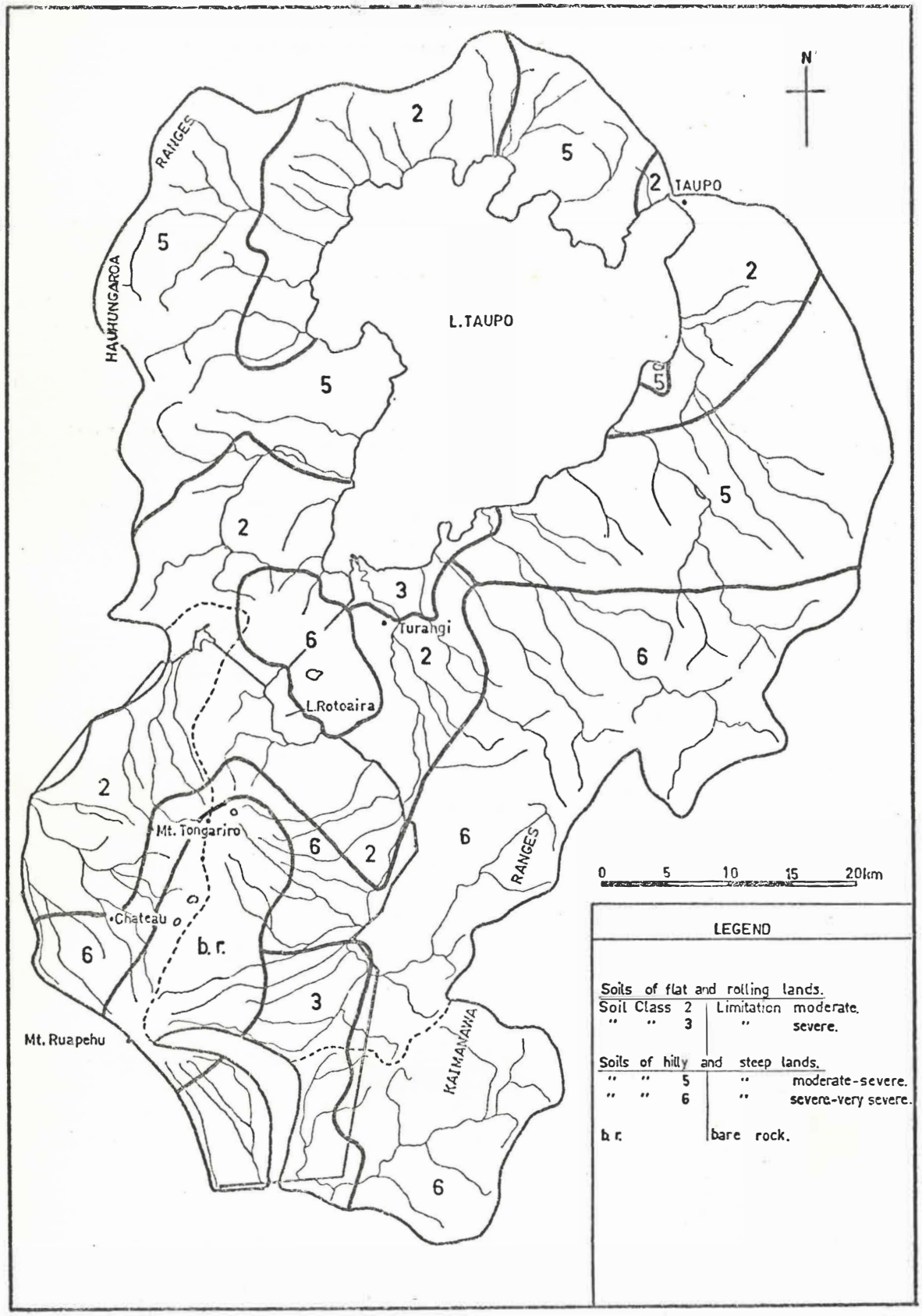


Fig. 2.19. Soil classes for potential pastoral use in Lake Taupo catchment (based on New Zealand Soil Bureau, 1964).

The soil classes for potential pastoral use and present catchment land use are given in Figs. 2.19 and 2.20 respectively.

2.5 VEGETATION

A detailed description of the catchment vegetation is given by Toohill and Fletcher (1971), and is summarised in Fig. 2.20. Vegetation remains largely in a pre-European state over much of the catchment, as indigenous forests, National Park and scrublands. Four geographic areas are characterised on the basis of vegetation.

1. Taupo Lowlands

Most land development has occurred on the flats of the Taupo Lowlands, much of which is now pasture grassland, particularly to the north and west of the lake, or exotic forest. Scrub cover (manuka, *Dracophyllum subulatum*, silver tussock, fern and tutu) remains on the steeper slopes of the lowlands, particularly to the east of the lake. Some podocarp regeneration is occurring amongst the scrub cover. On the less fertile, water-sorted gravelly pumice soils *Dracophyllum subulatum* and red tussock become dominant. A large area of swamp vegetation occurs around the Tongariro Delta.

2. Kaimanawa Ranges

In the northern Kaimanawas the forest is dominated by red and silver beech. Undergrowth is sparse due to deer browsing. Along the northwest margin and extending towards Lake Taupo beech is replaced by podocarp species (matai, rimu, miro, Hall's totara). Below the timberline, fern dominates the ridges, and manuka the flatter ground. Above the timber line danthonia tussock lands occur with associated sub-alpine herbs and shrubs.

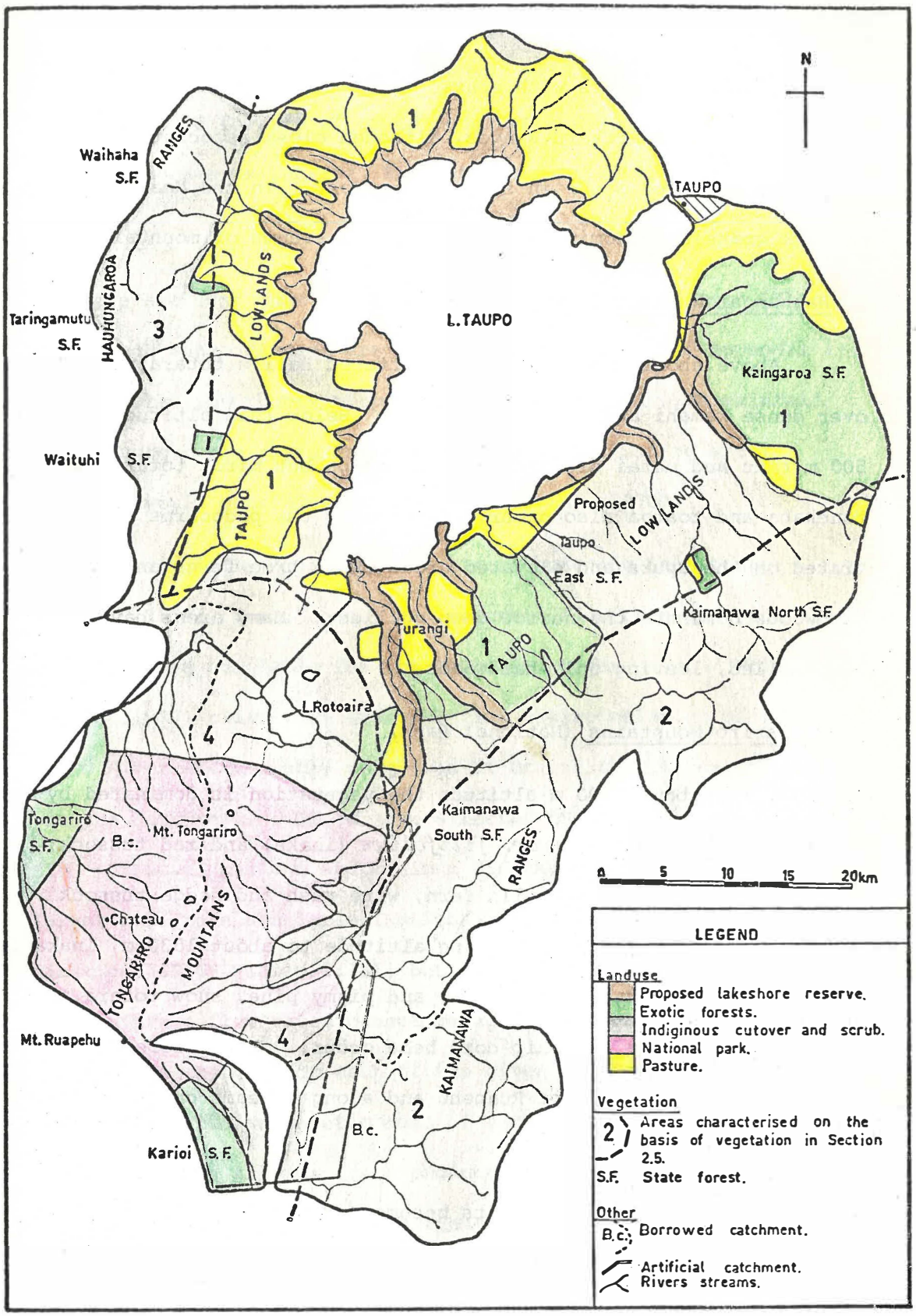


Fig. 2.20. Taupo catchment landuse (after W.V.A., 1973) and areas characterised on the basis of vegetation (after Toohill, and Fletcher, 1971).

Extensive screes with sparse vegetation are characteristic of the Middle and Umuarikaru Ranges, although close associations of snow grass and scabweed occur in sheltered areas. In the Moawhango Basin tussock grasslands dominate with localised stands of mountain beech.

3. Hauhungaroa Range

Above about 900 m altitude scattered Hall's totara are emergent over dense kamahi and scrub hardwoods. Below this altitude to about 500 m rimu and matai are the main podocarps but miro, totara, kahikatea, tanekaha and toatoa also occur. Generally the podocarps are concentrated on the spurs and elevated areas while tree ferns and scrub hardwoods dominate the narrow deep gullies. Many areas have, however, been milled, leaving only hardwoods.

4. Tongariro Mountains (National Park)

Below about 1200 m altitude the vegetation is dominated by *Dracophyllum longofolium var. filifolium* (inaka) and red tussock; in boggy areas, however, umbrella fern, wire rush and sedge tussock become dominant. With increasing altitude to about 1530 m, inaka is replaced by *Dracophyllum recurvum*, and pigmy pine, snow totara, mountain gaultheria and whip cord hebe occur. Beech forests occur on the southwest slopes of Ruapehu and along streams on the eastern slopes of Tongariro.

Above about 1370 m plants become more scattered with increasing altitude. Native forest and scrub give way to tussock grassland which in turn passes into gravel fields and bare rock.

Further north, fern and broom cover extensive areas around Lake Rotoaira, and forests of mixed podocarp emergent over hardwoods occur on the mountains Kuharua, Kakaramea and Pihanga.

2.6 HYDROLOGY

There are more than 60 streams and rivers flowing into Lake Taupo although many of these are ephemeral (Fig. 2.21 and Appendix 1). The high natural absorbancy of pumice soils, combined with rainfall spread throughout the year, has resulted in fewer running water courses than would otherwise be expected (Burton, 1970).

There is little flow data for rivers entering Lake Taupo (R. Pittams, 1978; pers. comm.) and accurate flow-rate and seasonal distributions are available for the Tongariro River only. White and Downes (1977) claim that seasonal flow characteristics of the Tongariro River are probably unique as it drains the highest rainfall area in the catchment. It is also affected by delayed snow-melt runoff. Observed maximum and minimum discharge figures for some of the larger rivers are available (National Water and Soil Conservation Organisation, 1976; Table 2.1a), but flow-rate frequency figures are not, thus average flow rates cannot be accurately calculated. Order of magnitude discharges for each of the given rivers have been calculated using the arithmetic mean of each discharge range (Table 2.1b). The river discharge figures are a product of a sub-catchment area (Fig. 2.21) and its specific discharge (Fig. 2.22). Specific discharge figures reflect rainfall characteristics, catchment steepness, the nature of the regolith and vegetation. The highest specific-discharge

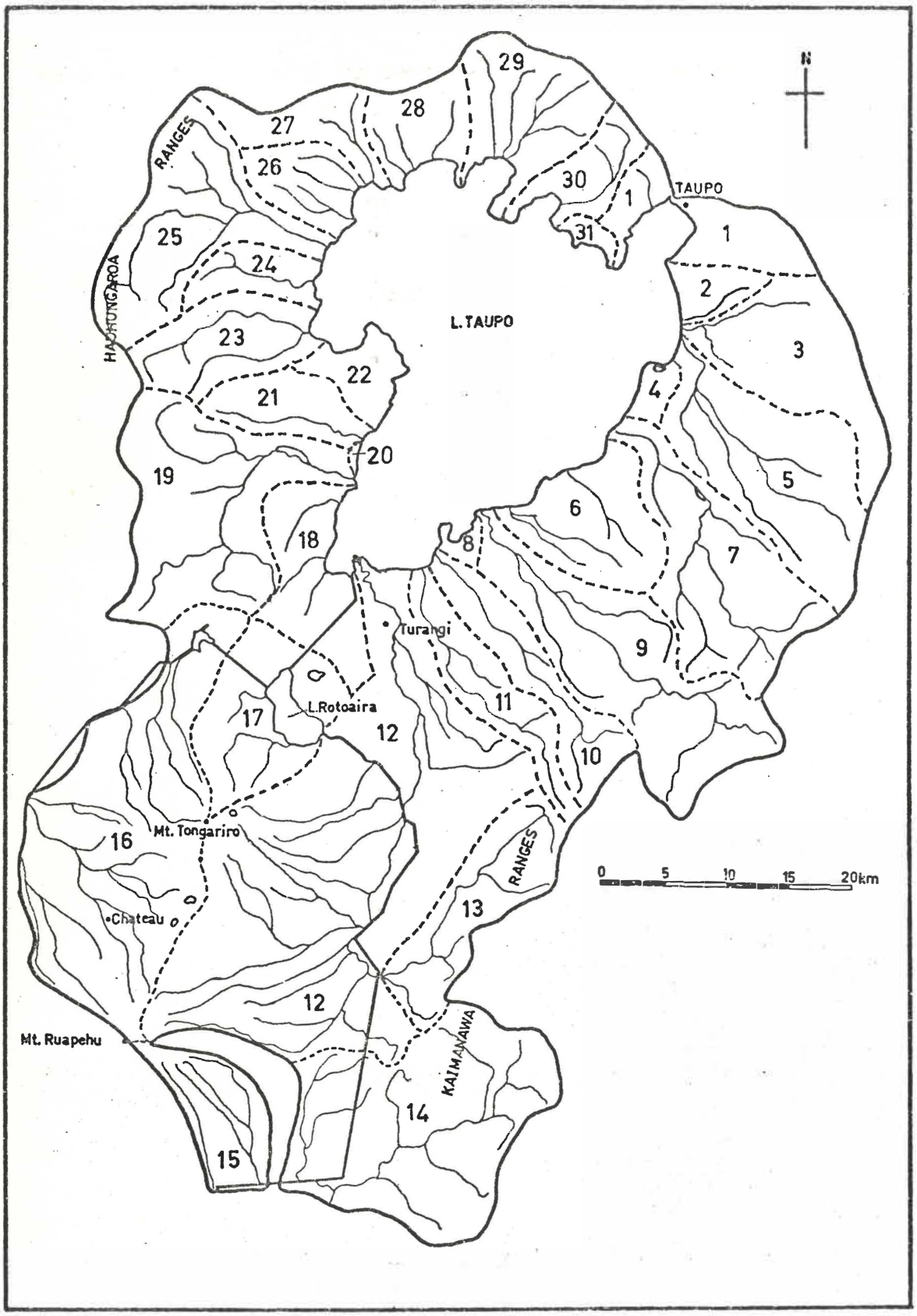


Fig. 2.21. Sub-catchments within Lake Taupo catchment.

N.B. 1. See Appendix 1 for stream names and sub-catchment areas.
2. Sub-catchments 13 and 17 drain into sub-catchment 12 and then into Lake Taupo
Runoff from sub-catchment 14, 15 and 16 will be diverted into Lake Taupo as a result of the Tongariro Power Scheme.

Table 2.1. (A) Ranges of observed river and stream discharges into Lake Taupo (based on National Water and Soil Conservation Organisation, 1976), and (B) approximate mean discharge percentages based on (A).

A.		River, stream	Discharge (l/sec)	B. Mean discharge (% of total)
1.	Mainly unmodified catchments			
		Waihaha	3000-11000	4
		Waimarino	800-5000	4
		Tokaanu	1000-2000	1
		Tailrace (Tokaanu)	31,000-112,000 (controlled)	43
		Tongariro	28,000-60,000	27
2.	Catchments partly modified by forestry			
		Hinemaiaia	5000-10,000	5
		Tauranga-Taupo	4000-16,000	6
		Waitahanui	6000-8000	4
		Mangamatu	± 2000	1
		Whanganui	700-2000	1
3.	Catchment mainly modified by agriculture			
		Kuratau	2800-10,000	4
		Whareroa	900-2000	
		Otahetahe	40-100	- (0.04)
		Omori	300-700	- (0.3)

N.B. (1) Mean discharge figures are means of the given discharge ranges, not necessarily real average flow rates.

(2) The frequency distribution of various flows within each range is not known.

(3) Mean discharge percentages have been calculated assuming 100% from only the above inflows.

(4) The outflowing Waikato River has an average flow of about 129,000 l/sec (White and Downes, 1977).

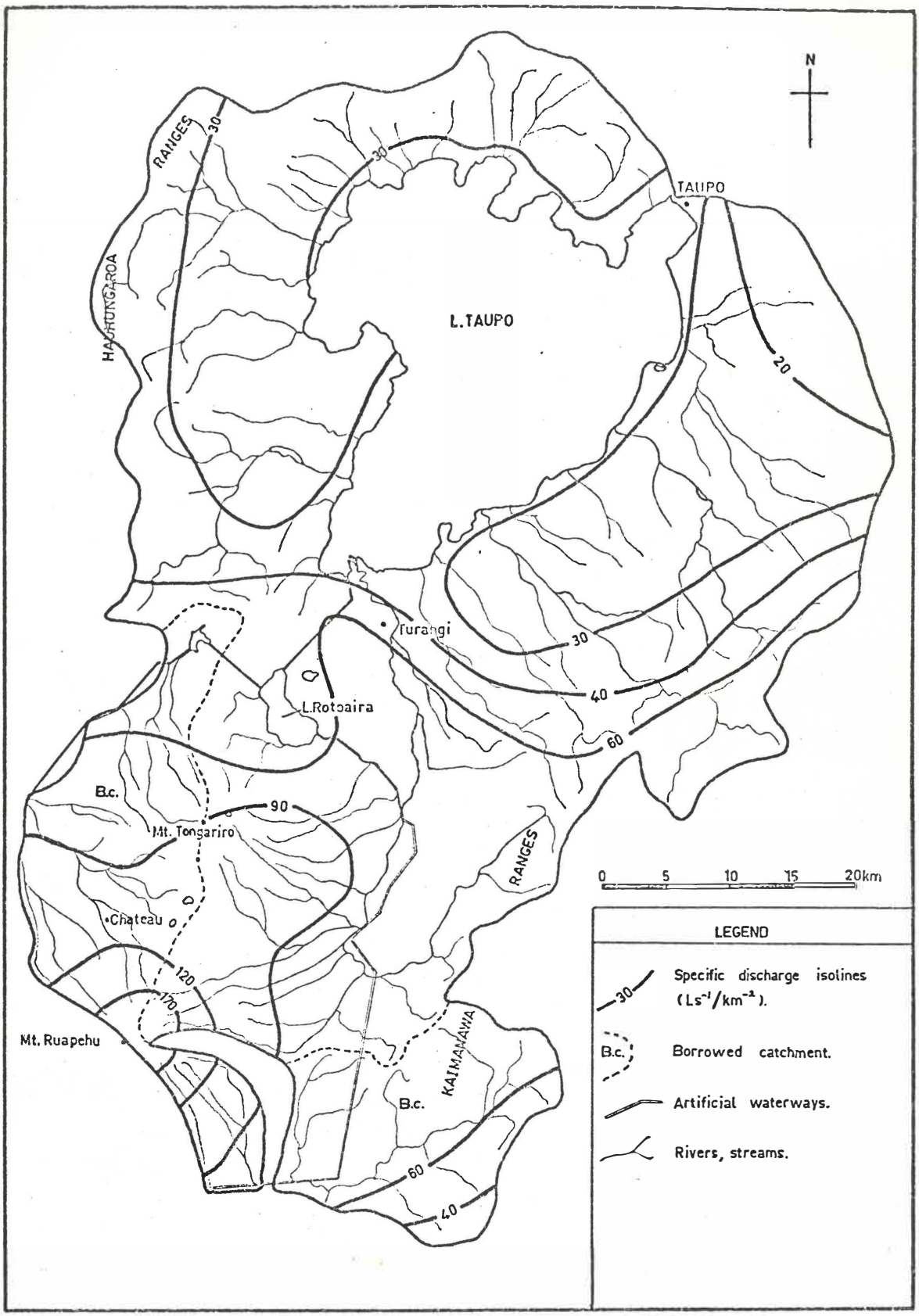


Fig. 2.22. Specific discharge (Ls^{-1}/km^{-2}) of surface water from Lake Taupo catchment (after Lands and Survey, 1975b).

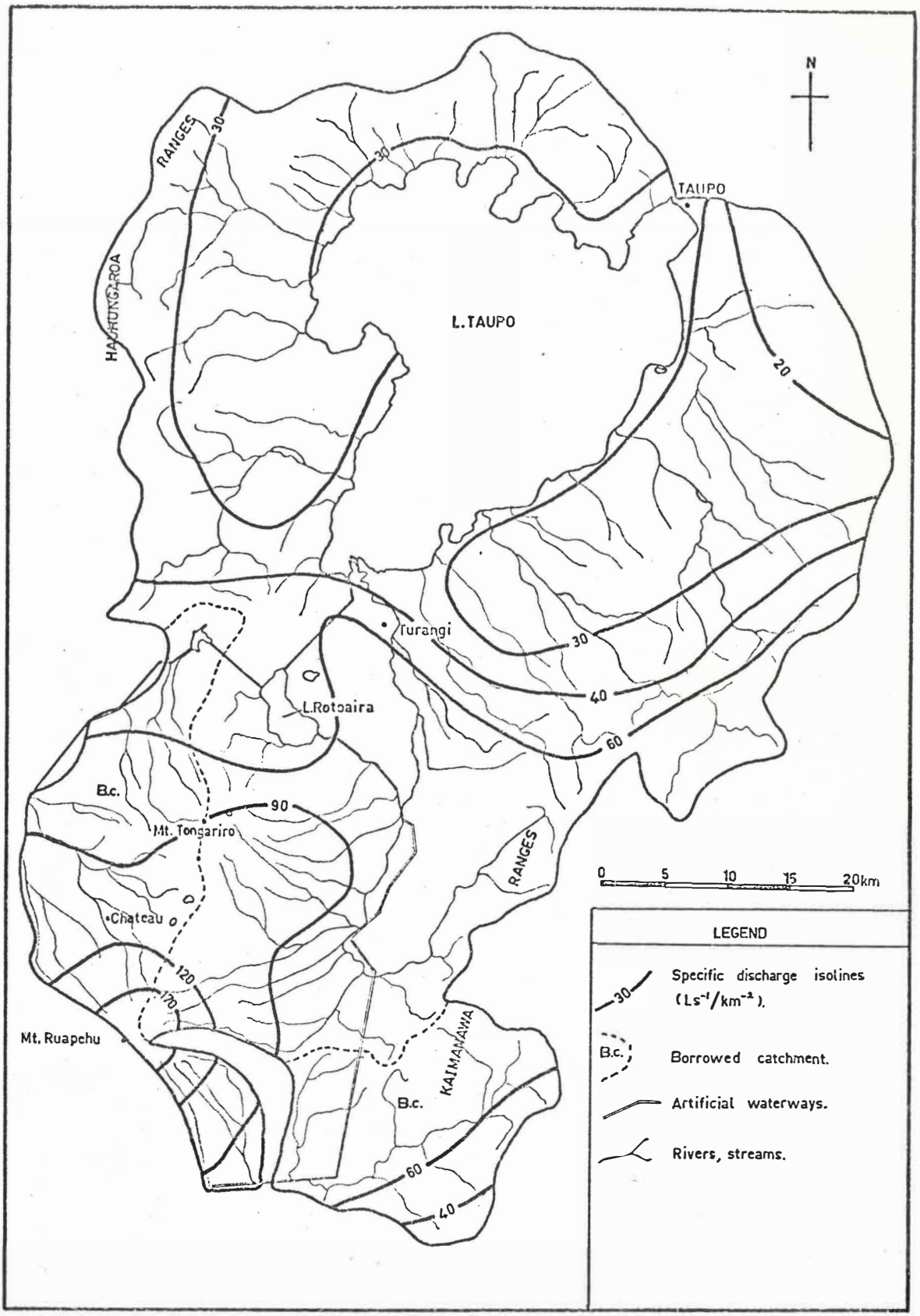


Fig. 2.22. Specific discharge (Ls^{-1}/km^{-2}) of surface water from Lake Taupo catchment (after Lands and Survey, 1975b).

figures occur at the southern end of the catchment where the highest rainfalls, mountainous terrain and poor vegetation cover or bare rock occur.

Tephra deposits, softer ignimbrites and coarse pumice breccias are both porous and permeable. Welded ignimbrites have little porosity but a high mass permeability due to numerous joints. The rhyolites and greywackes are less permeable and rivers flowing from the Kaimanawa Ranges are liable to violent flooding, particularly from short duration, high intensity storms.

A comparison of the average runoff figures from stations at Chateau Tongariro and Taupo indicate broadly similar trends with time, although the autumn runoff at Chateau Tongariro begins to increase a month earlier than at Taupo, and a runoff peak occurs at Tongariro during October, probably as a result of melting snow (Fig. 2.23) . The average annual runoff at Tongariro is about four times greater than that at Taupo.

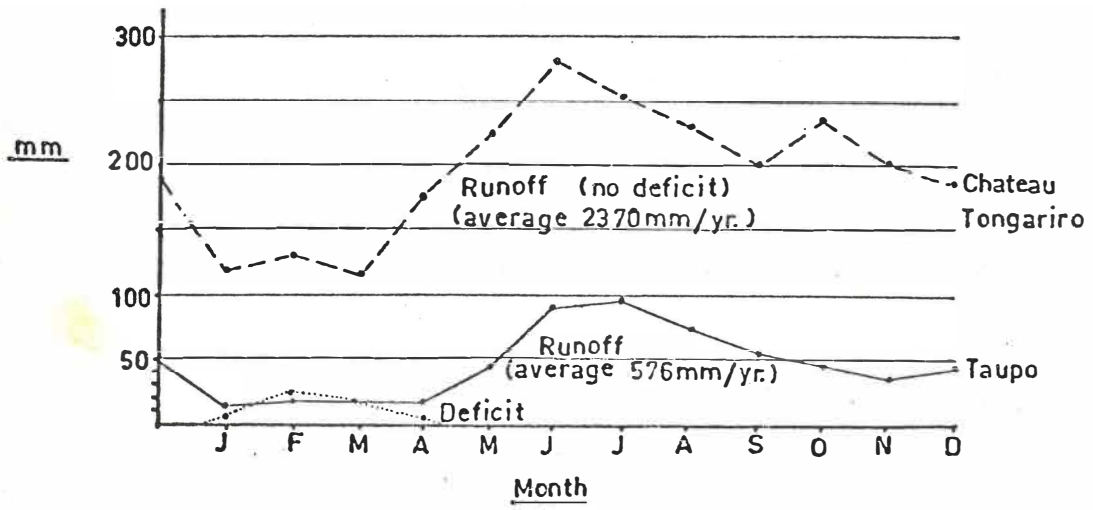


Fig. 2.23. Estimated average water balance for Taupo (1950-1970) and Chateau Tongariro (1940-1970; based on New Zealand Meteorological Service (1973).

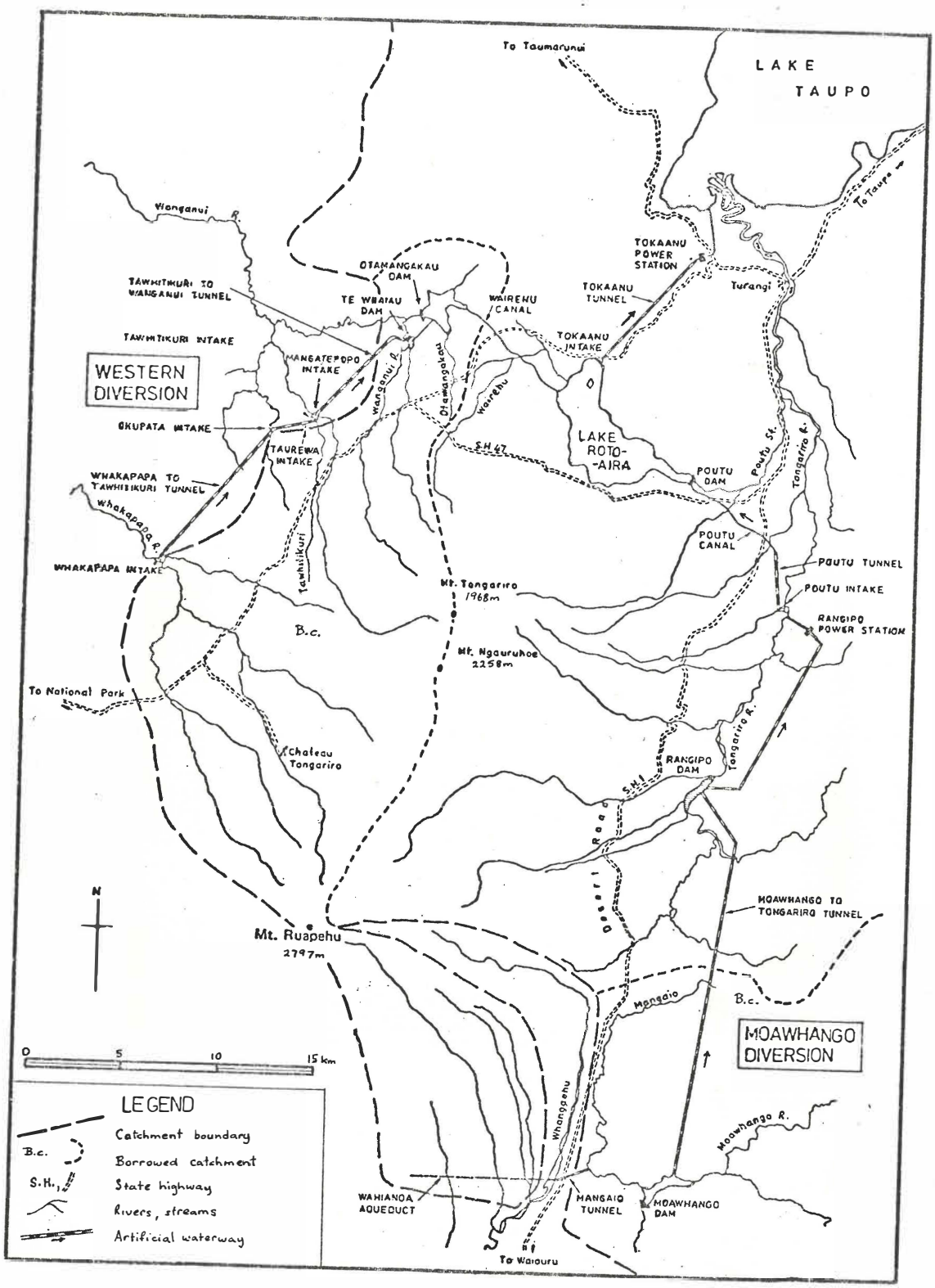


Fig. 2.24. The Tongariro hydro-electricity scheme, showing the diversions of borrowed-catchment runoff through Lake Rotoaira into Lake Taupo.

The magnitude of groundwater movement towards Lake Taupo is unknown. White and Downes (1977) have arbitrarily estimated groundwater flow directly entering the lake as one percent of the total land drainage.

Borrowed Catchment

The Tongariro hydro-electricity scheme to the south of Lake Taupo diverts the runoff from more than 2500 sq. km of land into Lake Taupo, and will eventually increase the lake outflow by about 27%. The development involves a series of intakes, tunnels and dams (Fig. 2.24). The Western Diversion has been in operation since 1972, and diverts a mean flow of 20 cumecs from the Wanganui River catchment on the western flanks of the National Park volcanoes, into Lake Rotoaira. The Moawhango Diversion will intercept a mean flow of 13.6 cumecs from the tributaries of the Rangitikei River which drain the southeastern side of Mt Ruapehu and the southwestern end of the Kaimanawa Ranges, and divert it into the Tongariro River. Further down the Tongariro River some flow is diverted into Lake Rotoaira at the Poutu Intake during peak discharges. Water from Lake Rotoaira eventually discharges into Lake Taupo via the Tokaanu tunnel, power station and tailrace. The tailrace maximum and minimum discharge figures are given in Table 2.1.

2.7 CATCHMENT EROSION

A map of Lake Taupo catchment erosion is included in the map pocket of this thesis (Map 2).

Erosion of soil and cover deposits is the first stage in sediment transport to Lake Taupo. The potential and actual erosion problems concerning both the lake and catchment have been primarily responsible for the proposed land-use and conservation measures adopted for catchment management under the Lake Taupo Catchment Control Scheme (W.V.A., 1973).

Immediately after deposition of the Taupo Ash (131 A.D.) widespread erosion of pumice occurred in the lower catchment areas and deep gullies were excavated that remain today as dry gullies (Healy, 1967). Huge amounts of pumice were washed into Lake Taupo. Eventually the unchoking of drainage channels and the return of vegetation reduced erosion rates. In higher country the mantle of Taupo Ash was protected by forests that largely survived the eruption.

Today erosion is not a serious problem (Map 2, map pocket) but potential erosion risks are high, the critical factors being the type and extent of vegetation, slope steepness, and the intensity and duration of rainfall. These factors are reflected in the classification for potential pastoral use (Fig. 2.19). On topographic highs, Taupo Ash tends to be finer textured and more compact, thereby preventing excessive runoff and erosion. Although in gullies and valley bottoms pumice material is coarser (Healy, 1967), it is also deeper, which gives soils a free drainage similar to that of uplands and hillslopes (Vucetich, 1960).

Low bulk density, poor particle cohesion, and the positive buoyancy of dry pumice particles make rhyolitic ash deposits susceptible to erosion by running water. Soil porosity reduction and the consequent increase in surface runoff result from conversion of scrub to pasture, stock trampling and camping, and track formation (Healy, 1967; Selby, 1967, 1973). Concentrated flow may initiate small scours which rapidly increase in size by lateral and/or headward erosion. Healy (1967) found that the Taupo Lapilli member is particularly prone to erosion of this type. Gully depths rapidly increase until underlying, more compact ash deposits or ignimbrite are reached. Such rill, sheet and gully erosion is common in the Hauhungaroa and northwest Kaimanawa Ranges as a result of logging tracks in pumice (W.V.A., 1973). Erosion of pumice becomes very severe when land development leads to the reactivation of dry gullies, and at present, gullies up to 12 m deep on some farms are causing serious concern.

Along stream and lake edges, native bush root structure is insufficiently fibrous to prevent serious slipping and erosion where runoff from adjacent farmland is extensive (Burton, 1970; Selby, 1974). Such slips have occurred in the Waimarino, Waiotaka and Lower Tauranga-Taupo catchments where vegetation has been severely depleted (W.V.A., 1973). Bank erosion occurs in most places where streams are entrenched in ignimbrite gorges.

Where hard rock is close to the surface the erosion risk is low, unless the rock is breccia where terracette creep, sheet and rill erosion may occur. Steep breccia faces are also liable to slip erosion and this is occurring on lake-shore cliff faces to the north of Hatepe (Fig. 2.25).

Where ignimbrite is close to the surface, the land is particularly stable because of the characteristic low, flat relief and the high mass permeability due to numerous joints (e.g. north-western catchment; Map 2, map pocket). Rhyolite is generally less permeable.

In the southern catchment Ngauruhoe Ash is liable to all types of erosion because of the higher altitude, heavy rainfall, wind exposure, frost action, and the existence of underlying, greasy, weathered Tongariro ash beds. Lahars have occurred recently in the Whangaehu River.

At high altitudes and where cover deposits have been removed, bare shattered rock suffers physical weathering. Debris avalanches occur on greywacke and schist, and extensive rock-fragment pavements, which scree creep, occur on argillite (W.V.A. 1973). This type of material is being carried from the Kaimanawa Ranges to Lake Taupo by the larger streams and rivers.

Recent erosional events affecting Lake Taupo that have been documented (W.V.A., 1973) include:

1. In 1971 a flash flood occurred in the Otakitaki catchment, which drains 2,550 ha., most of which has been developed by the

Lands Department. Extensive erosion damage occurred downstream in the scenic reserve area and a large debris deposit appeared in Lake Taupo offshore from the stream mouth.

2. Development and drainage of the Ruku Development block, (930 ha. of mainly peat), by the Lands Department led to downstream flooding and erosion problems.

3. Inland road building activities has resulted in a large silt load being deposited in Lake Taupo under the Waikino Falls. A sandbank now occupies water which was originally 4.5 m deep.

4. Flooding of 400 ha. of farmland and much of the residential area on the alluvial fan of the Tauranga-Taupo River occurred during the major flood events of February 1958 and March 1964. Proposed control works were designed to pass all flood water directly to the lake.

5. The Waimarino and Waiotaka Rivers have had similar flood characteristics to the Tauranga-Taupo River.

Flood control works that prevent sediment deposition on the natural flood plains must have inevitably increased the amount of sediment reaching Lake Taupo.

Wind may also transport eroded material to Lake Taupo. Mathews (1972) has calculated that an average of at least 3.8 tonnes of topsoil/ha./year are removed from cultivated land in New Zealand by wind. This is probably not a net loss as redeposition must occur, but his calculation suggests a massive movement of nutrients as the highest levels of fertility normally occur in the top few centimetres of soil. Cultivated or exposed yellow-brown pumice

soils are undoubtedly more susceptible to wind movement than other soils which have a higher bulk density and greater particle cohesion. Large areas of bare soil occur within the catchment at times as a result of drought, over-grazing, scrub removal, forest felling and fire.

Undoubtedly much of the material eroded within the catchment is not transported directly to Lake Taupo but is deposited within catchment "sub-traps", particularly in the southern part of the Basin where erosion is most severe.



Fig. 2.25. Erosion of pumice breccia cliffs to the north of Hatepe (right). Material slumps on to the beach, then is removed by wave action and northward longshore currents.

CHAPTER 3

MORPHOMETRY, HYDRODYNAMICS, AND AQUATIC FLORA OF LAKE TAUPO

3.1 MORPHOMETRY

Morphometric data for Lake Taupo are summarised in Table 3.1. A bathymetric map of the lake is included in the map pocket of this thesis (Map. 3), and three bathymetric cross-sections are given in Fig. 3.2a, b and c.

Terminology for lacustrine environments is based on bottom gradients, depth, and relationship to the lake shore (Fig. 3.1).

Approximately one third of the area of Lake Taupo is contained within the 120 m isobath at the northern end of the lake. Within this area deeper parts occur in the Whangamata (145-150 m) and Waitahanui (155-160 m) Basins (Fig. 3.2a). More than half the remaining area occurs as level or gently sloping plains between 100 and 120 m depth (Map 3, map pocket). Towards the eastern shore the bottom gradient progressively increases on the rise to about 15° near the foot of the slope (40-70 m). An angle of about 20-25° is maintained up the slope to the shelf-break at 5-10 m water depth after which the shelf gradually shallows shorewards (Fig. 3.2b and c). Towards the western and much of the northern shoreline, particularly where coastal cliffs plunge almost vertically into deep water, slope and shelf features are absent or poorly developed (Fig. 3.2b and c).

In the centre of the lake a considerable area rises above the 100 m isobath, with two topographic highs rising to within 60 m of

Table 3.1 Morphometric Data for Lake Taupo (mainly after Jolly, 1959, 1968; White and Downes, 1977).

Trophic status	Oligotrophic
Thermal classification	warm monomictic
Latitude	38°05' south
Altitude	369 m a.s.l.
Area	616 km^2
Maximum length	40 km
Maximum width	27 km
Maximum depth	164.6 m
Average depth	97.0 m
Volume	59.1 x 10^6 m^3
Direction of major axis	southwest-northeast
Length of shoreline	155 km
Length of shoreline as sand/gravel beaches	87 km
Length of shoreline as cliff/ deep water	68 km
Surface water temperature	21.5-10.6°C
Bottom water temperature	10.8-10.5°C
Lake level range (maximum controlled eater level - mean low water level)	1.4 m

Table 3.2 Estimated average annual water budget for Lake Taupo (White and Downes, 1977)

Outputs	1. Waikato River (Q_o)	4071.1 x 10^6
	2. Lake evaporation (E)	472.8 x 10^6
Inputs	1. Rainfall on lake (R)	723.2 x 10^6
	2. Total land drainage (Q_i)	3820.7 x 10^6

where Q_o = annual average discharge of Waikato River

E = annual average evaporation loss from the lake

R = annual average rainfall on the lake

$Q_i = Q_o + E - R$

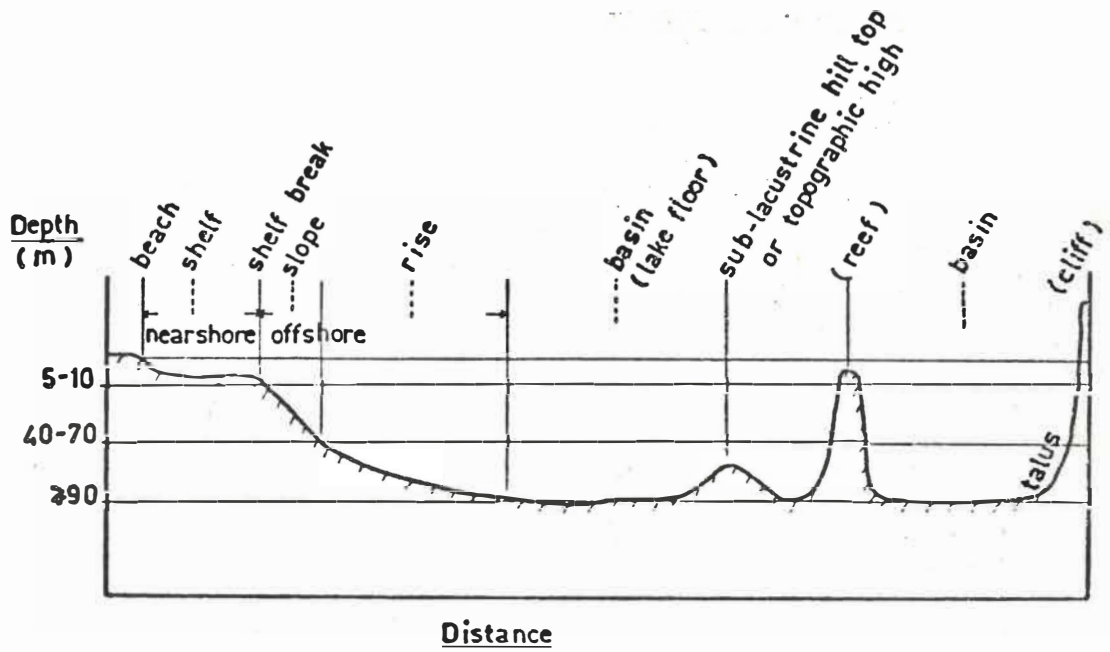
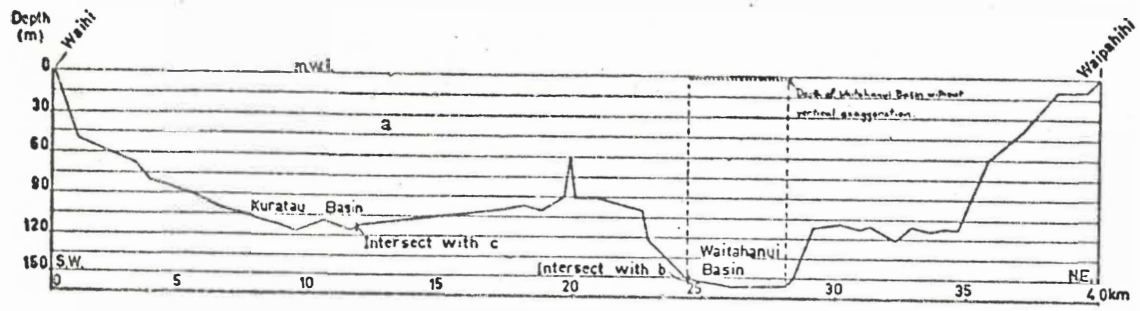
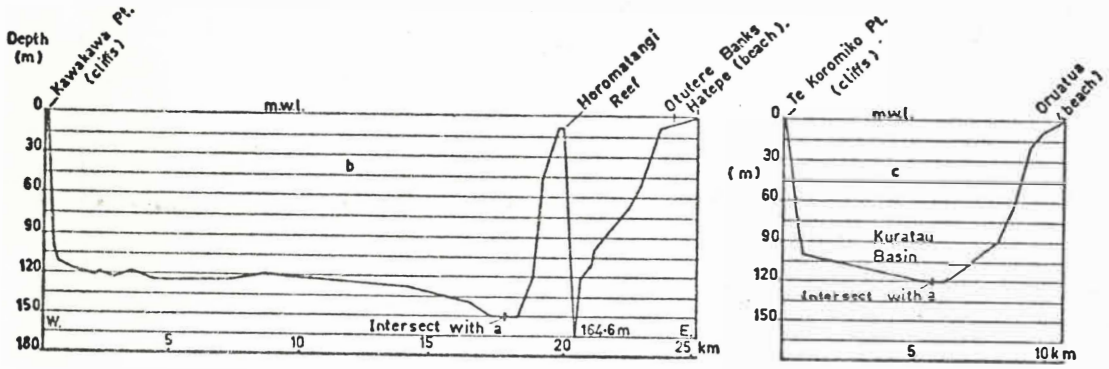


Fig. 3.1. Idealised bathymetric cross-section of a lake from a sandy shore to a cliffed shore. The terminology is based on bottom gradients, depth and relationship to the lakeshore (after Pickrill, 1978).





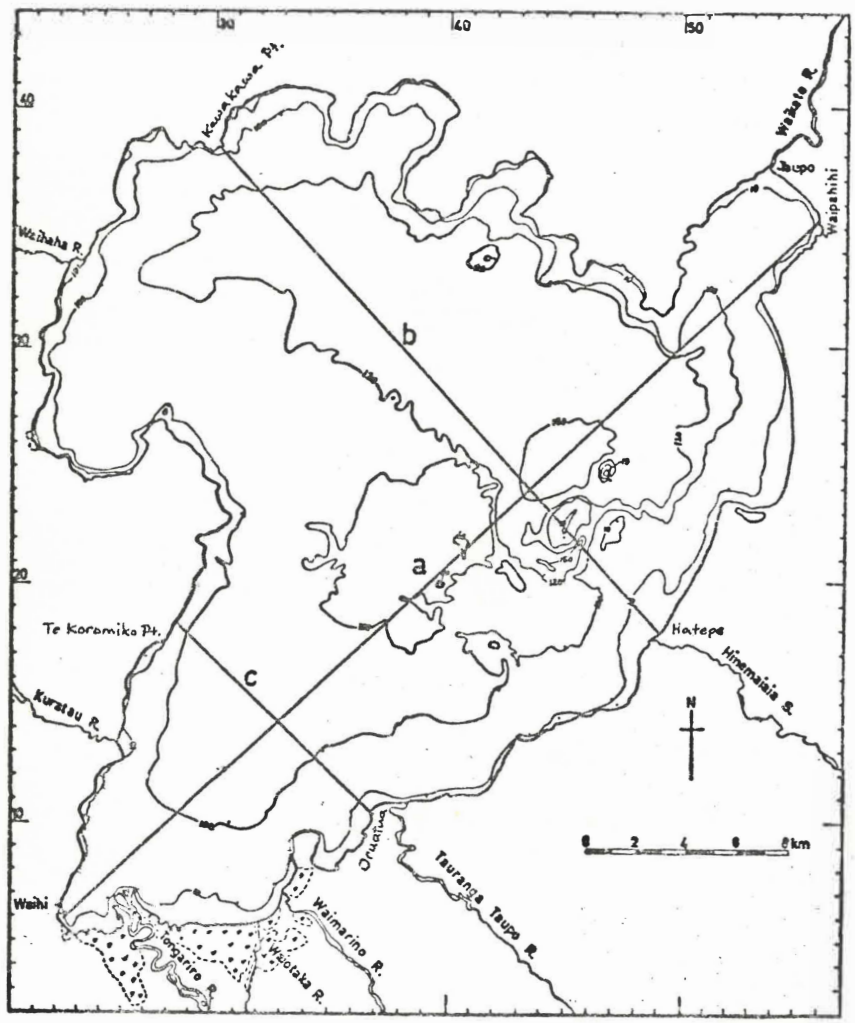


Fig. 3.2. Bathymetric cross-sections of Lake Taupo (Vertical exaggeration 50x).

the surface (Fig. 3.2a; Map 3, map pocket). To the east of this area the lake bed topography becomes very rugged. Motutaiko Island and Waitahanui Bank rise almost vertically for 140 m from the lake floor, and the Horomatangi Reefs (<5 m deep) enclose the deepest part of the lake (164.6 m; Fig. 3.2b).

Lake Taupo is not a very deep lake by New Zealand standards (e.g. Lake Hauroko and Lake Manapouri in the South Island reach depths of 462 m and 444 m respectively) but it has a fairly uniform depth, with only small areas shallower than 90 m, and consequently contains a relatively large volume of water (Table 3.1).

The average annual water budget for Lake Taupo is given in Table 3.2, and the residence time of a water particle in Lake Taupo (i.e. lake volume/average annual outflow + lake evaporation) has been calculated at 13 years (White and Downes, 1977).

3.2 LAKE HYDRODYNAMICS

Thermal structure

Lake Taupo is thermally classified as warm monomictic, that is, it is thermally stratified in summer and not below 4°C in winter (Hutchinson, 1957). When the lake is stratified a warm, almost homogeneous upper layer (epilimnion) is separated from relatively colder bottom water (hypolimnion) by a layer (metalimnion) showing a marked temperature gradient, the thermocline (Fig. 3.3). With the onset of winter heat is lost from the surface waters until the epilimnion temperature reaches that of the hypolimnion (Fig. 3.4), thermal stratification breaks down, the lake becomes homothermous and there is a general mixing of the waters by wind induced currents

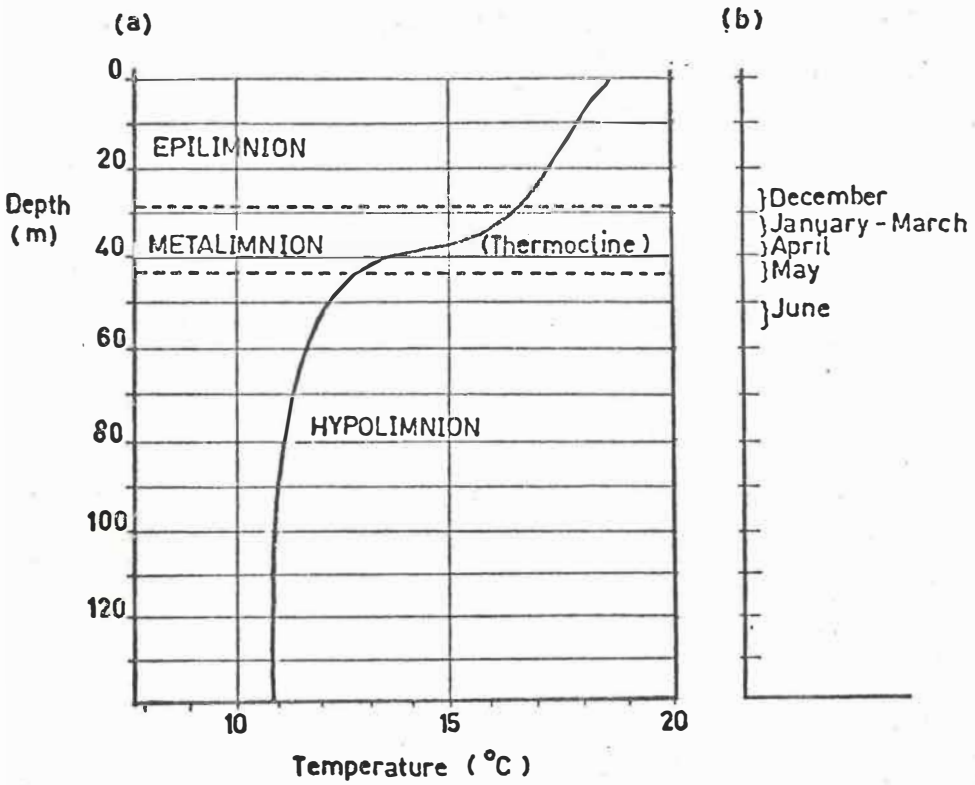


Fig. 3.3 (a) Temperature profile and (b) seasonal depth change of thermocline in Lake Taupo during 1955-56 (Jolly, 1959).

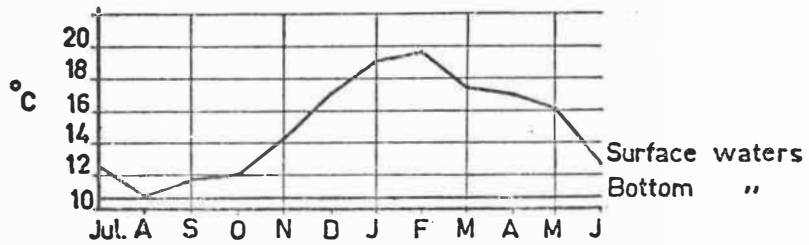


Fig. 3.4. Annual temperature range of surface and bottom waters in Lake Taupo during 1955-56 (Jolly, 1959). Subsequently surface water temperatures as high as 21.5°C have been recorded.

and wave action, inducing overturn. Lake Taupo is thermally stratified for about five months of the year, from December to April, with the epilimnion reaching about 50 m depth just before overturn (Fig. 3.3b).

The thermal structure is influenced by a number of factors including local climate variability, the area, depth and shape of the lake, and its exposure to wind. The main mechanism by which the lake stratifies results from the unstready and non-linear interaction between wind-induced turbulence and the stable buoyancy gradients in the lake due to surface heating (Sundaram and Rehm, 1973). Wind facilitates heat uptake by mixing the surface waters through swell and wave action, thus forcing down the thermocline (Stout, 1973; Jolly and Irwin, 1975). Because of the exponential relationship between wind velocity and wave magnitude, periods of strong winds could be expected to have a greater effect than longer periods of more moderate winds.

Lake Taupo water-level records show that surface seiches may produce 0.2 m water-level changes within 20-30 minutes (R. Pittams, 1978; pers. comm.). Internal seiches at the thermocline boundaries probably occur also. Internal seiches generally have greater amplitudes than surface seiches because of the smaller density difference between cold and warm water compared to that between air and water. They help to increase the depth of the thermocline by displacing hypoliminetic waters to the surface at the down-wind end of a lake, resulting in an increased heat uptake by the cooler water (Green, 1975; Sundaram and Rehm, 1973).

The existence of internal seiches in Lake Taupo would influence the dispersal of suspended sediments as the turbulence produced would help to maintain the suspension, while the rhythmic changes in current

direction, as the metalimnion waters were squeezed in alternate directions, would lead to lateral transport.

Wind effects are enhanced in Lake Taupo because it has a large surface area, it is in an exposed location, and it has its long axis parallel to the prevailing southwesterly winds (Fig. 2.1). The long fetch and deep mixing produce a relatively deep thermocline. Meteorological data (A.I. Tomlinson, 1977 pers.comm.) indicate that the strongest winds generally occur during spring and early summer when the lake is warming.

Lake circulation and inflow currents

No quantitative data on lake-circulation or inflow currents are available for Lake Taupo. However, the magnitude and direction of currents within a lake result from combinations of driving forces that are variable in time and space. Such currents include those that are wind, density, and thermally driven; inflow to outflow drift; geostrophic circulation (i.e. the faster response of shore zones to thermal forcing during spring and autumn); and deflection of flow by the Coriolis force. Wind is overall the most important force. Wind drag on a lake surface creates several types of currents including cyclonic surface flow (Emery and Csandy, 1973; Sundaram and Rehm, 1973; Bennett, 1974), upwelling, downwelling and lateral return flows (Bennett, 1974; Lambert and Lüthi, 1977; Lien and Hoopes, 1978), seiches, and currents associated with wave activity (e.g. longshore drift).

The Waimarino, Tauranga-Taupo, Kuratau, Waihaha Rivers and Hinemaiaia Stream all have spits extending approximately northwards across their mouths, indicating a similar net direction of longshore

drift and wave action in these areas. A shelf lobe to the north of Hatepe also extends northwards, although its proximity to the Horomatangi Reefs and a large bench cut into pumice breccia by higher lake levels suggest that it may not be entirely composed of unconsolidated sediment.

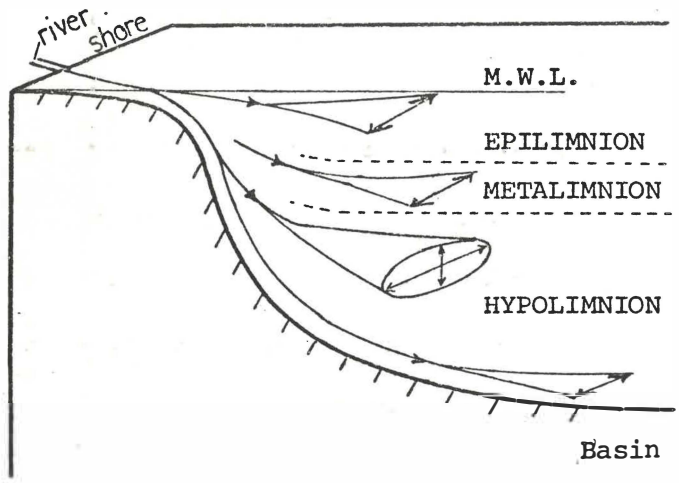
Waiotaka River (Stump Bay) and Whanganui Stream (southern Western Bay) have southward pointing spits at their mouths, probably because they are sheltered from the effects of prevailing southwesterly winds and exposed to longshore drift induced by winds from other quarters.

The directions of circulation currents in the deeper parts of Lake Taupo may be revealed by pattern of sediment deposition.

Inflow currents are the intra-lake extensions of streams and rivers discharging into a lake. In Lake Taupo the largest inflows occur around the southern end (Table 2.1) and the only outflow (Waikato River) is in the northeastern corner of the lake. The relative densities of stream and lake water, which determine the passage of inflowing water once it has entered the lake, are a function of water temperature and suspended matter content. Several variants of continuous density currents may occur (Fig. 3.5; Bates, 1953; Bates and Freeman, 1953), thus the type of inflow can be expected to have a strong influence on sediment transport and dispersal within a lake.

Flood discharges continuing as turbidity underflows have been detected in Lake Meade, U.S.A. (Grover and Howard, 1938), Lakes Thun and Walensee, Switzerland (Lambert and Lüthi, 1977), and have been artificially generated in Lake Superior, Canada/U.S.A. (Normark and Dickson, 1976).

(a) Stratified lake



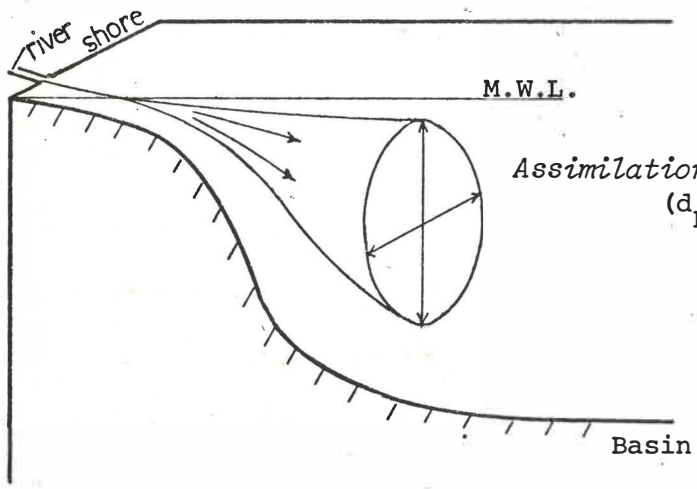
Surface flow, plane jet, 2D mixing ($d_R < d_E < d_M < d_H$)

Interflow, plane jet, 2D mixing ($d_E < d_R \simeq d_M < d_H$)

axial jet 3D mixing ($d_E < d_M < d_R \simeq d_H$)

Bottom flow, plane jet 2D mixing ($d_E < d_M < d_H < d_R$)

(b) Homothermous lake



Assimilation, axial jet 3D mixing ($d_R = d_L$)

where: d = Water density
R = River
E = Epilimnion
M = Metalimnion
H = Hypolimnion
L = Lake
D = Dimensions

Fig. 3.5. Idealised bathymetric cross-section of a lake nearshore-offshore region showing types of continuous density currents that may arise from river inflow (based on Bates, 1953; Bates and Freeman, 1953).

The exact hydrodynamics of interflow and underflow and their effects on the surrounding lake waters are not fully understood. Recent work in Switzerland by Lambert and Lüthi (1977) suggests that natural underflows are highly turbulent with a maximum velocity near the upper interface. A layer of overlying water with a thickness approximately equal to that of the underflow is dragged along, with a reverse flow above it. When interflow occurs the maximum return velocity occurs below it in the denser part of the lake basin.

When turbid flows disappear abruptly within a short distance of the shore, underflow or interflow is occurring. This type of situation was observed in Lake Taupo near the mouth of the Tongariro River during April 1978. Flow in the Tongariro River had increased as a result of heavy rain. The river water was noticeably discoloured and had a temperature of 11.8°C. At the mouth the river flowed about 40 m into the lake before disappearing abruptly beneath surface lake waters having a temperature of 17.6°C (Fig. 3.6). Calculated water densities based on temperature alone suggest that interflow in the region of the thermocline was probably occurring, as lake bottom-water temperatures remain at 10.4-10.6°C all year (Jolly, 1959). A layer of water containing suspended silt-sized material was observed at a depth of 25-30 m off the Kuratau delta in Lake Taupo by A. Devcich (1978, pers. comm.) while scuba diving on a zoology research trip during March, 1978. The water temperature was 19.7°C above the layer and 15.1°C below it. The layer was very distinct and swirled as he descended through it. There are also hearsay reports of scuba divers in Lake Taupo who, believing they have reached the lake bed, become alarmed to find themselves only sinking through a layer of discoloured water.



Fig. 3.6. Turbid water flowing from the Tongariro River (blind mouth) during April, 1978. At the shelf edge the turbid flow (11.8°C) disappears below the warmer 17.6°C surface waters of Lake Taupo.

If lake outflow and surface waters are clear at times of turbid inflow, it is reasonable to assume that a pool or layer of turbid water has formed at some depth in the lake from which particulate matter will gradually settle and that the outflow is being fed only by the epilimnion.

3.3 AQUATIC FLORA

Macrophytes

Rooted aquatic plants in Lake Taupo consist of a mixture of indigenous and introduced species. They grow in water depths down to about 10 m and are most abundant on less exposed shelf areas (e.g. Waihi, Stump, Motuoapa, Acacia and Whangamata Bays).

Native macrophyte species in Lake Taupo include *Myriophyllum*, *Potamogeton*, *Glossostigma* and characean algae. Introduced species include *Elodea canadensis*, *Lagarosiphon major*, *Ceratophyllum*, *Ranunculus* and *Egeria* (Chapman, 1970; Brown, 1975; Coffey, 1975; J. Clayton, 1977, pers. comm.).

Glossostigma is often first to colonise the substrate in water depths of 0.5-2.0 m, and mounds of entrapped sediment begin to form (Fig. 3.7). These mounds may develop as other species become established (e.g. *Myriophyllum*, *Potamogeton*) and reach heights of 0.5 m in Lake Taupo (Fig. 3.8). Wave action may subsequently cause mound migration or destruction (J. Clayton, 1977, pers. comm.). Chapman *et al.* (1971a, 1971b) have described a similar evolutionary sequence in the Rotorua lakes. *Myriophyllum* and *Potamogeton* species grow to depths of several metres but do not form closed canopies (Fig. 3.9).

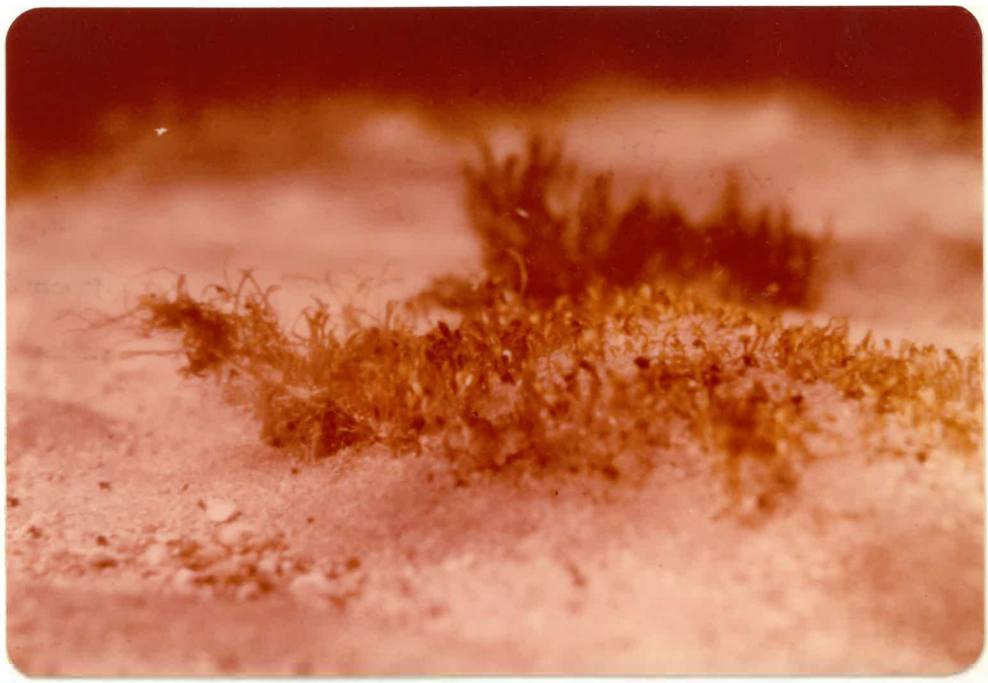


Fig. 3.7. Initial colonisation of shelf sediments by *Clossostigma submersum*. (Depth, ∿1 m; location, near Te Moenga; Photo - J. Clayton).

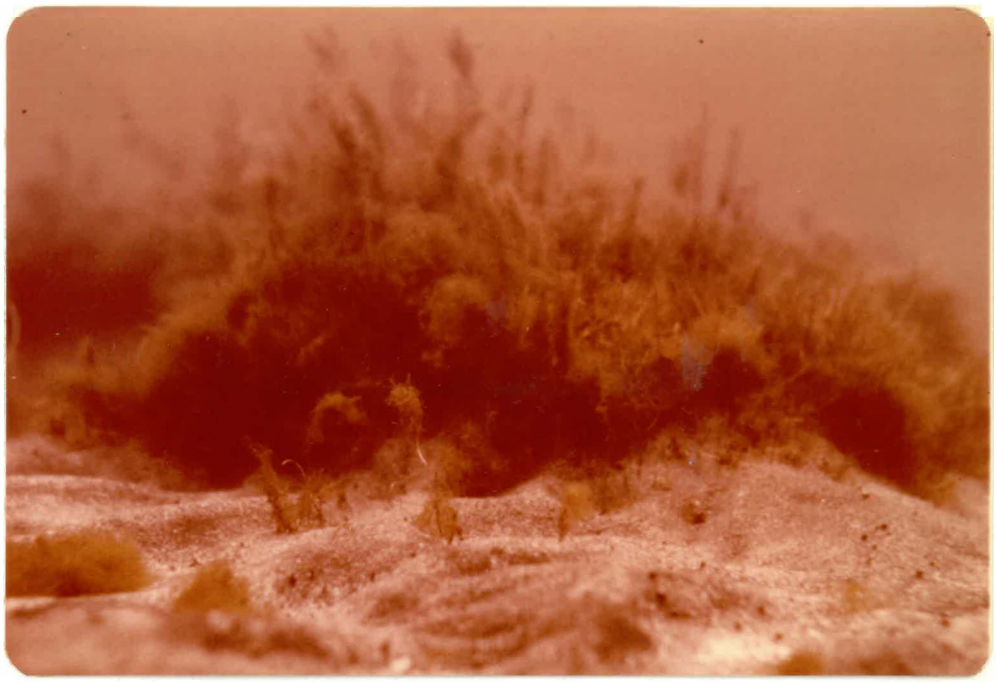


Fig. 3.8. A 0.3 m high mound of sediment entrapped by mainly *Myriophyllum elatinoides* and *Isoetes kirkii*. (Depth, ∿1.5 m; location, Kuratau shelf; Photo - J. Clayton).



Fig. 3.9. *Potamogeton crispus* growing on the lake bed near Waihi. Note the rounded pumice gravel. (Depth, ∿2 m; Photo - J. Clayton).



(a)

Fig. 3.10. Dense, encroaching stands of *Lagarosiphon major* (a) on the Kuratau shelf and (b) in Stump Bay, about 100 m off Waiotaka River mouth. (Depths, ∿3 m; Photos - J. Clayton).



Fig. 3.10(b)



Fig. 3.11. *Elodea canadensis* growing on slope sediments just below the Kuratau shelf-break. (Depth, ~6 m; Photo - J. Clayton).

Mixed indigenous macrophyte communities may be replaced by introduced macrophytes, which typically form single species communities with closed canopies, particularly in the case of *Elodea canadensis* and *Lagarosiphon major* (Brown *et al.*, 1973; Brown, 1975). *Lagarosiphon* grows at depths of 2-6 m generally, although it may occur at shallower depths in sheltered areas (Chapman *et al.*, 1971). In Lake Taupo, it presently dominates the inner zones of Waihi Bay (Wilson and Turner, 1971), Acacia Bay, and occurs around Kuratau and Stump Bay to Motuoapa (Figs. 3.10a and b; J. Clayton, 1977, pers. comm.). *Lagarosiphon major* will eventually dominate all submerged communities and may completely displace native plant communities within its depth range (Coffey, 1975). It became a serious problem in the Rotorua lakes in 1958 (Chapman, 1975). *Elodea canadensis* grows mostly on a silty substrate and may form dense beds, especially at the lower depth limits of *Lagarosiphon major*, as is the case in Waihi Bay (Wilson and Turner, 1971) and Kuratau (Fig. 3.11 J. Clayton, 1977, pers. comm.). Characean algae (*Nitella* spp.) may also form dense meadows at the lower limits of macrophyte growth (Coffey, 1970).

Algal Flora

Algae occur in three communities; floating or freely suspended (phytoplankton), attached to, or moving on, a living substrate (aufwuchs) or the lake bottom (benthos; Cassie, 1974). A list of common algal species in Lake Taupo is given by Hill (1975).

Phytoplankton in Lake Taupo are characteristic of an oligotrophic environment, being relatively sparse (circa 50 cells/ml), having fewer than twelve common species and dominated by diatoms, particularly

Melosira sp. 'A' (Jolly, 1959; Hill, 1975; Table 3.3). Diatoms are also the major constituents of aufwuchs and benthos (Cassie, 1974).

Diatom cells are encased in rigid, opaline, silica frustules and may be solitary, colonial, or filamentous in habit. Classification is based largely on distinctive frustule characteristics of which there are two general expressions of form giving two orders; pennales one elongate (cigar-, boat- or wedged-shaped) and have bilateral symmetry, centrales have a circular outline (pillbox-shaped) with radiate ornamentations. After death the frustules usually sink to the lake bottom and are incorporated into the sediment.

Bacillariophyceae	Abundance
Cyclotella stelligera Cleve and Grun	P
Cyclotella spp.	P
Melosira sp. 'A'	A
Asterionella formosa Hass.	P
Synedra acus Kütz	P
Synedra ulna (Nitzsch.) Ehr.	R
Fragilaria sp.	R

A = Abundant component of the phytoplankton. Species often dominant for some period.

P = Species relatively common in both sedimented and net plankton, but species never dominates plankton.

R = Species rarely seen in sedimented plankton but present in moderate numbers in net plankton.

Table 3.3. Diatom species observed in Lake Taupo by Jolly (1959) and Hill (1975). Abundances were observed at the lake outflow (Waikato River) by Hill. *Melosira* sp.'A' are least abundant at the outflow when the lake is stratified (Thomason, 1960; Hill, 1975).

CHAPTER 4

FIELD WORK AND PRELIMINARY INVESTIGATION

4.1 OUTLINE OF FIELD WORK

95 surficial bottom sediment samples and six cores were collected at Lake Taupo from the University of Waikato's barge, or from a run-about supplied by H. Larsen, during February 1977. A further 22 surficial samples were collected from a launch supplied by Ecology Division, D.S.I.R., Taupo in May 1977.

An echo-sounding survey was carried out from the N.Z.O.I. boat 'Taraiti' in April 1978 with a Raytheon RTT-1000(A) Portable Survey System using 200 kHz and 7kHz frequency signals.

4.2 SAMPLING NETWORK

Ideally, the accurate determination of sediment facies boundaries requires a sampling network of sufficient density so as to minimise subjective interpolation and to 'average out' samples which for any reason are not representative of the area from which they were taken. Systematic sampling along a grid has greater accuracy than random sampling (McCammon, 1975).

At Lake Taupo a basic grid-system approach was modified by the need to obtain a greater sampling density in the southern part of the lake where the largest inflows occur, by the resources and time available for both field and laboratory studies, and by field conditions and practical logistic requirements. The closest site densities occur along transects across several shelf-slope and delta areas where sediment characteristics change most rapidly with bathymetry.

Core samples

Sediment cores were obtained primarily for identification of any reflectors revealed by echograms, and minor sedimentological events which could not be resolved by seismic methods. The main southwest-northeast profiling transect coincides with the core transect.

The sediment sample sites and seismic profiling transects are shown in Map 3 (map pocket).

4.3 POSITION FIXING

Steel superstructure on the barge prevented accurate compass use. Close-to-shore positions were fixed using adjacent landmarks, visual estimations of distance offshore, and bathymetry.

Further offshore, positions were fixed by taking several pairs of sightings on landmarks.

Each pair of sightings was made simultaneously in opposite directions along a 2 m 'sighting staff' and plotted directly on to a chart. This method gave greater accuracy than the Sestrel hand-held compass bearings used for position fixing during the echo-sounding survey.

The barge is equipped with a Marlin DIR60 recording depth sounder capable of registering depth to 110 m. This assisted exact position fixing on a bathymetric chart in areas of unique lake-bed topography. In deeper areas the calibrated winch wire was used to determine depth at the moment of sampling.

4.4 SAMPLING TECHNIQUES AND EQUIPMENT

Surficial bottom sediments

These samples were collected using a 500 cc capacity Marukawa sampler. Minimal disturbance of samples by this device permitted inspection of any vertical changes in sediment character immediately after recovery. These were recorded and, in some cases, subsamples separated. Samples were stored in sealed plastic containers.

Sediment penetration varied from about 2 cm in sandy sediments to 20 cm in some deep water muds. Temperatures of several samples were recorded immeidately after recovery, and Eh/pH values were recorded at the end of the day.

Core samples

Sediment cores were obtained with an Alpine model piston corer capable of penetrating 2 m of sediment. After recovery the 3 cm internal diameter P.V.C. core liners were removed from the corer barrel and immediately plugged at the lower end. Excess core liner was removed to within 2 cm of the sediment top, the top sealed and the cores stored in an upright position. At all core sites secchi disc readings and temperature profiles to 44 m depth were also recorded.

River sediment samples

One bed-load sample was collected from each of the rivers and major streams discharging into Lake Taupo. Low flow conditions in February, 1977 allowed sample collection at midstream, straight-reach sites within a few hundred metres of the lake. A suspended-load sample and water temperature measurements were obtained from the Tongariro River mouth during the falling stage of a flood in April, 1978.

4.5 SEDIMENT FIELD CHARACTERISATION

Shelf sediments are almost entirely sands and gravelly sands. Weed-free shelf areas display long, parallel bifurcating sand ripples which are sub-parallel or oblique to the shoreline. These increase in wavelength with depth across the shelf, ranging from a few centimetres nearshore to tens of centimetres towards outer shelf areas. The troughs frequently contain pumice sands and pebbles (Fig. 4.1) where heavy weed beds occur (e.g. south of the Tongariro Delta, Stump Bay and Motuoapa Bay) entrapment of finer material occurs and the sands become muddy. A cobble lag occurs out to about 50 m offshore from the Oruatua headland (Fig. 4.2).

With rapidly increasing depth beyond the shelf-break the sediments commonly grade into muds, which occasionally contain pumice clasts (Fig. 4.3).

With only a few exceptions (samples 67, 76, 77, 86, 87, 115) the deep-water muds showed no obvious vertical changes in texture, but all showed a colour change from olive-brown or khaki in depth to dark brown or reddish-brown in their top 0.5-1.0 cm (Fig. 4.4). A subsample was separated from sample 27 as sample 28, and from sample 47 as sample 48. All deep-water muds contained sparse sand grains that appeared to be randomly dispersed, and a few small (<1 mm) horizontal laminae, lenses, or specks of black iron-sulphide pigmentation (Fig. 4.4). The sand:mud ratio increases considerably on isolated topographic highs (e.g. samples 56, 57, 76, 77, 120, 121).

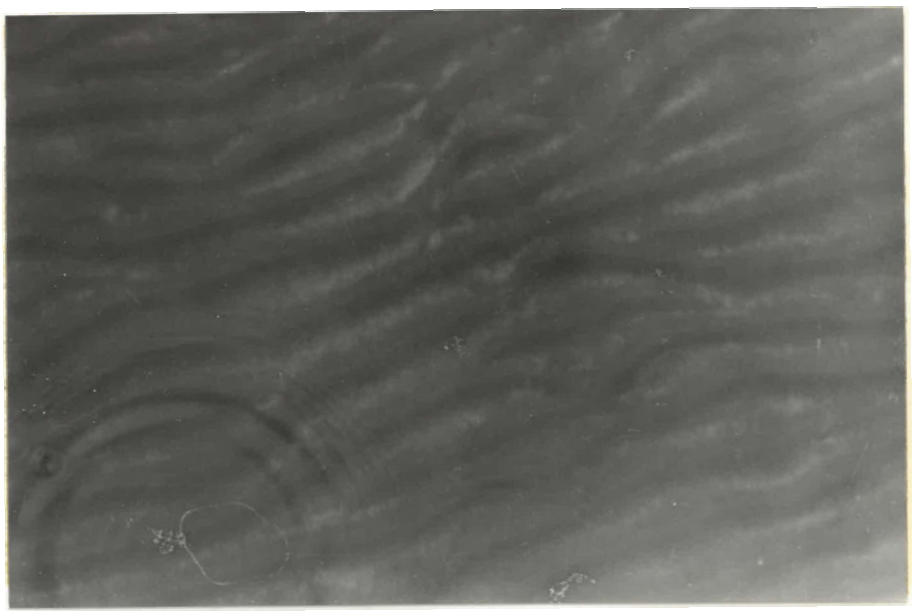


Fig. 4.1. Ripples (wavelength 10-15 cm) formed by swell action on weed-free shelf sediments to the north of Otutere Banks. Pumice grains have accumulated in the troughs. (Depth, ∿1.5 m).

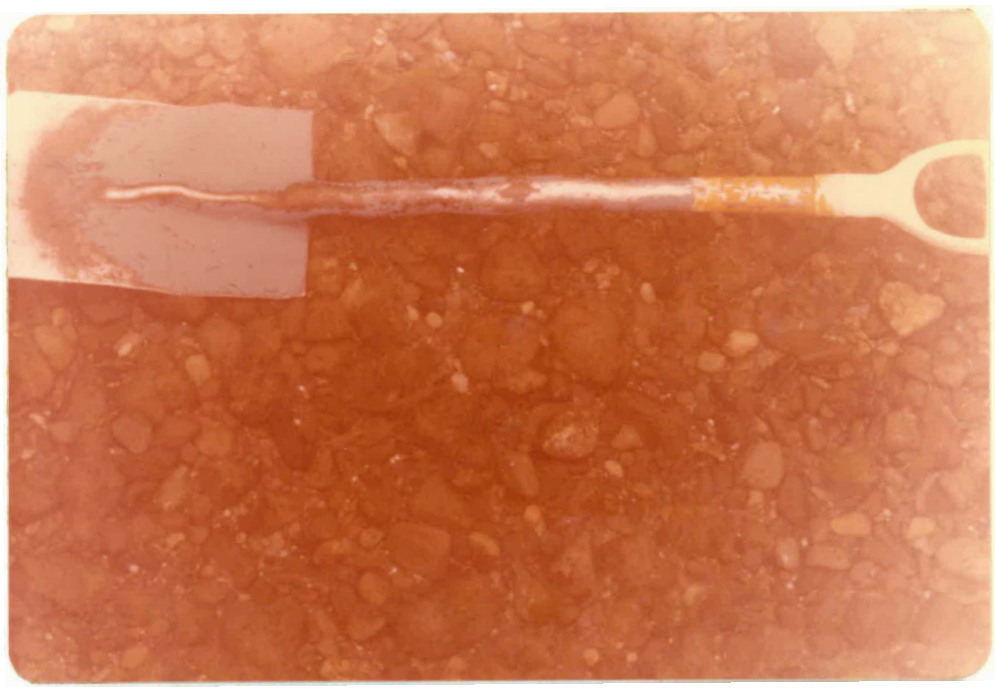


Fig. 4.2. A cobble/gravel lag which extends to about 50 m offshore from Oruatua headland. This material was probably deposited by a pre-existing Tauranga-Taupo River mouth. (Depth, ∿0.5 m).

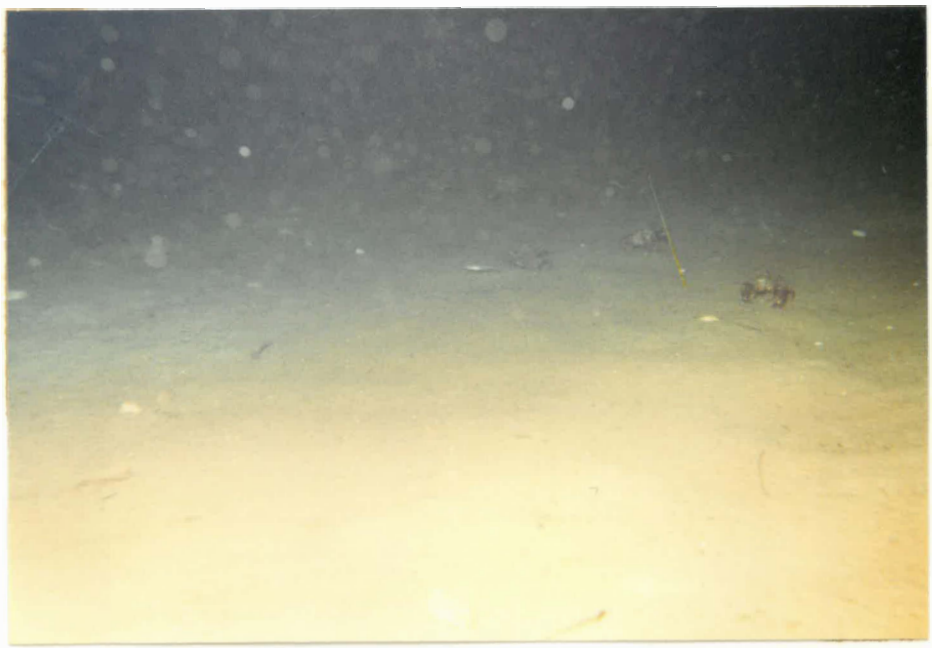


Fig. 4.3. Slope/rise sediments at about 40 m depth near Kuratau. The muds contain occasional pumice clasts and wood fragments. Freshwater crayfish (*Potamopyrgus* sp.) are common. (Photo - A. Devcich).

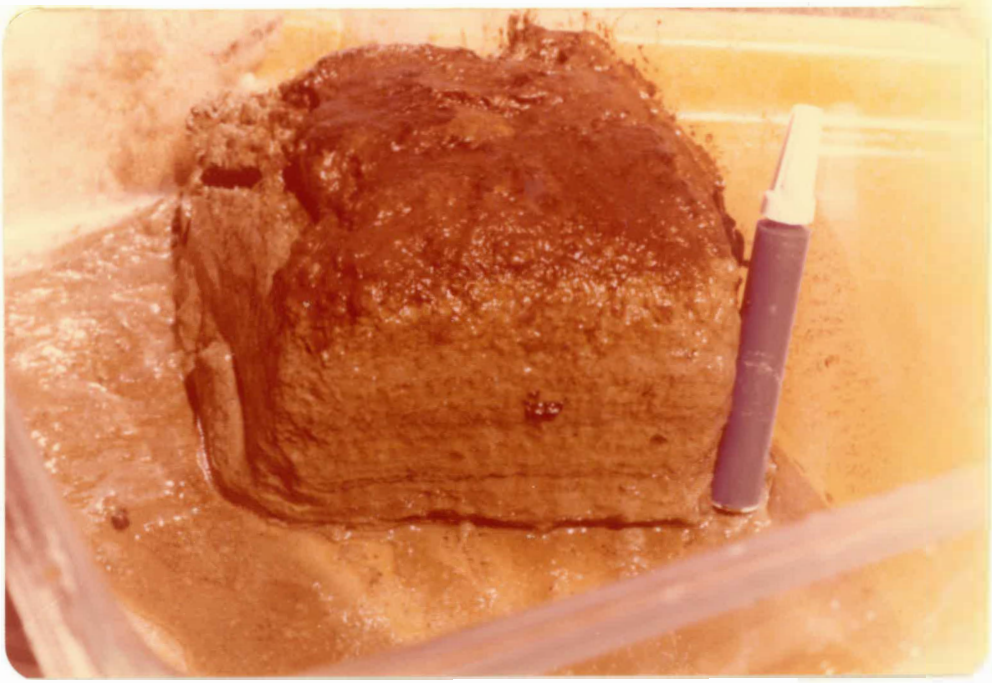


Fig. 4.4. A typical basinal sediment sample (number 66) immediately after recovery from the bottom of Lake Taupo. Note fine laminae of iron sulphide pigmentation at depth, and the surface layer of oxidised sediment. (Scale-marking pen is 12.5 cm long).



Fig. 4.5. Sample 67 immediately after recovery from the lake bed near Motutaiko Island. Note ∿0.5 cm thick sand layer at ∿6 cm sediment depth and a yellowish colour layer above it. Sand on the oxidised surface layer may have been emplaced during sample recovery. (An apparent sand layer below the marking pen is in part of the sample tipped towards the camera).

4.6 UNUSUAL DEEP-WATER SAMPLES

Sample 67 contained a 0-5 cm thick sand layer about 6 cm below the surface and a yellowish coloured layer about 3 cm below the surface (Fig. 4.5).

Sample 76 had a 1 mm thick hard crust at the surface with several pumice pebbles embedded in it (Fig. 4.6). The underlying 2 cm of ediment had a high sand content showing some bedding, and an unu ually pale, buff coloured mud fraction.

Sample 115 contained a 1 cm thick layer of small, well rounded pumice pebbles, and sand 5 cm below the surface (Fig. 4.7).

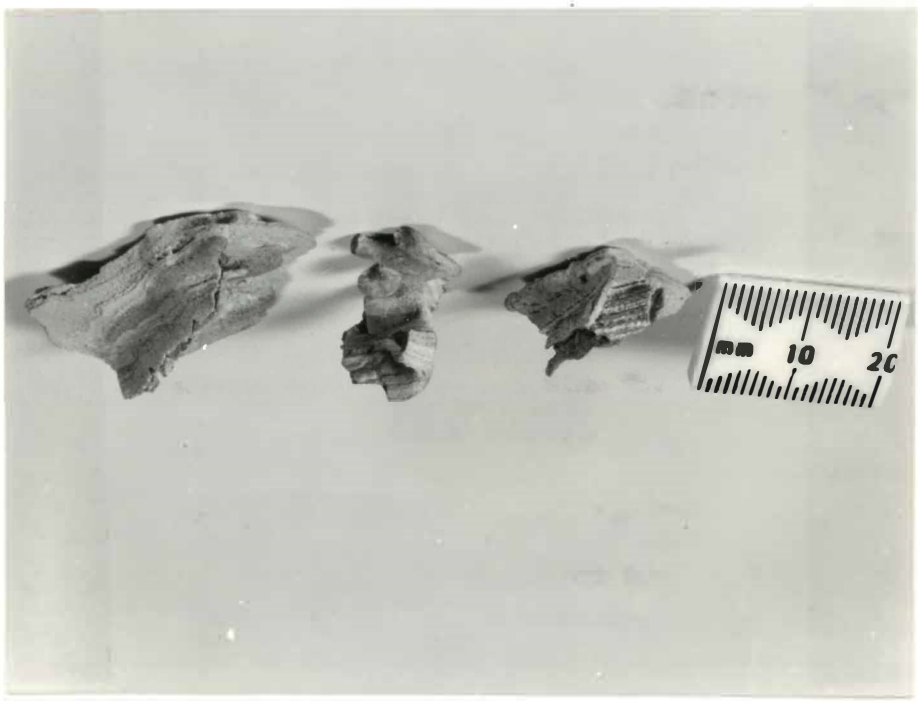
Sample 99 was almost entirely dark brown stained pumice and sand.

Sample 86 contained about 1 cm of dark brown sediment with a high sand content and stiff consistency separated by a sharp contact from the underlying paste-like mud, also with a high sand content. The two layers were separated, the top layer becoming sample 87.

Close to cliffs of rhyolite and ignimbrite, where no shelves occur, the sediments are very poorly sorted. Angular rock fragments of all sizes frequently caused sampling problems.

Fresh water mussels (*Hyridella menziesi*), mussel shells (Fig. 4.8a), and small (<3 mm) water snails (*Potamopyrgus* sp.) occurred in some samples. Dead mussel shells were commonly decomposed on those parts that were buried in the mud (Fig. 4.8b) indicating instability of calcium carbonate in the sediment.

(a)



(b)



Fig. 4.6. Parts of the sinter crust which overlay sediment sample 76. (a) Undersides of crusts showed cleaved, blade-like extensions in which sand grains are cemented, thus preserving the bedding structure of sub-surface sediment. Hydrothermal water may have coursed through the cleavages. (b) Pumice fragments cemented on to the upper surface of sinter crusts. The upright position of the pumice fragment on the left indicates a lack of bottom currents during its deposition on to a soft-sediment surface. This suggests that subsequent hydrothermal flow in the immediate vicinity was no more than a seepage.



Fig. 4.7. Sediment sample 115 immediately after recovery from the lake bed. Note the layer of redeposited pumice gravel and sand.

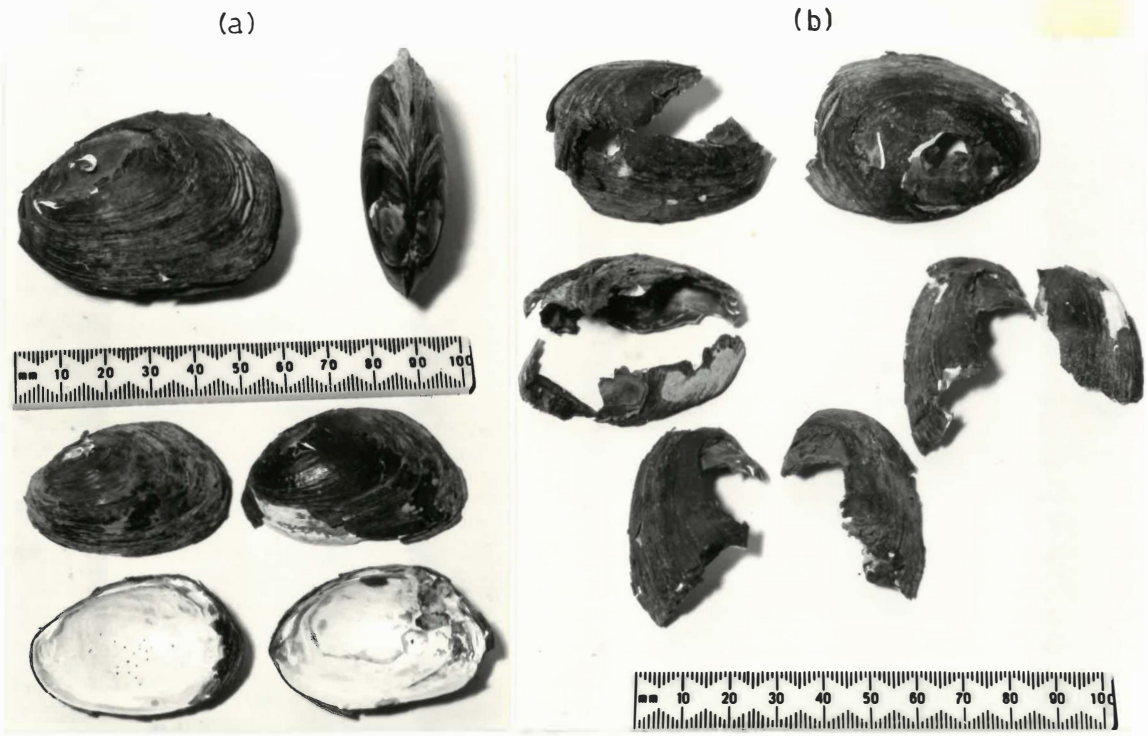


Fig. 4.8. Freshwater mussel shells (a) from live specimens and (b) from dead specimens.

4.7 SEDIMENT HYDROGEN ION CONTENTRATIONS (pH) AND REDOX POTENTIALS (Eh)

Sediment pH values range from 3.5-7.1, and Eh values range from 40-450 mV (Appendix 2; Figs. 4.9a and b). The highest pH values (6.5-7.1) occur around the southern end of the lake, with lower values occurring locally. Over much of the rest of the lake, pH values are commonly 5.0-6.0 with the higher values occurring on the eastern side (Fig. 4.9b). An unusually low pH value (3.5) occurs in the eastern central part of the lake (sample 74).

Sediment Eh values are always positive, and over most of the lake exceed 100 mV, the potential below which measurable oxygen disappears (Mortimer, 1942). Eh values less than 100 mV occur locally around the southern end of the lake, particularly off the northern and western sides of the Tongariro delta (Fig. 4.9a).

The surface 'colour layer' (0.5-1.0 cm thick) was removed from samples 27 (as sample 28) and 47 (as sample 48) and the pH-Eh values of each sub-sample determined separately. In both cases the top layer showed slightly lower pH values and much higher Eh values than the underlying sediment.

A plot of Eh against pH (Fig. 4.10c) shows two intersecting Eh-pH trends:

(a) pH values increase as Eh values increase from about 100-400 mV. This trend is possibly depth related.

(b) pH values increase as Eh values decrease from about 200-50 mV. This trend is caused largely by a grouping of low Eh-high pH values at the southern end of the lake, with pH having the stronger influence.

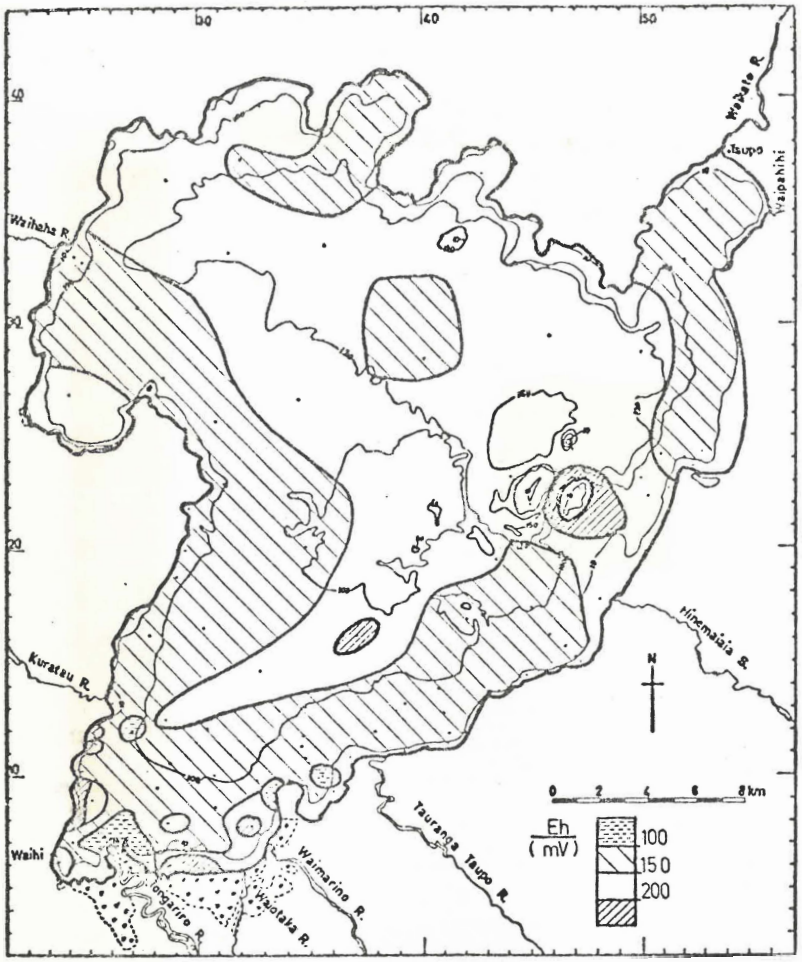
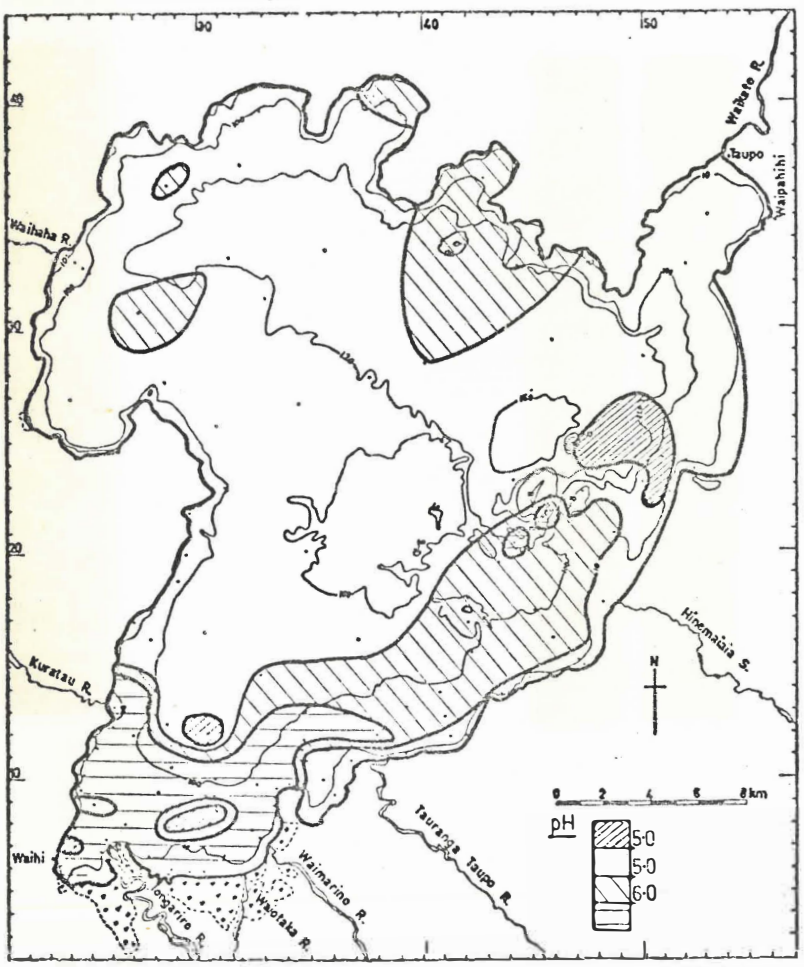


Fig. 4.9.

(a) Surficial sediment Eh values



(b) Surficial sediment pH values

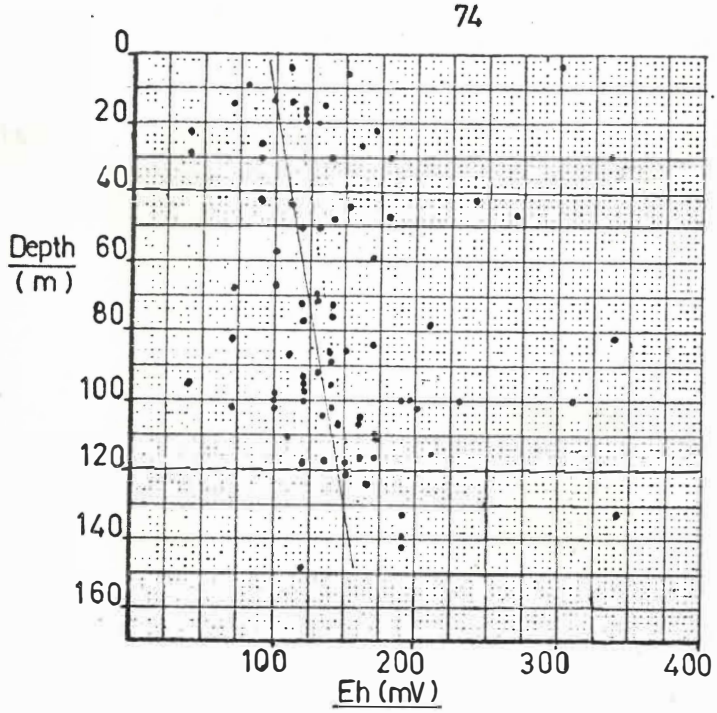
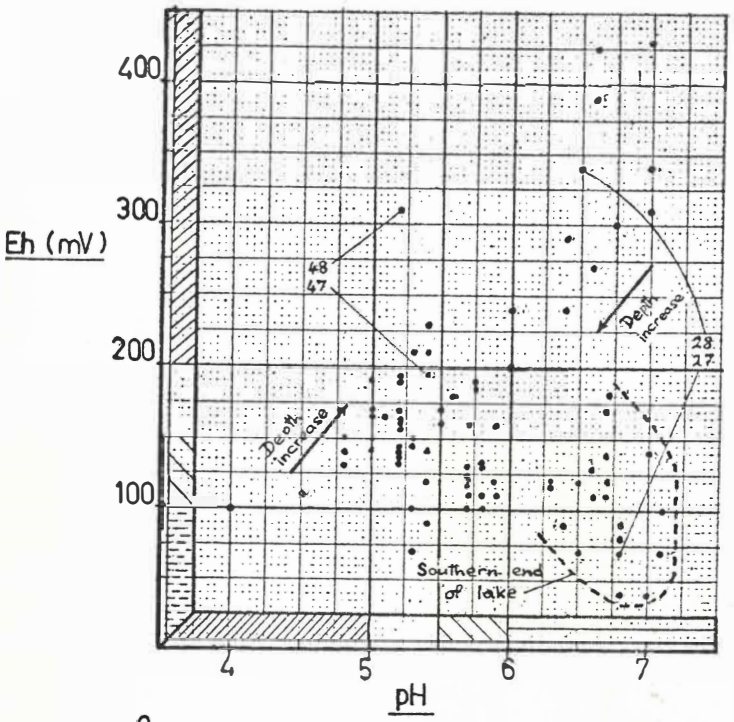


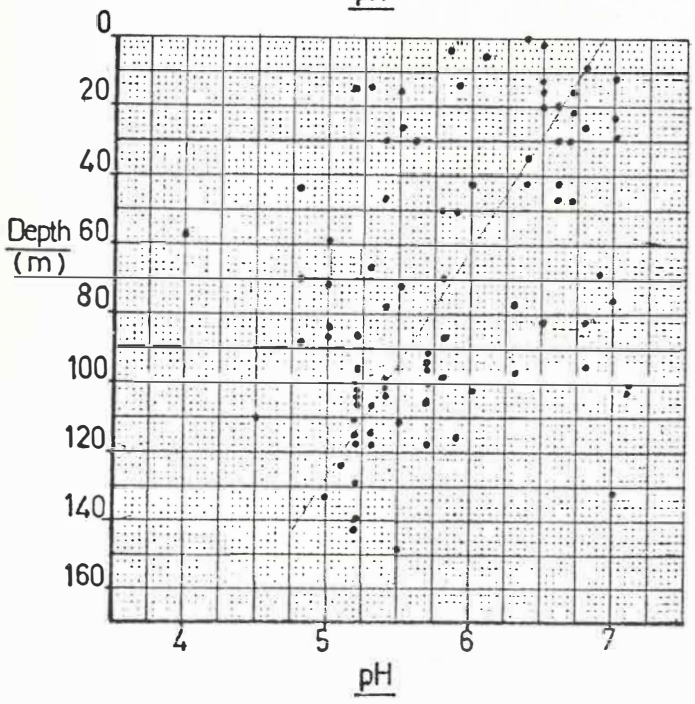
Fig. 4.10

(a) Sediment Eh vs. water depth.



(c) Sediment Eh vs. pH.

Axes are hatched according to Fig. 4.9 a and b for cross reference.



(b) Sediment pH vs. water depth

Both Eh and pH values are determined largely by reactions such as the oxidation of iron or the microbial degradation of organic matter in the sediment (Blatt *et al.* 1972; McColl, 1977); however, geothermal influences (acid-sulphate-chloride waters) may also decrease lake sediment pH values (e.g. Lake Rotowhero sediments have a pH range of 3.8-5.3; McColl, 1977). Sediment redox potentials are controlled mainly by the supply of gaseous oxygen in relation to the amount of material being oxidised. In Lake Taupo the minimum dissolved oxygen in bottom water is 78% (Stout, 1975) so oxidation of sedimentary particles occurs at the sediment-water interface. As sediments are incorporated into the top 0.5-2.0 cm thick layer they are largely cut off from the overlying water having pH7.0-7.6 (Stout, 1975). Aerobic bacterial degradation of sedimentary organic matter reduces the oxygen content of the interstitial water, resulting in an increase in the partial pressure of dissolved carbon dioxide, the production of organic acids and sulphate, and a consequent decrease in pH relative to the super-adjacent water (Zobell, 1942; Emery and Rittenberg, 1952; Fairbridge, 1967). Further burial of the sediments leads to replacement of aerobic bacteria by anaerobic bacteria as the dissolved oxygen content and redox potential decrease. In this environment pH values may rise slightly as a result of microbial reduction processes (e.g. conversion of sulphates to sulphides).

A range of sediment Eh and pH values occur at all depths in Lake Taupo. A weak trend occurs in both; pH values decrease and Eh values increase with increasing depth (Fig. 4.10a and b). Higher Eh values in deeper parts of the lake suggest low rates of bacterial activity and therefore low organic matter inputs. Conversely,

lower pH values suggest higher rates of bacterial activity in central lake areas relative to shallower areas. At the southern end of the lake the opposite relationship between Eh and pH exists with high pH values and low Eh values occurring. These conflicts suggest factors other than bacterial activity are involved in the Eh-pH relationship, or the possibility of instrumental error or drift during Eh-pH determinations. Certainly remeasurement of some samples in the field showed that Eh and pH values could not be accurately reproduced, and McColl (1977; pp515-516) has mentioned doubts about the value of redox potential data for making accurate comparisons between sediments from different lakes. More detailed work on the relationships between causal factors and Eh-pH values in the sediment is required before the given Eh-pH values and their spatial variations can be confirmed.

4.8 LAKE WATER TEMPERATURE AND CLARITY

Water temperatures were measured at some core sites at 2 m intervals from 0-44 m depth using a reversing thermometer. Temperature profiles and secchi disc readings at core sites 3, 4, 5 and 6 are given in Fig. 4.11 together with a temperature profile observed in 1956 by Jolly (1959). Water temperatures at a given depth vary by up to 3° between sites. The depth at which rapid temperature decrease begins varies by up to 6 m (16-22 m) from site to site, suggesting the possibility of internal seiche action, and occurs about 10 m shallower than observed in March-April, 1956 by Jolly (1959).

Water depths at which the secchi disc disappeared (av. 13.6 m) are less than the maximum of 18 m observed by Jolly (1958). Readings were taken on the shaded side of the craft under calm-small wave lake conditions. The subjectivity in determining water clarity by this

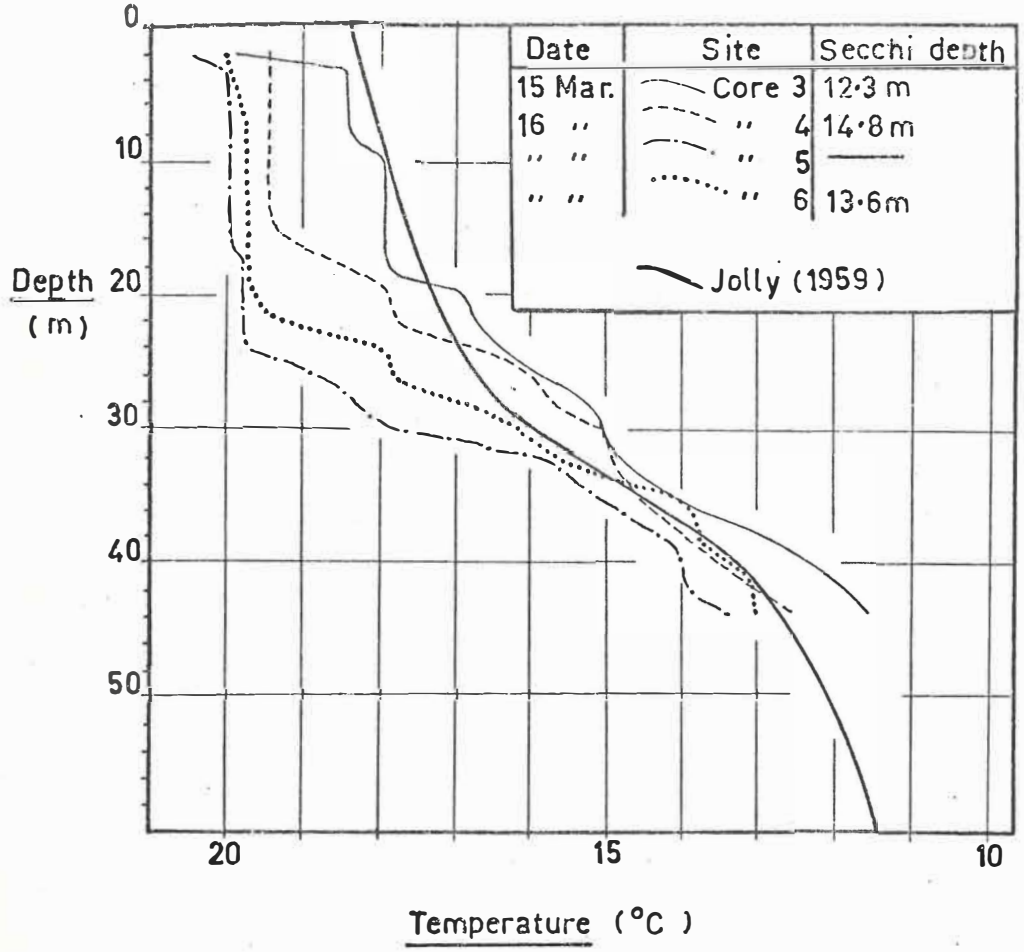


Fig. 4.11. Water temperature profiles and water clarity at core sites in Lake Taupo.

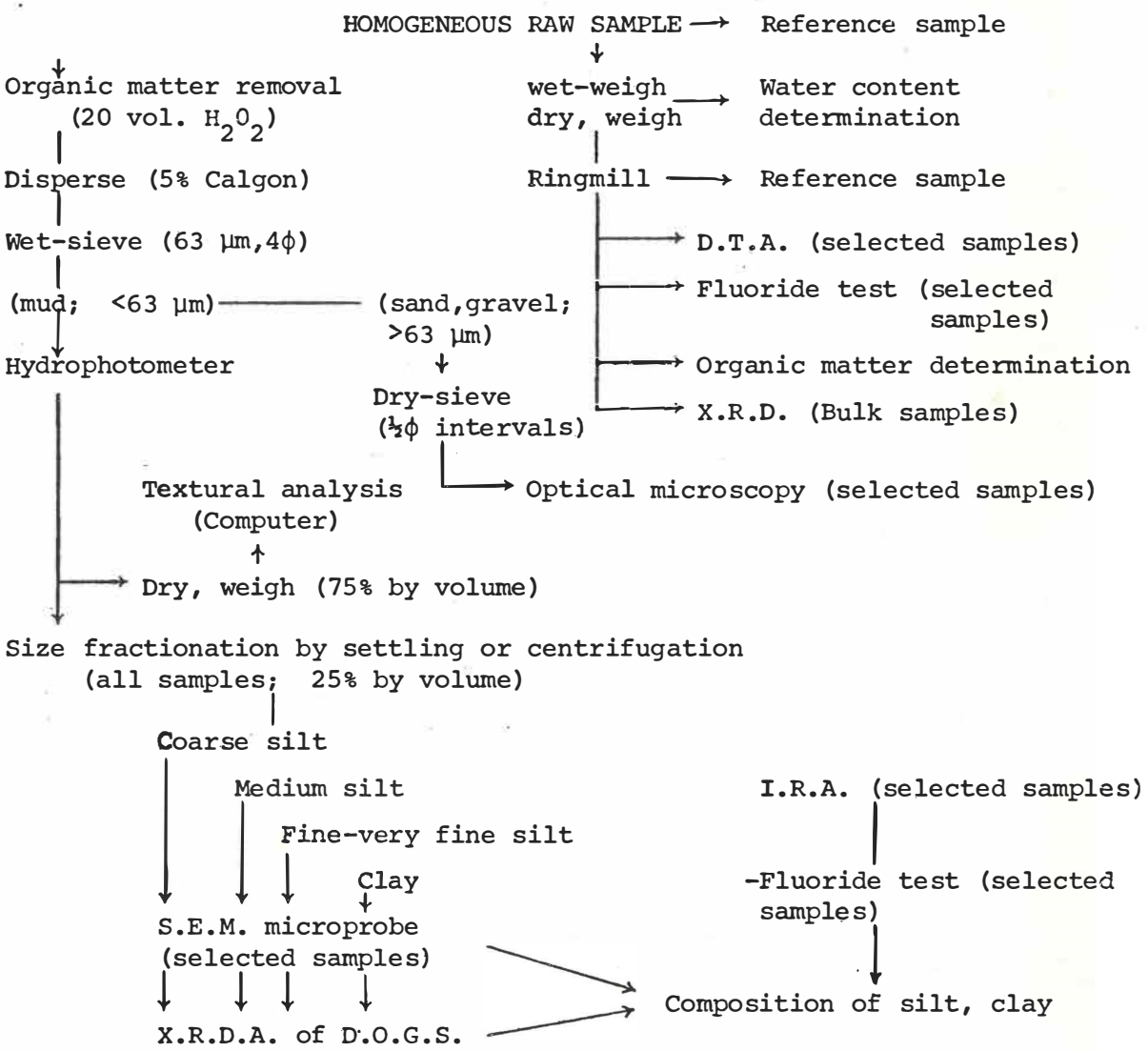
method has been discussed by Jolly (1968) and Irwin (1974). Lake-water clarity is determined by phytoplankton density, dead organic material, particulate inorganic matter, and dissolved matter such as humic material leached from the catchment. Although observed water clarity in Lake Taupo was less than that observed by Jolly the values are still high and typical of an oligotrophic lake, indicating a very low content of both particulate and dissolved matter in the epilimnion.

4.9 PRELIMINARY INVESTIGATION

Twelve dry bulk samples (9, 25, 45, 53, 65, 66, 75, 78, 84, 93, 94, 96) were subjected to a fluoride field test for allophane (Fieldes and Perrot, 1966). The test was negative for all samples suggesting that any allophane content was less than 5-10%. Organic-free samples (H_2O_2) in distilled water required very little dispersion (less than about 50 ml of 5% Calgon per litre of sediment/water mixture), further suggesting little, if any, allophane. The bulk of sediment in each sample settled to the bottom of the container within a few minutes of mixing, indicating a high proportion of coarser than clay (0.004 mm) material. After removal of larger than silt (0.0625 mm) material by wet-sieving through a 4.0ϕ screen, samples were centrifuged into silt fractions and a clay fraction. The bulk of each sample proved to be silt with a mode below coarse silt (5.0ϕ, 0.031 mm). Further centrifugation of the twelve clay samples indicated that all contained only negligible amounts of fine clay (<0.2μm). Fluoride tests on the twelve air-dried clay fractions were again negative, suggesting an absence of allophane.

This preliminary investigation determined the subsequent techniques and experimental approach used for sample analysis. A flow chart summarising laboratory procedures is given in Fig. 4.12.

Fig. 4.12. Flow chart for laboratory procedures used on Lake Taupo sediment samples.



Abbreviations

X.R.D.A.	X-ray diffraction analysis
S.E.M.A.	Scanning-electron microscope analysis
I.R.A.	Infra-red analysis
D.T.A.	Differential thermal analysis
D.O.G.S.	'Drop on glass slide' oriented sediment mounts

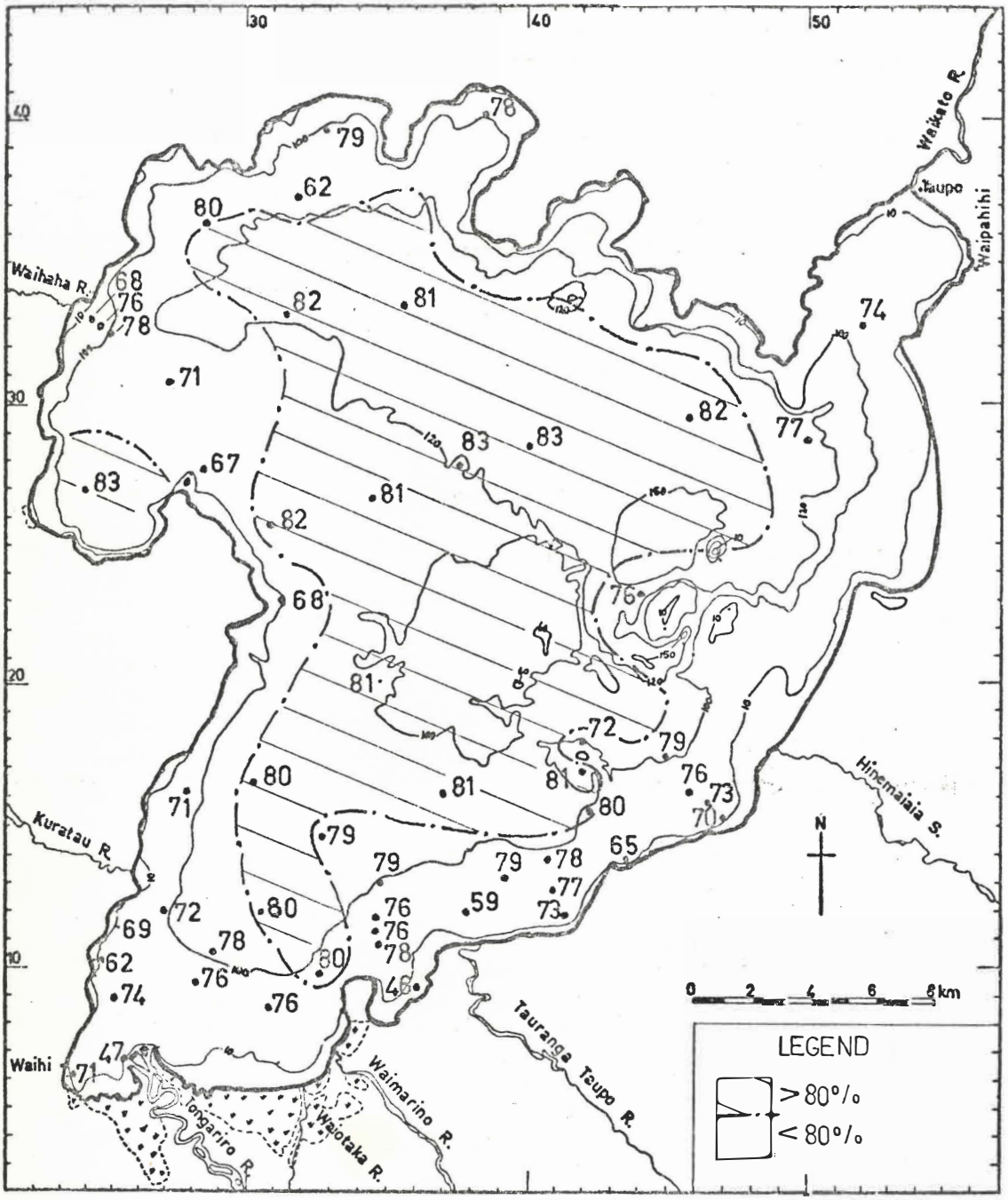


Fig. 4.13. Water content (wt.%) in surficial sediment.

4.10 SEDIMENT COLOUR AND WATER CONTENT

The pulpy consistency of deep-water sediments helped prevent drainage losses during sample recovery. Sediment samples were stored in watertight containers. Growth of small black iron sulphide patches occurred between the field and laboratory, and chironamid larvae were observed in most samples.. Samples were thoroughly homogenised prior to subsampling.

Sediment water content was determined from the weight difference between wet and dried (24 hours at 55°C) subsamples. Sediment water content increases with lake depth towards a constant value of about 80% in basinal regions (Fig. 4.13). The trend is probably a result of the increasingly finer texture of sediments towards basinal regions, where the constant values reflect texturally similar sediments.

Wetted deep-water sediment colours were determined using a Munsell soil colour chart (1954). Sediments in central northern parts of the lake have the lightest average colour (2.575/3; yellowish grey). Patches around the southern end of the lake, particularly off the Tongariro, Waiotaka, Waimarino and Tauranga-Taupo river mouths, have the darkest average colour (2.57 3/2-3/3; brownish black-dark olive brown; Fig. 4.14). Sediment mineralogy, organic matter content, and the products of microbial processes largely determine sediment colour. McColl (1977) found that surface sediment colour in eight Rotorua lakes darkened through the oligotrophic-mesotrophic-eutrophic lake sequence. The different colours also correlated with surface sediment redox potentials, which, in turn, inversely correlated with organic matter concentrations in the sediments. In Lake Taupo, darker sediments off the Tongariro Delta and in the southwestern corner of

Waihi Bay (Fig. 4.13) correlate with lower Eh values (<100 mV; Fig. 4.9a), and the lighter sediments in central northern regions of the lake correlate with higher Eh values (150-200 mV). This suggests that bacterial activity, and thus organic matter content, exert a significant control on sediment colour (c.f. McColl, 1977).

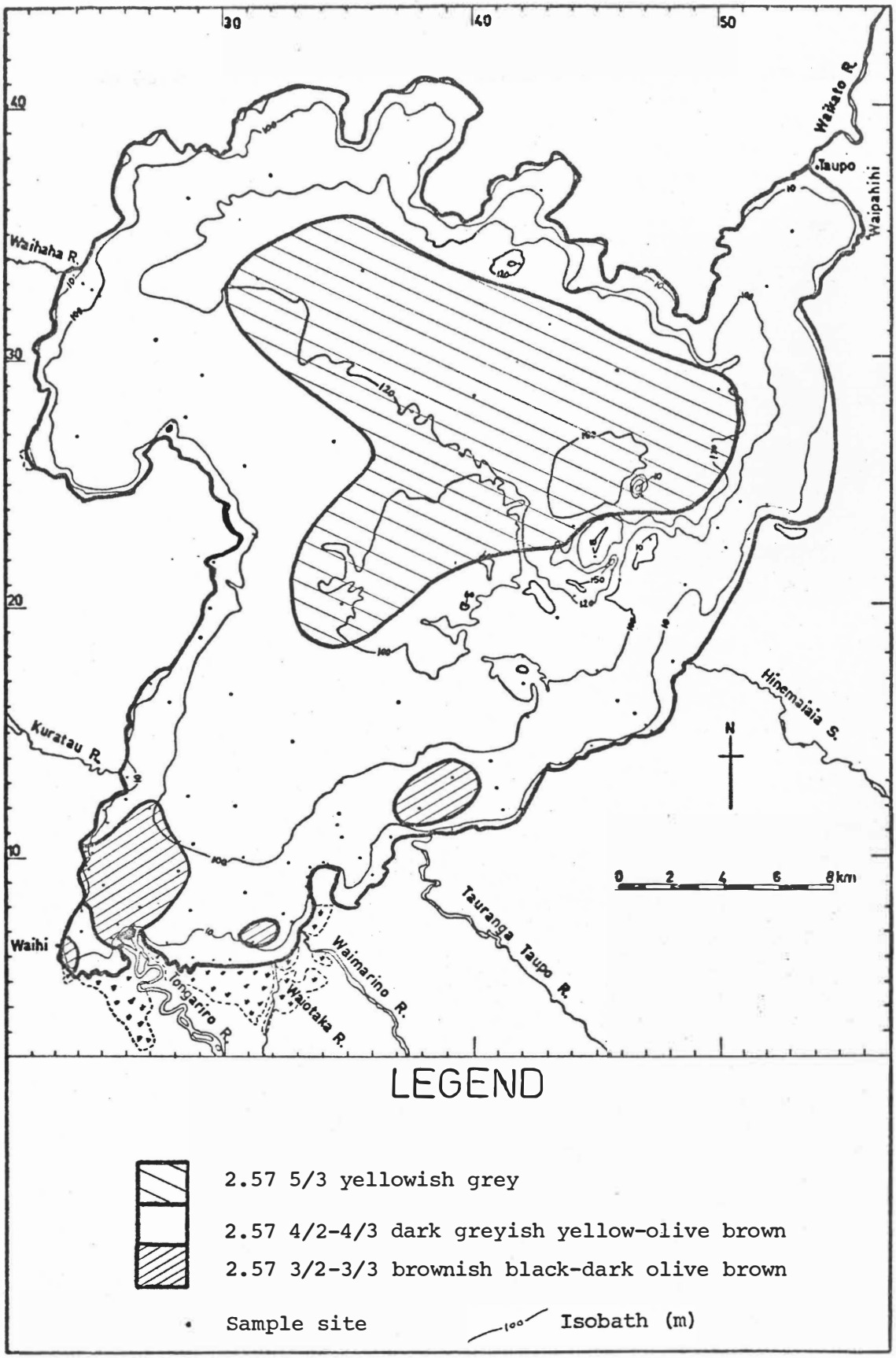


Fig. 4.14. Colour of homogenised wet sediment (Munsell, (1964) Soil Colour Chart).

CHAPTER 5

TEXTURAL ANALYSIS

5.1 METHOD

Mud and sand were separated by wet-sieving samples through a 4ϕ (0.0625 mm) screen following digestion of organic matter with 20% H_2O_2.

Grain size distributions of the coarser than 4ϕ fractions were obtained using ½ϕ interval sieves on a Rotap sieve shaker. Non-pumiceous material was sieved for 15 minutes; samples containing considerable amounts of pumice were sieved for shorter periods to minimise abrasion effects. The small amounts of sand (commonly only a few grams) in the basinal silt deposits were either hand sieved or considered as very fine sand.

Particle size distribution data for the mud fractions were obtained using a hydrophotometer model 7313 (Jordan *et al.* 1971). Diluted mud aliquots were homogenised (end over end) and allowed to stand for 10 seconds before initial transmission readings were made. Consecutive ½ϕ interval readings were taken for silt (4ϕ-8ϕ) and a single reading for clay (8ϕ-14ϕ).

A computer programme (Kamp, 1978) was used to combine all particle size distribution data and to produce a textural characterization of each sample. This information is summarised in Appendix 3 and includes weight percentages of gravel, sand, silt and clay; sand/mud and silt/clay ratios; the number of modes present and their ϕ values; verbal classifications of Folk and Ward (1957) statistics (mean, median, sorting, skewness, kurtosis); and textural terms (Folk *et al.* 1970).

5.2 TEXTURAL CHARACTER

Triangular textural plots of sediment texture show groupings that relate to lake bed topography (Fig. 5.1a and b). The relationship is emphasised by plots of sediment texture against lake bed depth (Fig. 5.2a and b) and can be summarised as follows:

(a) Shelf sediments include sands, gravels and sand-gravel mixtures.

(b) Slope sediments are generally sandy silts and silty sands, but may include some gravel.

(c) Sub-lacustrine talus slope sediments are gravel, sand and subordinate mud mixtures.

(d) Rise sediment textures intergrade between those of slope and basinal sediments. These sandy silts and silts rarely contain small amounts of gravel.

(e) Basinal sediments are entirely silts.

(f) Sub-lacustrine hilltop sediment textures are variable ranging from sandy silts to muddy sandy gravels, but the mud content is usually dominant.

Rise and basinal sediments containing redeposited material from shallower water are generally 'slightly gravelly muddy sands' to 'slightly gravelly muds', although higher gravel contents occasionally occur.

Gravel-sized material at all sites except on sub-lacustrine talus slopes and near river mouths is almost entirely pumice.

The distribution of sediment textural types in Lake Taupo is summarised in Fig. 5.3.

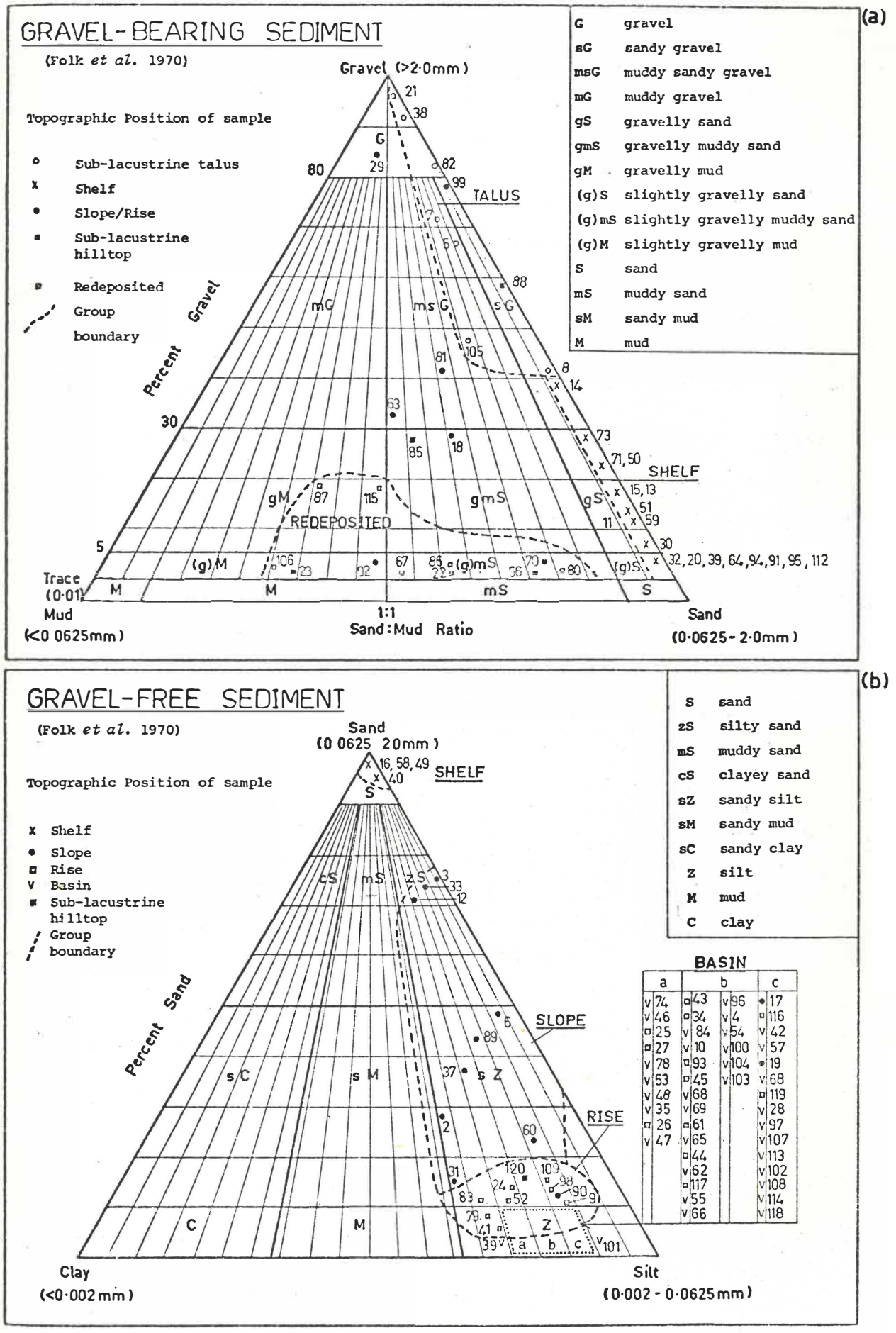


Fig. 5.1. Positions of Lake Taupo sediments on ternary textural diagrams, showing textural composition and terminology for individual samples, and groupings related to lake-bed topography.

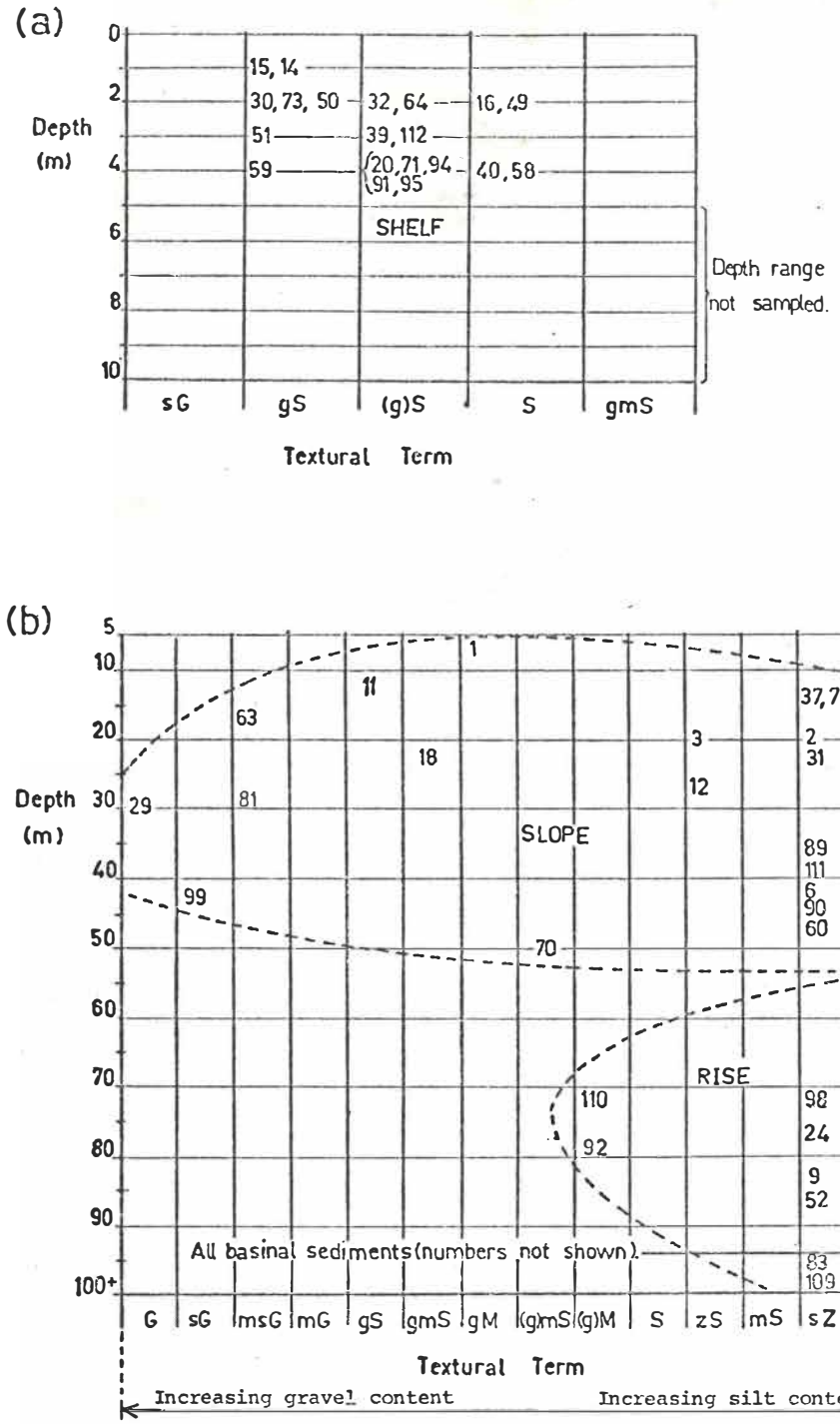


Fig. 5.2. Sediment texture vs. water depth for (a) shelf sediments (b) slope, rise and basinal sediments in Lake Taupo.

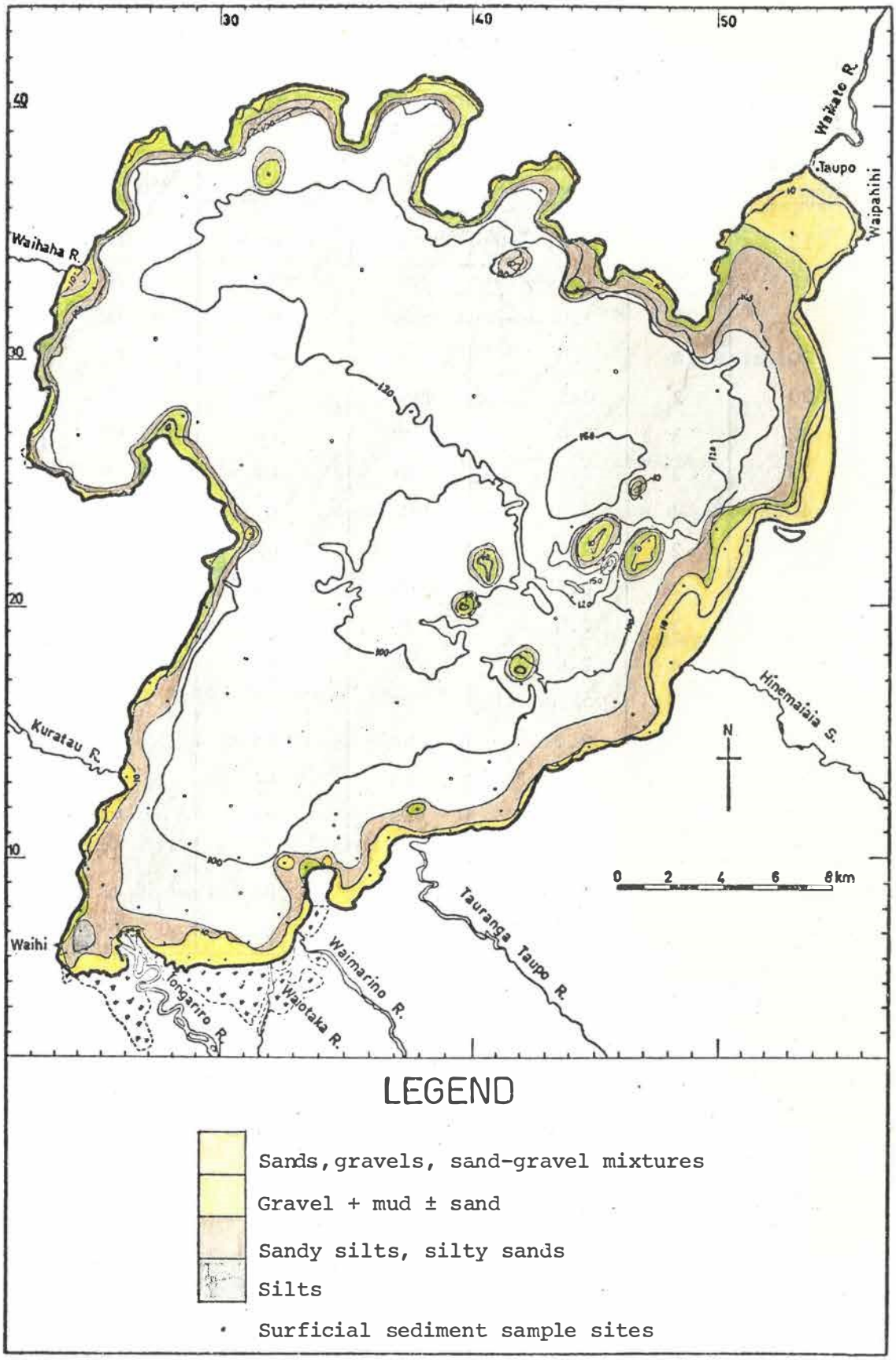


Fig. 5.3. Sediment textural types in Lake Taupo

Table 5.1. Shelf sediment textures

Sample number	Depth (m)	Mode Φ value	Sorting	Skewness	Kurtosis	Textural term
13	1	0.0, 3.0	ps	ns	lk	gS
15	1	1.5,-2.5	ps	scs	vlk	gS
16	2	2.0	mws	ns	lk	S
20	4	3.0	ms	cs	lk	(g)S
30	2	0.5	mws	ns	lk	gS
32	3	2.0	ms	cs	mk	(g)S
39	3	2.0	ms	cs	lk	(g)S
40	4	4.0	vws	cs	mk	S
49	2	2.0	ms	ns	mk	S
50	2	0.5	ms	scs	mk	gS
51	3	2.0	ps	scs	mk	gS
58	4	2.0	mws	ns	mk	S
59	4	polymodal	ps	-	-	gS
64	2	2.0	mws	ns	mk	(g)S
73	2	0.0,-2.5	ps	cs	mk	gS
91	4	1.0	vws	ns	mk	(g)S
94	4	0.5	mws	cs	lk	(g)S
95	4	3.0	mws	ns	mk	(g)S
112	3	2.0, 1.0	ms	cs	pk	(g)S

N.B. See Appendix 3 for expansion of textural abbreviations.

5.3 SHELF SEDIMENTS

Shelf sediments occur along most of the eastern side of the lake, and on the western side between Poukura Pa and Pukawa. They are commonly unimodal, moderately to very well sorted sands and gravelly sands (Table 5.1). Poor sorting occurs near some river mouths and in sheltered areas (e.g. Waihaha River (73), Hinemaiaia Stream (51), Whareroa Stream (112) and Stump Bay (13, 15). All shelf samples are near-symmetrical to strongly coarse-skewed. In depths of 1-5 m the mode is commonly in the 2ϕ-3ϕ grain size range.

5.4 SLOPE, RISE AND BASINAL SEDIMENTS

The shelf-break occurs in water depths of 5-10 m beyond which slope angles may reach 30° and depth increases rapidly. With increasing depth the mud content increases rapidly, and particle sizes are commonly polymodal and the sediments poorly sorted. Where gravel occurs sorting deteriorates further as a result of additional modes. Silty sands occur to depths of abour 45 m and sandy silts to depths of 100 m or more (Fig. 5.2b). Beyond approximately 50 m depth the slope angle progressively decreases down the rise to flat basinal regions. Sediments become silts containing only a few percent sand and commonly up to 25 wt.% of clay-sized material. These silts persist across basinal regions.

5.5 MIXED SEDIMENTS

Deviation from the general pattern for deep-water sediments occurs in a number of situations:

1. Proximity of deep water to steep cliffed areas can produce very poorly sorted mixtures involving all sizes of material (e.g. samples 5, 7, 22, 80, 81).

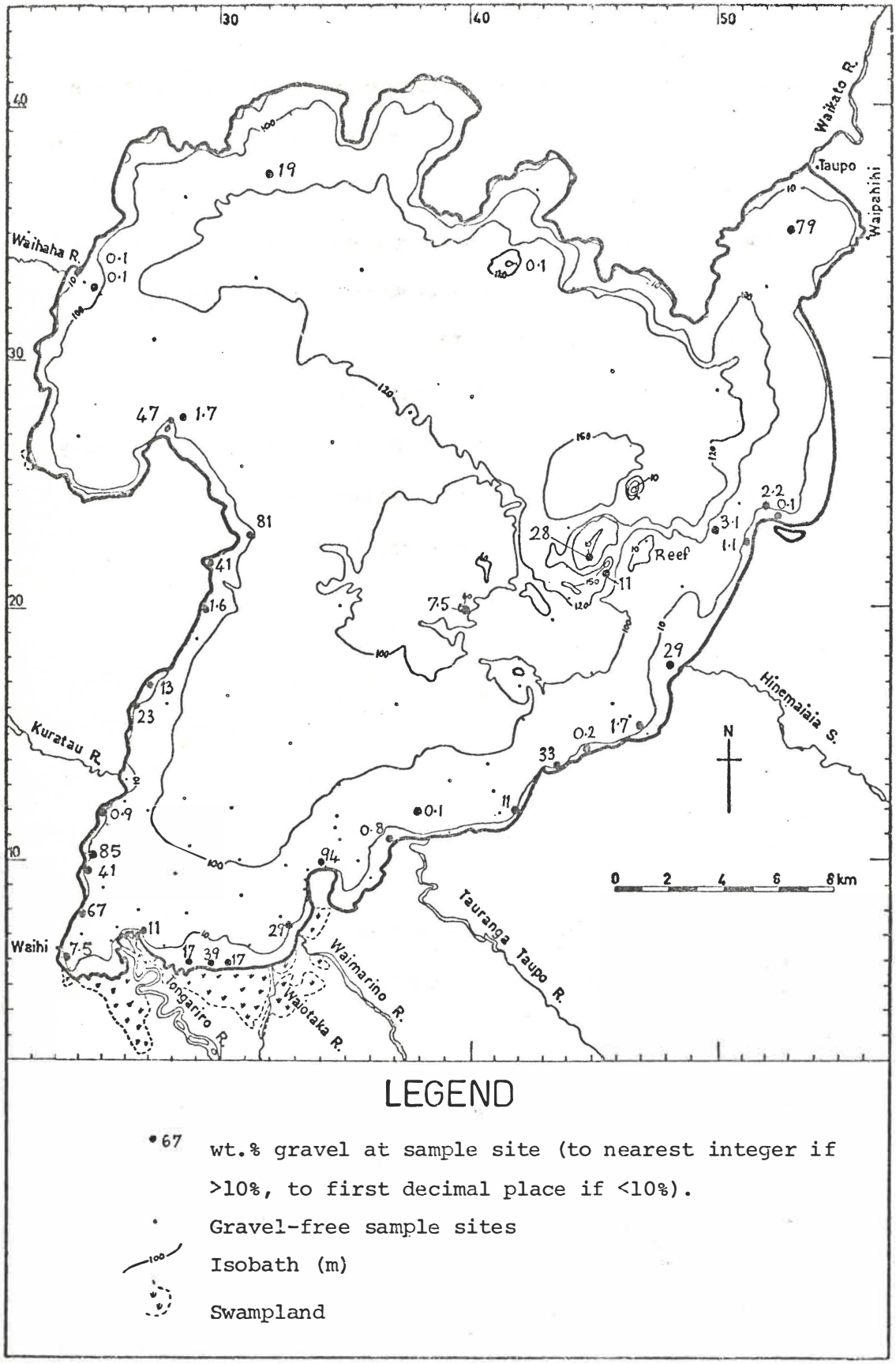


Fig. 5.4. Weight percent gravel (>2.0 mm) in organic-free sediment. Gravel contents occur mainly in shelf sediments (east coast) but are also found on slopes, sub-lacustrine hilltops, and as redeposited material in basinal sediments. Except for sub-lacustrine talus slopes near cliffs (e.g. West Coast), shelf areas near present and pre-existing river mouths (e.g. Oruatua), and Horomatangi Reef, the gravel content in the sediment is almost entirely pumice.

2. Redeposition of sediments can produce poorly sorted mixtures of mud, sand and/or gravels (e.g. samples 67, 70, 86, 92, 105, 106, 110, 115).

3. Sediments on sub-lacustrine hilltops generally have a higher sand-gravel content than the surrounding deeper areas (e.g. samples 56, 57, 85, 88, 120, 121).

4. An unusually high content of gravel (78.7%) occurs at 43 m depth in Tapaueharuru Bay, where the lake bottom is gradually shallowing towards the outflowing Waikato River. Together with 20.6% of sand this accounts for 99.3% of the sediment.

5.6 GRAVEL AND SAND TRENDS

The wt.% of gravel and sand in samples is shown on bathymetric maps (Figs. 5.4 and 5.5 respectively). Gravel-sized material is generally confined to nearshore areas and sub-lacustrine hilltops. Sand content decreases with depth down to about 100 m and then remains fairly constant across basinal areas. Small random variations in basinal sand content from site to site may relate to microtopography or sediment penetration depth during sampling. This sand invariably occurs as a discrete 3.5-4.0ϕ mode.

5.7 SILT AND CLAY TRENDS

Maps of wt.% silt and wt.% clay in samples (Figs. 5.6 and 5.7) both display broad areal trends. Two areas in the southwestern part of the lake have about twice the clay content of those areas at the northern end. An unusually high clay content occurs in the centre of the lake (sample 76). Silt shows a reciprocal pattern, as expected, as wt.% mud is approximately constant over deep areas.

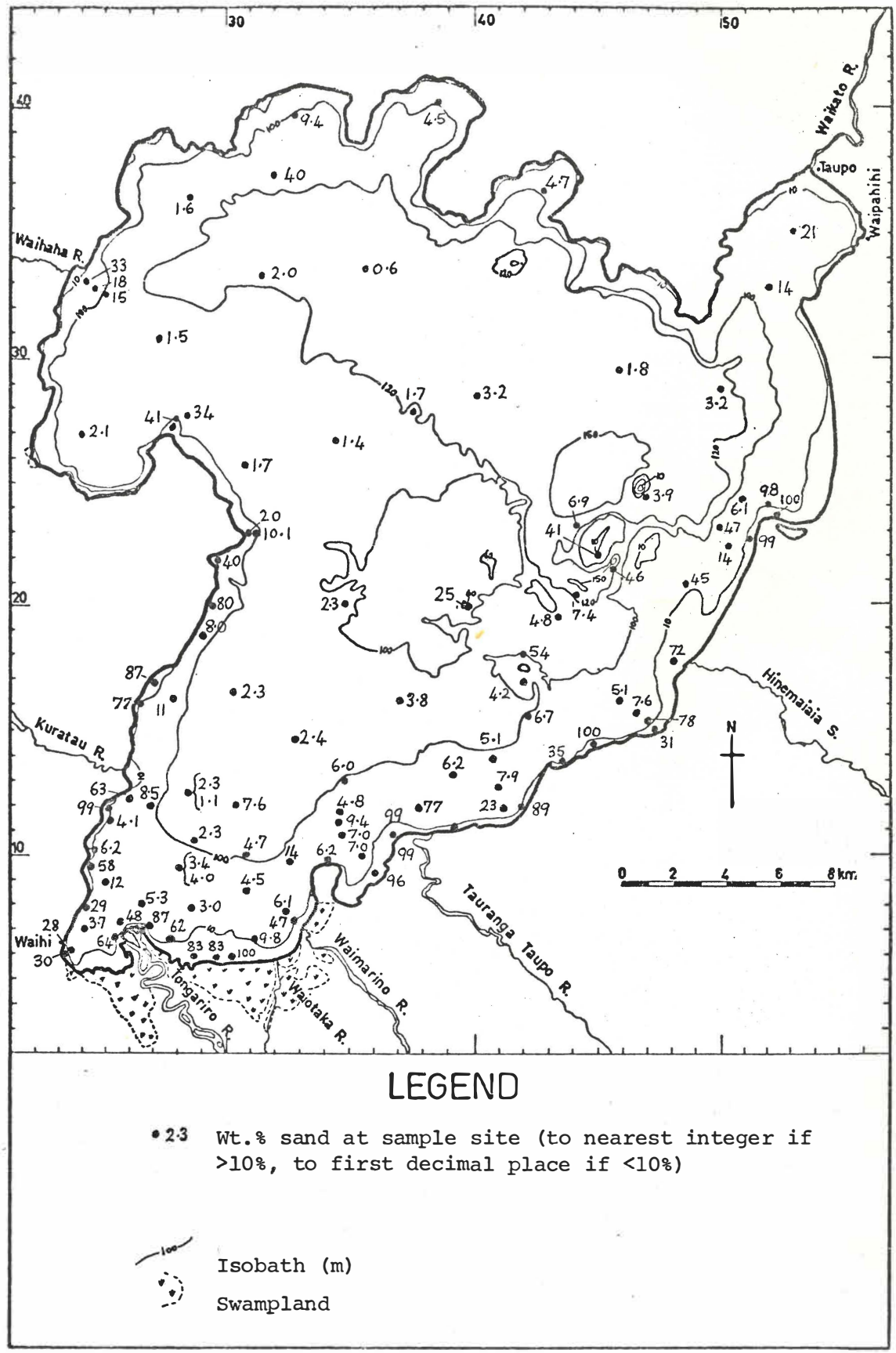


Fig. 5.5. Weight percent sand in organic-free sediment decreases with increasing water depth to about 100 m depth and then remains approximately constant across the lake floor.

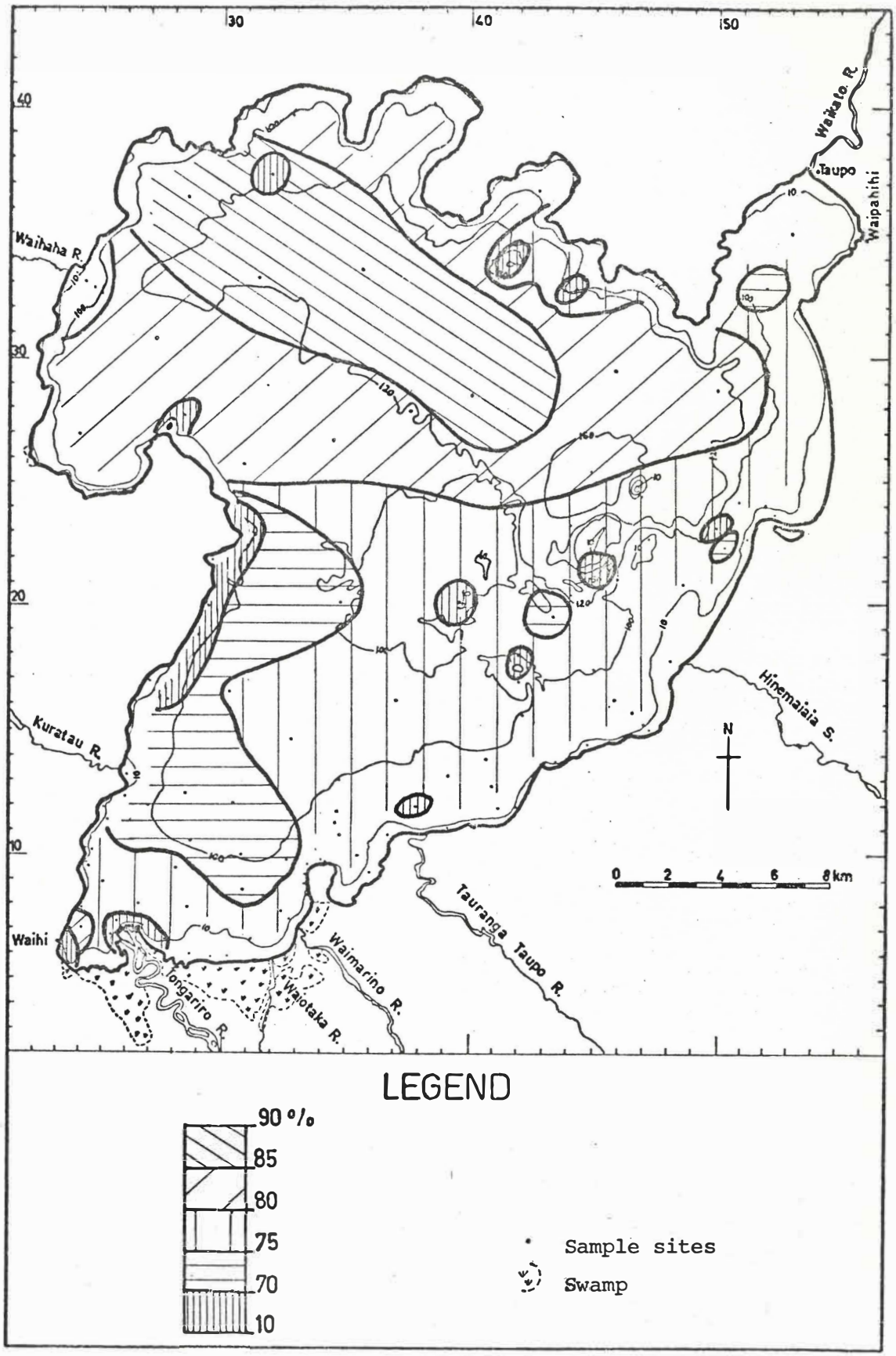


Fig. 5.6. Weight percent silt in organic free sediment

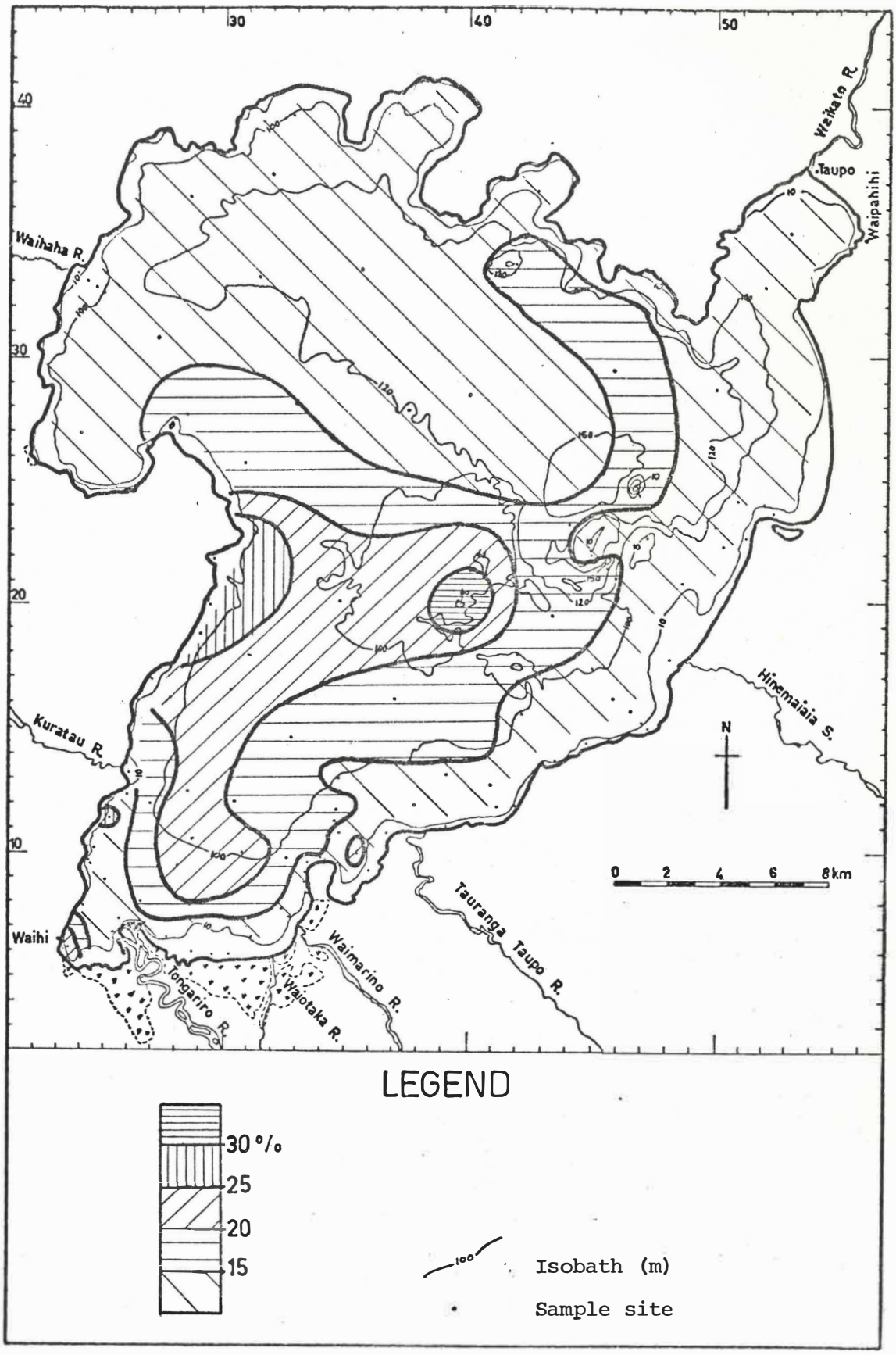


Fig. 5.7. Weight percent clay in organic-free surficial sediments in Lake Taupo.

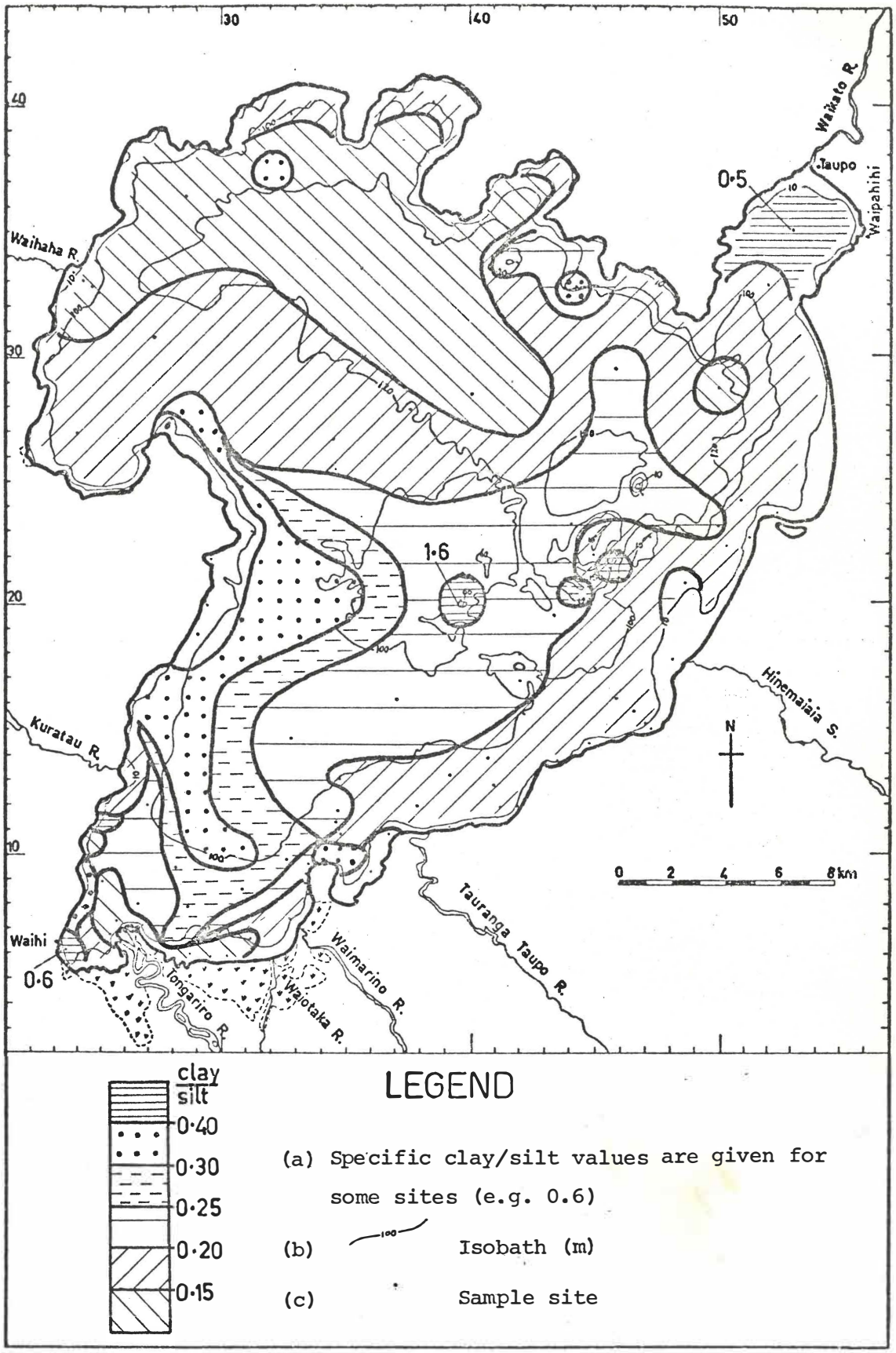


Fig. 5.8. Clay/silt ratio in the surficial sediments of Lake Taupo.

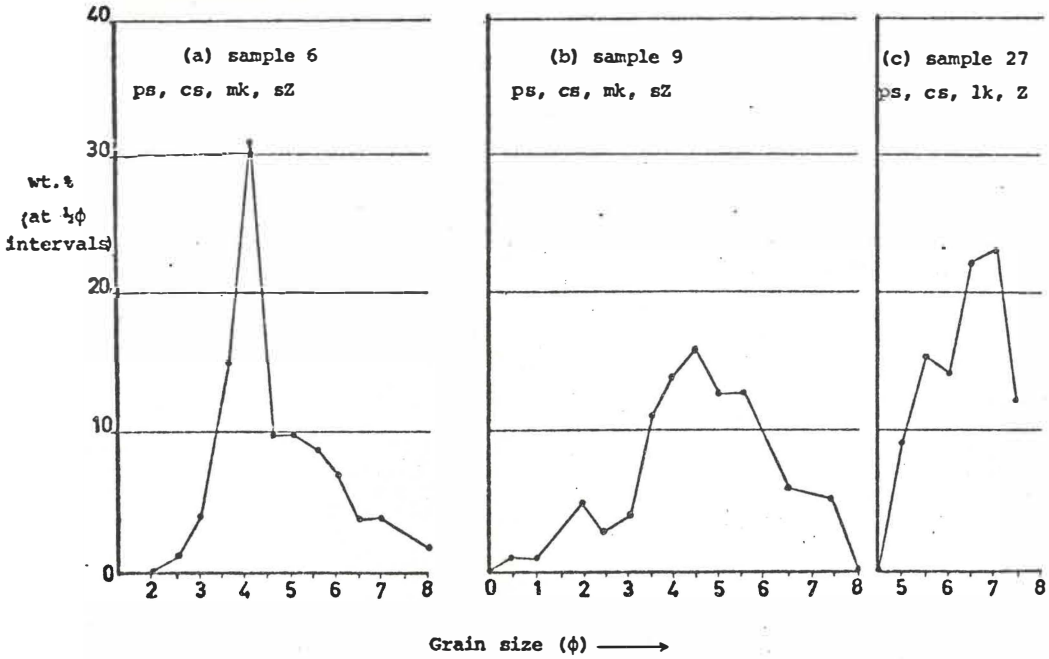
Because of the reciprocal relationship, a map of the ratio of clay/silt produces a clearer pattern which also remains useful at shallow depths as it is independent of sand content (Fig. 5.8). The patterns are likely to be a product of lake and inflow hydrodynamics, sediment source areas and sediment composition, so a discussion of pattern significance is postponed until these factors have been established.

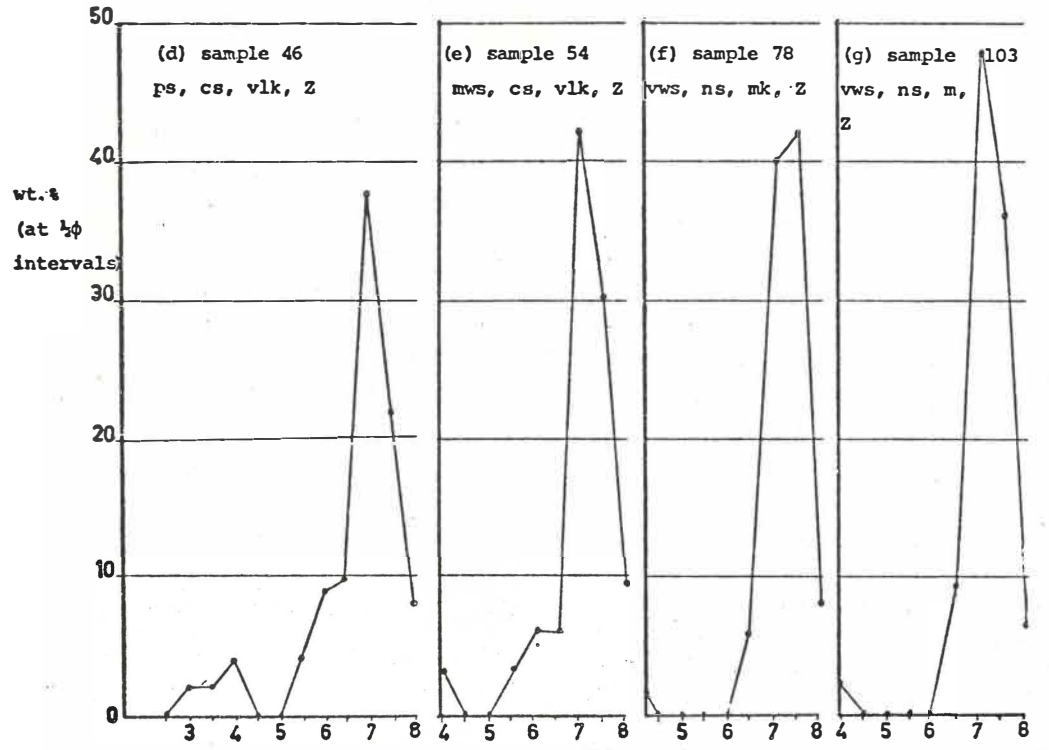
5.8 SILT MODES

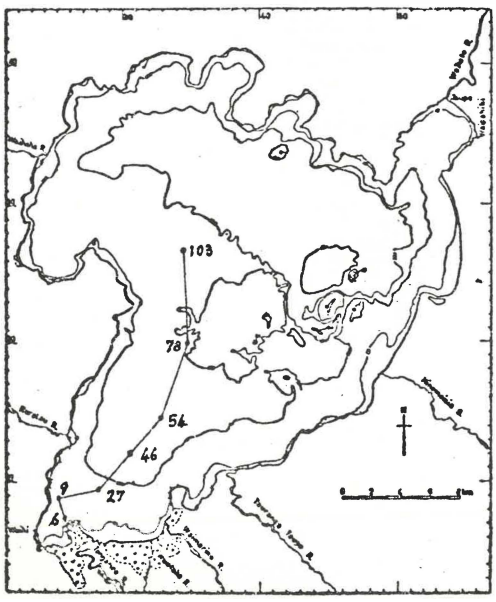
Two persistent modes occur in the silt fraction of samples, one at 5.5-6.0ϕ and the other at 7.0-7.5ϕ. They display a reciprocal relationship, with the 7.0-7.5ϕ mode becoming increasingly abundant towards central lake areas. An example of this trend is shown by the change in relative heights of frequency curve peaks along a transect (Fig. 5.9).

The two modes partly overlap, and the coarse end of the 5.5-6.0ϕ mode often overlaps with the ubiquitous 4.0ϕ sand mode. The fine end of the 7.0-7.5ϕ mode appears truncated at the lower frequency-curve limit (8ϕ) suggesting that this population continues into the coarse clay fraction. For these reasons the weight-percent of each population cannot be accurately determined.

The base width of both modes is approximately the same so the peak heights may be used semi-quantitatively. Values for the ratio 5.5-6.0ϕ mode height:7.0-7.5ϕ mode height show a well defined pattern that is independent of both sand and clay contents (Fig. 5.10). The relative abundance of these two modes is largely responsible for the mean grain size trends in basinal sediments (Fig. 5.11). In the central and central western parts of the lake where silts are almost







Location of sample sites in Lake Taupo

Fig. 5.9

Frequency / grain-size curves for selected sediment samples

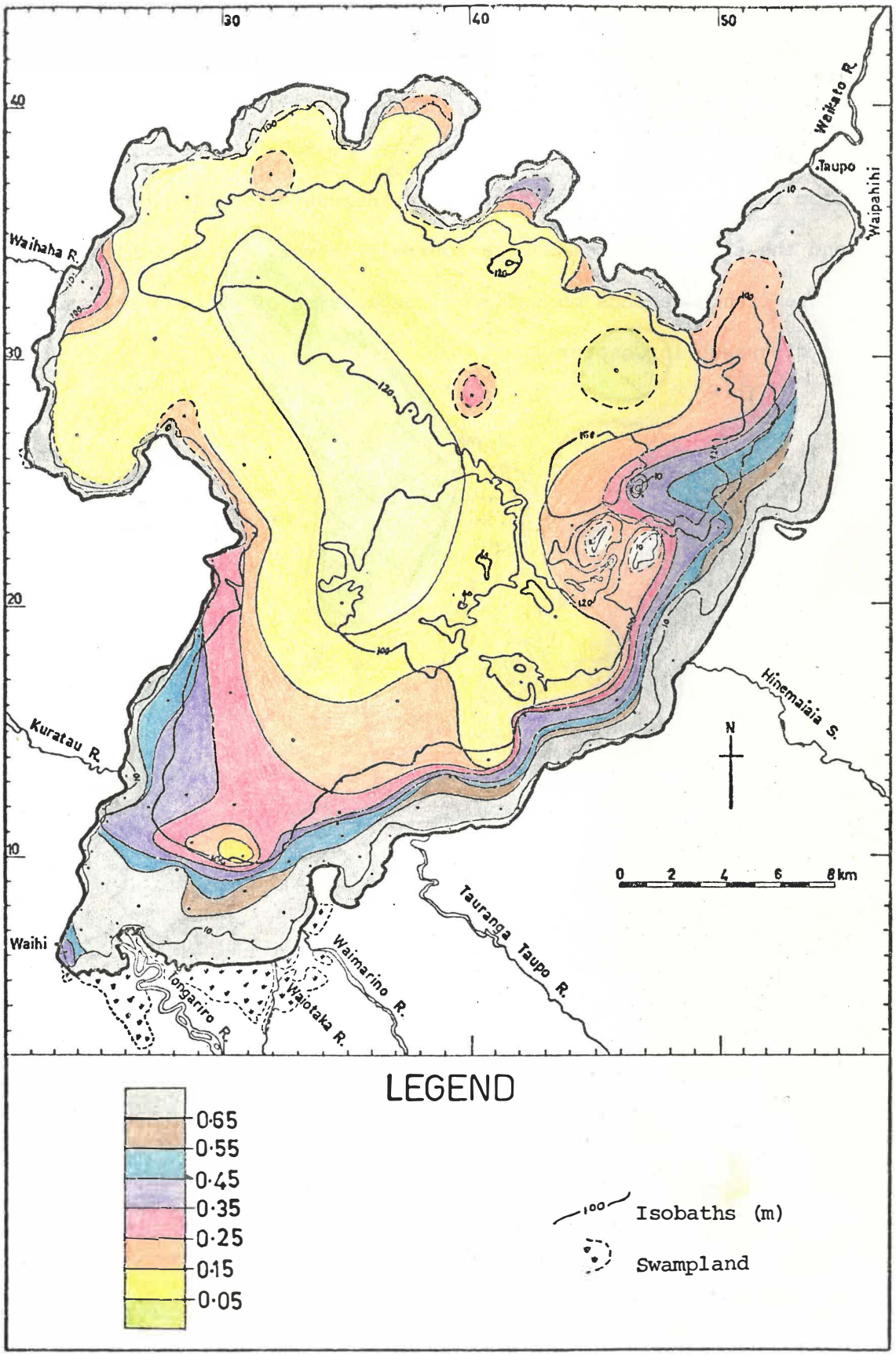


Fig. 5.10. Ratio of the 5.5-6.0ϕ/7.0-7.5ϕ grain size mode heights in the surficial sediments of Lake Taupo.

entirely in the 7.0-7.5ϕ mode the sediment is commonly very well sorted, near-symmetric, mesokurtic silt. As the 5.5-6.0ϕ mode increases away from this area, the mean grain size increases, sorting deteriorates, and the sediment becomes more coarsely skewed. The significance of these trends depends on sediment composition of the two silt modes and is discussed in Chapter 7.

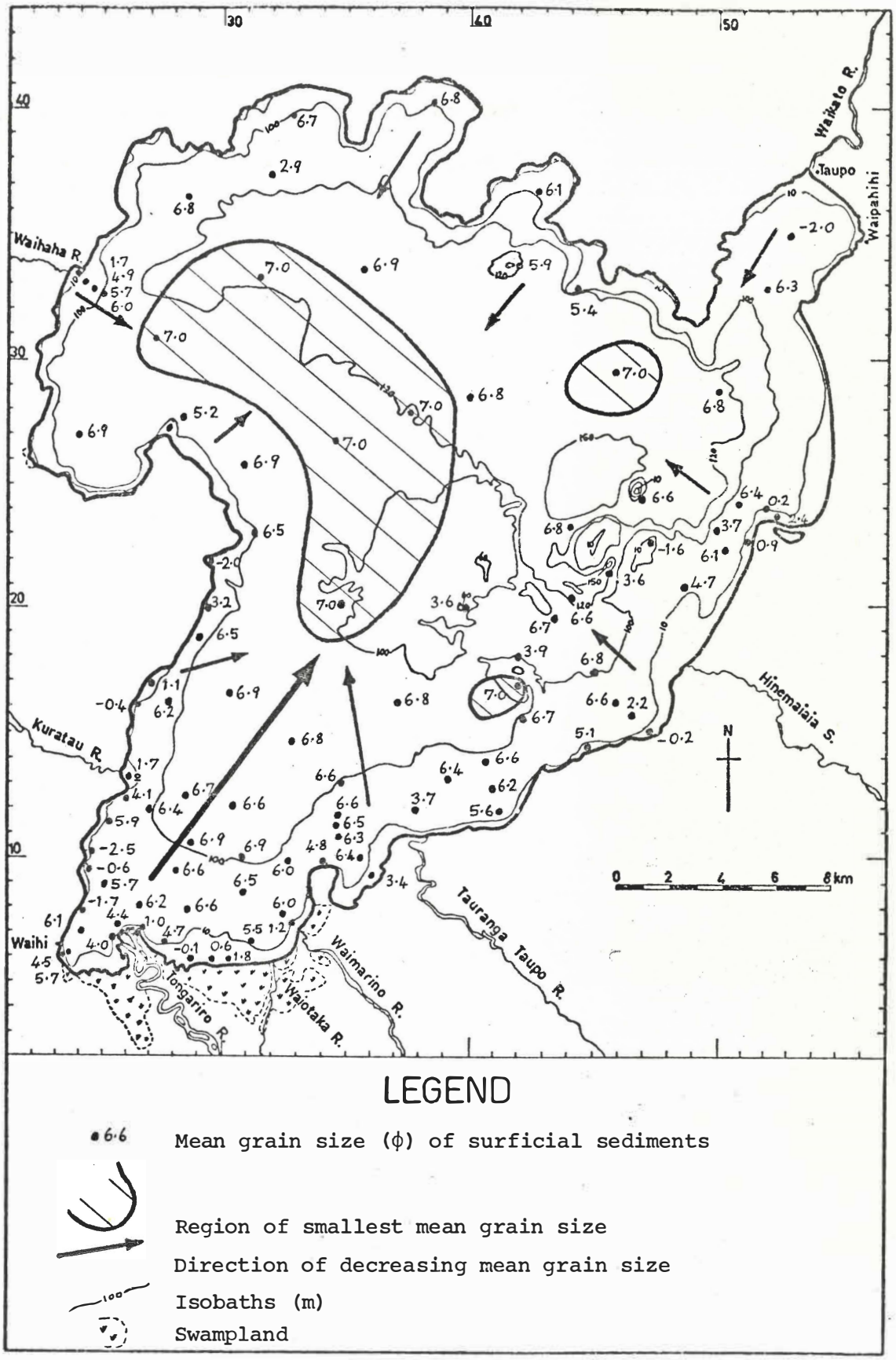


Fig. 5.11. The mean grain size of surficial sediments in Lake Taupo show a general decrease away from river mouths, and all shores towards the central and central northwestern lake regions.

CHAPTER 6

SEDIMENT COMPOSITION

The analysis techniques used to determine sediment composition are discussed under each sub-heading in this chapter. The significance and interpretation of the following experimental results are presented and discussed in Chapter 7.

6.1 ORGANIC MATTER

Method

Sediment organic matter contents were determined from the weight loss following ignition of oven-dried (105°C/8 hours) sediment sub-samples in a muffle furnace for two hours at 500°C. To determine whether or not part of the weight loss on ignition was due to dehydration of clay material (e.g. allophane), four samples Nos. 26, 46, 74 and 90) were subjected to differential thermal analysis. No endothermic dehydration peaks occurred.

Results

Distribution of surficial sediment organic matter content is shown in Fig. 6.1. No significant trends in wt.% organic matter are apparent across basinal regions of the lake. Most deep-water muds have an organic matter content close to the overall mean value of 7.4 wt.%, although contents of 8% or more occur in the deeper parts of Stump Bay, Waihi Bay, and around the Waihaha River mouth. Values lower than this mean correspond to samples with increased sand/gravel content. Shelf sediments are generally free of organic matter except where weed beds occur, as at Stump Bay and Motuoapa Bay.

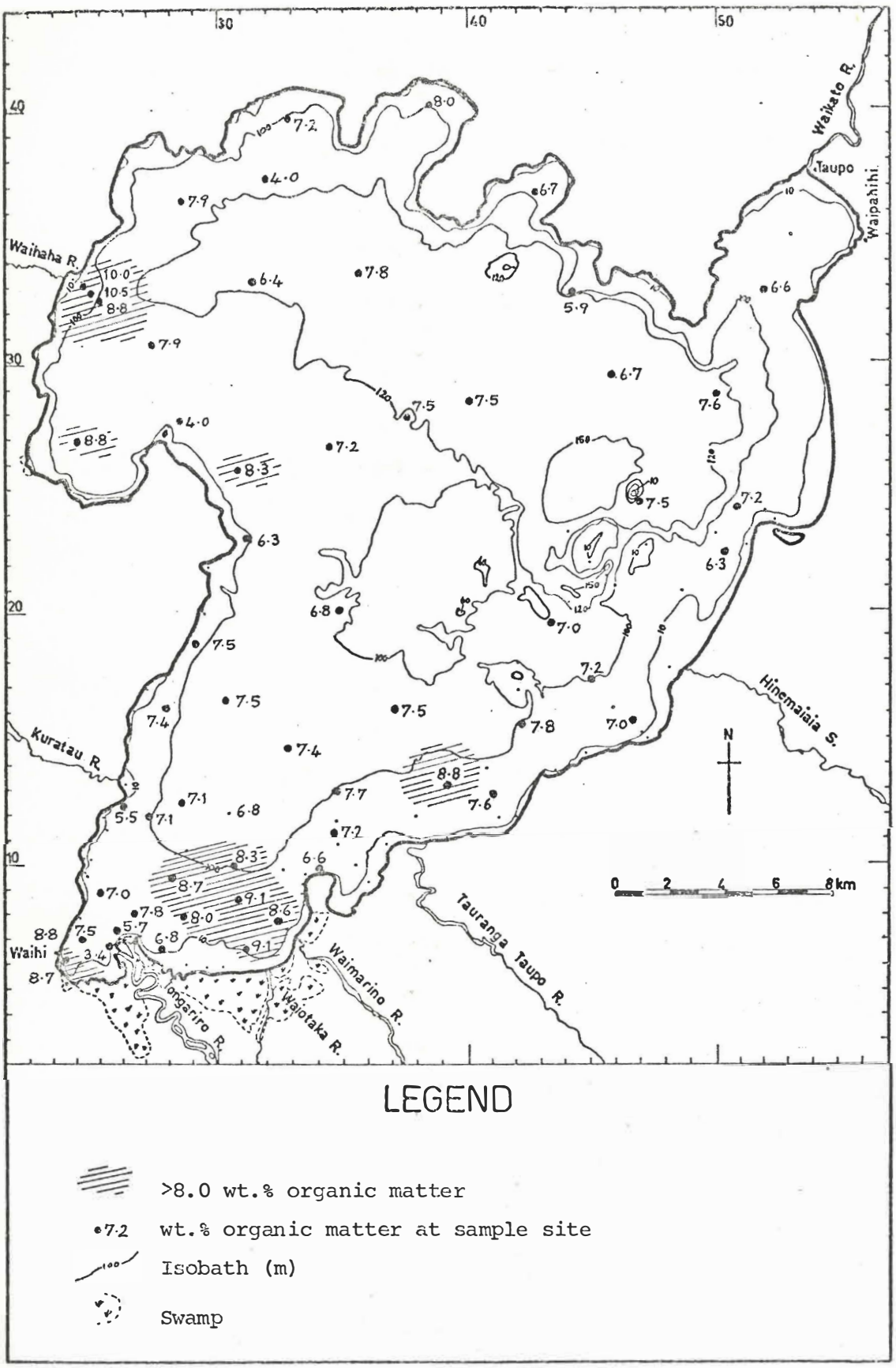


Fig. 6.1. Organic matter content (weight %) in the surficial sediments of Lake Taupo.

Sources of organic matter in the sediments are discussed in Chapter 7.

6.2 X-RAY DIFFRACTION (X.R.D.) OF BULK SEDIMENT

Method

Bulk X.R.D. was used qualitatively to determine the gross mineralogy, and semi-quantitatively for quartz, plagioclase feldspar and crystalline clay mineral content using a modification of the method of Nelson and Cochrane (1970).

Samples were scanned on a Phillips X-ray Spectrometer using Cu Kα radiation with 1° divergence and 1 mm scatter slits, a scanning speed of 2°2θ per minute, a chart speed of 20 mm per minute, a time constant of four seconds and a rate meter setting of 400 counts per second.

Initial scans indicated relatively small amounts of plagioclase feldspar and quartz in a large amount of X.R.D. amorphous material. Quartz concentrations were too low in silt samples for semi-quantitative use of the 4.25Å peak, so the 3.34Å quartz peak was used. No plagioclase feldspar peak occurs in the same region, and the quantitative accuracy of the 3.34Å quartz peak is enhanced by the greater slope angle of the intensity-concentration curve.

Radiation generated at 30 kV and 13 mA gave the most useful 3.34Å peak height range for this work.

Standard Intensity-Concentration Curves

A series of quartz standards were prepared using crushed quartz (<30 μm) and pumice mixed in weight percent ratios from 0 to 45% quartz at approximately 5% intervals. Pumice was used to

simulate the amorphous silica in the sediments. No magnetite was added (*cf.* Nelson and Cochrane, 1970). The resulting 'line of best fit' curve showed a maximum error of 14% and passed through the ordinate intersection (Appendix 4).

An intensity-concentration curve for plagioclase feldspar was modified from that given by Nelson and Cochrane (1970, p.158) by applying the linear relationship between their quartz (4.26Å) and feldspar (3.20Å) intensity-concentration curves to the quartz (4.26Å) intensity-concentration curve obtained above (Appendix 4). Quartz and acid plagioclase feldspar have similar X-ray mass absorption coefficients under Cu Kα radiation(e.g. albite, 34; quartz, 35; Carroll, 1970), and Nelson and Cochrane used Oligoclase standards claiming (p.153) "...other plagioclase varieties would exhibit small differences in peak height intensities".

Sample Preparation

Dried samples (8 hour at 55°C) were crushed in a ring mill to less than 30 μm and packed into sample holders using the 'back-filling' method. These unoriented mounts were scanned from 3° to 40°2θ. Samples were selected at random to reduce the possibility of instrumental drift creating artificial areal concentration patterns in the semi-quantitative results. A quartz-in-araldite standard was scanned prior to each sample as a check on possible instrumental drift.

Results

Quartz and plagioclase feldspar were the only minerals identified in bulk samples.

In sandy sediments the feldspar basal spacings and relative reflection intensities (e.g. Fig. 6.2), correspond to high temperature albite. In deep-water muds, the feldspar content is too low to give sufficient peak resolution for positive identification of the dominant plagioclase composition. Semi-quantitative use of the 3.20Å plagioclase X.R.D. peak assumes that only one plagioclase composition is present, although more than one may be present, giving superimposition of the main peaks.

Plagioclase and quartz contents as weight percentages (wt.%) of organic-free sediment are given in Appendix 5, and areal trends within the lake in Figs. 6.3 and 6.4 respectively. The highest concentrations of both quartz and plagioclase in deep-water sediments, occur around the southern end of the lake, and generally decrease in abundance towards the northeast, reaching approximately constant concentrations in central and northern parts of the lake. The pattern of decreasing plagioclase content generally extends further northwards than that of quartz, and the feldspar:quartz ratio generally decreases towards the northern regions of the lake (Fig. 6.5), but perhaps the most significant difference between the two patterns is the local increase in plagioclase content alone on several sub-lacustrine topographic highs (e.g. sample site nos. 76, 120) and in deep-water sediments containing redeposited material (e.g. sample site nos. 67, 105, 106, 115). The significance of quartz and plagioclase content trends is discussed in Chapter 7.

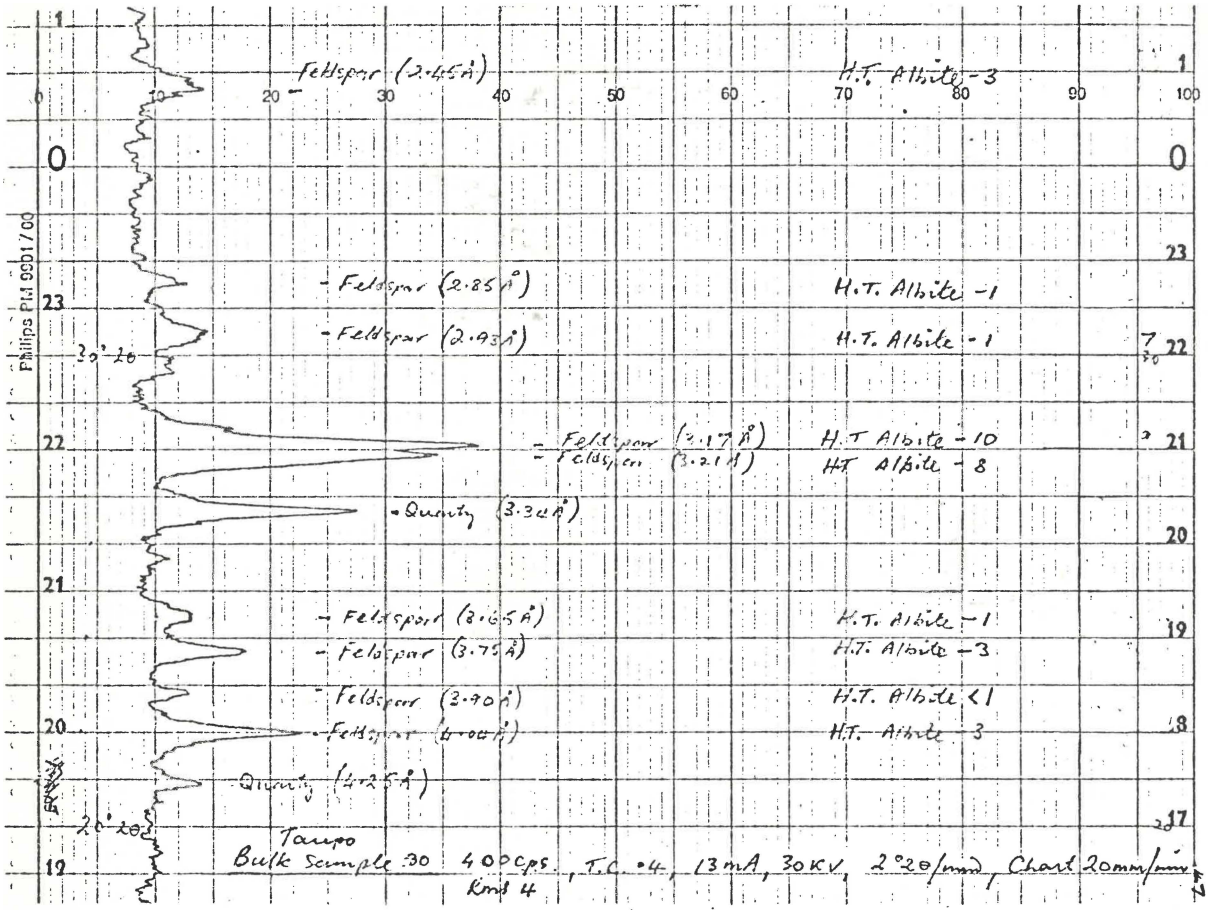


Fig. 6.2. A typical X-ray diffractogram of sand-rich sediment showing basal spacings and reflection intensities for quartz and plagioclase feldspar (?high-temperature albite).

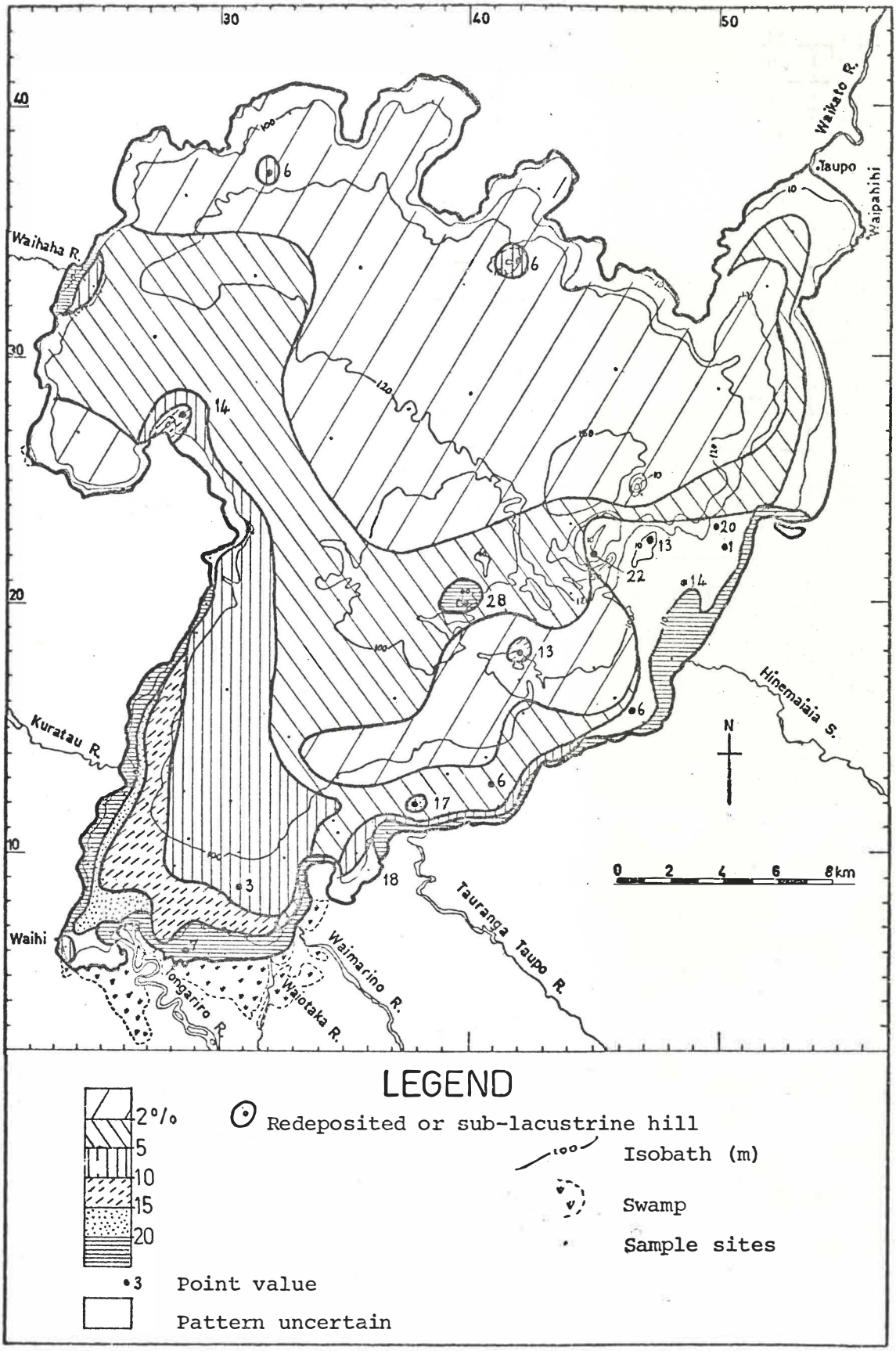


Fig. 6.3. Weight percent plagioclase feldspar in the organic-free surficial sediments of Lake Taupo.

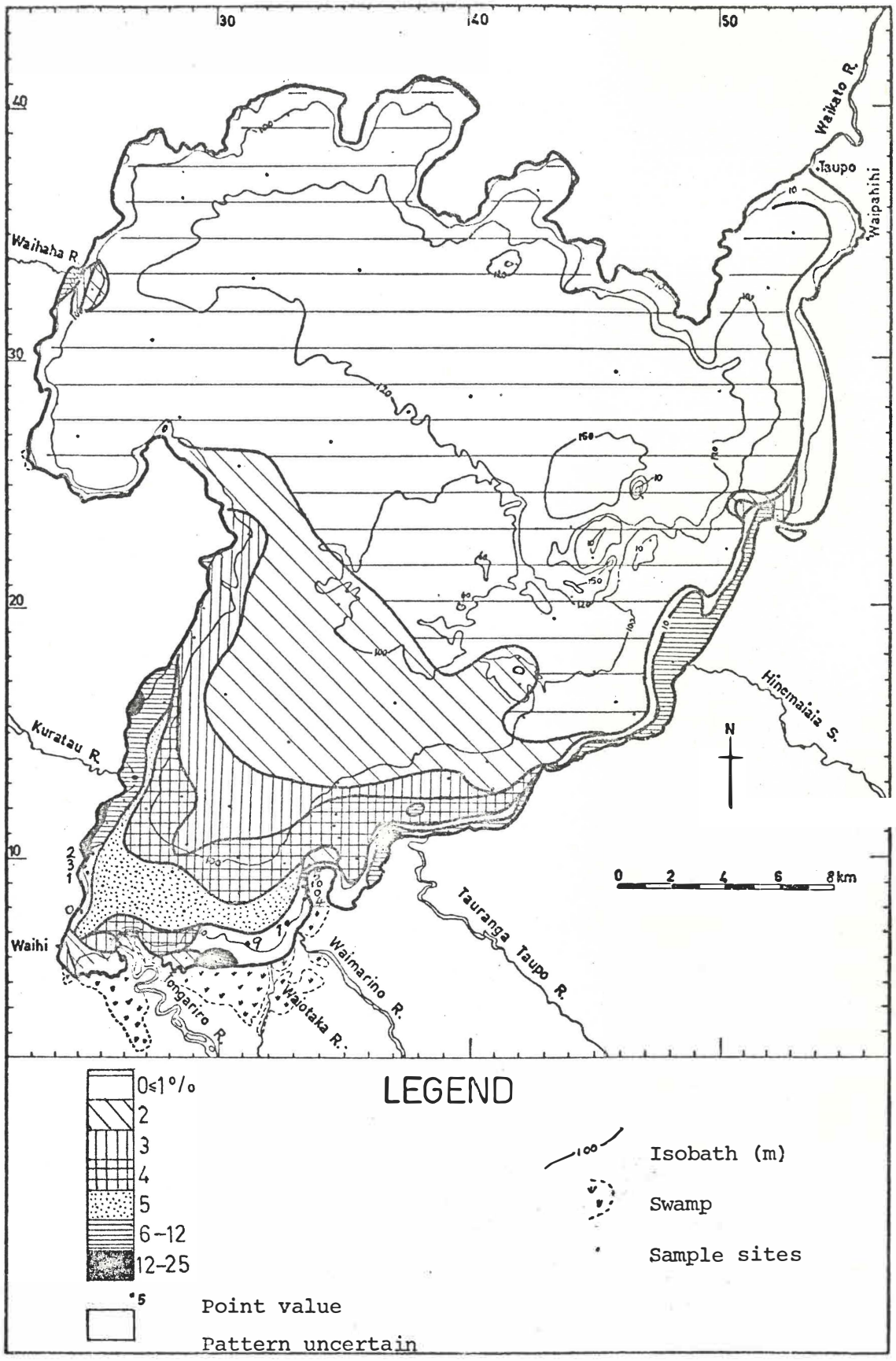


Fig. 6.4. Weight percent quartz in the organic-free surficial sediments of Lake Taupo.

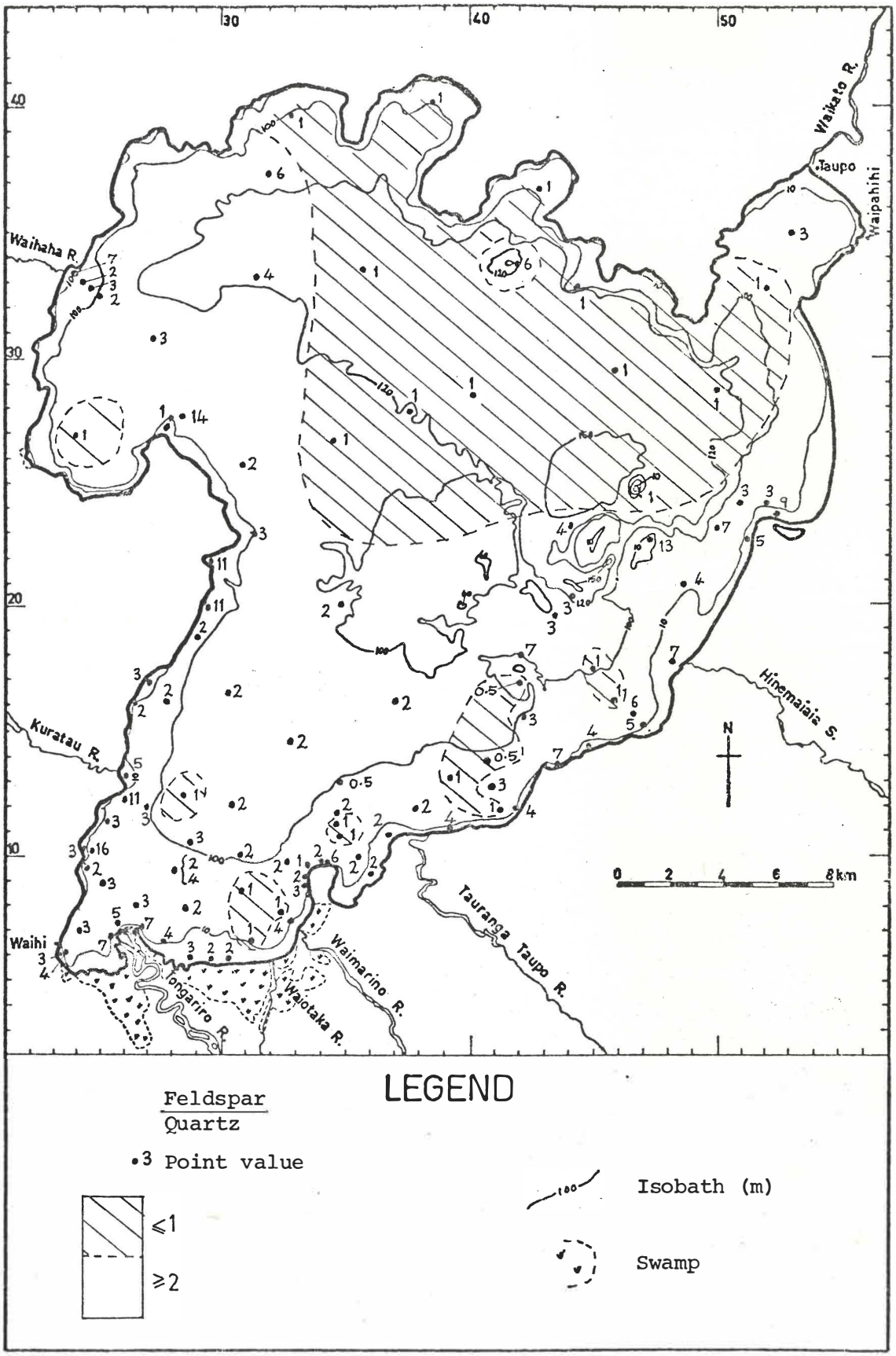


Fig. 6.5. Approximate plagioclase feldspar/quartz ratios in Lake Taupo sediments.

6.3 X.R.D. OF ORIENTED MOUNTS

Method

Organic-free, less than 4ϕ (63 µm) sized material was fractionated into coarse silt (4-5ϕ, 63-31 µm), and medium silt (5-6ϕ, 31-16 µm), according sedimentation times for particles of specific gravity (S.G.) 2.65 (Tanner and Jackson, 1947), and fine-very-fine silt and clay by centrifugation (after Murley, 1965) assuming a particle S.G. of 2.3. Each fraction was decanted twice to minimise the content of material smaller than the given size range. Oriented drop-on-glass-slide (D.O.G.S.) mounts of all samples were prepared for each size fraction using thick slurries to minimise differential settling effects. These were dried at room temperature and scanned on the Phillips X-ray Spectrometer using the bulk XRD analysis instrument settings.

Results

Silt fraction

Feldspar and quartz occur in all silt fractions, with the feldspar:quartz ratio decreasing in the medium to very fine silts (31-2 µm; Table 6.1). Generally the feldspar and quartz contents in the silt fractions of a given sample are of the same order of magnitude as their respective contents in the corresponding bulk sample, assuming the feldspar and quartz intensity concentration curves used for bulk sample determination apply equally well to the oriented silt-fraction mounts. However, this assumption is tenuous for several reasons. The coarse silt (31-63 µm) grain size exceeds that of the crushed standards and bulk samples (<31 µ), orientation

No.	SILT									Bulk sample		
	2-16μ			16-31μ			31-63μ					
	Q	F	F/Q	Q	F	F/Q	Q	F	F/Q	Q	F	F/Q
34	4	7	1.8	4	7	1.8	3	7	2.3	4	10	2.5
36	4	7	1.8	4	7	1.8	2	8	4.0	4	8	2.0
12	2	6	3.0	2	3	1.5	2	17	8.5	4	14	3.5
68	1	0	-	0	0	-	0	0	-	0	1	-
53	3	6	2.0	2	6	2.0	1	6	6.0	2	6	3.0
55	2	3	1.5	3	6	2.0	4	13	3.3	2	4	2.0
84	1	0	-	0	0	-	0	0	-	1	4	4.0
97	0	0	-	1	1	1.0	0	3	-	0	0	-
101	1	1	1.0	1	3	3.0	0	14	-	0	0	-
104	2	3	1.5	4	7	1.8	2	11	5.5	2	3	1.5
109	1	1	1.0	0	1	-	1	3	3.0	2	4	2.0
115	2	4	2.0	1	1	1.0	1	6	6.0	1	6	6.0

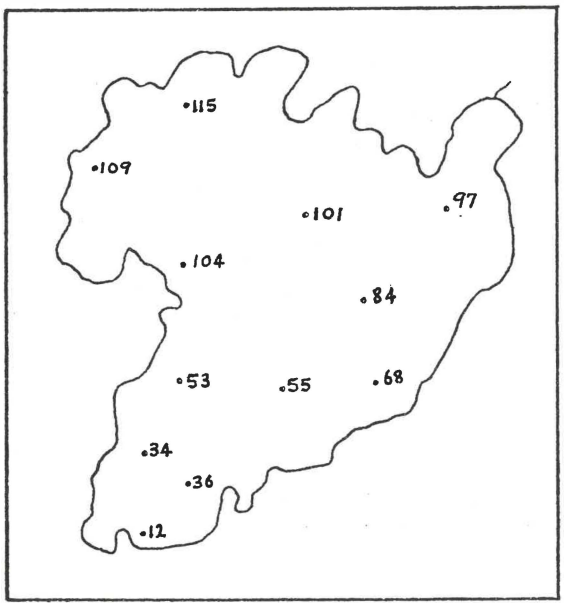


Table 6.1. Variation of quartz and feldspar (wt.%) through silt fractions (selected representative samples).

of grains increases as grain size decreases, and fractionation may have altered any masking effects of amorphous material. In the fine-very fine silt fraction (2-16 μm) the 001 peaks of plagioclase and quartz may be enhanced by illite peaks (114 reflection at 3.50Å, 006 and 024 reflections at ∿3.35Å, respectively). Trace amounts of illite (10Å) and kaolinite (7Å) occur in the 2-16 μ fraction in most samples towards the southern end of the lake (see section 6.4).

Clay fraction

The bulk of clay fractions in all samples is amorphous to X-rays. Small amounts of crystalline clay minerals, including illite, kaolinite and montmorillonite, commonly occur but in amounts that are collectively insufficient to make quantitative use of the 4.46Å peak (Nelson and Cochrane, 1970). Identification of the crystalline clay minerals is based on diagonistic basal spacings, relative reflection intensities, and changes in these with glycol and heat treatments (Table 6.2; Carroll, 1970). Effects of these procedures on a typical clay fraction are shown in Fig. 6.6. Sample 99 (Tapaueharuru Bay) is the only sample containing no illite and detectable amounts of montmorillonite, so shift of the 17.0Å glycolated montmorillonite peak to 10Å on heating to 300°C is clear (Fig. 6.7).

The relative peak heights of kaolinite, illite and montmorillonite are given for all samples in Appendix 6. Neither absolute quantities of each of these clay minerals, nor their relative abundance with respect to one another, can be calculated from the reflections obtained, however, maps of the reflection intensities

Table 6.2. Identification of crystalline clay minerals (oriented mounts) using X-ray diffraction (after Carroll, 1970).

Clay mineral	Basal d(001) spacing	Glycolation effect (8 hrs., room temperature)	Heating effect (1 hour)
Kaolinite	7Å	No change	At 550-600°C becomes amorphous to X-rays.
Illite	10Å	No change	May become more intense
Montmorillonite (Ca/Mg + $2H_2O$)	15Å	Expands to 17Å	At 300°C shifts to 10Å.
Vermiculite	14Å	No change	Dehydrates in steps
Feldspar	3.2Å	No change	No change

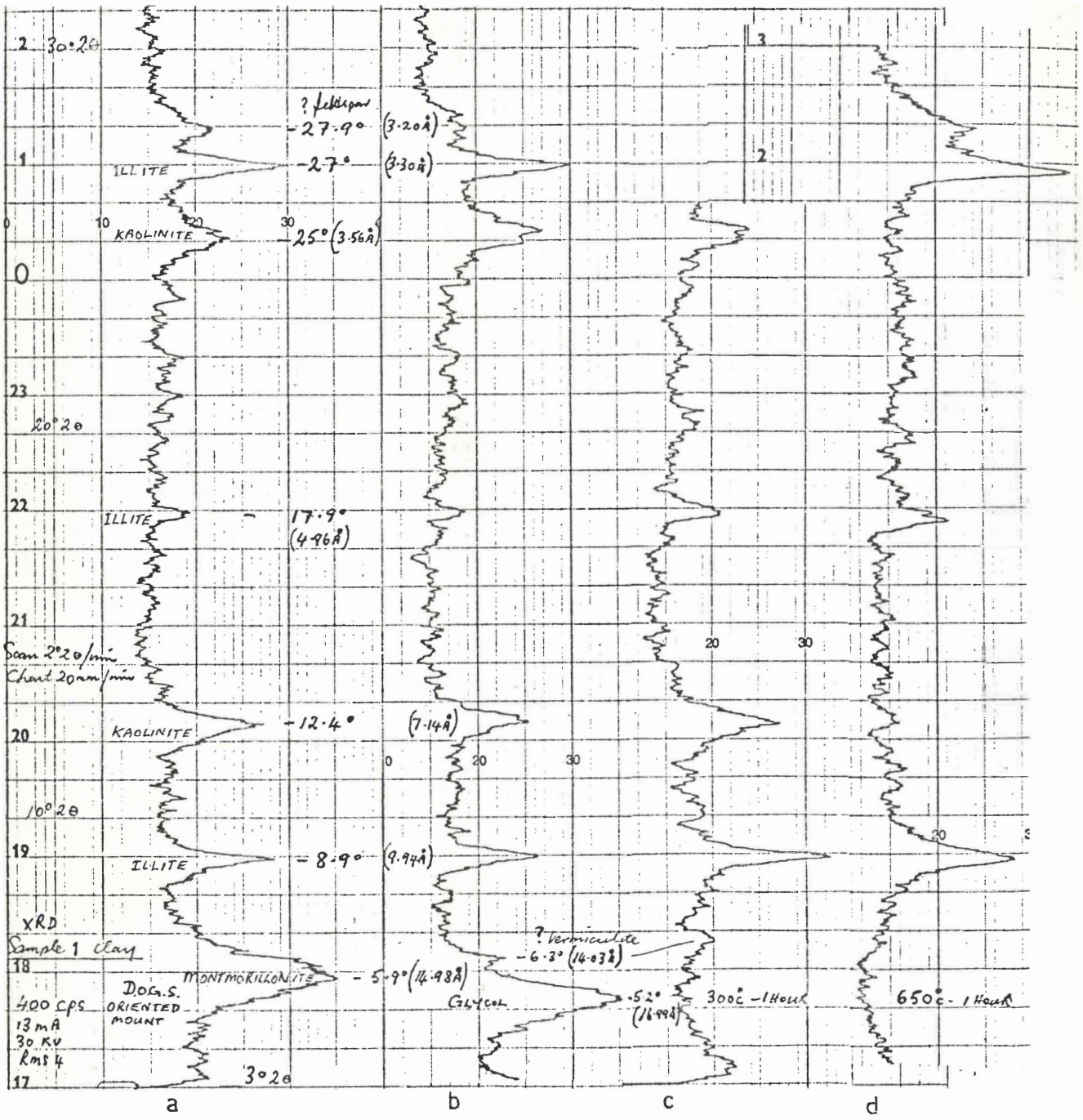


Fig. 6.6. A series of X-ray diffractograms of the clay fraction (D.O.G.S) from sample 1 showing the reflection peaks of (a) the untreated clay (b) glycol treated clay (c) clay heated to 300°C and (d) clay heated to 650°C.

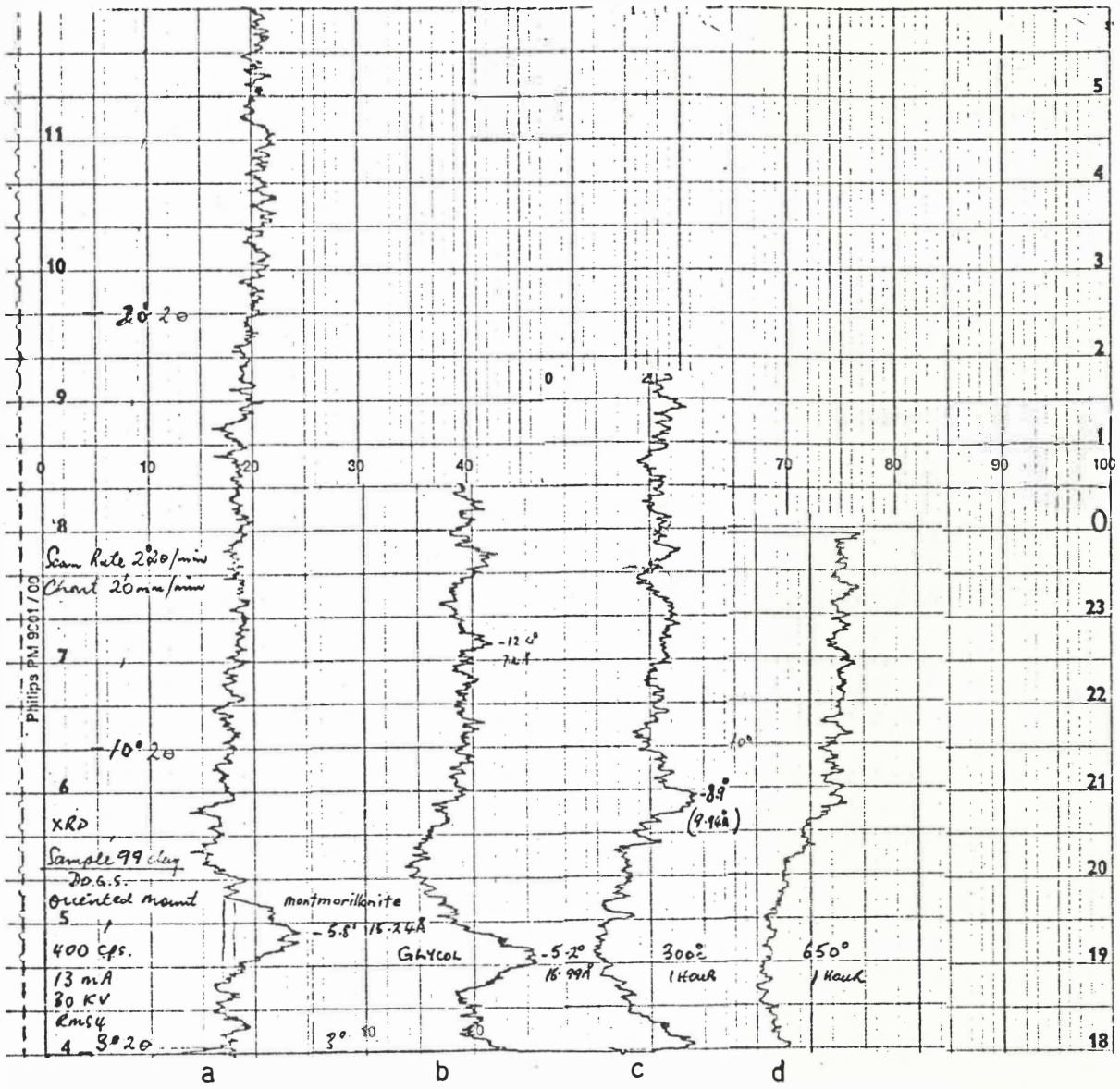


Fig. 6.7. A series of X-ray diffractograms of the clay fraction (D.O.G.S) from sample 99 showing (a) the reflection peak of untreated montmorillonite (b) peak shift after glycol treatment (c) peak shift on heating to 300°C and (d) peak collapse on heating to 650°C.

(peak height) of a given basal spacing for each crystalline clay mineral show strong areal trends. These are given for kaolinite (7Å peak) in Fig. 6.8, for illite (10Å peak) in Fig. 6.9, and for montmorillonite (15Å peak) in Fig. 6.10. The areal trends of both kaolinite and illite concentrations in the clay fraction are broadly similar, decreasing northeastwards from their highest values at the southern end of the lake. Such a trend is less apparent for montmorillonite, which shows high concentrations in the clay fraction from central and northeastern lake positions (Fig. 6.10). Montmorillonite abundances in the clay fraction multiplied by total clay abundance in the sediment shows that the highest montmorillonite concentrations in the sediment occur in the southwestern corner of Waihi Bay and on a central lake topographic high (Fig. 6.11).

Further discussion and interpretation of the areal trends of crystalline clay mineral abundance are presented in Chapter 7.

6.4 DIFFERENTIAL THERMAL ANALYSIS (D.T.A.)

Method

Dry bulk (55°C) and clay (<2 μm) samples (9, 25, 46, 54, 74, 89, 93) were subjected to differential thermal analysis using Stone D.T.A. equipment. Samples were heated in air to 1000°C at a rate of 10°C per minute.

Prior to analysis, samples were stored for 96 hours with $MgNO_3.6H_2O$ to equilibrate moisture content (r.h. 55% at 18°C) for reproducibility of low temperature peaks, and mixed with calcined Al_2O_3 in a ratio of 1:3 by weight.

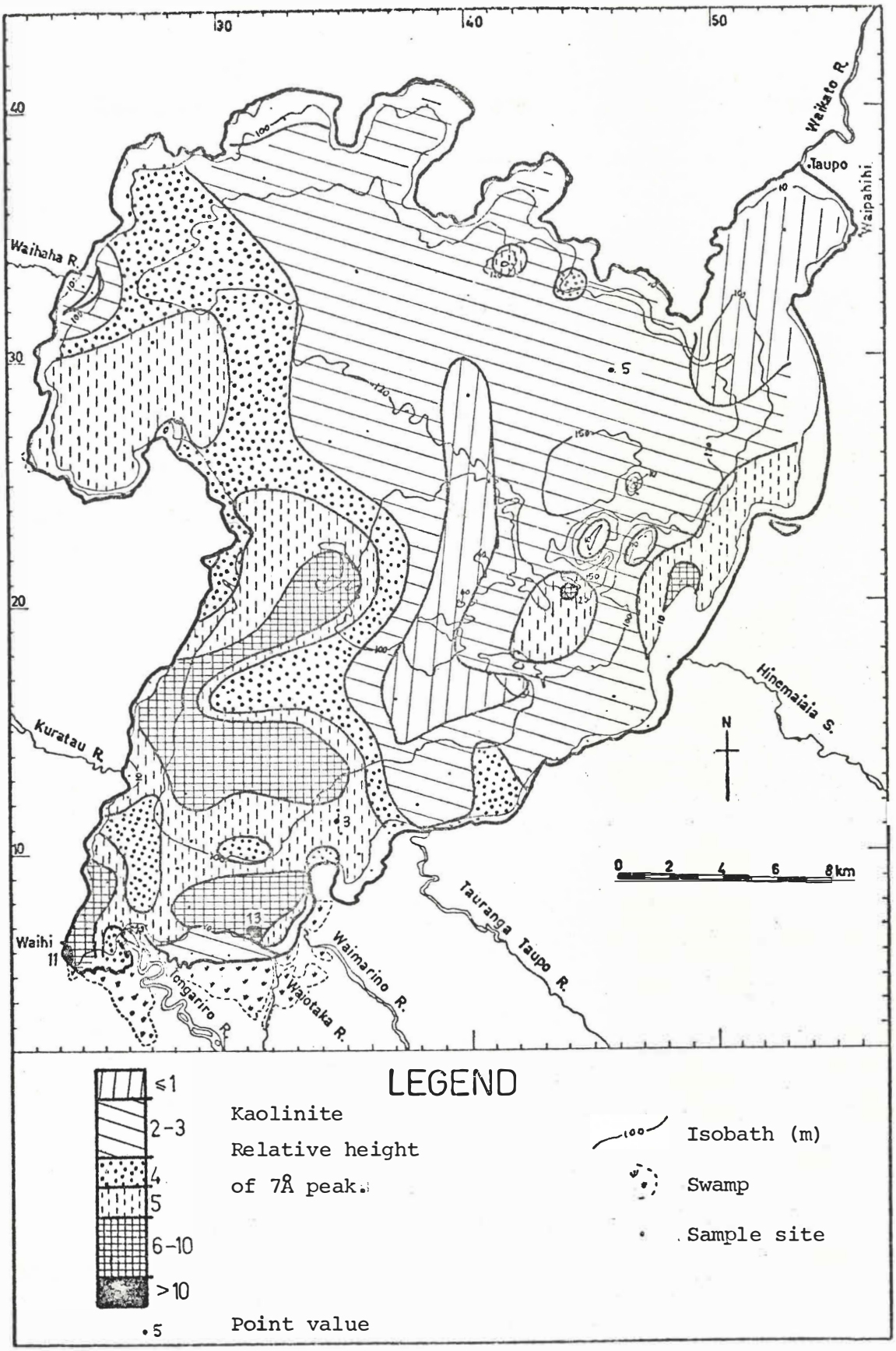


Fig. 6.8. Relative heights of 7Å kaolinite peaks obtained from X.R.D. of oriented clay mounts (D.O.G.S.).

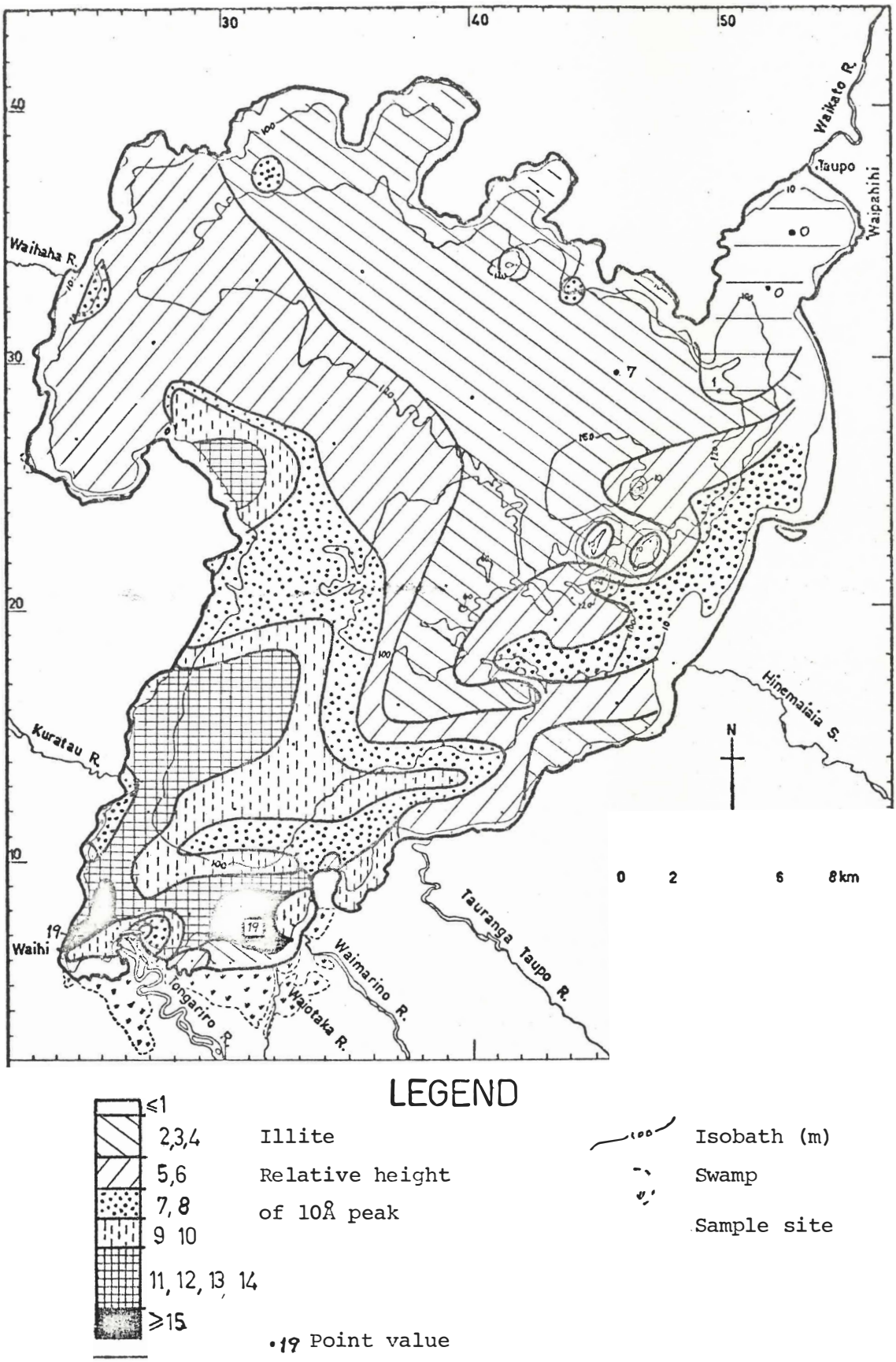


Fig. 6.9. Relative heights of 10Å illite peaks obtained from X.R.D. of oriented clay mounts (D.O.G.S.).

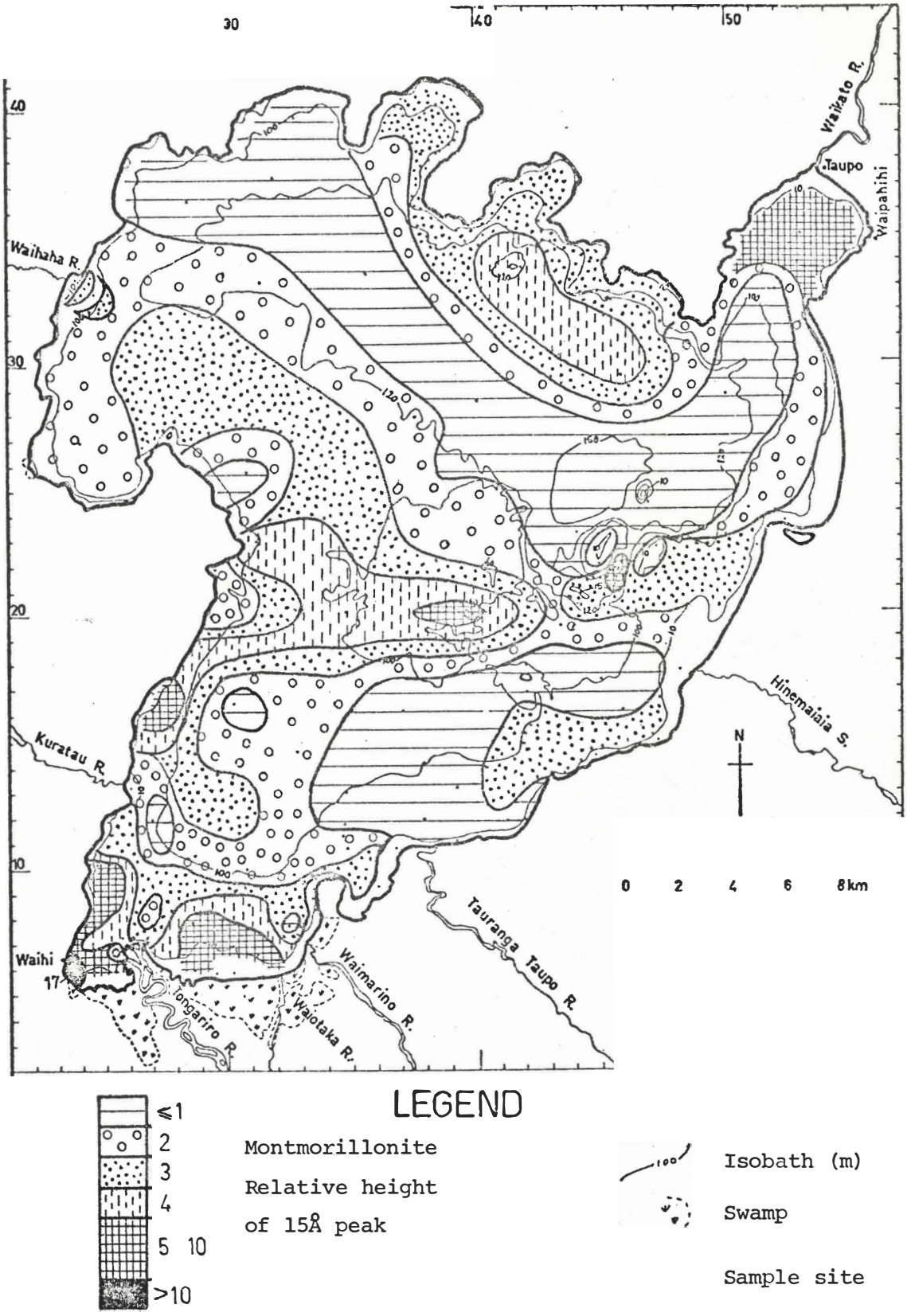


Fig. 6.10. Relative heights of 15Å montmorillonite peaks obtained from X.R.D. of oriented clay mounts (D.O.G.S.)

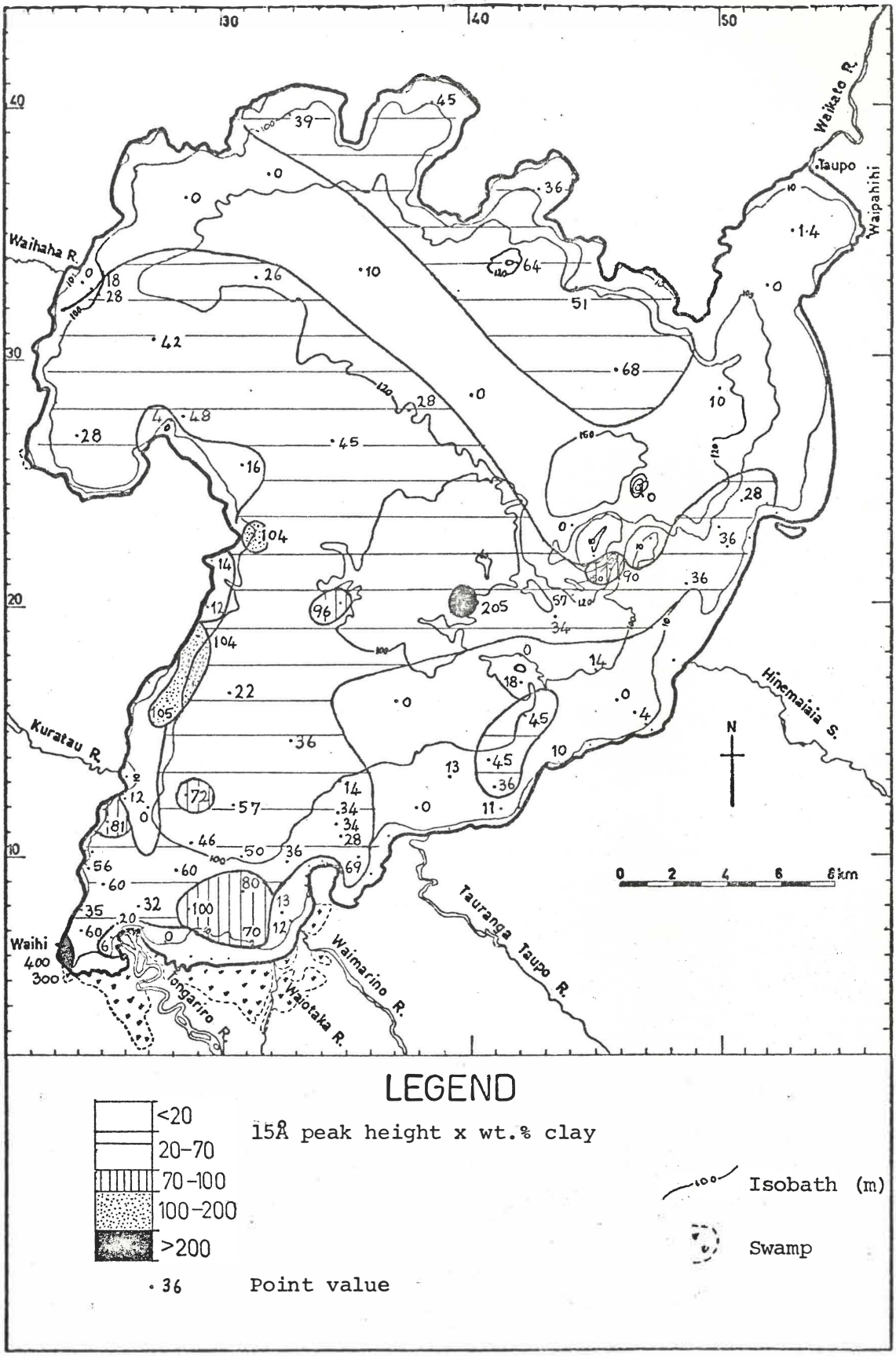


Fig. 6.11. Relative abundance of montmorillonite in the sediment as a product of the 15Å X.R.D.peak height and wt.% clay.

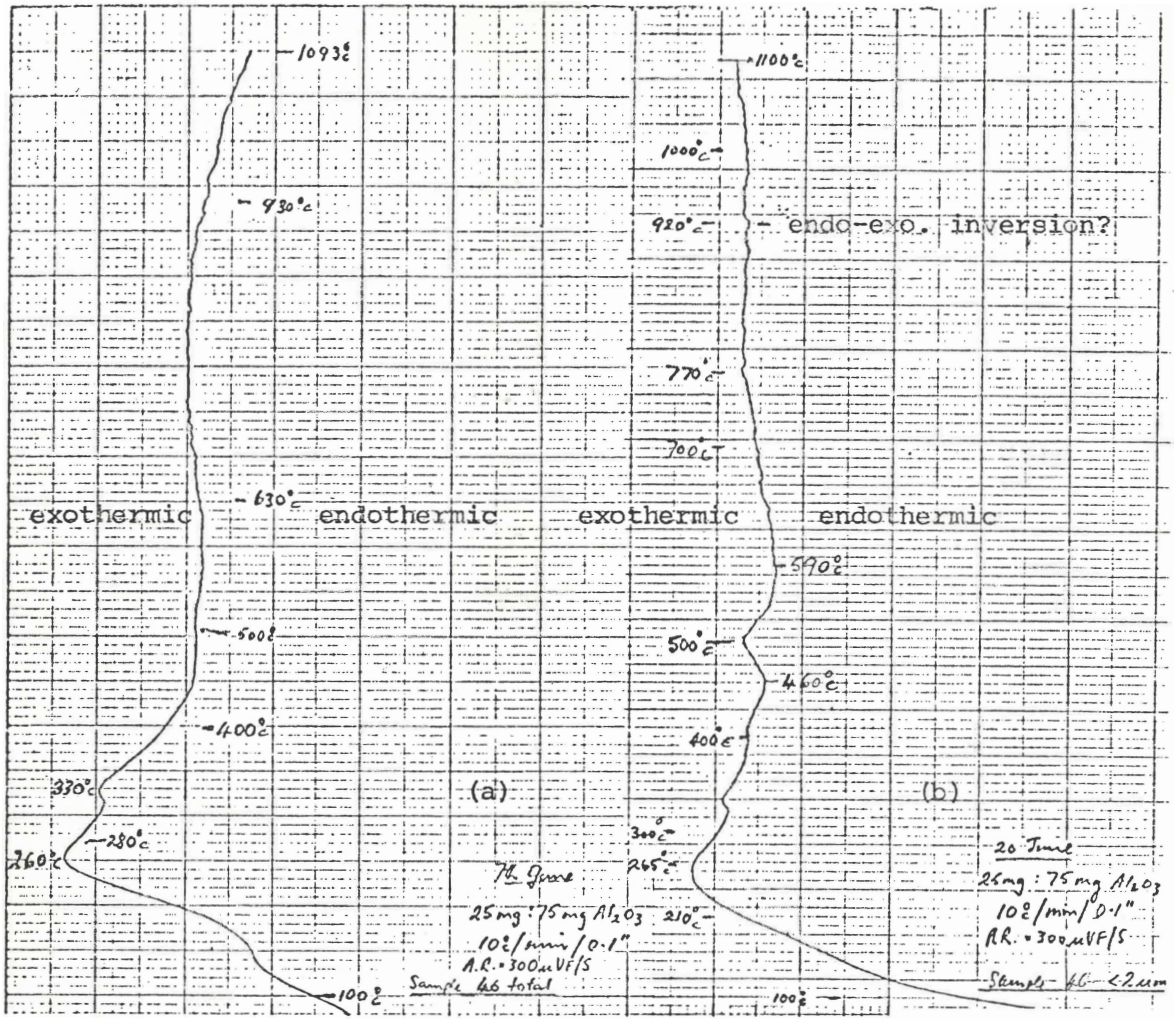


Fig. 6.12. D.T.A. thermographs of (a) a typical, dry, basinal mud, and (b) the corresponding clay fraction.

Results

The bulk samples have generally similar thermographs, showing only organic matter combustion peaks at 260°C and 330°C (Fig. 6.12a).

In the clay samples (treated with hydrogen peroxide) these peaks are smaller or non-existent. Small endotherms occur at approximately 460°C and 590°C (broad) and/or a small exothermic peak 500°C in all clay thermographs (Fig. 6.12b). Montmorillonite has a main endotherm at about 600°C, a smaller endotherm at 700°C and an endotherm-exotherm inversion at about 900°C (Mackenzie and Caillére, 1975). The latter two may be present in Fig. 6.12b but are inconclusive. Kaolinite also has an endotherm at about 600°C but the characteristic sharp exotherm at about 980°C is absent, suggesting that any kaolinite contribution to the 590°C endotherm is negligible. The thermal characteristics of illite and allophane (Mackenzie and Caillére, 1975) do not occur. Mackenzie and Caillére (1975) suggest that the diluting effects of non-clay minerals result in only very small clay-mineral peaks when non-clay minerals account for 80% or more of a sample.

6.5 INFRA-RED ABSORPTION (I.R.A.)

I.R.A. analyses of clay fractions (<2 μm) were carried out on samples 3, 27, 57, 86, 89, 103 and 116, using a slight modification of the method described by Fieldes *et al.* (1972).

Sample Preparation

1 mg of air-dried (55°C), H_2O_2 treated, clay sample was added to 500 mg of pure dry (8 hours at 105°C) potassium bromide (kBr) and thoroughly mixed by grinding. 10 mm diameter discs were

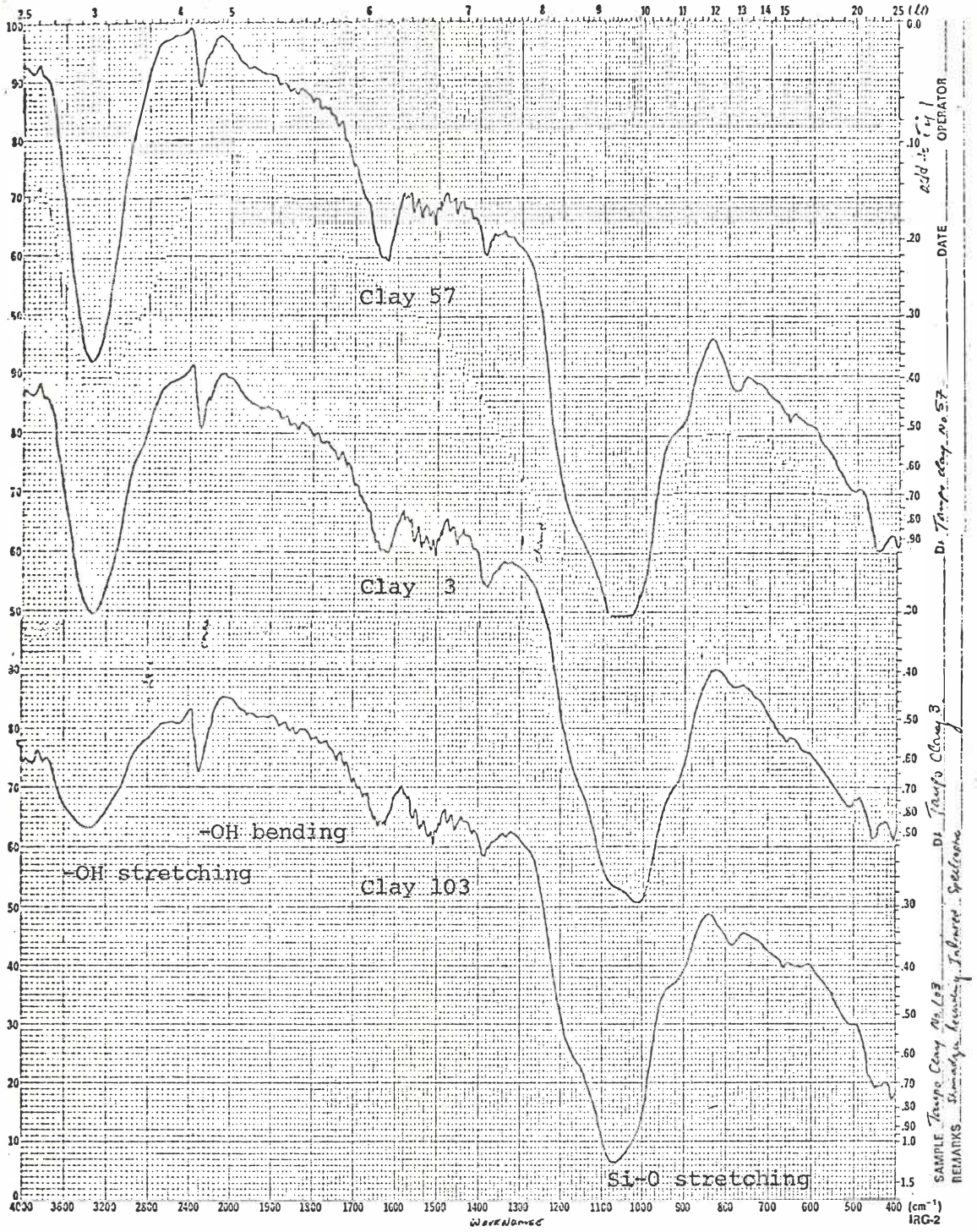


Fig. 6.13. Typical infra-red absorption spectra of clay-sized material (<2 μm) in Lake Taupo sediments.

prepared by vacuum pressing at 8000 kg/sq cm for 10 minutes. Very even packing of the mixture into the pressing die was necessary to avoid opaque areas in the pressed disc.

Prepared discs were scanned relative to a pure kBr disc, from 4000 to 400 cm^{-1} with a Shimadzu Recording Infra-red Spectrophotometer IR27G.

Results

Clay fractions and silt fractions

Qualitatively, all clay samples showed similar patterns. The intensity of the absorption peaks at 3450 cm^{-1} (-OH bond stretching (e.g. Si-OH, Al-OH) and absorbed water), 1630 cm^{-1} (-OH bond bending), and 1070 cm^{-1} (Si-O bond stretching) co-vary by a few percent from sample to sample (Fig. 6.13). Absorption peaks at, or close to these wavelengths are common to a number of minerals, particularly unweathered rhyolitic pumice, micaceous minerals, silica gel, allophane, illite, montmorillonite and vermiculite (Fig. 6.14; Fieldes *et al.* 1972; Kirkman, 1976).

Diatom frustules are composed of hydrous silica (opal) or polymerised silicic acid (Lewin, 1962) and so contain both Si-O and -OH bonds. The organic-free medium silt fraction (16-31 μm) of sample 113 is, from X.R.D. and S.E.M. evidence, almost entirely composed of diatom frustules and has a lower particle size limit considerably larger than clay (<2 μm). KBr discs of both this material and the course silt fraction (31-63 μm) were scanned. Both fractions produced spectra that are qualitatively similar to the clay fractions, with the medium silt (16-31 μm) giving larger

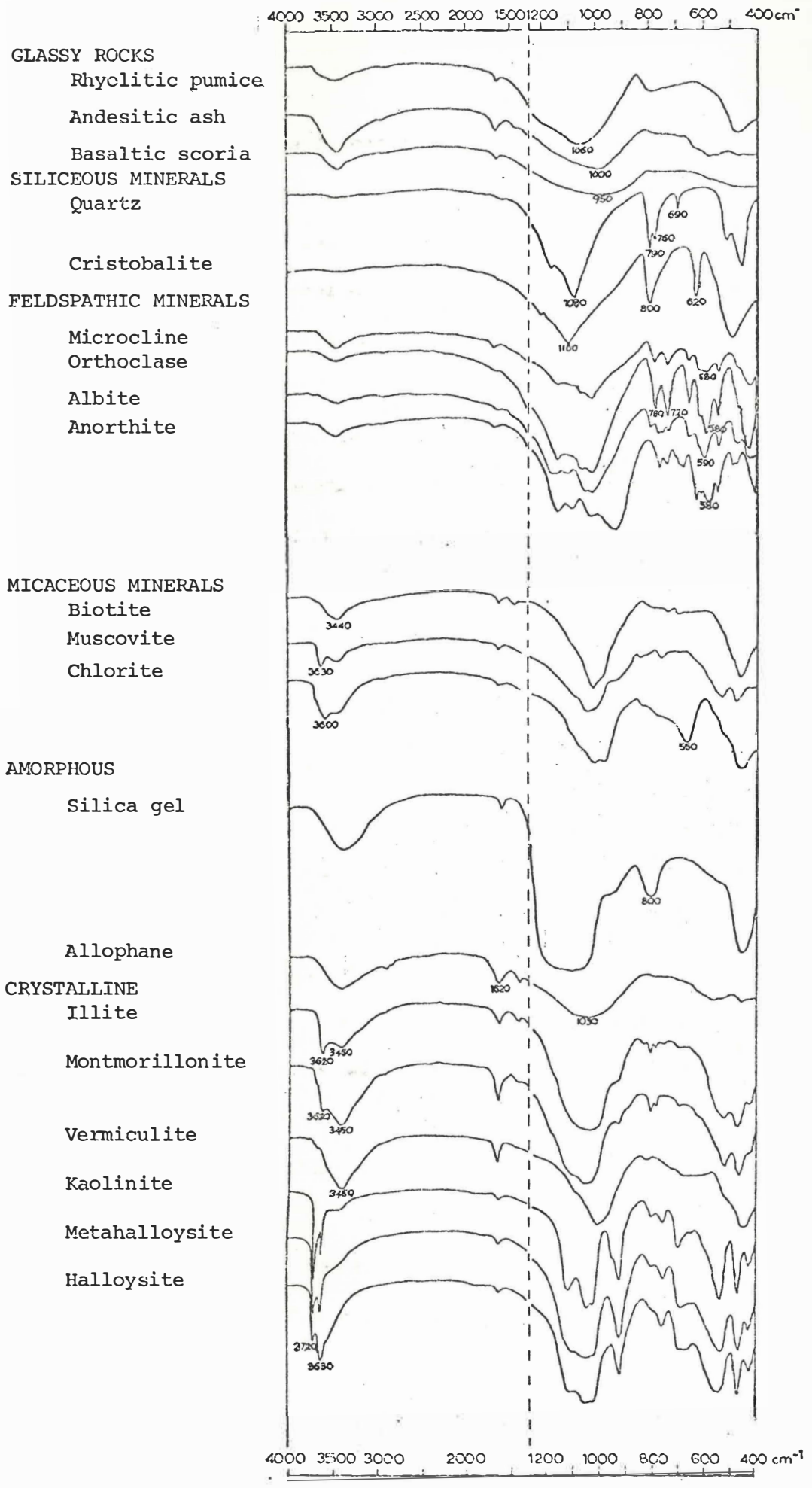


Fig. 6.14. Characteristic I.R.A. spectra of selected rocks and minerals (Fieldes *et al.* 1972)

-OH and Si-O absorption peaks than either the clay or coarse silt fraction (Fig. 6.15a, b, and c). The coarse silt fraction, from X.R.D. and S.E.M. evidence, has a much lower diatomaceous silica content than the medium silt fraction indicating that the larger -OH and Si-O absorption peaks of the medium silt fraction are probably due to diatomaceous silica. Farmer and Palmieri (1975) claim that substitution of Si-O-Al links for Si-O-Si links decreases the intensity and frequency of Si-O stretch absorbance maxima, so relatively sharper, more intense Si-O absorption peaks are expected from diatomaceous silica than from volcanic glass or clay minerals. This combined evidence suggests that the -OH and Si-O peaks in the clay fractions are due mainly to diatomaceous opal. The clay spectra undoubtedly include small contributions from other clay-sized materials which are masked by the dominant biogenic silica. Although this prevents exact quantitative use of the absorption peaks, semi-quantitative inferences may be made. Incident infra-red radiation conforms to the Beer-Lambert law:

$$\log (I_o/I) = \varepsilon cd = A$$

where I_o is baseline intensity, I is peak intensity, ε is the extinction coefficient, d is the disc thickness, c is the concentration and A is absorbance. Thus absorbance is a linear function of concentration. If it is assumed that Si-O absorbance from non-diatomaceous material in the clay samples and medium silt sample 113 is small and approximately equal, that the disc thickness are equal and that there are no variations due to grinding (e.g. Fieldes *et al.* (1972) claim that quartz absorption peaks are a function of grain size, then relative Si-O peak heights of the clay samples and medium silt sample

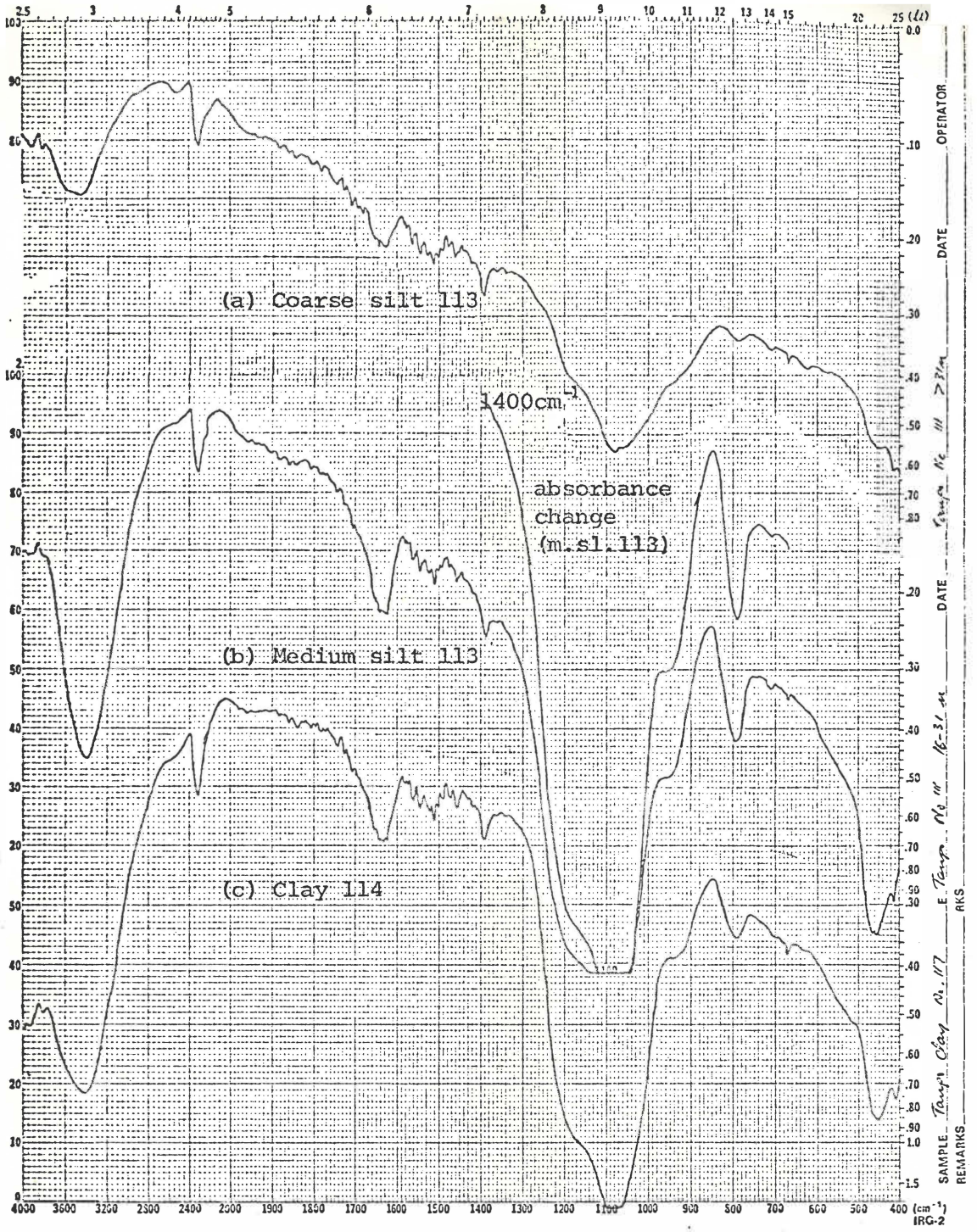


Fig. 6.15(a). Sample 113 coarse silt (31-63 μm). Non-diatomaceous silt dominant.

(b) Sample 113 medium silt (16-31 μm). Almost entirely diatomaceous silica.

(c) Sample 114 clay (<2 μm). Diatomaceous silica probably dominant.

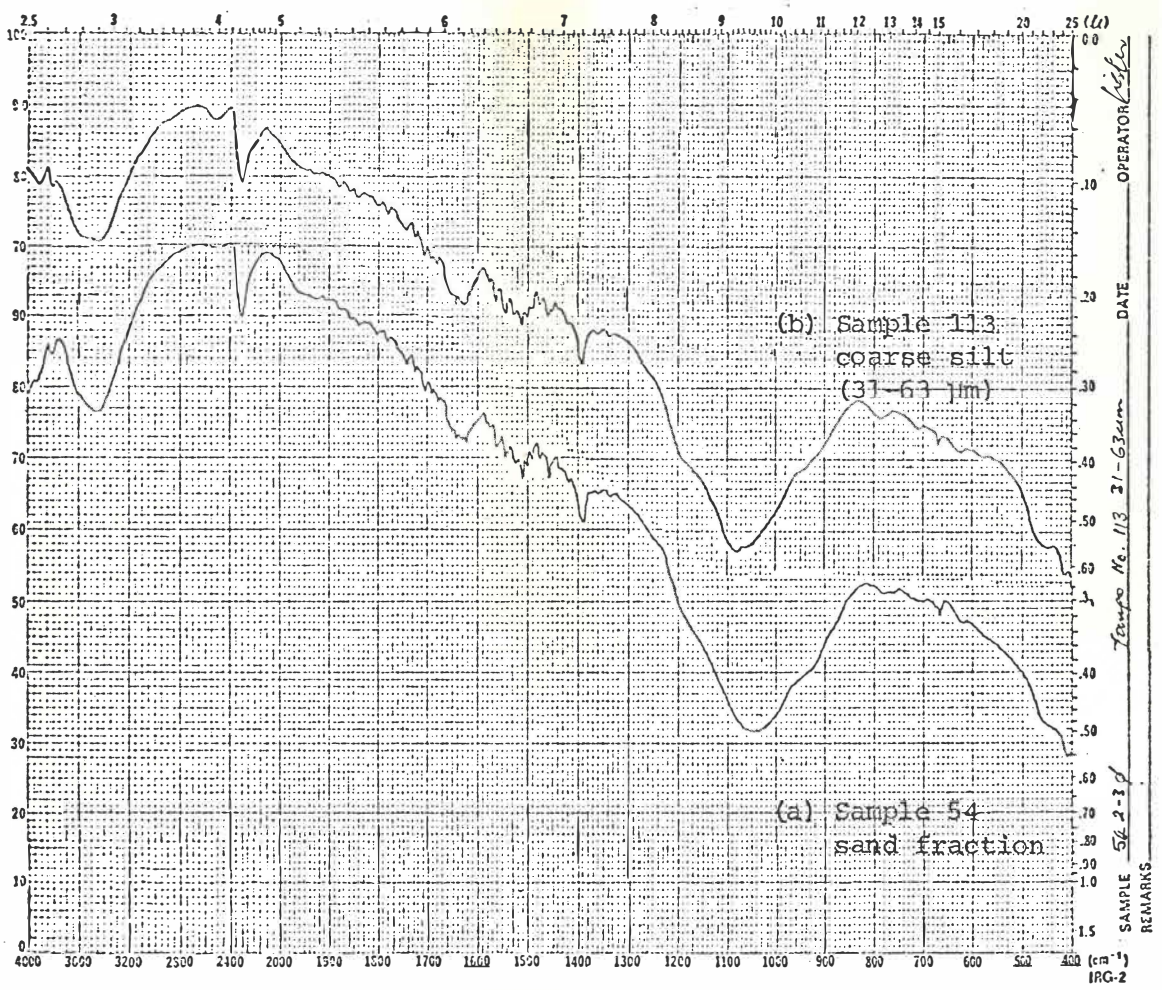


Fig. 6.16. Infra-red absorption spectra of a typical basinal sand fraction (sample 54) and coarse silt fraction (sample 113)

113 indicate relative amounts of diatomaceous silica. On this basis, diatomaceous silica forms approximately 50-60% of the clay samples.

Other absorption, peaks, or shoulders include those at 2900 cm^{-1} and 2300 cm^{-1} which may be due to residual organic matter (Farmer and Palmieri, 1975), a slight absorption at 800 cm^{-1} which may be due to volcanic glass (Kirkman, 1976), and a shoulder at 915 cm^{-1}, possibly due to phyllosilicates (Kirkman, 1976).

Deep-water Sand Fractions

I.R.A. spectra of deep-water sand fractions away from shelf and cliff areas were scanned to establish whether they were rhyolitic or andesitic. This proved unsuccessful because of the close similarities of the published spectra of rhyolitic pumice and andesitic ash (Fig. 6.14) and the possibility that both types of material are present. The I.R.A. spectra of the sand fractions (e.g. Fig. 6.15) are similar to each other and also to the coarse silt fractions (compare Figs. 6.16 a and b). These spectra both suggest a high proportion of volcanic glass (Kirkman, 1976).

Thus I.R.A. suggests that the sand and coarse silt fractions of deep-water sediments are dominated by rhyolitic and/or andesitic volcanic glass, the medium-very fine silt fraction is dominated by diatomaceous silica, and the clay fraction is commonly 50-60% diatomaceous silica.

6.6 SCANNING ELECTRON MICROSCOPY

Method

Silt and clay samples were scanned with a JEOL JSM-35 scanning electron microscope (S.E.M.) to identify sample components on the basis of particle morphology. Qualitative elemental compositions

for selected particles were determined using an S.E.M. X-ray energy dispersive microprobe coupled with an Ortec multichannel analyser (M.C.A.).

Silt sample preparation

Organic-free silt samples were settled or centrifuged (see X.R.D. sample preparation) to obtain either (a) a coarse-medium silt fraction (63-16 μm) and a fine-very fine silt fraction (16-2 μm), or (b) a coarse silt fraction (63-31 μm), a medium silt fraction (31-16 μm), and a fine-very fine silt fraction (16-2 μm). These fractions were oven dried (55°C), mounted on brass stubs using double-sided sticking tape and initially coated with gold/palladium (Au/Pd) to a thickness of 500Å using an E5000 diode sputter coater. High proportions of amorphous silica frequently caused poor conductance which resulted in a build up of negative charge on particles, producing abnormal contrast (e.g. Fig. 6.18a), image deformation and shifting (e.g. Fig. 6.21c), particle movement and burning, and a reduction in resolving power. Recoating of samples with Au/Pd to a total thickness of 750Å, and lowering the accelerating voltage reduced the build up of negative charge.

Results

The silts comprise two major components (Fig. 6.17a and b): siliceous diatom tests (biogenic component), and siliceous rock and mineral fragments (terrigenous component). Diatom tests are most abundant in the fine-very fine silts and the inorganic fragments in the coarse silts (Fig. 6.21c and a). In the medium silt fraction a variable mixture of these two components occurs (Fig. 6.21b).

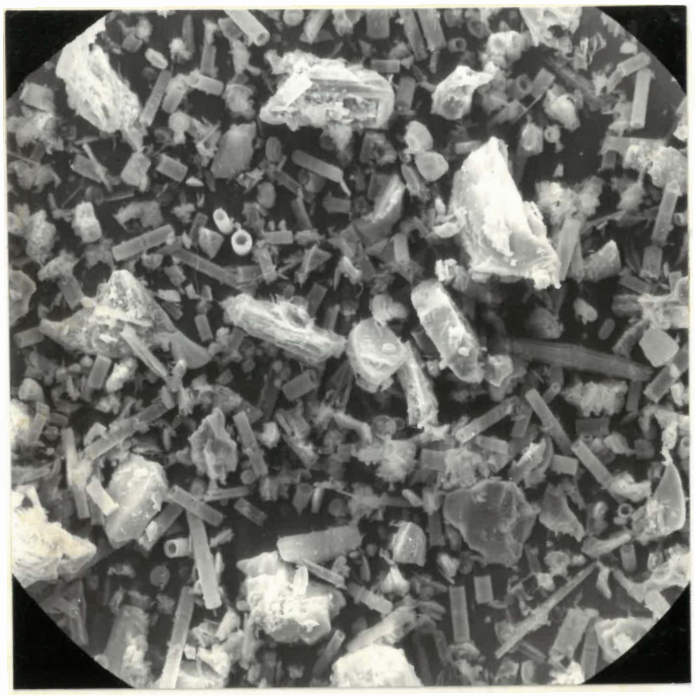


Fig. 6.17

(a)

Sample 74

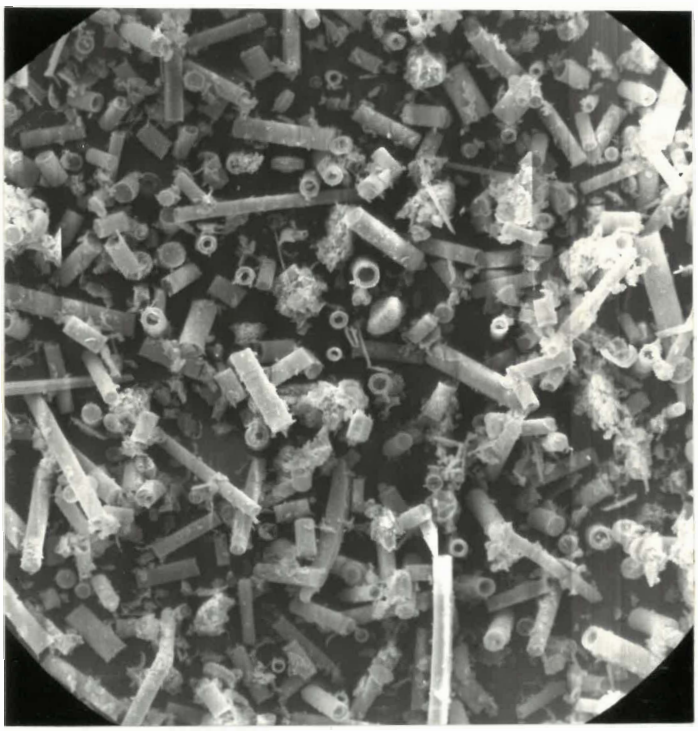
Total oven-dry (55°C) untreated sediment.

x200

⟵ 50 µm

No. 0004 (film negative number)

25 kV (S.E.M. accelerating voltage)



(b)

Sample 103

Total oven-dry (55°C) untreated sediment.

x220

⟵ 40 µm

Broad areal trends occur in the relative abundance of biogenic and terrigenous components in the lake, with the latter decreasing fairly rapidly away from shelf areas, and more slowly away from the southern end of Lake Taupo. This trend along a south to north transect (Fig. 6.19c) is illustrated by Figs. 6.18 to 6.21.

The terrigenous component comprises two categories of particles. The first includes pumice fragments and glass shards, which are compositionally similar. The gradational change from one to the other is essentially a function of particle to vesicle size. Pumice particles are vesiculated (Fig. 6.22a) while glass shards display parts of vesicle walls with variable shapes, including flat plates with or without ridges, and curved, concave, and Y-shaped fragments (Fig. 6.22b). The second category includes unidentifiable particles (e.g. Fig. 6.22b).



Fig. 6.18 Sample 2

(a)

Coarse silt (31-63 μm)

x200

50 μm

P.No. 2635

13 kV



(b)

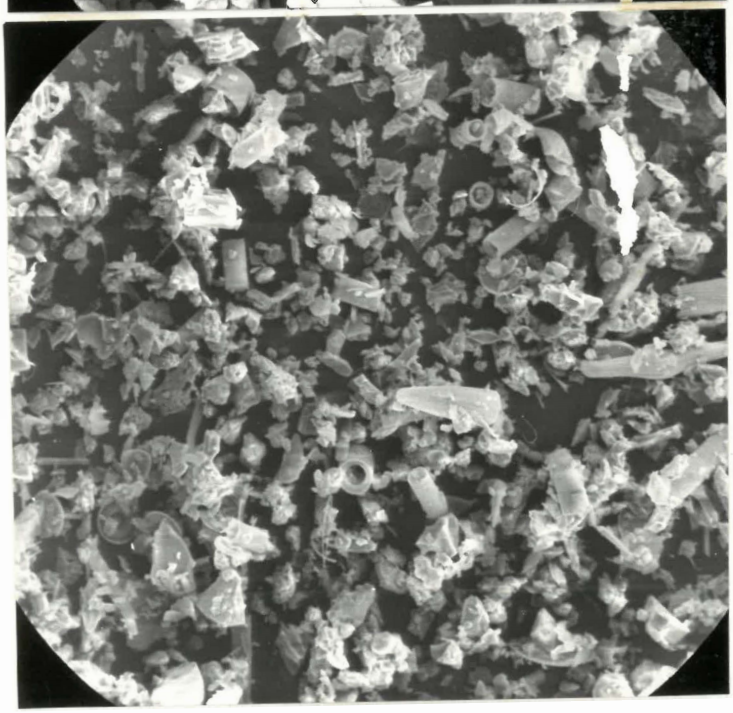
Medium silt (16-31 μm)

x220

40 μm

No. 2629

13 kV



(c)

Fine-very fine silt (2-16 μm)

x360

30 μm

No. 2631

13 kV

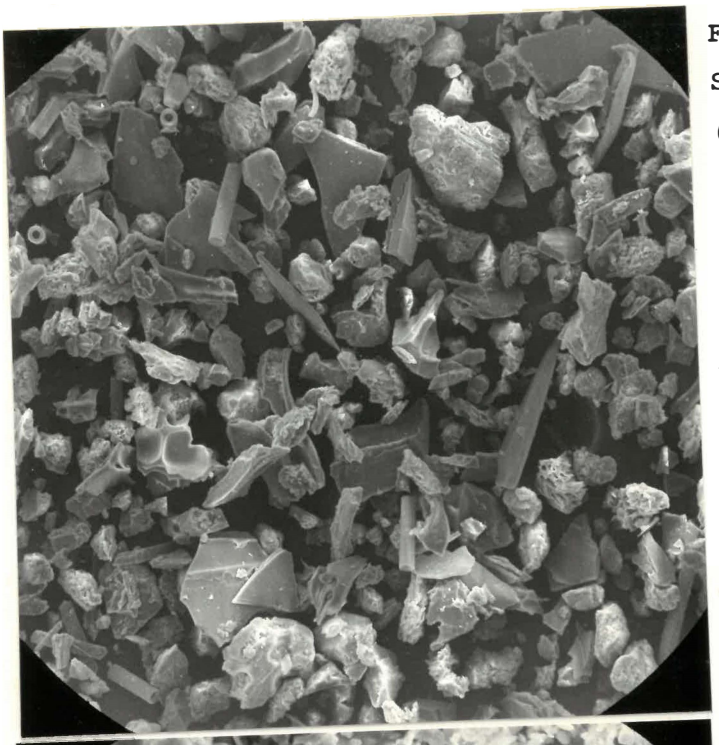
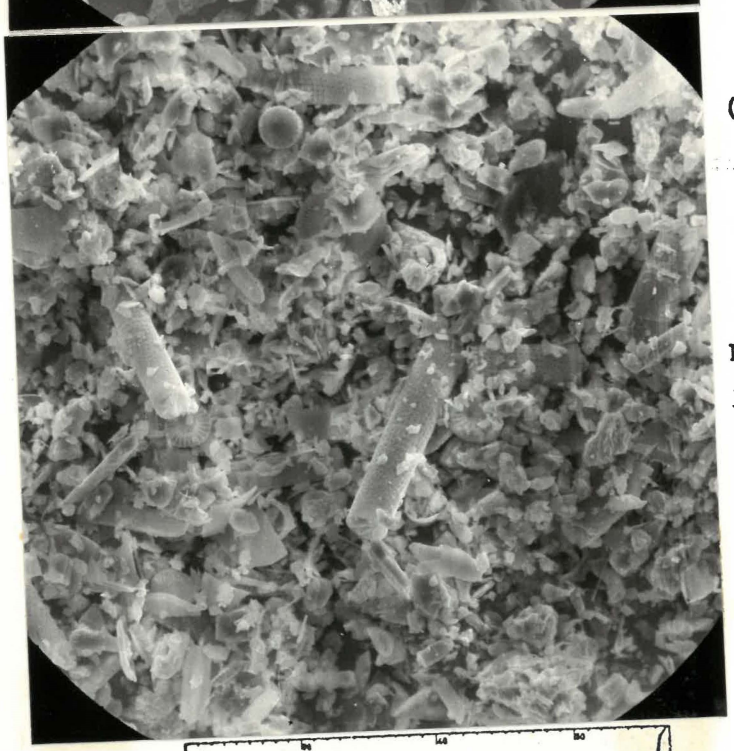


Fig. 6.19

Sample 4

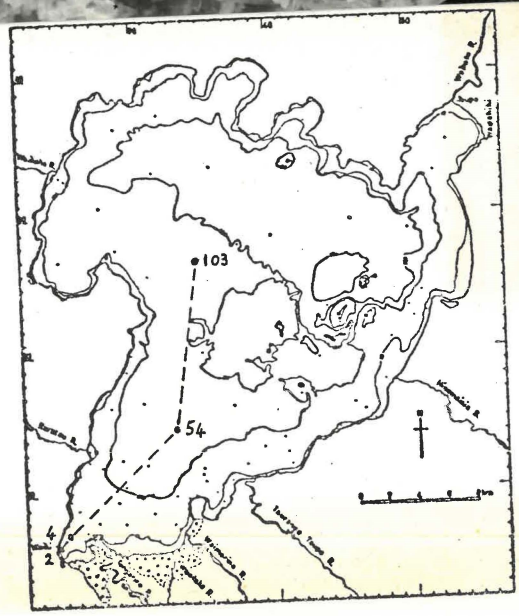
(a) Coarse-medium silt
(16-63 μm)
x240
⟵40 μm

No. 0490
15 kV



(b) Fine-very fine silt
(2-16 μm)
x660
⟵10 μm

No. 0456
18 kV



(c) Sample sites in Lake Taupo for samples illustrated in Figs. 6.18 to 6.21.



Fig. 6.20. Sample 54

(a)

Coarse-medium silt

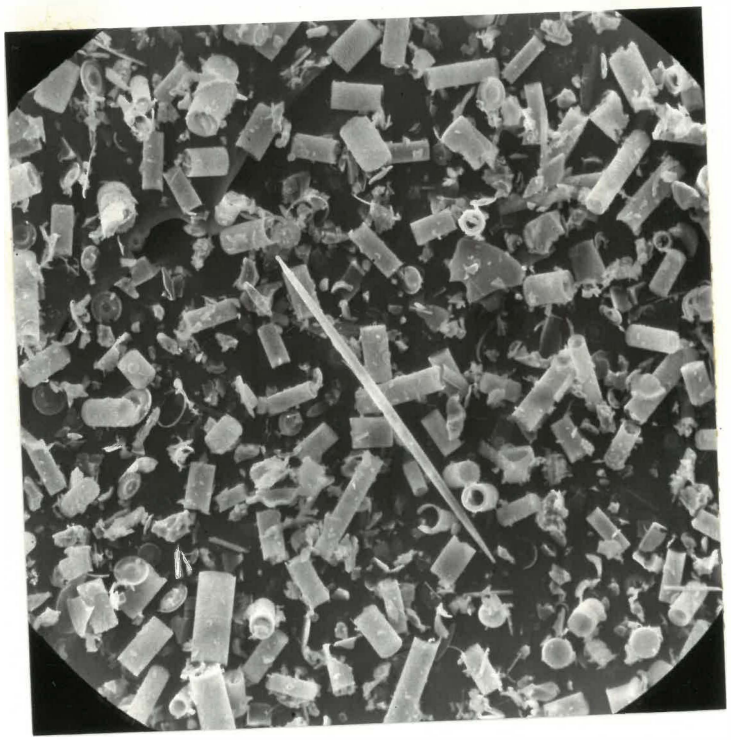
(16-63 μm)

x200

50 μm

No. 0486

18 kV



(b)

Fine-very fine silt

(2-16 μm)

x320

20 μm

No. 0481

18 kV



Fig. 6.21 Sample 103

(a)

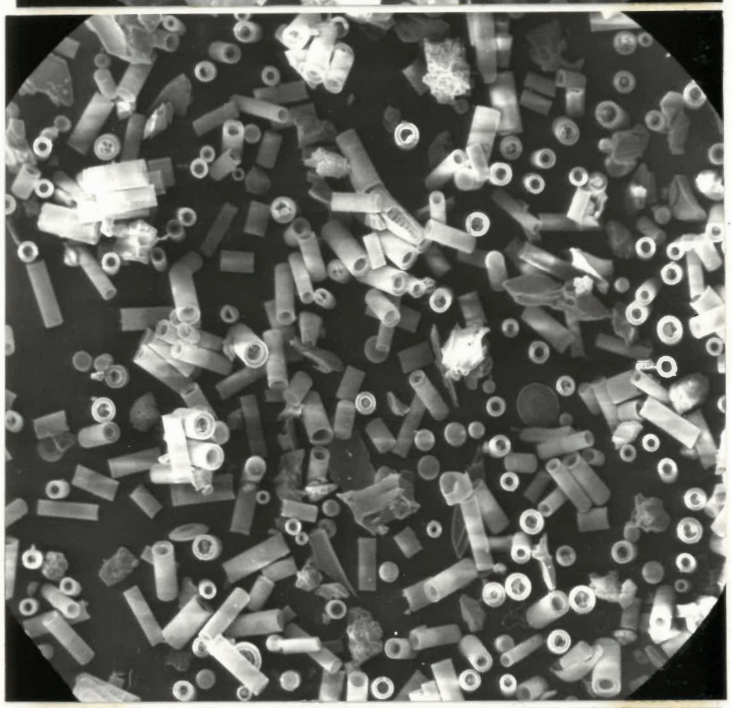
Coarse silt (31-63 µm)

x220

40 µm

No. 2625

13 kV



(b)

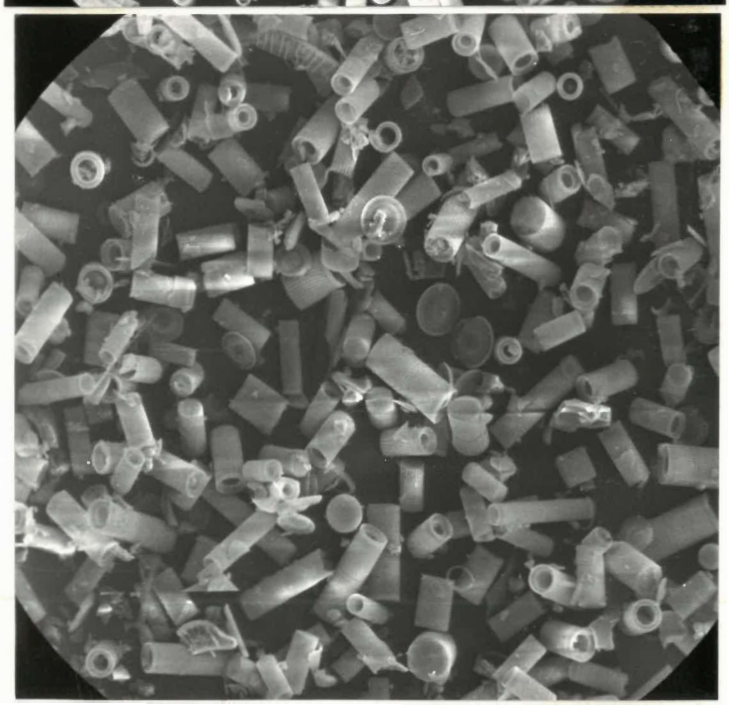
Medium silt (16-31 µm)

x220

40 µm

No. 2630

13 kV



(c)

Fine-very fine silt

(2-16 µm)

x360

30 µm

No. 2626

13 kV

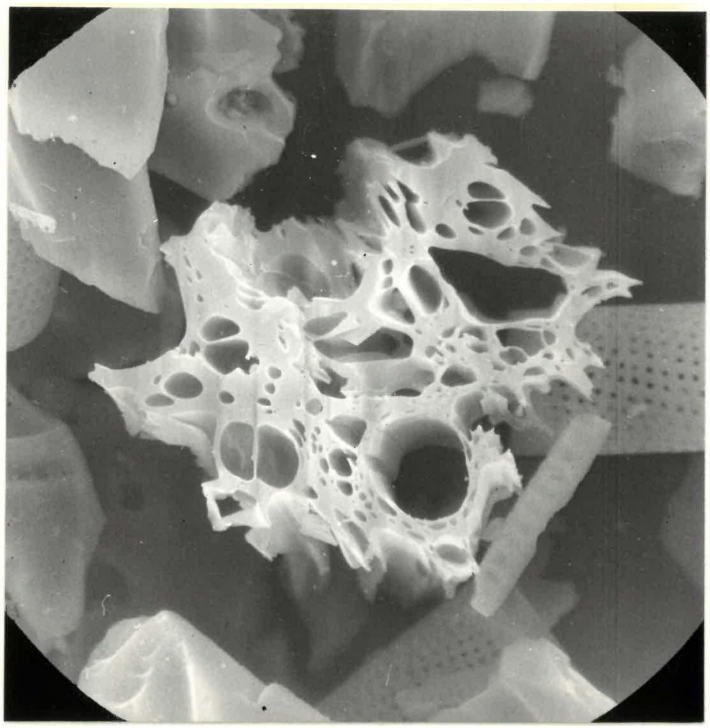


Fig. 6.22

(a)

Sample 93

coarse-medium silt

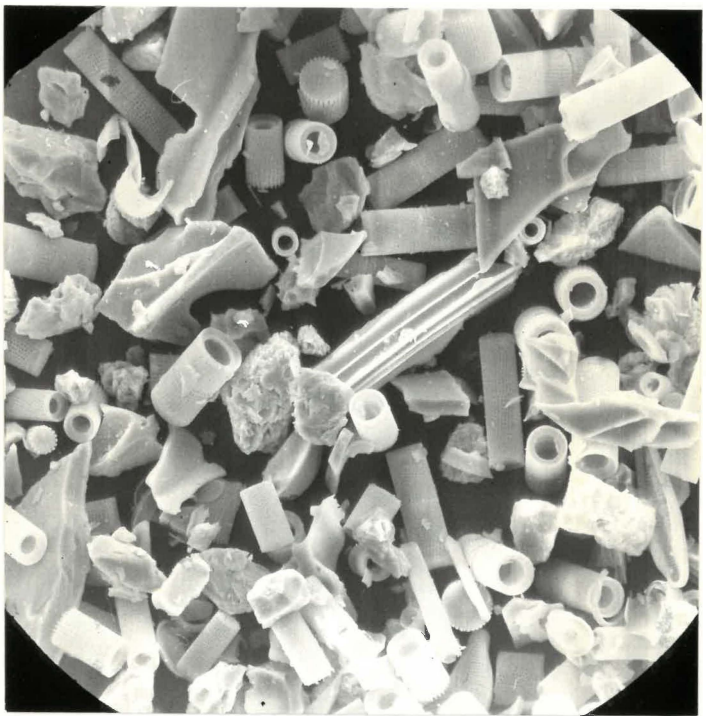
x1800

10 µm

Vesiculated pumice fragment

No. 0675

18 kV



(b)

Sample 46

Coarse-medium silt

x440

20 µm

(1) Glass shards

(2) Terrigenous particles lacking distinct morphology

No. 0552

18 kV

IDENTIFICATION OF DIATOM FRUSTULES

The occurrence, physical characteristics, and ecological significance of diatoms in the Lake Taupo plankton community were described in Chapter 3, section 3.

The identification and relative abundance of the various species of diatom frustules observed in the sediments of Lake Taupo in the course of this study are given in Table 6.3 and are illustrated in Figs. 6.23-6.39. Wherever possible, the authority and reference is given with each identification (based on Patrick and Reimer, 1966; V. Cassie, 1978a, pers. comm.).

Subsequently, V. Cassie (1978b, pers. comm.) has identified further diatom species in several of the Lake Taupo sediment samples, and in a "diatomite" sample, probably of Huka Group origin (Fig. 6.41), collected by the author from a large (several metres across) partly buried slab of similar material in 1 m of water just offshore in the northern part of Scenic Bay, Lake Taupo (Table 6.4). Micrographs of diatom species from this subsequent study are not included in this thesis.

Clay Sample Preparation

The sediment remaining after removal of the silt fractions was either further centrifuged into coarse (0.2-2 μm) and fine clay (<0.2 μm) fractions (samples 12, 34, 36, 53, 55, 68, 84, 97, 101, 104, 109, 115), or flocculated by adding a few crystals of $MgCl_2$ to 200 mls of sample (all other samples). The latter group was then centrifuged and decanted twice to remove any $MgCl_2$ in solution.

Table 6.3. Diatoms in Lake Taupo Sediments (Identification based on Patrick and Reimer, 1966; Cassie, 1978, pers. comm.)

Species	Relative abundance	Fig.
Silt fraction		
Melosira sp. (?ad *pyxis* > *varians*)	v.a.	6.23
Cyclotella stelligera	c.	6.24,6.25
Rhopalodia gibba (Ehr.) O.Müll var. *gibba*	o.	6.26
Epithemia sp.	c.	6.27
Cocconeis placentulata (Ehr.) var. *lineata*	r.	6.29
Fragillaria sp.	r.	6.30a and b
Coscinodiscus sp. ad *lacustris* GRUN	r.	6.31
Synedra ulna (Nitzsch) var. *amphirhynchus* (Ehr.) GRUN	o.	6.28
Valvocopula (diatom girdle band)	o. (as separate particles)	6.32a and b
Fine-very fine sand fraction (of samples close to some shallow water areas; cf. Fig. 7.4)	Relative abundance in sample 40	
Synedra ulna (Ehr.) Nitzsch var. *ulna*	o.-v.a.	6.37c
Surirella sp.	o.	6.33,6.34
Surirella tenera GREG	o.	6.35,6.36
Cymatopleura solea	r.	6.37a
Cymbella sp. (?*aspera*)	r.	6.37b
Nitzschia sp.	r.-c.	6.38
Non-diatom particles		
?L.R.G.T. (little round green thing; Paerl, 1977)	r.	6.39
Sponge spicules (siliceous)	r.-o.	6.35
Unidentified biogenic object	r.	6.40
very abundant (>50%)	v.a.	
common (5-50%)	c.	
occasional (1-5%)	o.	
rare (<1%)	r.	

Table 6.4. Further diatom species observed in several of the Lake Taupo sediment samples by V. Cassie (1978, pers. comm.).

SPECIES	SAMPLE NUMBER AND SEDIMENT SIZE FRACTION						
	2 v.fs.-f.s.	10 sl.	41 v.f.s-f.s.	66 sl.	78 sl.	97 sl.	"diatomite" (?Huka Gp.)
Asterionella formosa	—	1	1				
Capartogramma crucicula	—	1					
Cocconeis placentula	1	1	—	1	—	—	1
Cyclotella stelligera	2	3	2	4	5	5	
?Cymbella aspera	—	—	—	—	1	—	1
Cymatopleura solea	—	—	1				
?Diploneis smithii	—	—	—	—	—	—	1
Epithemia argus	1	1	2	—	—	—	3
Epithemia sorex	—	1	1	—	—	—	2
Eunotia sp.			1				
Fragilaria construens	—	—	1	r			
Melosira pyxis	2	5	2	5+	5	5+	1
Melosira varians	1	—	1				
Navicula sp.1 (long, narrow)	1	1	1				
Navicula sp.2 (short, wide)	—	1					
Meidium iridis var. *amphigomphus*	1	1	—	—	—	—	1
Nitzschia vermicularis	5	—	2				
?Pinnularia mesogongyla	—	—	1				
Rhopalodia gibba	1	1	—	—	—	—	1
Surirella biseriata	3	—	1				
Surirella contorta	2	—	3				
Surirella ovalis	—	—	2				
Synedra ulna	1	—	1				

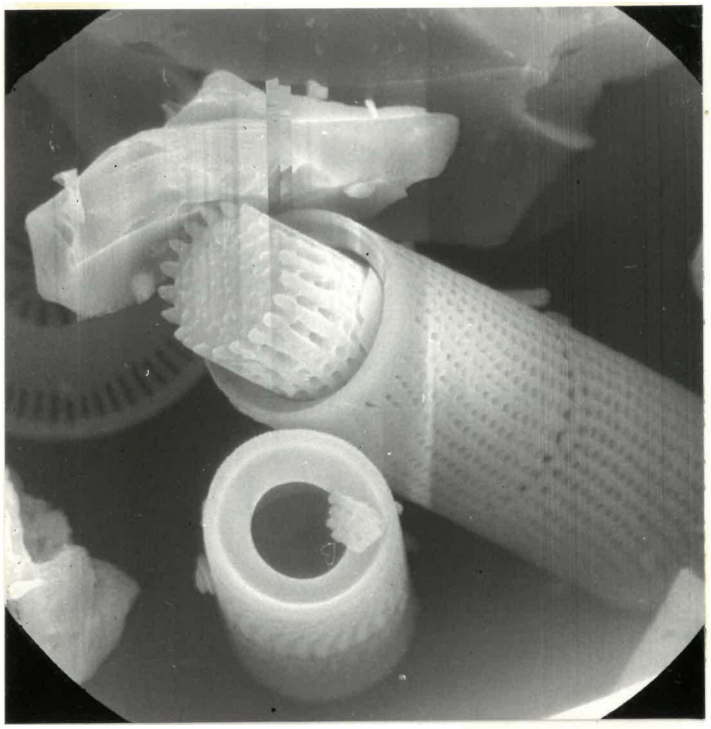


Fig. 6.23

Melosira sp.

x2400

6 µm

No. 0662

18 kV

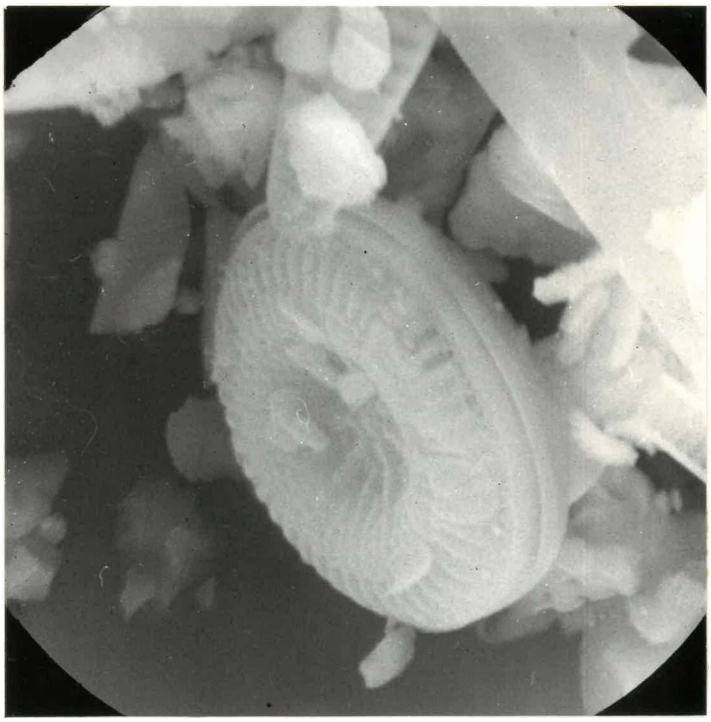


Fig. 6.24

Cyclotella stelligera CLEVE et GRUN

(Ref. Huber-Pestalozzi)

Tilted specimen

x4000

5 µm

No. 0681

18 kV

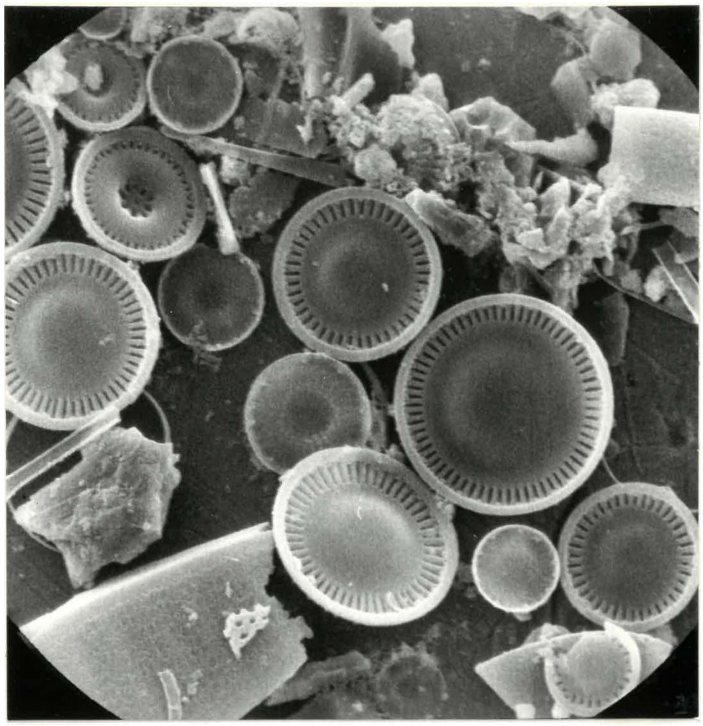
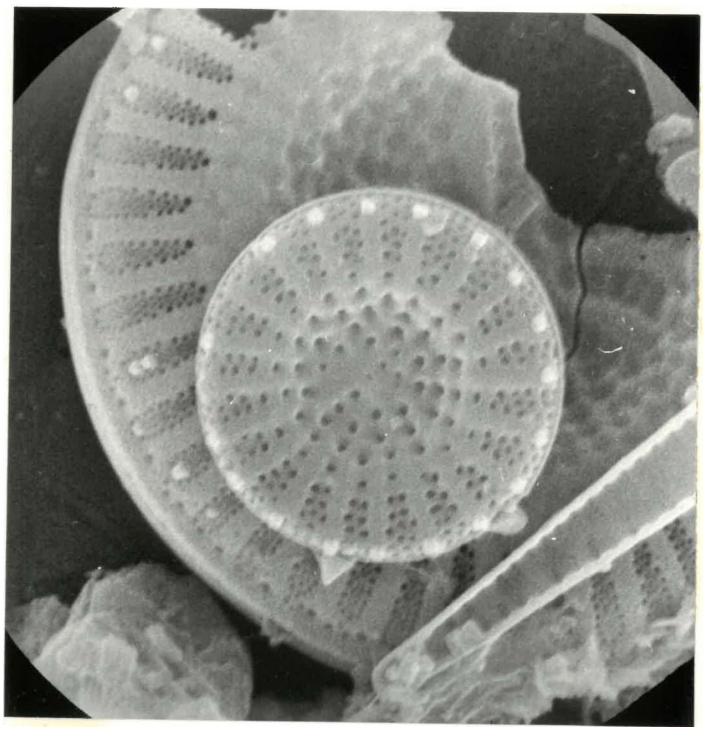


Fig. 6.25
Cyclotella stelligera

CLEVE et GRUN
(Ref. Huber-Pestalozzi)

(a) Valve interior
x1500
10 µm

No. 2064
18 kV



(b) Valve exterior
x7200
2 µm

No. 2009
18 kV



Fig. 6.26
Rhopalodia gibba
(Ehr) O. Müll.
Var. *gibba*
(valve interior)
x750
15 µm

No. 0804
7 kV

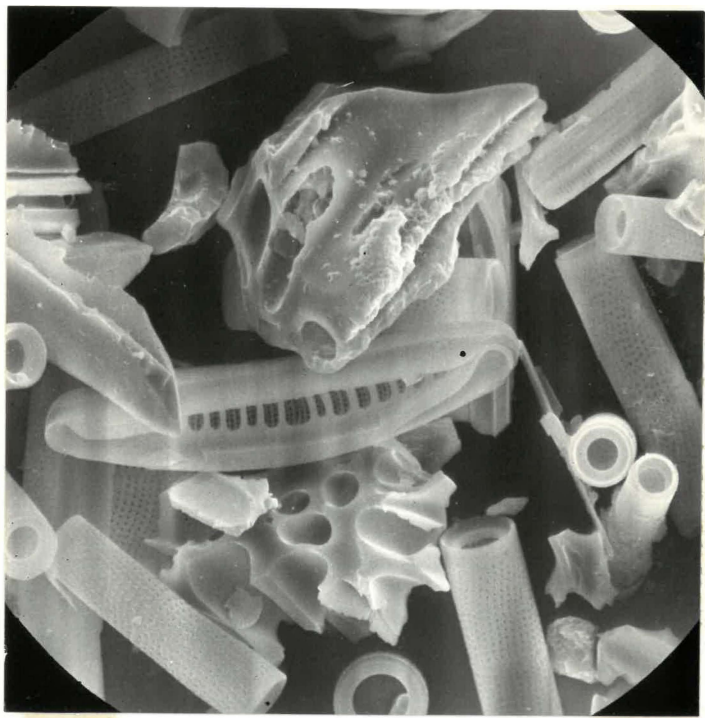


Fig. 6.27
Epithemia sp.
(valve interior)
x900
20 µm

No. 0435
18 kV

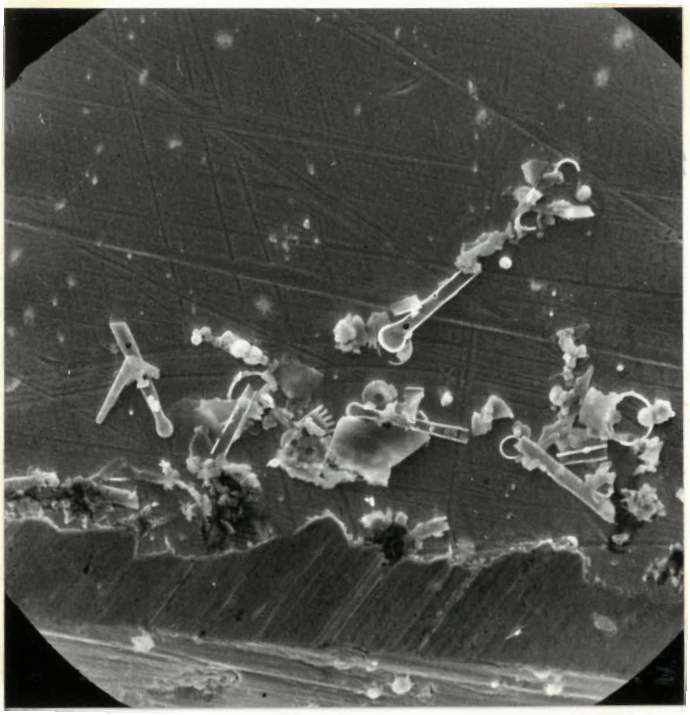


Fig. 6.28
Synedra ulna
(Nitzsch)
var. *amphirhynchus*
(Ehr.) GRUN

x1000
10 µm

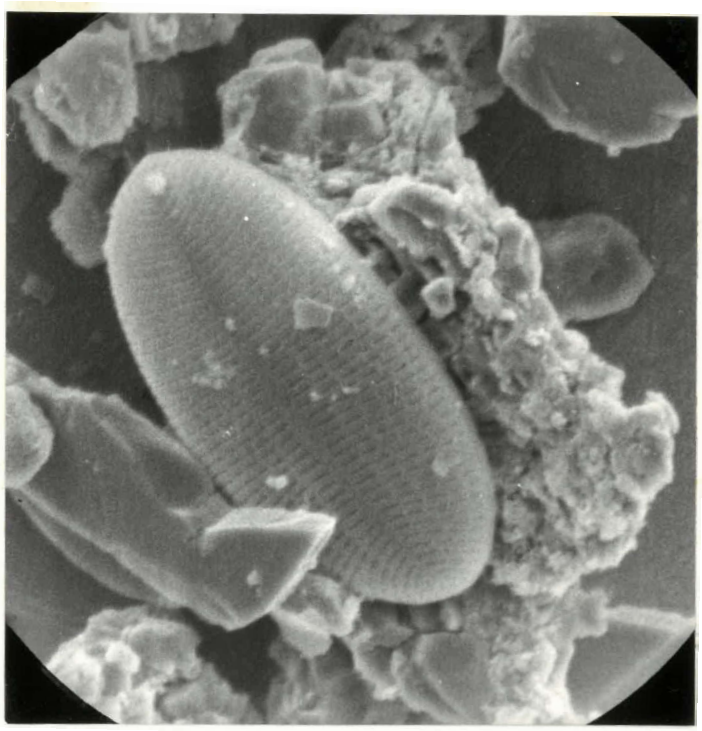


Fig. 6.29
Cocconeis placentulata
(Ehr.)
var. *lineata*
(Pseudoraphe valve)

x3900
5 µ

No. 2023
8 kV

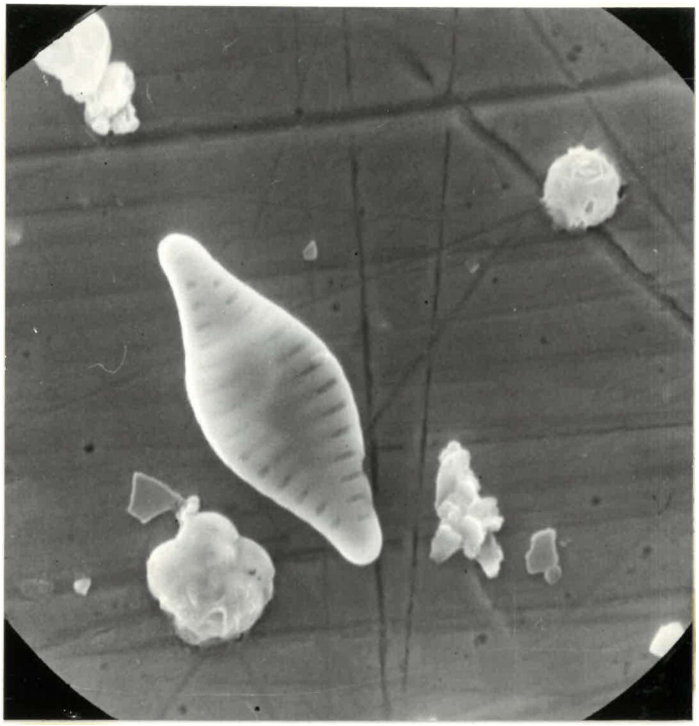


Fig. 6.30

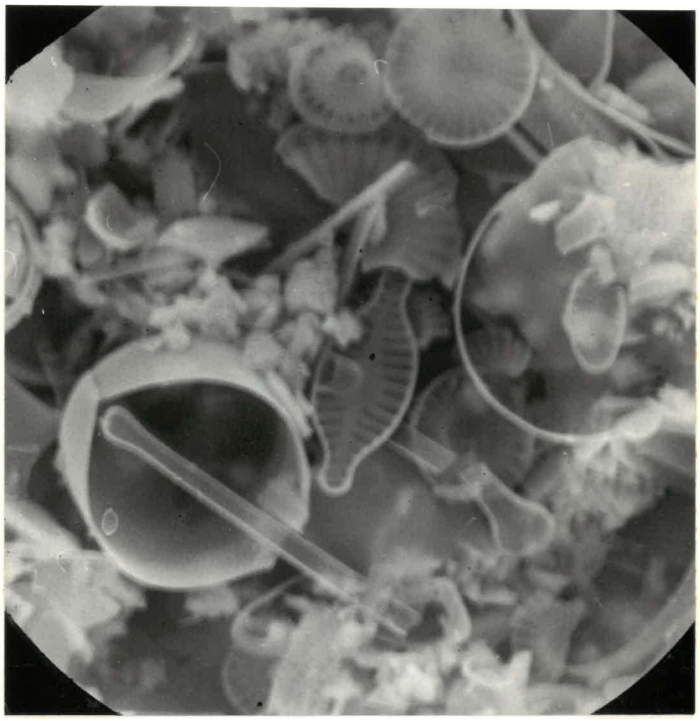
(a) ?*Fragillaria* sp.

x4800

2 µm

No. 0978

15 kV



(b) ?*Fragillaria* sp.

x2200

5 µm

No. 0988

15 kV

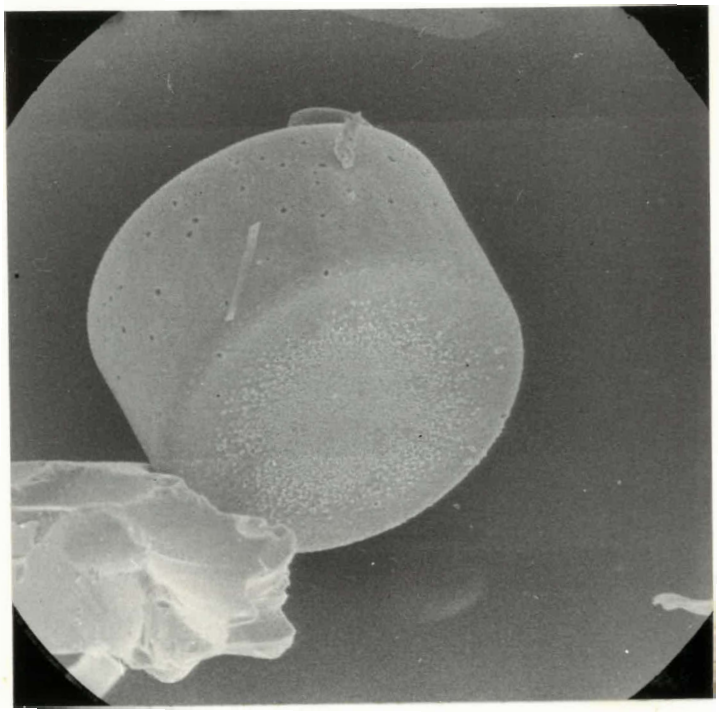


Fig. 6.31
Coscinodiscus sp.
ad *lacustris*
GRUN

x1300
10 µm

No. 0795
7 kV

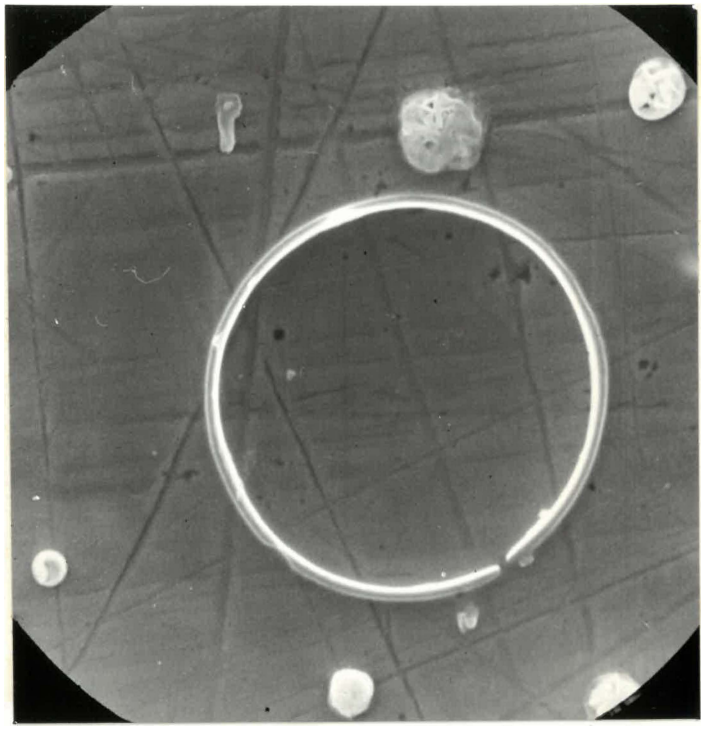


Fig. 6.32
Valvocopula
(diatom girdle band)
Ref. Anonymous, 1975

(a) x4000
5 µm

No. 0980
15 kV



(b) x6600
2 µm

No. 0965
15 kV

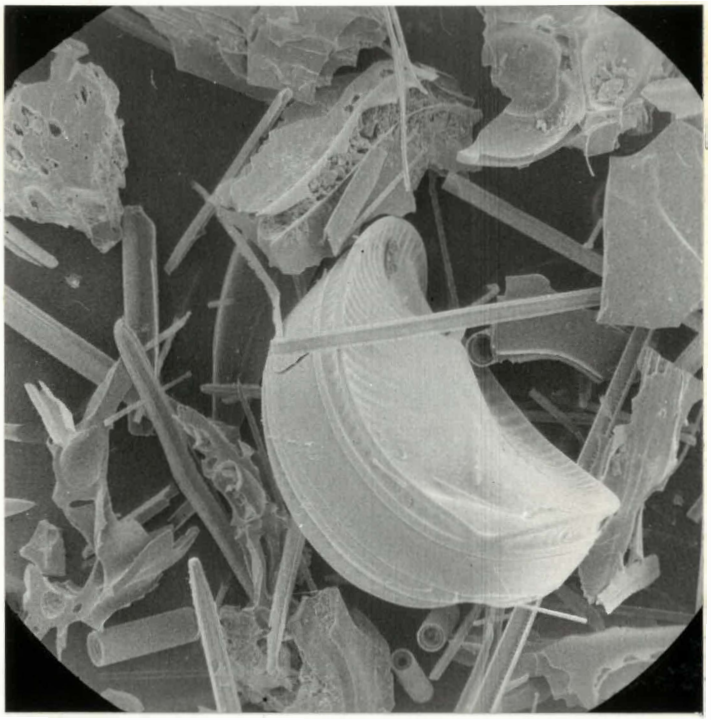


Fig. 6.33
Surirella sp.
(with girdle)

x360
60 µm

No. 0798
7 kV

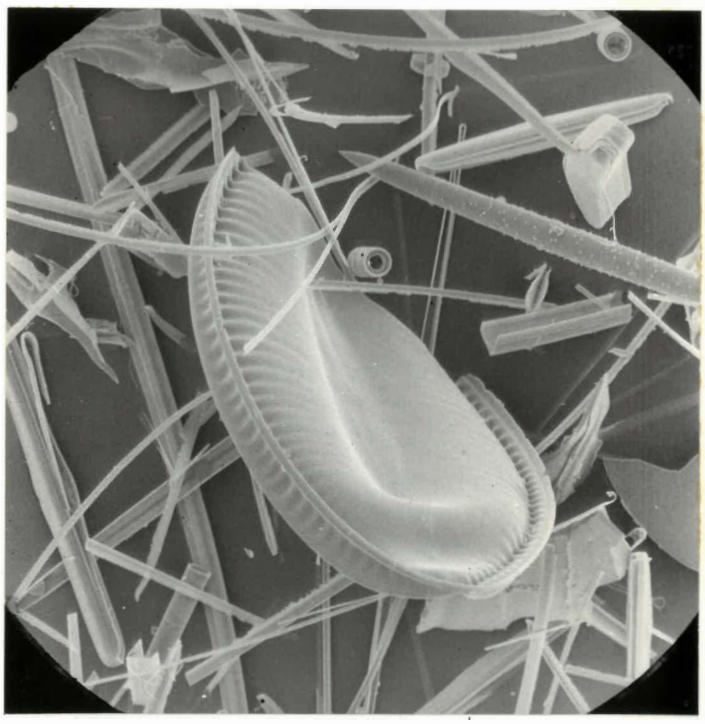


Fig. 6.34
Surirella sp.
(assymmetrical valve)

x360
60 µm

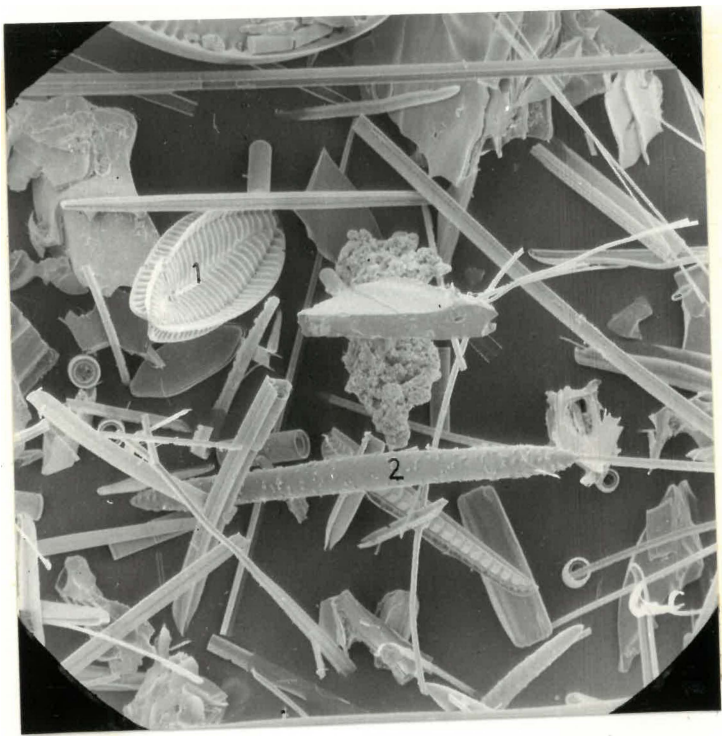


Fig. 6.35

1. *Surirella tenera*
   GREG.
   Ref. Huber-Pestalozzi
2. Siliceous sponge
   spicule

x300

40 µm

No. 0793

7 kV



Fig. 6.36

Surirella tenera

GREG.

Ref. Huber-Pestalozzi

x500

20 µm

No. 0800

8 kV

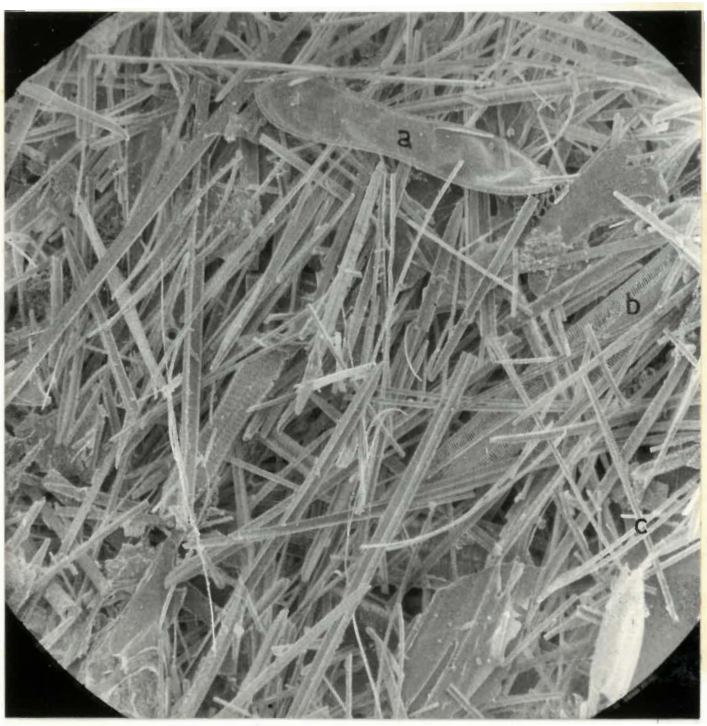


Fig. 6.37
(a) *Cymatopleura solea*
(b) *Cymbella* sp.
(?*aspera*)
(c) *Synedra ulna*
(Ehr.) Nitzsch
var. *ulna*

x200
50 µm

No. 0805
7 kV

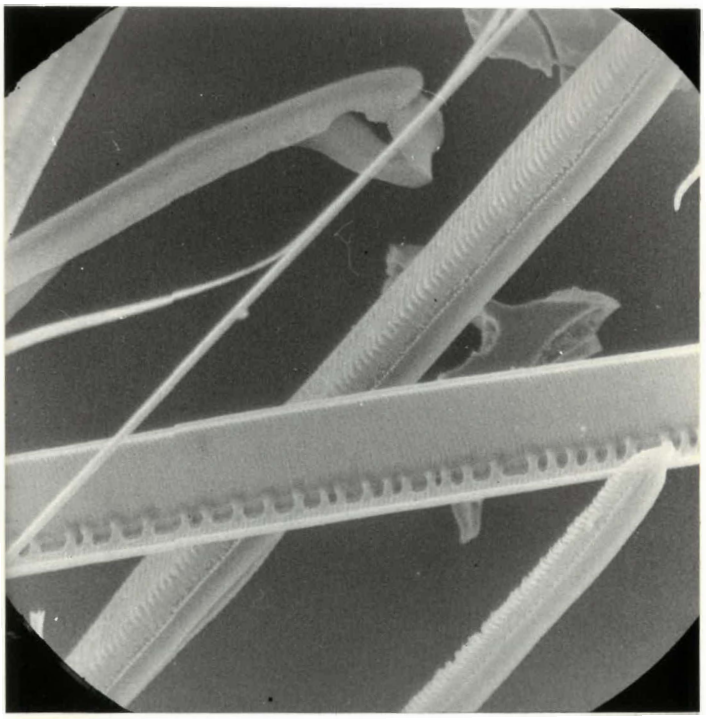


Fig. 6.38
Nitzschia sp.

x1800
10 µm

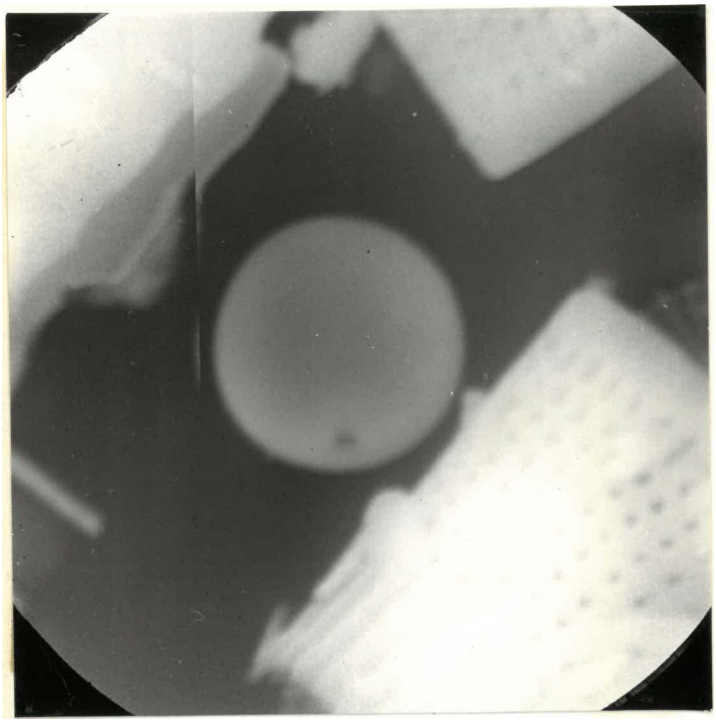


Fig. 6.39
?"Little round green thing" (L.R.G.T; Paerl, 1977).

x4000

5 µm

No. 0484
25 kV

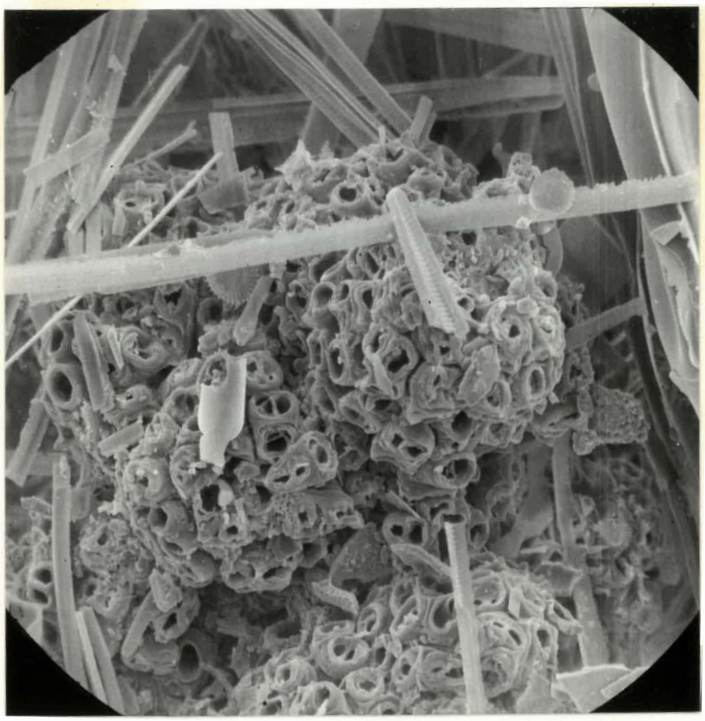


Fig. 6.40
Unidentified biological structure (Sample 14)

x720
10 µm

No. 0801
8 kV



Fig. 6.41. Diatomite sample collected from Scenic Bay, Lake Taupo. Note sand-rich laminae and pumice clast.

As a preliminary step on which subsequent procedure was based, sample 12 coarse clay was mounted directly on to a brass stub, using a dropper, and scanned with the S.E.M. Both diatomaceous and non-diatomaceous components are evident (Fig. 6.42). The twelve coarse clay samples were then mixed with distilled water and allowed to settle in 15 cm long test tubes. In every case differential settling produced three distinct colour layers with approximately similar layer-thickness ratios (e.g. Fig. 6.43). Each of these three layers was subsampled and S.E.M. mounts prepared using brass stubs. Corresponding fine clay fractions were mounted on carbon stubs to eliminate elemental peaks of the metals in brass during microprobe investigations. Mounts were also prepared from flocculated total clay samples (52, 54, 74, 86, 89) using brass stubs.

The clays were mounted on stubs by mixing clay/water suspensions with variable quantities of tertiary butyl-amine (t.b.a) and applying the suspension with a dropper. Beutelspacher and Van der Marel (1968) suggested a clay suspension:t.b.a. ratio of 1:700. As the result is a compromise between the effects of reducing surface tension by increasing the t.b.a. content and an adequate clay particle density, the initial clay suspension partly determines the ideal ratio. In this invesitgation a ratio range of 1:40 to 1:100 generally gave good results.

Results

Sample 55 (Figs. 6.44-6.46) is representative of the clay fractions examined. Visual identifications of the components in this sample are listed in Table 6.5 together with approximate dimensions and abundances in a particular layer. In some cases

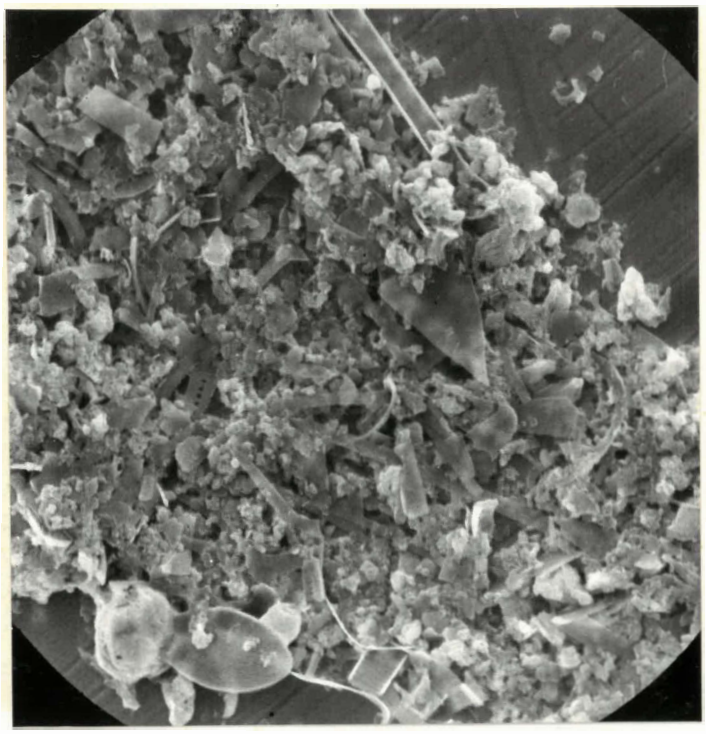


Fig. 6.42. Sample 12 coarse clay fraction (0.2-2.0 µm)

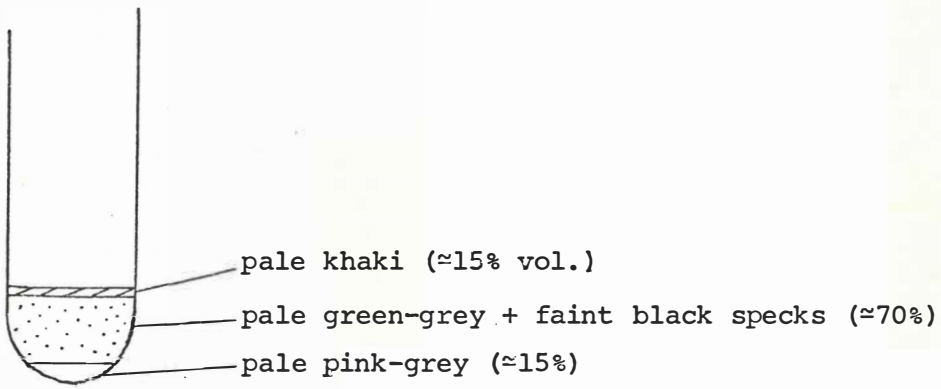


Fig. 6.43. Layers formed by differential settling of sample 55 coarse clay (0.2-2.0 µm) particles through a 15 cm water column.

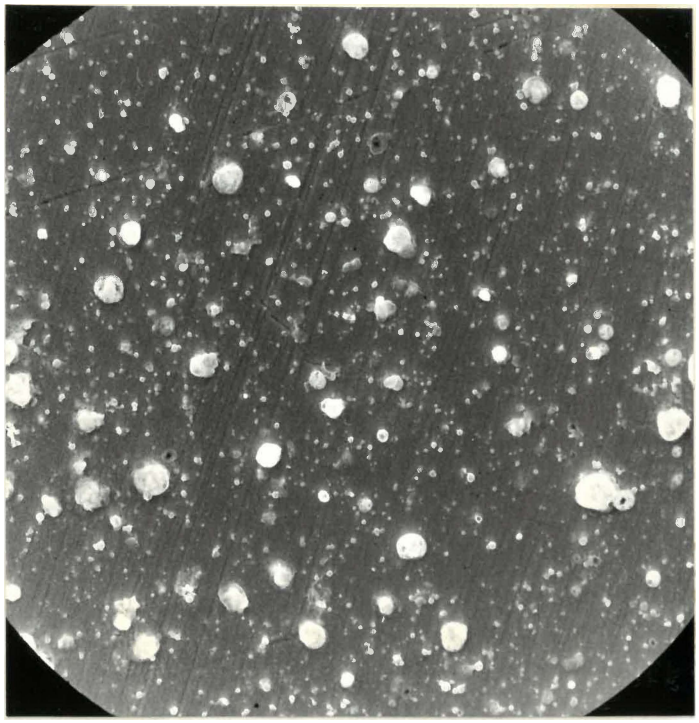
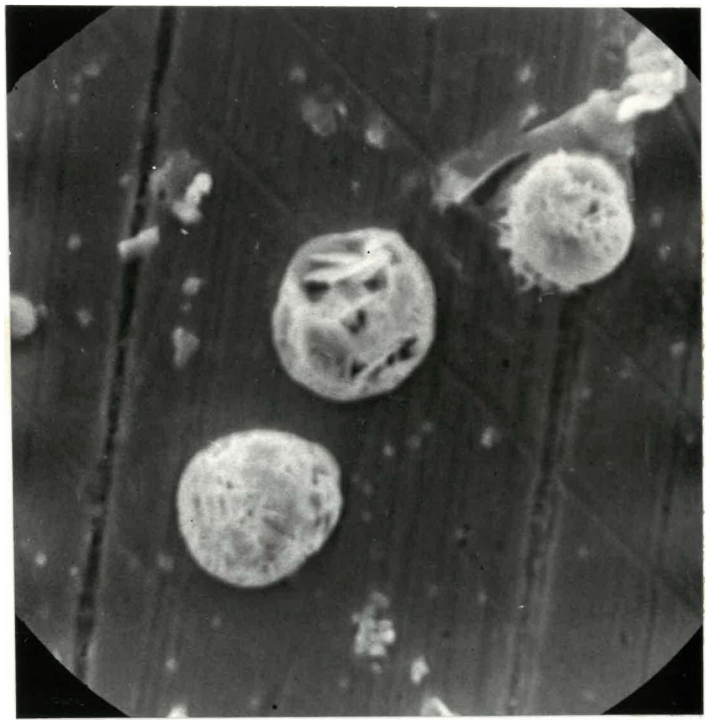


Fig. 6.44
Sample 55 clay
(top layer; Fig. 6.43)

(a) x720
10 µm

No. 0960
25 kV



(b) x3000
5 µm

No. 0992
15 kV

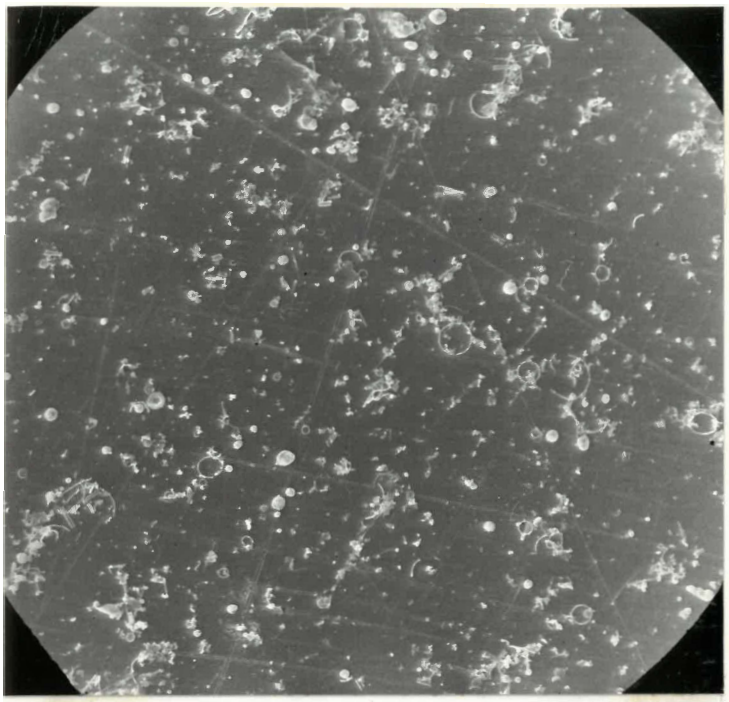
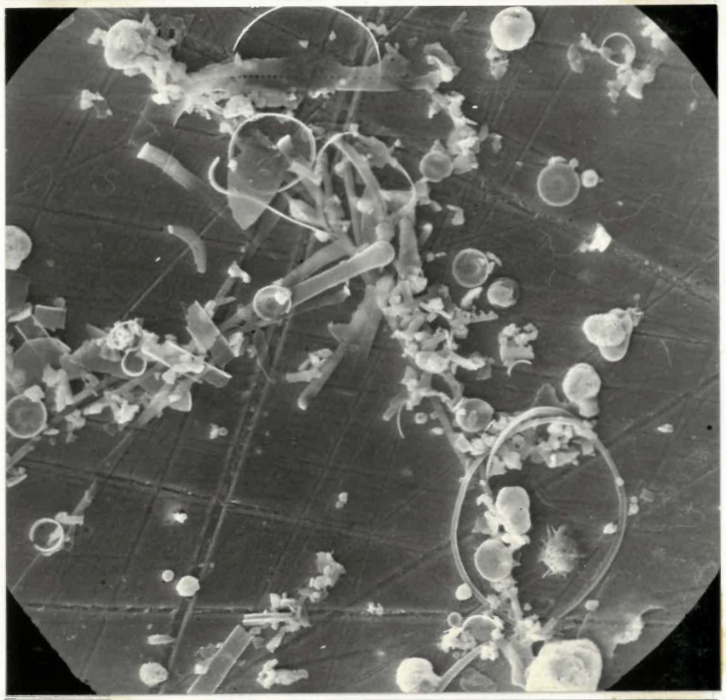


Fig. 6.45
Sample 55 clay
(middle layer; Fig. 6.43)

x320
20 µm

No. 0974
15 kV



(b) x1500
10 µm

No. 0976
15 kV



(c) x6000
2 µm

No. 0977
15 kV

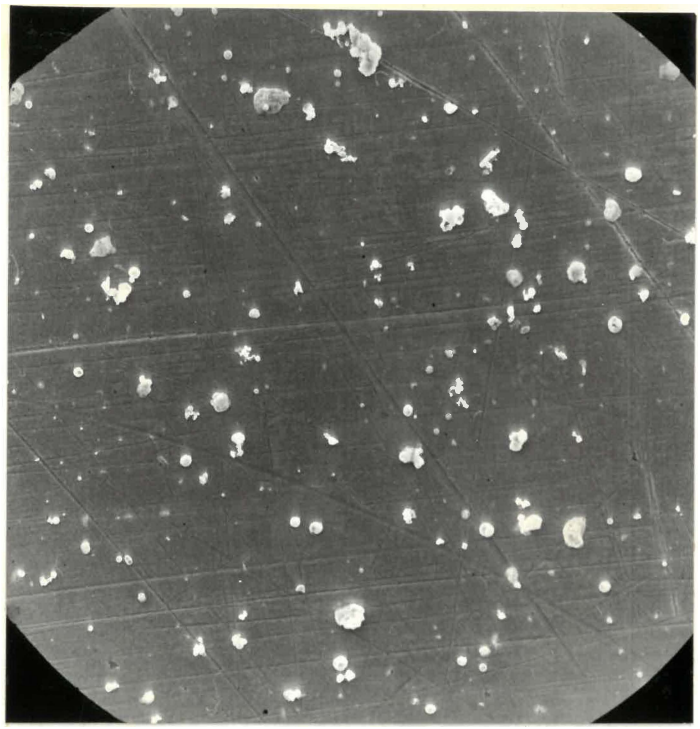
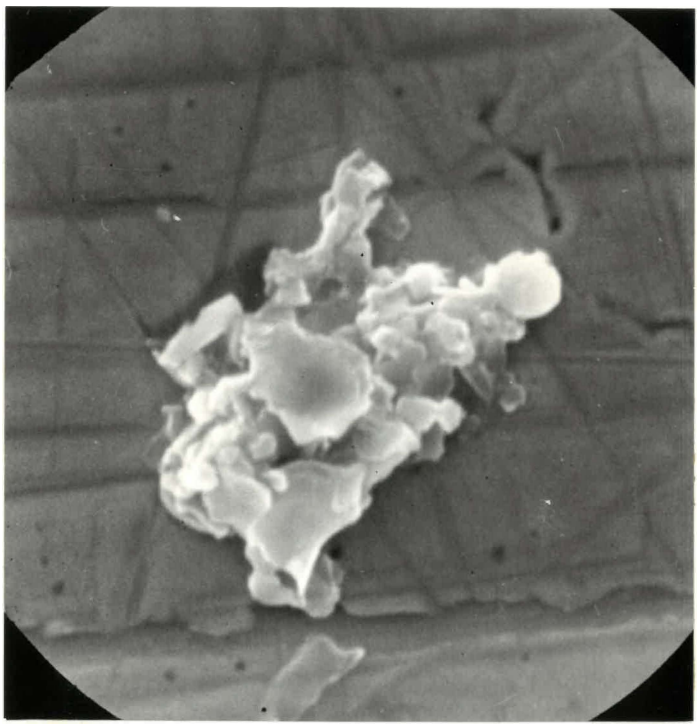


Fig. 6.46
Sample 55 clay
(bottom layer; Fig. 6.43)

(a) x720
20 µm

No. 0981
15 kV



(b) x8600
2 µm

No. 0982
15 kV

(e.g. girdle bands, long fragments) dimensions have little meaning with respect to size classification or settling rates in a fluid medium, and so are not given.

Component distribution

"Spherical objects" occur in all layers but are smaller and less abundant near the bottom; angular fragments and flake-like particles occur in all layers; diatom tests and test fragments occur only in the middle layer, where they are the most abundant component; and aggregates of flakes occur only in the bottom layer, where they also form the major component (Table 6.5). By converting component layer percentages to total percentages and summing these for each morphologically distinct component, the abundance of each as a percentage of the total clay sample is obtained (Table 6.6).

Non-diatom particle morphology

Spherical particles occurring throughout the clay fractions have several distinct morphologies (Figs. 6.47-6.49). Fig. 6.47a shows an apparently hollow body with surface crystal growths. Other sphericical particles show a surface crystal structure but no evidence of being hollow (e.g. Fig. 6.47b). Composition of these particles was not determined, however their morphology suggests they may be partly or wholly authigenic silica. $SiO_2\ nH_2O$ is a common authigenic mineral in diatomite and characteristically forms fibrous spherulites (Heinrich, 1965). Amorphous silica (e.g. diatom tests) is one of the most soluble forms of silica (equilibrium solubility approximately 120 ppm in water at room temperature) and saturation of interstitial waters may result in precipitation of crystalline

Table 6.5. Sample 55 Coarse Clay (0.2-2 μm) Components

LAYER		COMPONENT MORPHOLOGY	APPROX. DIMENSION	ABUNDANCE IN LAYER
Top (≃15%)	1	Approximately spherical)	5-10 μm	
	2	" " ") same?	<2 μm	≃ 70%
(Fig. 6.44)	3	Angular fragments, flake-like particles	1-2 μm	≃ 30%
MIDDLE (≃70%)	1	Diatom tests (mainly *Cyclotella* sp.)	3-6 μm	≃ 5%
	2	Diatom test fragments (girdle bands, flakes and strips with regular perforations, *Synedia* sp.)	-	≃ 55%
(Fig. 6.45)	3	Approximately spherical, some have the appearance of crystal growths or aggregates	2-10 μm	≃ 20%
	4	Angular fragments, flake-like particles	0.2-1.5 μm	≃ 20%
BOTTOM (≃15%)	1	Aggregates (2-8 μm) of flakes	0.3-1.5 μm	≃ 55%
(Fig. 6.46)	2	Approximately spherical	2-5 μm	≃ 40%
	3	Individual flakes	<2 μm	<5%

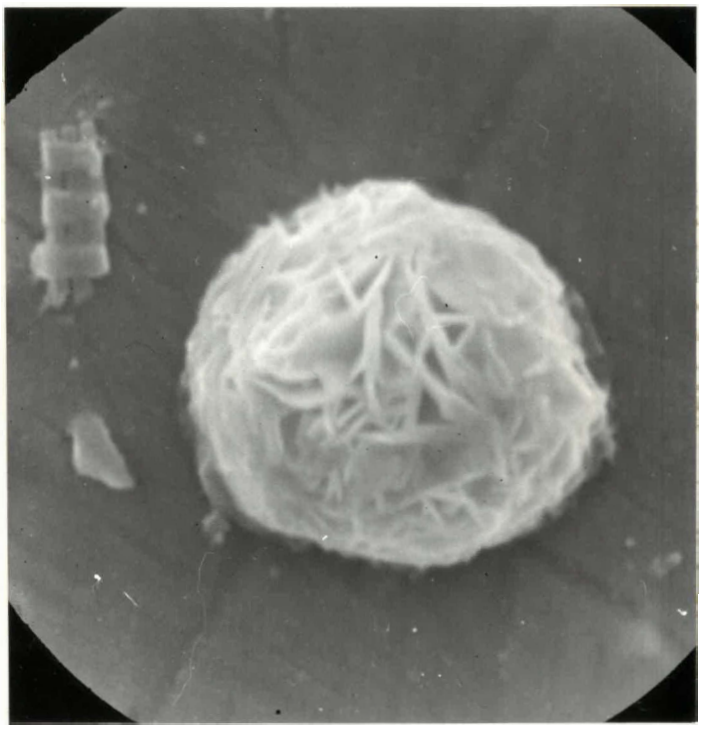
Table 6.6. Approximate abundance of morphologically distinct components in the coarse clay fraction of sample 55

Particle morphology	Approximate abundance
Spherical particles	30%
Diatom tests and fragments	40%
Angular fragments and flake-like particles	20%
Aggregates of flakes	10%



Fig. 6.47
Sample 55 clay
(middle layer; Fig.6.43)
? Authigenic siliceous
micro-spherulites
(a) x2600
5 µm

No. 0993
15 kV



(b) x10,000
1 µm

No. 0975
15 kV

silica (Blatt *et al.* 1972). For example, particles of a similar morphology to the above particles from Taupo, commonly line microfossil moulds in opaline Eocene claystone deposits (altered diatomites) of the Atlantic and Gulf Coast Plain, U.S.A. (Weaver and Wise, 1973; S.E.M. micrographs p.900). These particles consist of, pp.899-900 "... unidimensionally disordered alpha-cristobalite in the form of bladed microspherulites", probably as a result of "... *in situ* dissolution of biogenous opal with silica reprecipitated inorganically as authigenic disordered alpha-cristobalite".

Other "spherical" particles (e.g. 6.48a and b) are hollow and have some symmetry, suggesting a biogenic origin. Because of the possibility that biogenic particle morphology may have been modified during sample preparation, it is unclear whether or not these particles are distinct from the round particles illustrated in Fig. 6.49a and b, each of which has the appearance of a partially collapsed sphere with at least one pore-like opening. Spherical cells, <2 μm to 5 μm in diameter and having a pore-like opening, dominate the ultraplankton (0.2-3 μm phytoplankton) in Lake Taupo (Paerl, 1977; S.E.M. micrograph, p.299). Several such cells have been observed in the very fine silt fraction of Lake Taupo sediments (e.g. Fig. 6.39). Little is known of the taxonomy of these ultraplankters, which Paerl (1977) has referred to as LRGTs (little round green things). Ultraplankton is more prominent in oligotrophic lakes (e.g. Lake Taupo) where it may form up to 35% of the biomass and 76% of the primary productivity (Paerl, 1977).

S.E.M. X-ray energy dispersive mocroprobe spectra of many of the round particles illustrated in Fig. 6.49a and b show they consist

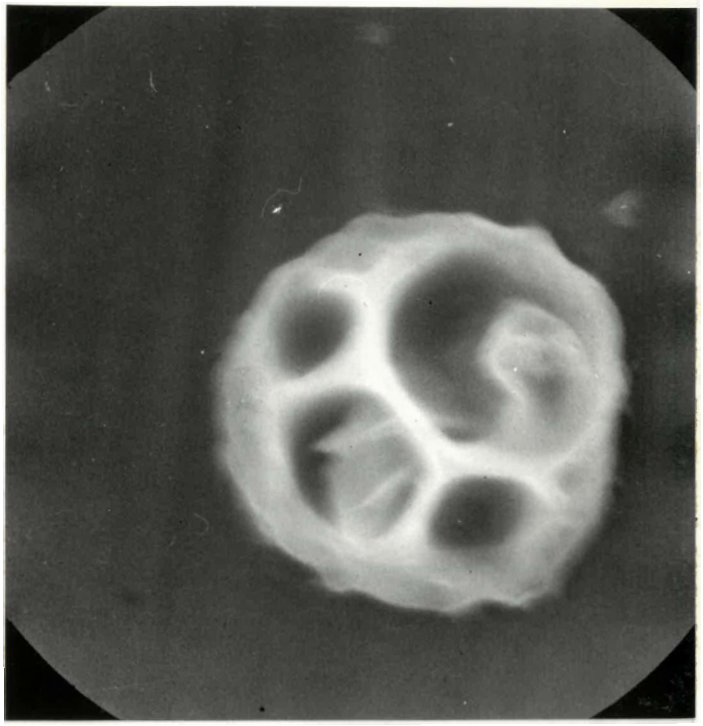


Fig. 6.48

(middle layer)

Sample 55 clay

(middle layer; Fig. 6.43)

(? bio-capsule)

x8600

2 µm

No. 0994

25 kV



(b) Sample 104

clay

(? bio-capsule)

x18000

1 µm

No. 0956

25 kV

largely, or entirely, of sulphur (e.g. Fig. 6.50). The nature and source of such sulphur in the sediment is unclear. A general sulphur cycle for lacustrine environments is well established (e.g. Reeves, 1968; Berner, 1971; Brock, 1974), and shows that particulate sulphur or sulphur compounds may exist in lake sediments in a number of forms depending on the immediate microenvironment. For example, sulphur may initially reach the sediments through the water column as organic sulphur compounds, elemental sulphur particles and dissolved sulphate anions (SO_4^{2-}); or directly from sub-lacustrine hydrothermal activity. Under anaerobic conditions in lake sediments, these forms of sulphur are reduced to H_2S and HS^- mainly by bacteria of the genus *desulphovibrio*. Dissolved H_2S in the sediments may bleed back into the water column, where spontaneous oxidation in the presence of dissolved oxygen produces SO_4^{2-} and colloidal particles of elemental sulphur (S^o), or react with iron minerals and precipitate the finely disseminated monosulphides largely responsible for the black colouring in anaerobic lake sediments (fine black lenses and patches were observed in freshly recovered Lake Taupo sediments, and rapid growths of black-coloured patches in the stored sediment samples occurred in the laboratory, probably as a result of such bacterial action). These monosulphides are predominantly mackinawite (non-crystalline $Fe_{1.05}S$) and greigite (cubic Fe_3S_4), together referred to as hydrotroillite. In the presence of oxygen, metastable hydrotroillite is oxidised producing elemental sulphur (i.e. $4FeS + 3O_2 \longrightarrow 2Fe_2O_3 + 4S^o$; Reeves, 1968).

Reduced sulphur in lake sediments may also be oxidised by bacteria belonging to the families *Beggiatoaceae*, *Nitrobacteriaceae*,

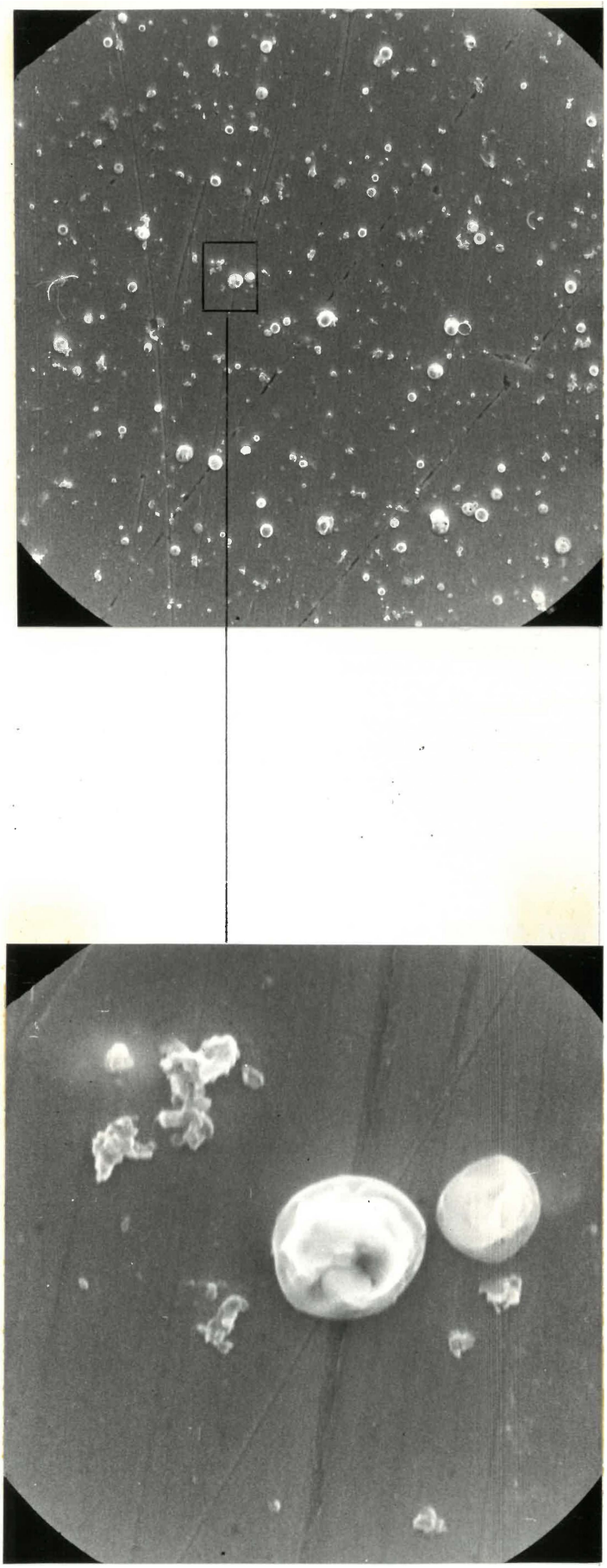


Fig. 6.49
Sample 104 clay
(top layer)

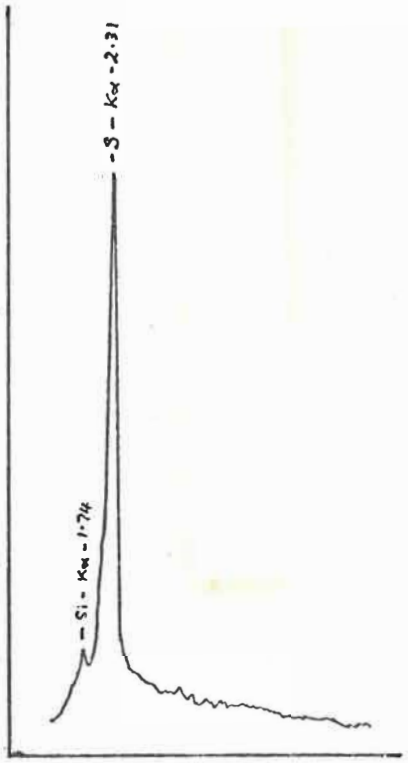
(a) x600
10 µm

No. 0954
26 kV

(b) x6000
1 µ

"spherical" particles
(?collapsed L.R.G.T's,
? sulphur particles)
and clay flakes.

No. 0955
26 kV



↑
Counts

Counting time = 80 seconds at 18 kV.

Energy →

Fig. 6.50. S.E.M. X-ray energy dispersive spectrum of the approximately spherical particle illustrated in Fig. 6.49b.

Pseudomonadaceae and *Rhodospirillaceae*. Most of these bacteria deposit elemental sulphur granules internally (e.g. Beggiatoa occur as filaments which are often filled with 0.5-1.0 μm sulphur granules; Brock, 1974, p.639). Species of the important genus, *thiobacillus* (*Nitrobacteriaceae*) may deposit amorphous elemental sulphur granules externally.

Where sufficient light is present (mostly infra-red; 700-900 nm), photosynthetic bacteria may also produce 0.5-1.0 μm granules of elemental sulphur by reduction of H_2S. These bacteria are divided into two broad groups on the basis of pigmentation; green photosynthetic bacteria (*Chlorobiaceae*) deposit elemental sulphur granules externally, and purple photosynthetic bacteria (*Chromatiaceae*) deposit them internally (Brock, 1974; p.622). It is likely that such granules would be released during organic matter removal from sediment samples.

On this basis, the sulphur-containing particles observed under the S.E.M. (figs. 6.49a and b) are possibly elemental sulphur resulting from:

(a) Inorganic precipitation near the sediment/water interface or from hydrothermally active sites.

(b) Organic precipitation near the sediment water interface.

(c) Release from organic sulphur compounds and bacteria destroyed during organic matter removal.

(d) Oxidation of sulphides during S.E.M. sample preparation.

S.E.M. X-ray energy dispersive microprobe analysis of the angular fragments in the coarse clay fractions indicate essentially siliceous material. Both diatom tests and pumice are capable of producing such fragments (e.g. Figs. 6.51a and b).

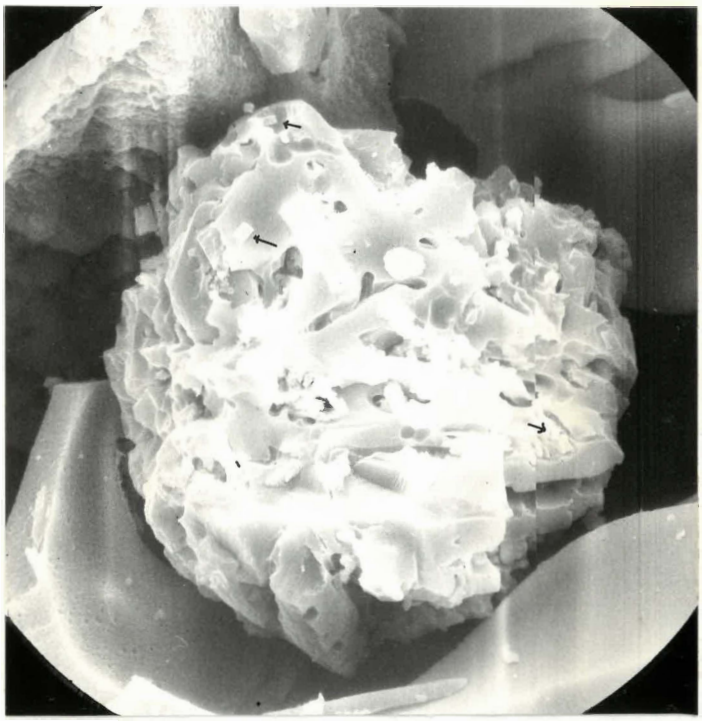


Fig. 6.51

Sample 52

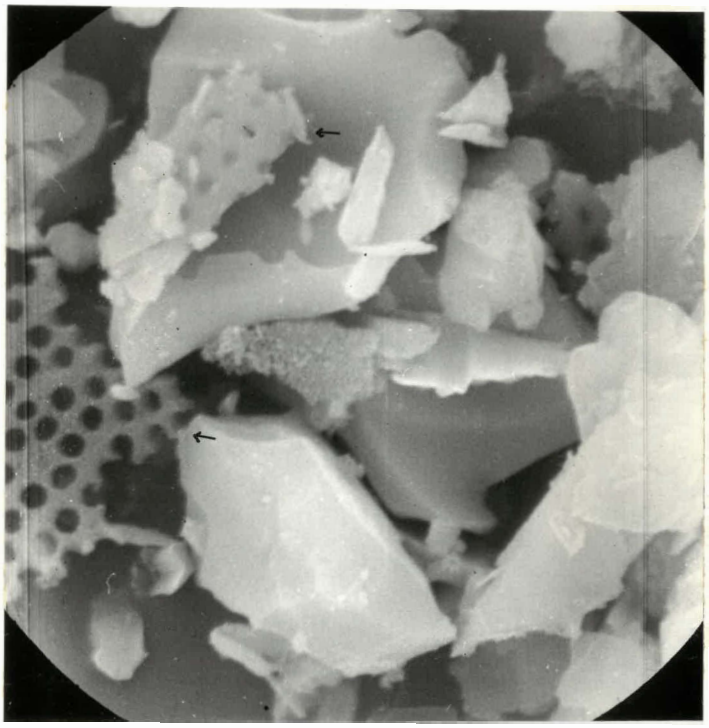
(a) Clay-sized pumice fragments

x2000

5 µm

No. 0556

18 kV



Clay-sized diatom fragments

x4800

2 µm

No. 0678

18 kV

The "fine clay" (based on estimated specific gravity of particles and centrifuge times) fraction formed less than 1% of the twelve centrifuged clay samples. The particles are commonly up to 1 μm in diameter and exhibit flake-like morphology typical of crystalline clay minerals (e.g. Fig. 6.52a and b). Microprobe analysis of individual flakes or small aggregates of flakes proved unsuccessful. Low S.E.M. accelerating voltage and small amounts of material prevented adequate elemental counts being obtained, and an increase in accelerating voltage resulted in particle destruction.

Larger aggregates of clay-sized material microprobed over an area, rather than at a point, gave 'average' elemental counts that were similar from sample to sample (e.g. Figs. 6.53, 6.54), comprising mainly Si, Al, P, K, Fe and Mn.

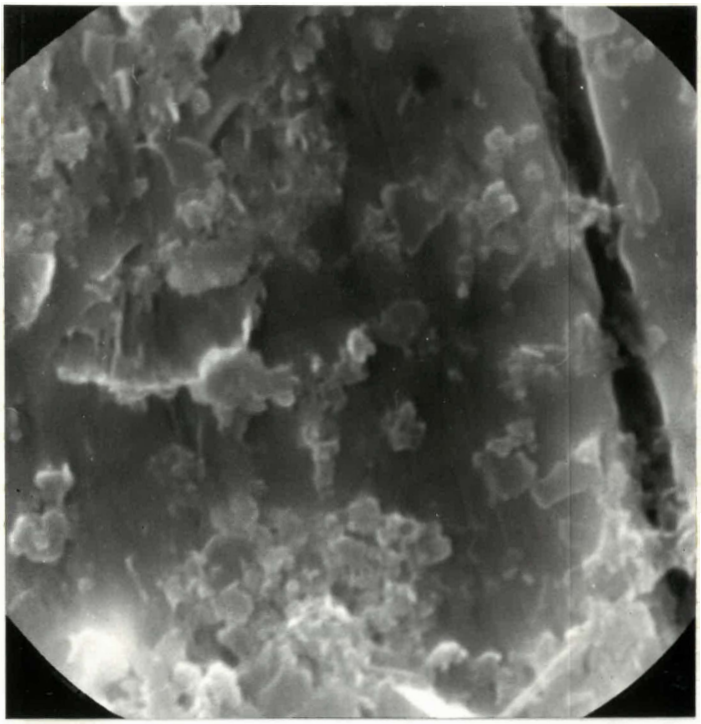
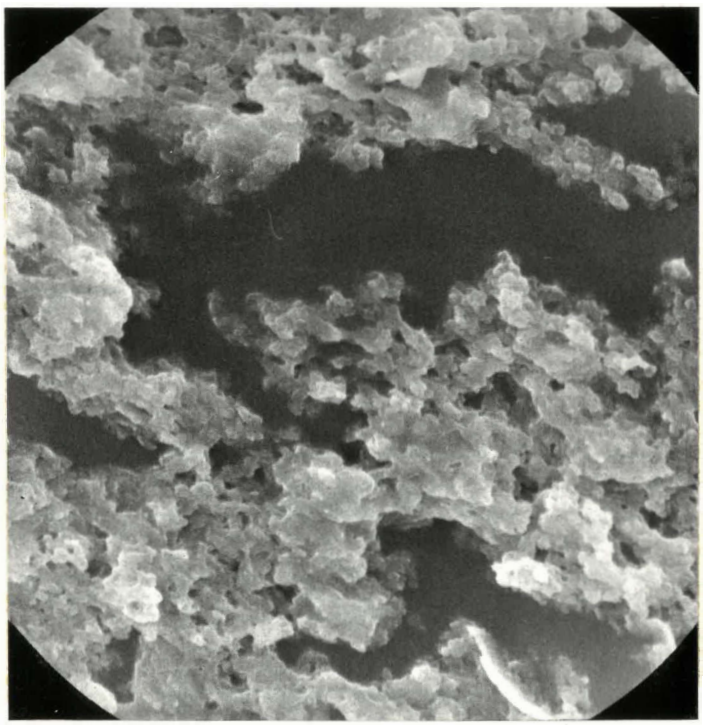


Fig. 6.52

(a) Sample 34 "fine clay" mounted on brass stub.
x10,000
1 µm

No. 2057
28 kV



(b) Sample 104 "fine clay" mounted on carbon stub
x2200
5 µm

No. 2061
18 kV

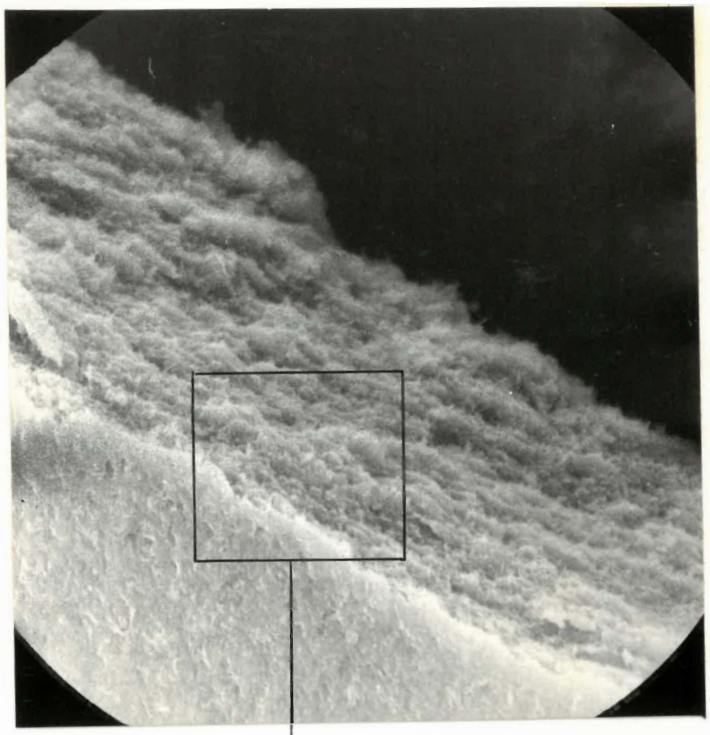


Fig. 6.53
Sample 104 "fine clay"
(Broken edge of aggregate.
Inset shows area on which
microprobe was focussed.
Ref. Fig. 6.54).

x1000

10 μ

No. 2056
18 kV

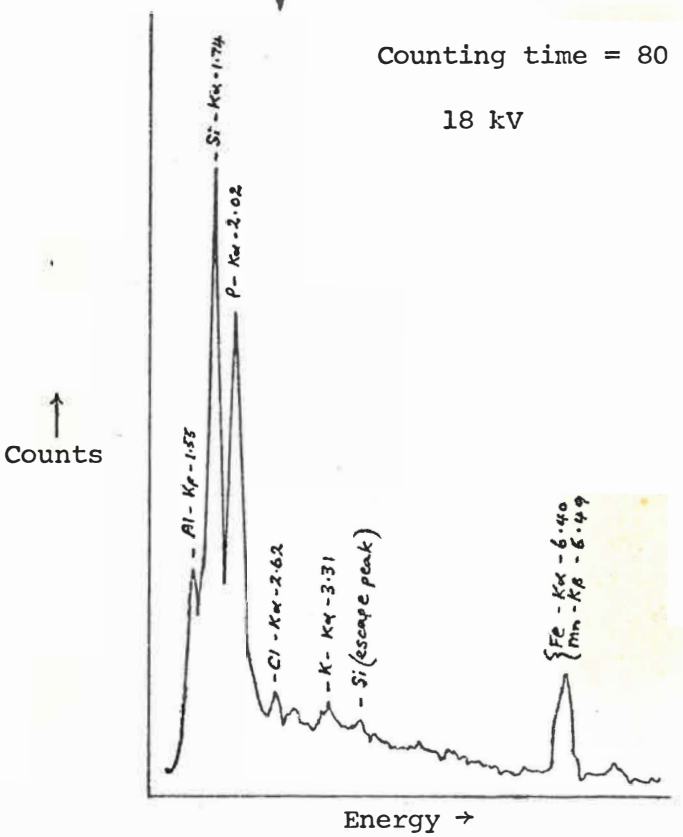


Fig. 6.54. S.E.M. X-ray energy dispersive spectrum showing average elemental composition for clay sample 8. Sample area scanned is shown as an inset in Fig. 6.53.

CHAPTER 7

DISCUSSION AND INTERPRETATION OF EXPERIMENTAL RESULTS

7.1 INTRODUCTION

On the basis of experimental work several maps have been presented in the previous chapters showing areal changes in textural and compositional properties in Lake Taupo bottom sediments. These are intended to reveal trends in each parameter by grouping values between certain limits, without creating unnecessary or artificial details. Isolines have been interpolated assuming linear changes between point values, unless bathymetric considerations, changing bottom slope, or evidence of redeposition dictates otherwise. Subjectivity due to choice of isoline values, their positioning, and the semi-quantitative nature of the values of some parameters, all affect the comparative interpretation of the patterns on these maps.

7.2 SEDIMENT TEXTURAL IMPLICATIONS

Textures of the lake sediments are a function of the nature of the source material, sorting processes during transport to the lake, and reworking in the lake. Sorting depends on distance transported from source, energy of transporting media, rates of deposition, and energy at the site of deposition (Allen, 1970). Sediment composition has implications for source areas and consequently transport mechanisms and directions of sediment dispersal within the lake.

Broad relationships exist between sediment texture and environment in Lake Taupo and interpretation of textural data is made below

in terms of processes operating in the major lake environments.

Sub-lacustrine talus environment

Coarse, very poorly sorted sediments occur in deep water close to cliffed areas along the western and northern shores of the lake. Textures of this material reflect the lack of river or nearshore-transport sorting processes on material falling from the cliff faces, and the simultaneous deposition of silt and clay-sized material transported from other areas in suspension (Fig. 7.1).

Shelf environment

In contrast to sub-lacustrine talus material, shelf sands, gravels and sand-gravel mixtures along the eastern and southern sides of the lake lack mud and show better sorting, having first been transported to the lake and then subjected to swell and wave action at the lake margin. Shelf sediment textural characteristics are determined mainly by the effects of wave action (King, 1972; Pickrill, 1978). Deep-water waves consist of orbital motions of water which decrease exponentially to negligible values at water depths approximately equivalent to half their wavelength (Fig. 7.2). Thus the depth at which wave motion first impinges on the bottom (i.e. effective wave base) is determined by wave amplitude and period, both of which increase with wind speed and length of exposed fetch. Thereafter, incoming wave interaction with the bottom increases as the shelf depth decreases, and bottom sediment movement is initiated when orbital flow velocity at the bottom exceeds the threshold velocity needed to move sediment particles of a particular size and specific gravity. The wave energy gradient across a shelf produces shore-normal

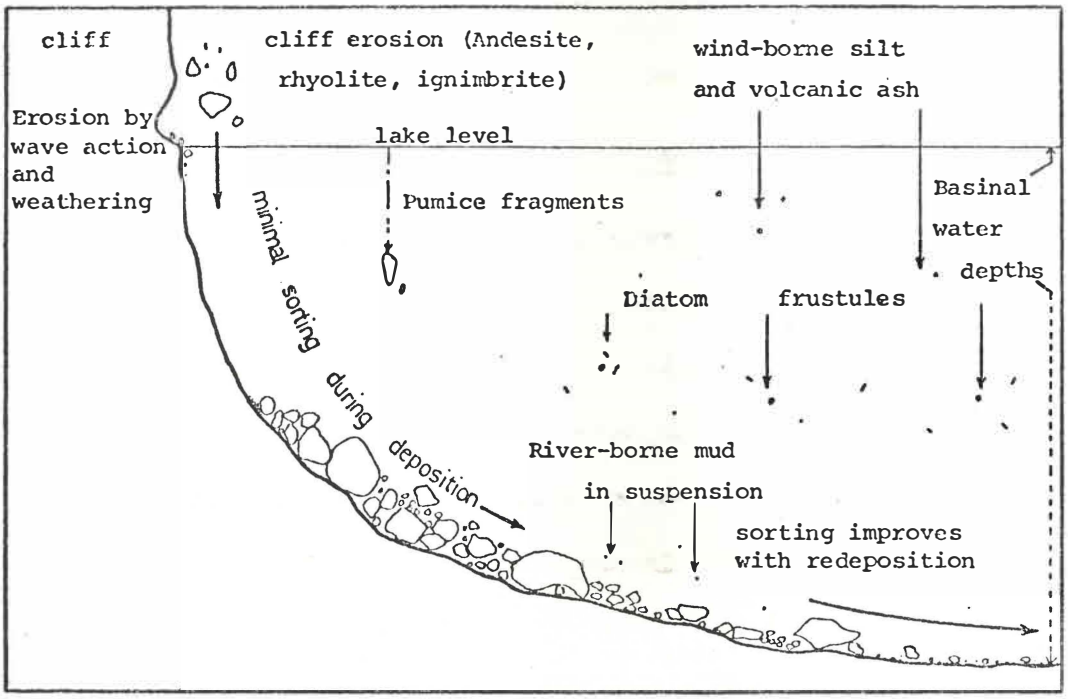


Fig. 7.1. Idealised cross-section of sub-lacustrine talus facies showing types of sediment input.

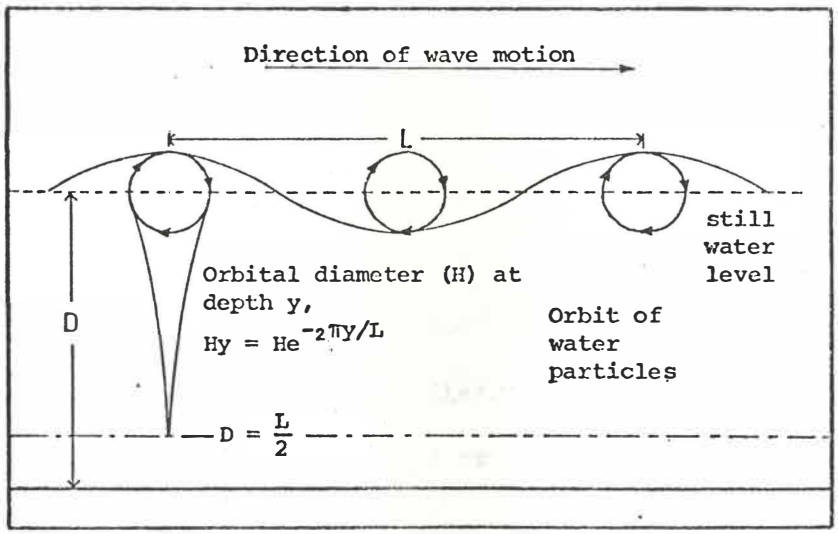
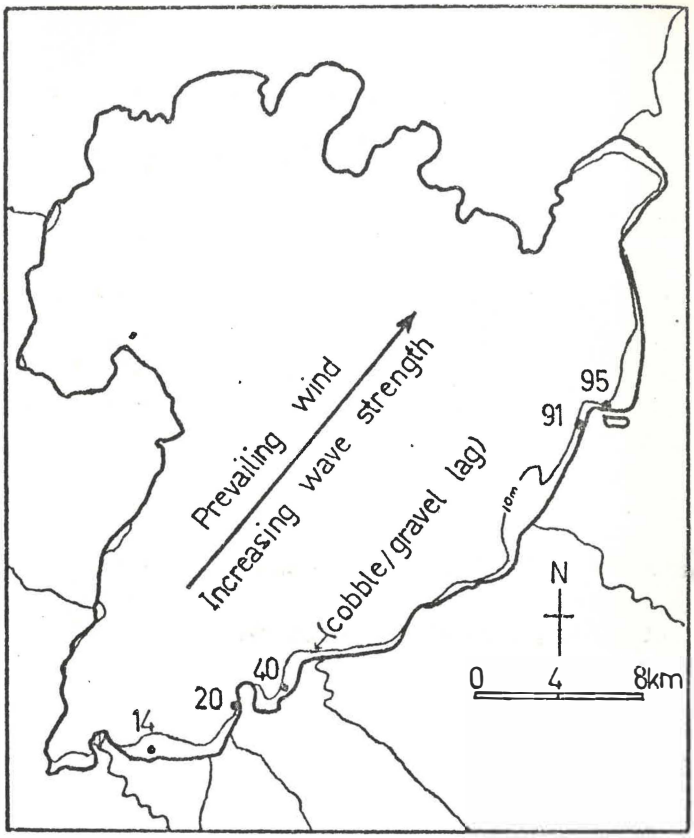


Fig. 7.2. Idealised cross-section of wave motion in deep water. Wave orbital diameter decreases approximately 50% for each increment in water depth equal to $\frac{L}{9}$ and reaches negligible values at about $D = \frac{L}{2}$.

sorting by selective bed-load and suspension transport. Mean grain size decreases and sorting deteriorates with increasing water depth (Pickrill, 1978).

In Lake Taupo, shelf-sediment textural trends are apparent although they are partly obscured by the presence of pumice. Sand and gravel-sized pumice produces textural data that are difficult to interpret in terms of classical hydrodynamic energy and transport processes. Pumice fragments have variable buoyancy, ranging from positive through neutral to negative, depending on their degree of vesicularity and waterlogging. Fragments floating on the lake become progressively waterlogged and may sink anywhere. Larger fragments may be carried right across the lake, become beached, and eventually dry out again. Fragments with slight negative buoyancy are easily moved across the bottom by weak currents and tend to collect in sheltered areas, such as in ripple troughs and on the slope. Shelf sediments in which the above pumice problem is minimal have textures that may reflect the degree of exposure to prevailing wind-wave activity. For any given depth, modal grain size is larger and sorting is generally better on more exposed shelf areas. For example, at the southern end of the lake the presence of a 3ϕ sand mode (and weed beds) indicates one of the lowest energy shelf environments in the lake (Fig. 7.3).

The texture of shelf sediments may also reflect the competence of river and stream waters entering the lake, particularly during times of flood. For example, a predominantly greywacke cobble and pebble lag has formed off the Oruatua headland, presumably from material jetted into the lake by the Tauranga-Taupo River, and a coarse/very



Location of selected shelf-sediment sites in Lake Taupo

Sample Number	Water depth (m)	Pumice sand Content	Modal ϕ value	Sorting	Textural term	Exposure to prevailing wind-wave activity
14	1	negligible	0 and 3	ps	gS	low
20	4	low	3	ms	(g)S	moderate
40	4	low	4	vws	S	low
91	4	high	1	vws	(g)S	high
95	4	high	3	mws	(g)S	low

Fig. 7.3. Shelf-sediment sample textures reflect degree of exposure to prevailing wind-wave action. The modal grain size at a given depth reflects both sediment composition and the competence of wave-induced bed-load transport at that depth.
From site 20 to 40 and site 91 to 95 there is both a decrease in exposure and modal grain size.

coarse sand mode of rhyolite and greywacke fragments occurs close to a pre-existing Tongariro River mouth in Stump Bay (site 14, Fig. 7.3).

Slope and Rise Environments

Lake Taupo bathymetry shows that the steepest slope section occurs immediately lakewards of the shelf-break. The slope progressively decreases with increasing depth, producing an approximately concave profile. The slope is almost entirely below effective wave base, so sediment may be deposited either from shelf spill-over (sands, pumice gravels) or suspension (silt and clay-sized material). Creep, slumps, slides and density flows may redeposit sediments further downslope, particularly in areas where high rates of sedimentation near the shelf edge lead to oversteepening (Brodie and Irwin, 1970; Pickrill, 1978).

The rate of sediment accumulation from an areally uniform suspension increases with decreasing slope angle because the vertically projected area of the slope increases. This, together with both decreased environmental energy and increased remoteness from shelf spill-over with depth, produce the downslope transition from silty sands through sandy silts and silts across the rise to basinal regions in Lake Taupo.

Diatom frustules frequently occur in the fine sand fraction of slope and rise sediments and occasionally dominate this fraction (Fig. 7.4). Species include abundant *Nitzchia* sp. and *Synedra* sp., together with *Surirella* sp. and *Cymbella* sp. Occasional siliceous sponge spicules also occur (see chapter 6, Figs. 6.33-6.38). These species live in shelf-depth waters attached to the substrate or

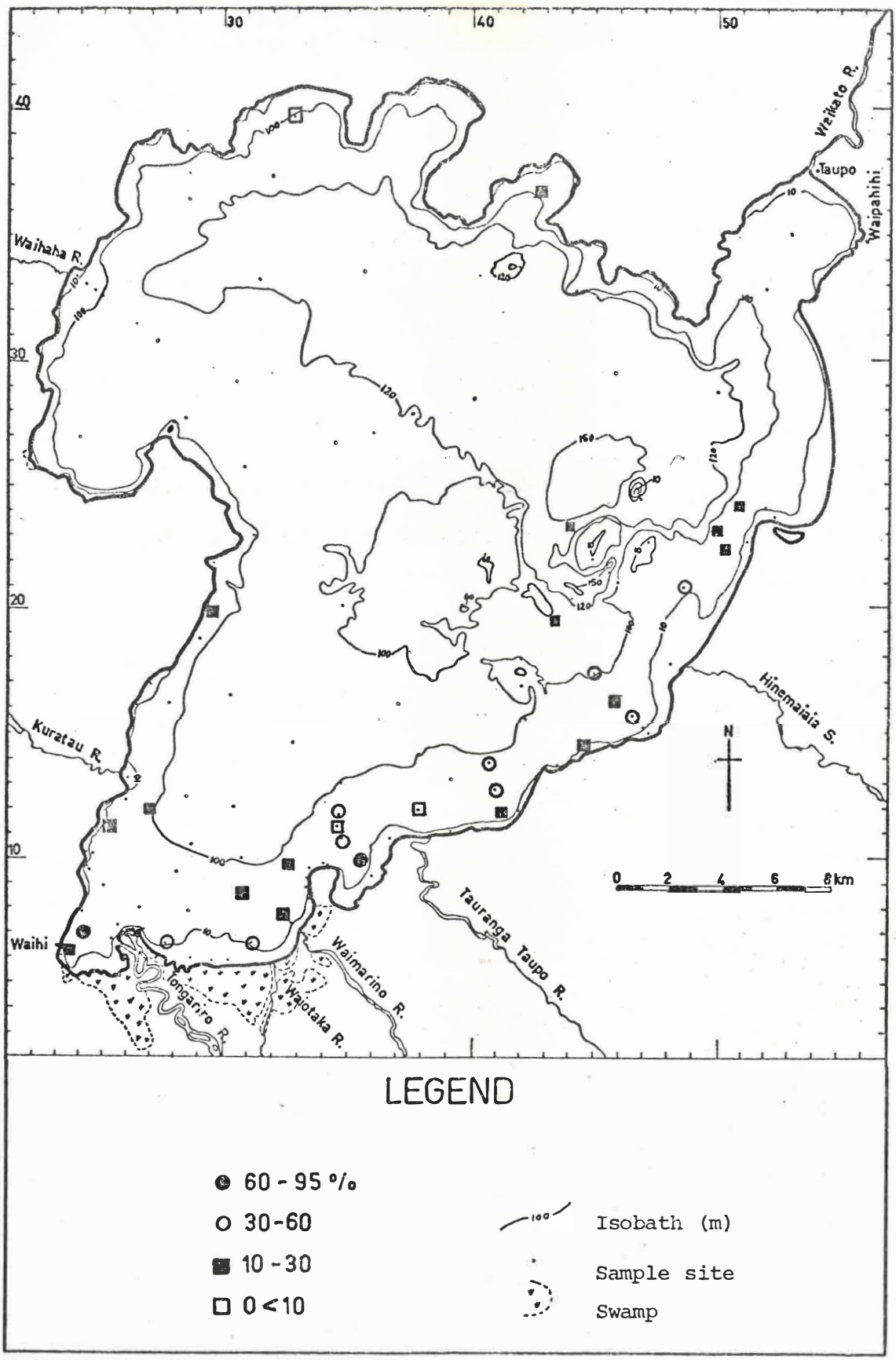


Fig. 7.4. Approximate quantity of benthic/aufwuch diatom tests in the sand fraction of surficial sediment samples from Lake Taupo.

aquatic vegetation (Cassie, 1974), and are probably winnowed to slope-rise areas, after death, by current energy gradients.

Thus a relatively large number of sources contribute material to slope and rise regions, commonly producing polymodal, poorly sorted sediments.

Basinal Environment

Together silt- and clay-sized material generally account for more than 95% of the basinal sediments. Two modes, having an inverse relationship, dominate the silt fraction (Fig. 5.9). S.E.M. indicates that the 5.5-6.0ϕ mode is due to terrigenous material (Fig. 6.18b), and the 7.0-7.5ϕ mode to diatom frustules (Fig. 6.21c). In the absence of any evidence to the contrary, it is assumed that the average sedimentation rate of diatom frustules is similar in all deep-water parts of the lake, so that variations in the mode-ratio values (Fig. 5.10) reflect variations in the terrigenous silt component alone (Fig. 7.5).

Terrigenous material dominates the silt fraction at the southern end of the lake and close to shelf areas. The decrease in terrigenous silt away from shelf areas, despite an increase in total silt content, suggests that much of it has been winnowed from adjacent shelf areas. The terrigenous silt content of the basinal sediments decreases almost linearly in a northeasterly direction, attaining negligible values in central and northern parts of the lake. The relatively low terrigenous silt content in a small area near the southern end of the lake suggests that turbid currents rarely traverse this area. Extensive erosion of high cliffs of pumice-breccia to the north of the Hinemaiaia Stream mouth probably contributes the

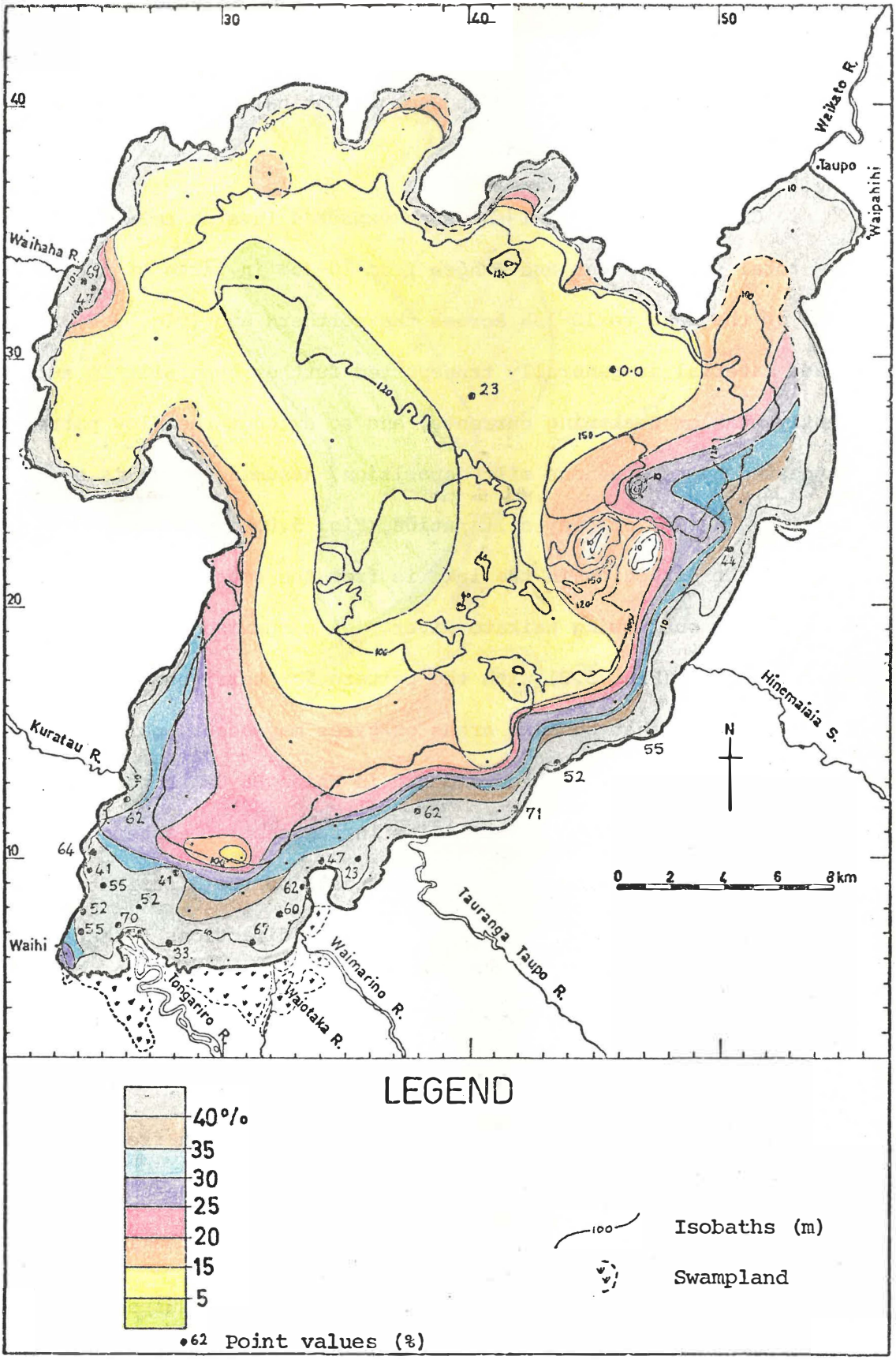


Fig. 7.5. Terrigenous silt as a percentage of total silt content in deep-water sediments of Lake Taupo.

increased terrigenous silt component to basinal sediments northeast of the Horomatangi Reef.

Clay-sized material shows an expected inverse relationship with the total silt content and ranges from 20-25% in parts of the southern half of the lake to 10-15% across the northern end (Fig. 5.7). Clay-sized material is generally transported further than silt in sufficiently weak or weakening currents, and so extends the flow patterns suggested by terrigenous silt deposition, assuming there is a common source. A plot of clay:silt ratios (Fig. 5.8) indicates that the net current direction in the lake is from the southwestern side towards the outflowing Waikato River. A comparison of the clay:silt ratio pattern (Fig. 5.8) with the pattern for terrigenous silt (Fig. 5.10) suggests that ponding areas or gyres may occur, particularly to the west of Motuoapa headland and in Waihi Bay. Abnormally high clay contents at two localities in the central eastern part of the lake remain unexplained. On the basis of the distribution of terrigenous silt and clay in the lake, flow directions for suspended sediment-laden currents are proposed (Fig. 7.6a). Further evidence for these flow directions is provided by a Band 4 Landsat image of Lake Taupo taken on the 22 December, 1975 (Fig. 7.6b). The image clearly shows a plume of suspended sediment extending from the Tongariro delta up the western side of the lake to the cliffs north of Poukura and across to the northeastern region of the lake.

Campbell (1977) has identified four zones of suspended-sediment density from a Photowrite enlargement of the Band 4 Landsat image (Fig. 7.6c). He suggested that the Kuratau and Waitahanui Rivers and the Whareroa Stream contributed significantly to this

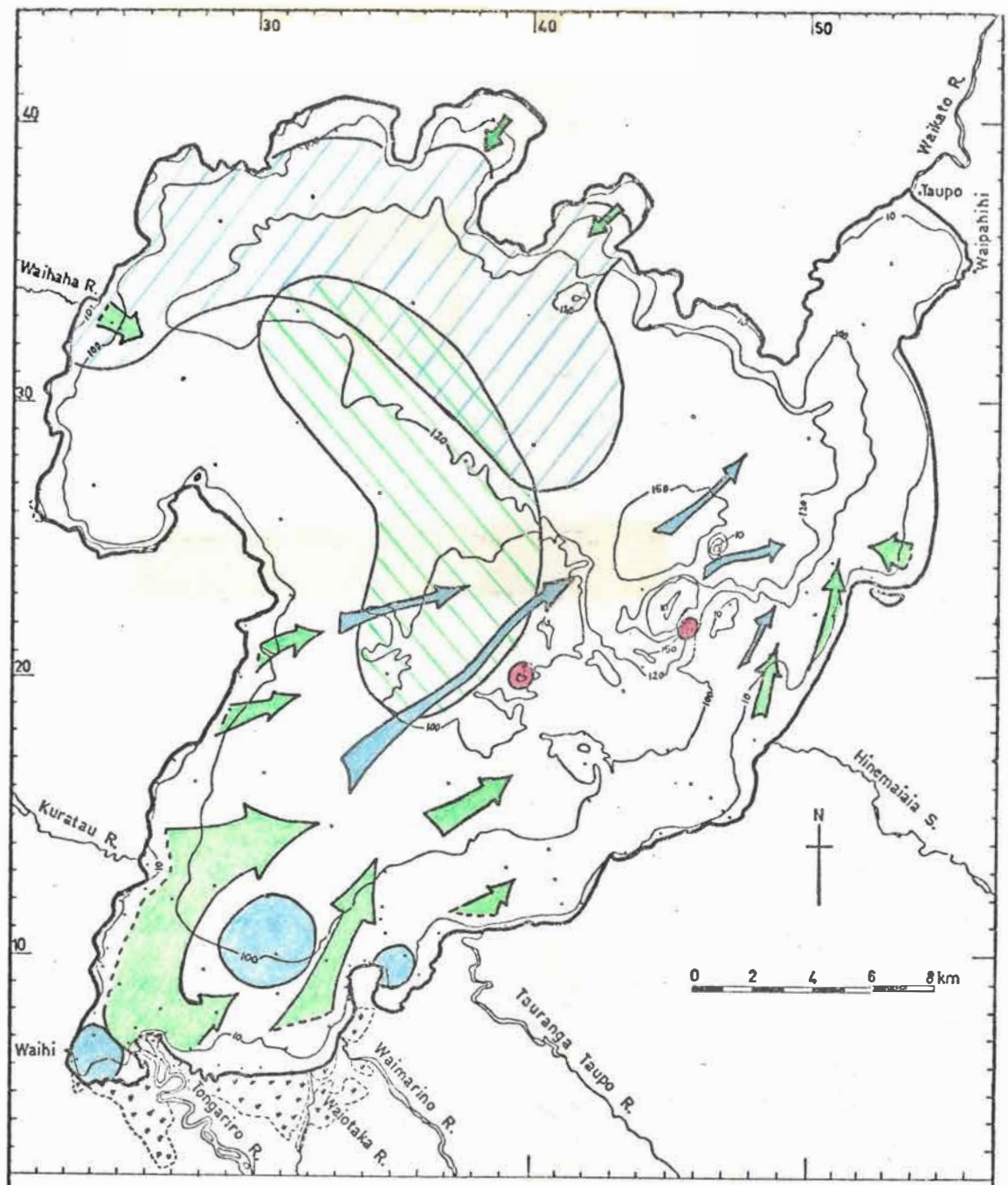


Fig. 7.6a. Flow directions of sediment laden currents based on areal changes of terrigenous silt and clay content.

sediment load. However, a comparison of the image with lake bathymetry (Map3, in map pocket) indicates that the zones depicted in Fig. 7.6c as 'heavy density' probably result largely from shelf areas being recorded on the Landsat image (e.g. Kuratau shelf, Stump Bay, Motuoapa Bay, Otutere Banks, northern Tapaueharuru Bay). Suspended sediment resulting from wave action along the coast to the north of Hatepe may also contribute to the 'density' in that region. Photographic penetration to depths of at least 8 m (i.e. outer shelf depths) suggest that suspended sediment was being transported in the lake by either surface-flow or inter-flow at the time.

Sand content in the basinal sediments is generally less than 5%, with grain sizes ranging from very fine to medium sand. The relatively uniform content over most of the lake, and its occurrence as a distinct mode, suggest that the bulk of this sand has not been transported and dispersed by the same mechanism as the silt. Settling rates of these grain sizes preclude transport in suspension for any great distance from a stream mouth by either surface-flow or inter-flow, both of which rapidly lose competence by dispersal in at least two directions. Bottom flow may transport sand considerable distances over a lake floor, but this process creates textural patterns that correspond to channelisation of flow and overbank deposits. Channels and levees resulting from underflow of stream currents have been observed in Lake Wakatipu (Brodie and Irwin, 1970). However, none of these features occur in Lake Taupo, suggesting that inflowing currents disperse mainly by surface-flow, inter-flow or assimilation, and do not transport sand to central deep-water regions of the lake.



Fig. 7.6(b) A Band 4 Landsat image of Lake Taupo on 22 December 1975 (E-2334-21123). A Suspended sediment plume curves away from the Tongariro delta towards the northeastern region of Lake Taupo.

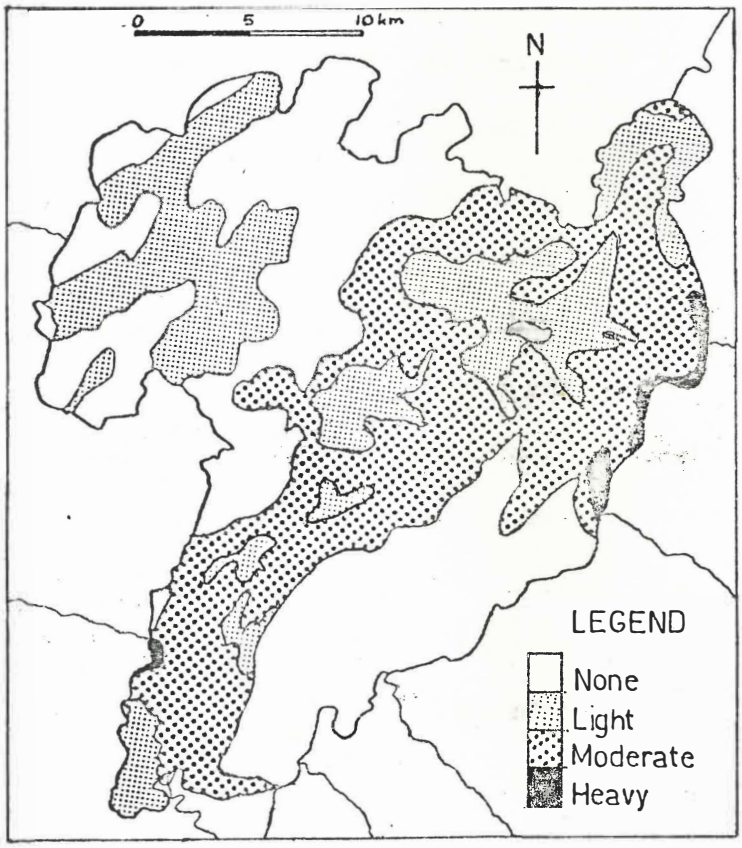
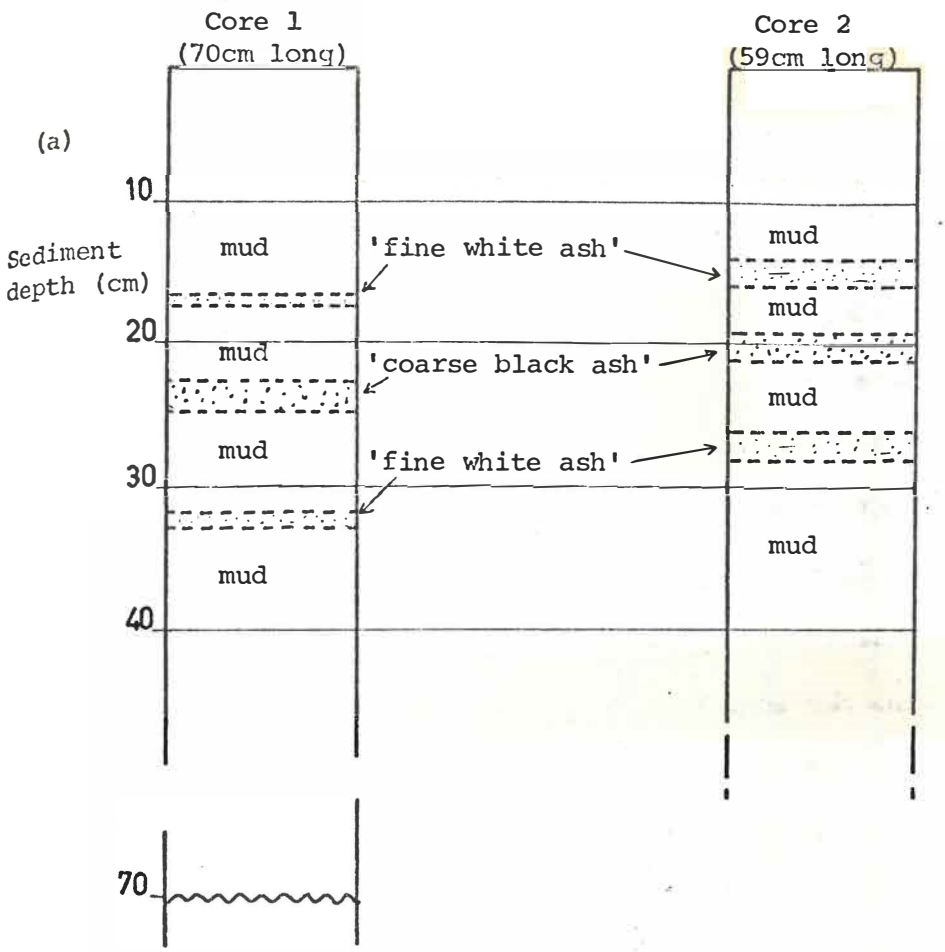


Fig. 7.6(c). Relative density of suspended sediment illustrated in 7.6(b) (after Campbell, 1977).

Wind transport might account for the relatively uniform distribution of sand. High country immediately to the south and west of the lake, and the volcanoes of Ruapehu and Ngauruhoe, are possible sources. Ngauruhoe Ash (Gregg, 1960) is periodically still accumulating on land, and is likely to have been deposited over the lake area by prevailing winds (Fig. 7.7). Rawlence (1973) claimed to have observed ash layers in two sediment cores from Lake Taupo but does not identify them (Fig. 7.7). The sand content does not decrease appreciably towards the southern end of the lake, as might be expected because of the higher rates of river-borne silt deposition there. This may reflect an increasing river-borne sand content towards the southern end of the lake and/or proximity to National Park volcanic sources.

Basinal silts occasionally contain lenses of redeposited pumice gravel and/or sand. The additional grain-size modes generally result in very poorly sorted sediments that are unusually coarse for their lake-bed situations.

The types and extent of sediment input and transport mechanisms for basinal, rise, slope and shelf facies are summarised in an idealised cross-section (Fig. 7.8).



Taupo Pumice (131 A.D). Overlying sediments have accumulated at an average rate of 0.38 mm/year.

(b)

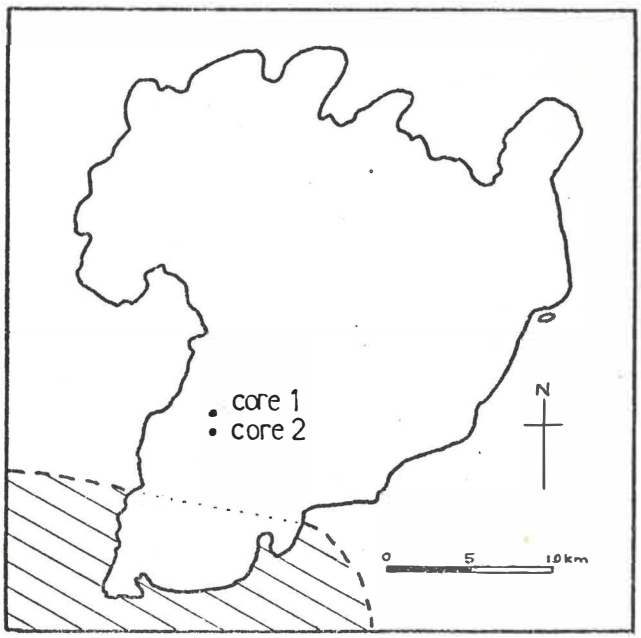


Fig. 7.7. (a) Volcanic ash layers observed in Lake Taupo sediment cores by Rawlence (1973), and

(b) Extent of andesitic Ngauruhoe Ash as a soil parent material (N.Z. Soil Bureau, 1973).

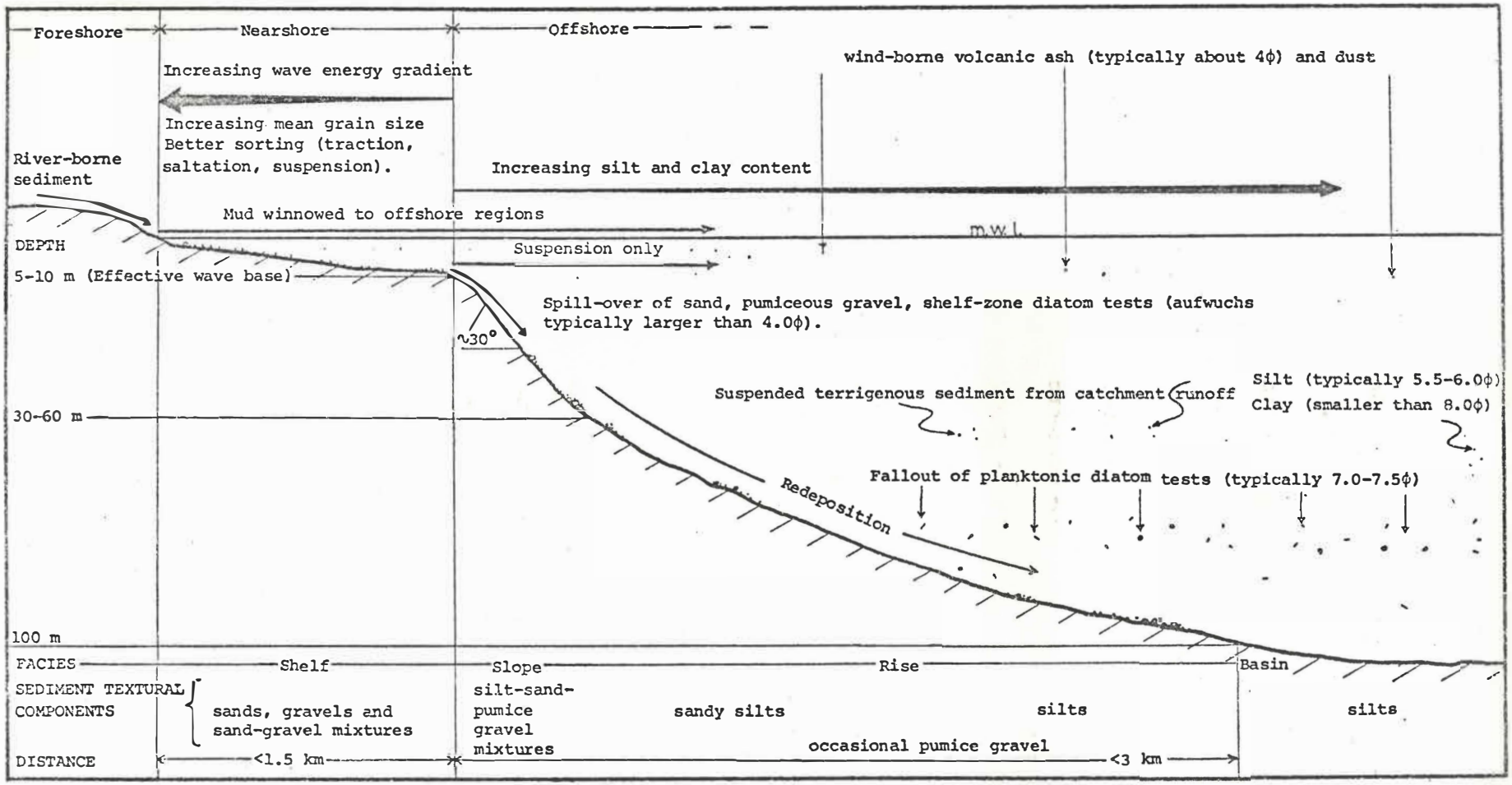


Fig. 7.8. Idealised cross-section of shelf-slope-rise-basin area showing types and extent of various sediment inputs and transport mechanisms. The modal grain sizes of each type of sediment input are given where they have been established. Adjacent facies are inter-gradational and the cross-section has variations in different parts of the lake.

Sub-lacustrine hilltop environment

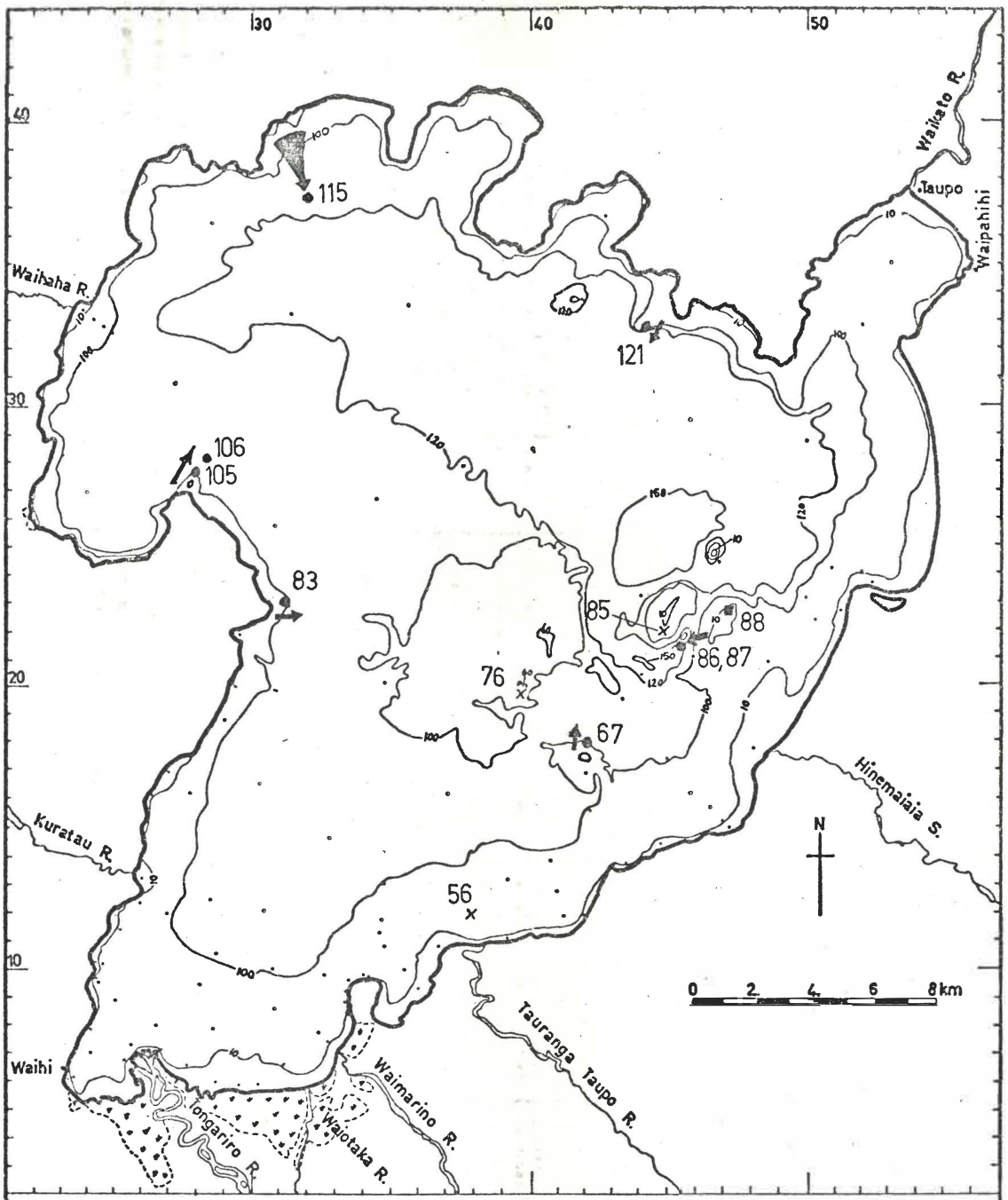
Sediments on sub-lacustrine topographic highs in Lake Taupo commonly contain higher pumice gravel and/or sand contents than the surrounding basinal sediments, even though the tops may be several tens of metres under water. On the basis of previous discussion on lake hydrodynamics, transport mechanisms, and sediment sources, it is likely that this is largely due to lower mud sedimentation rates, caused perhaps by special lake currents such as internal seiches. The presence of pumice gravel supports a low sedimentation rate in one of two ways. Either pumice has sedimented at the same rate as in basinal areas and has been concentrated by the lack of permanent mud deposition, or it is relict from the high influxes of pumice following the Taupo Pumice eruptions of about 131 A.D. In either case an accumulation of sand, from the same source as that in basinal sediments, is likely to have occurred also. Sand coarser than 3.5ϕ may be relict from volcanic activity, and is possibly in basinal sediments at greater sediment depths than were sampled. Sites below the peak of a sub-lacustrine hill may have accumulated sands by redeposition from further upslope.

Sands and rhyolite gravels on the Horomatangi Reef, the top of which is only a few metres below water, have probably been produced by wave action on the rhyolite forming the reef.

Textural characteristics of both redeposited and sub-lacustrine hilltop sediments and likely sources of redeposited sediments are summarised in Table 7.1 and Fig. 7.9.

	Sample Number	Depth (m)	Silt Diatom	Modes (ϕ) Terrigen.	Sand modes observed in basinal sediment	Sand modes not obs. in basinal sediment	wt.% sand	Gravel modes Pumice	Gravel modes (ϕ) Other	wt.% gravel	Mean grain size	Sorting	Skewness	Kurtosis	Textural term	Nearest upslope source
REDEPOSITED	67	100	7.0	-	-	3.0,2.0,-0.5	54.2	-	-	0.3	3.9	vps	sfs	vpk	(g)mS	Rhyolite cliffs
	83	96	7.5	6.0	4.0	2.0	10.1	-	-	-	6.8	ps	scs	vlk	sZ	Rhyolite cliffs
	86	132	7.5	5.5	4.0	3.0,2.0	62.4	-1.5	-	1.5	2.5	vps	sfs	lk	(g)mS	Rhyolite reef
	87	132	7.5	-	4.0	-	28.7	-1.5,-2.5	-	19.6	2.2	vps	ns	vpk	gM	Rhyolite reef
	105	92	7.0	6.0,5.0	4.0	2.0,-0.5	40.8	-3.0	-	46.6	-0.6	vps	ns	mk	msG	Ignimbrite cliffs
	106	112	7.0	6.0	4.0	2.0	33.6	-	-	1.7	5.2	vps	scs	vpk	(g)M	Ignimbrite cliffs
	115	107	7.5	6.0	3.5	2.0	40.4	-2.0	-	18.5	2.9	vps	cs	pk	gM	Beach/shelf deposits
SUB-LACUSTRINE HILL	56	42	7.5	5.0	3.5	-	76.5	-	-	0.1	3.7	ps	sfs	vlk	(g)mS	Slope deposits (possibly).
	76	60	7.0	-	-	3.0,2.0	24.8	-1.5,-3.0	-	7.5	3.6	vps	ns	pk	gM	Higher parts of sub-lacustrine hill
	85	15	-	6.0,5.0	4.0	1.5	40.6	-1.5,-2.5	-	27.9	2.0	vps	scs	vpk	gmS	Rhyolitic reef top
	88	3	-	-	-	-0.5	41.3	-	-1.5, -2.5, -3.5 (Rhyolite)	58.7	-1.6	ps	ns	pk	sG	
	120	102	7.0	5.5	4.0	2.0	15.5	-	-	-	5.9	vps	scs	pk	(g)M	
	121	116	7.0	-	4.0	2.0	24.0	-	-	0.1	5.4	ps	scs	vlk	sZ	Higher parts of sub-lacustrine hill

Table 7.1 Textural character of deep-water sediments containing redeposited pumice gravel and/or sand, and of sediments on sub-lacustrine hills. (For sample positions and likely sources of redeposited material see Fig. 7.9) sorting, skewness, kurtosis and textural term abbreviations are expanded in Appendix 1.



LEGEND

- • Sediment containing redeposited material.
- ➘ Likely direction of redeposition.
- ▪ Sediment on sub-lacustrine hilltops.
- x Sediment below the highest point of a sub-lacustrine hill which may have been influenced by redeposition from higher parts.

Fig. 7.9. Positions of deep-water sediments containing redeposited sand and pumice gravel, and of sub-lacustrine hilltop sediments enriched in sand and pumice gravel.

7.3 FELDSPAR AND QUARTZ TRENDS

The distributions of feldspar and quartz in Lake Taupo sediments are shown in Figs. 6.3 and 6.4 respectively.

The highest content of feldspar (>20%) occur in the shelf sediments and on a topographic high near the centre of the lake. The major deep-water trend in feldspar content involves a steady decrease in a northeasterly direction from about 15% near the Tongariro delta to less than 2% across the northern and southeastern parts of the lake. The higher value isolines tend to hug the western shore, except in Waihi Bay. A locally high feldspar value decreases to background levels over about 2 km offshore from the Waihaha River mouth.

The major trend in feldspar content indicates that the most important sources for this mineral occur at the southern end of the lake.

The highest quartz contents also occur in the shelf sediments where values are typically 5-10%, although there are local shelf areas of higher content. While overall the contents of quartz are lower than for feldspar, the deep-water trends are broadly similar, decreasing from about 5% to 1% or less in the northern half of the lake. There are, however, some important differences. The pattern of decreasing quartz does not extend as far north as that of feldspar, and the feldspar/quartz ratio in the central and northern parts of the lake is frequently 1/1, while at the southern end it is commonly 2/1 or more (Fig. 6.5). This suggests there are at least two distinct lake-sediment provenances. Furthermore, quartz does not display a

marked increase on some topographic highs (sites 76, 120) or in redeposited sediments (e.g. 67, 115, 106) that is evident for feldspar. At all of these sites the sediments have enriched sand contents and it is in this fraction where most of the feldspar occurs. Similarly, the sand fraction of basinal sediments has a high feldspar and very low to undetectable quartz content. Microscopic examination of the sand has shown that it is dominated by dark volcanic glass fragments, many with feldspar inclusions. X-ray diffraction analyses of fine, medium and coarse silt fractions show an increase in the feldspar/quartz ratio from fine to coarse silt (Table 6.1). These mineralogical differences with texture suggest two distinct transport mechanisms and/or two sources of material. Comparison of the lake sediment mineralogy with that for catchment cover deposits and rock types (Table 7.2) suggests that the sand content in the basinal sediment is derived primarily from andesitic ash. Deposition over the lake from minor, intermittent volcanic eruptions (e.g. Ngauruhoe Ash) would account for the dispersal of grains throughout deep-water sediments and also for its accumulation on sub-lacustrine hilltops, where the sedimentation of mud is limited.

The quartz content in basinal sediments is confined to the silt fraction and relative to feldspar is highest in the fine to medium silt grade. The feldspar:quartz ratio in the silt fraction (Table 6.1) suggests a substantial content is derived from greywacke and/or rhyolite, as alternative terrigenous sources (Table 7.2) have very high feldspar:quartz ratios and selective sorting of these two minerals during transport is unlikely. Greywacke is probably dominant because of its wide extent in the major tributary catchments

Mineral	Yellow-brown pumice Soil (in sand)	Recent Soil from Volcanic Ash (in sand) %	Soil Parent Rock				
			Rhyolitic Ash (%)	Andesitic Ash (%)	Rhyolite (%)	Andesite (%)	Greywacke (%)
Quartz	-	-	<1	<1	30	<1	35
Acid feldspar	<1	-	30	-	30	5	40
Andesine	1-4	5-9	-	40	-	40	10
Glass	50±	5-50	60	30	30	5	1
Hornblende	<1	<1	-	10	1	10	2
Hypersthene	1-9	5-9	1-3	5	1	5	-
Augite	<1	1-9	1	5	-	5	1
Chlorites	-	<4	-	-	-	-	5
Mica	<1	<1	-	5	1	5	10

Table 7.1. Approximate contents of some minerals in Yellow-brown pumice Soils, Recent Soils from Andesitic Ash and different soil parent rocks (Fieldes and Weatherhead, 1968).

(Fig. 2.17). The increased feldspar:quartz ratio in the coarse silts and towards the southern end of the lake indicates a feldspar-rich/quartz-poor component. Rhyolitic tephra and andesitic material are probable sources.

Gregg *et al.* (1977) have shown that up to 1% of diatomaceous silica in freshly killed, cultured, freshwater diatoms may occur as strained α-quartz. Lake Taupo samples having the highest contents of diatom frustules show quartz contents of up to 1%, but the origin of this quartz is unknown. However, if this quartz occurred in the diatom frustules, rather than as detrital grains, it would still not affect appreciably the terrigenous quartz concentration patterns.

The confinement of quartz to the silt fraction of the deep-water sediments indicates that transport within the lake is by suspension only. The quartz concentration patterns more accurately represent the directions and extent of river-borne material as any airfall component is minimal or absent.

Obviously, neither quartz nor feldspar patterns indicate the direction or extent of sedimentation of the amorphous silt content derived from catchment pumice soils or tephra. However, the pattern shown by terrigenous silt (Fig. 7.5) represents variations in the sum of both crystalline and amorphous terrigenous components (discussed in section 7.2), thus the amorphous terrigenous component is partly represented by the difference between the terrigenous silt pattern and the quartz-content pattern.

In the southern part of the lake the terrigenous silt pattern is very similar to that of the quartz content, indicating a homogeneous

mixture of crystalline and amorphous components during transport and deposition, or, a subordinate amorphous content. In other parts of the lake the difference between the two patterns represents amorphous silt derived from the catchment rather than from airfall deposition. Evidence includes an area of very low content in the central lake regions, the absence of higher terrigenous silt contents on topographic highs (e.g. site 120), and the overriding fact that very little airfall material occurs in surface sediment samples. On this basis a relatively large input of pumiceous silt occurs from the northeastern shore of the lake (Fig. 7.10).

This conclusion is supported by the obvious evidence of past and present erosion of extensive pumice breccia cliffs along the lake shore to the north of Hatepe (Fig. 2.25), from which silt-sized material is undoubtedly winnowed by wave action. Nearby shelf, slope and rise sediments contain high contents of pumice gravels and sands, and pumice transported from the base of the cliffs by northward longshore currents has largely built the flats upon which Waitahanui now stands.

7.4 CLAY-SIZED MATERIAL

Diatomaceous silica, kaolinite, illite, montmorillonite and traces of vermiculite have been identified in the clay fraction of Lake Taupo sediments.

Infra-red and S.E.M. analyses indicate that approximately half the clay fraction in the central region of the lake is diatomaceous silica. The diatomaceous silica content probably increases from this value to the north and northwest, and decreases to the south. The ratio of diatomaceous:non-diatomaceous components in the

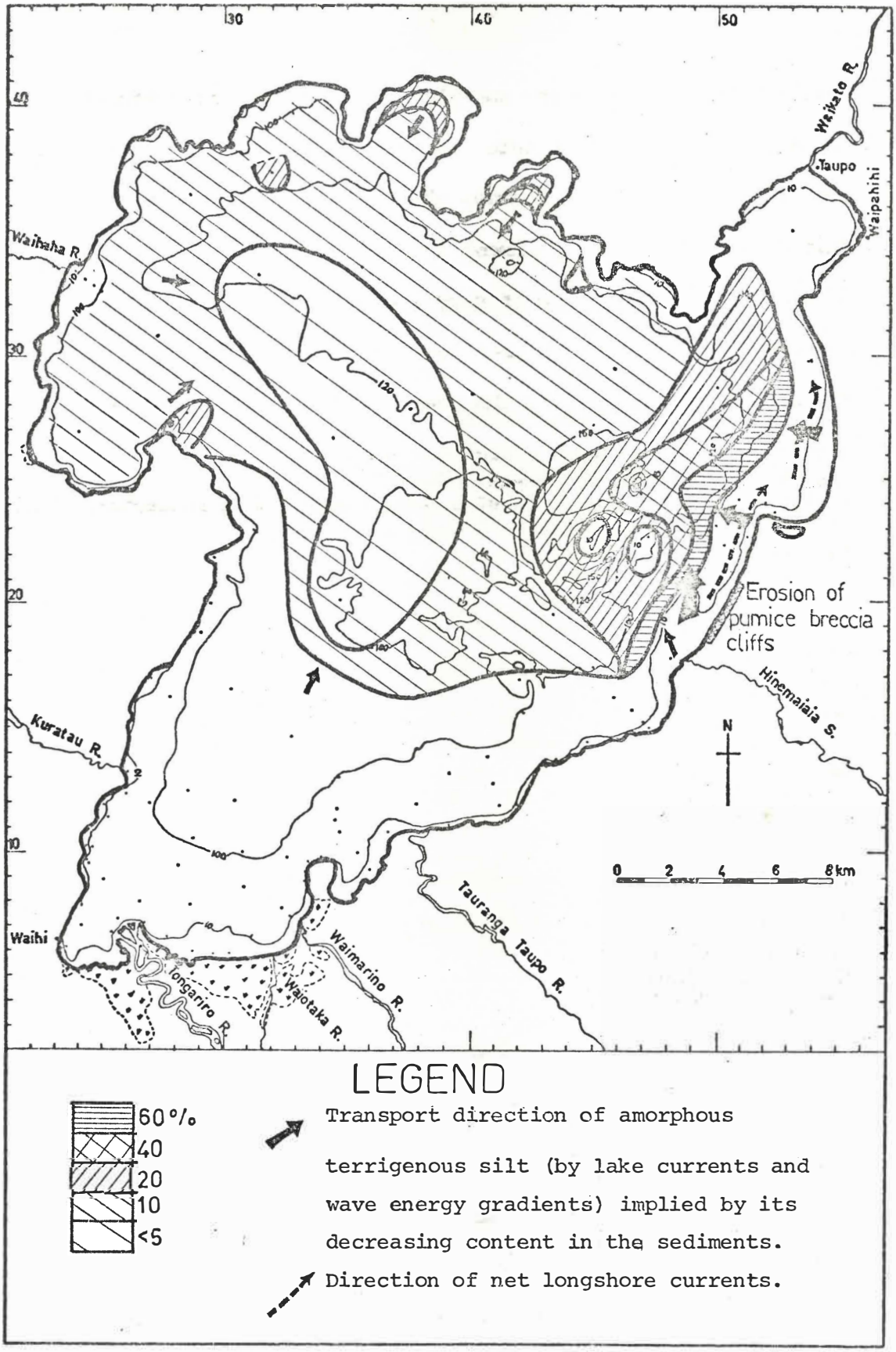


Fig. 7.10. Approximate content of amorphous terrigenous silt in surficial sediments of central and northern Lake Taupo.

clay fraction is less variable over the lake than in the silt fraction, because non-diatomaceous clay is further and more evenly dispersed by transport in suspension than is non-diatomaceous silt. The ratio undoubtedly decreases in the clay grade close to stream-borne sediment inputs as a result of the masking effects and inflow of plankton-free waters.

Crystalline clay mineral content

Differential thermal analysis suggests that crystalline clay minerals form less than 20% of the total clay fraction; S.E.M. analyses suggest a value between 10 and 20%. The total content of clay-sized material in deep water sediments ranges from 9 to 25%, which means that crystalline clay minerals account for less than about 5% of the total sediment.

Crystalline clay mineral trends

Figs. 6.8-6.10 indicate areal variations in the relative abundance of clay minerals in the clay fraction of sediments. The relationship between the height of a particular X.R.D. peak and the corresponding clay mineral may not be linear, thus the variations for a particular clay mineral may not be absolute.

Kaolinite and illite show strong areal patterns that are broadly similar (Figs. 6.8 and 6.9). Lower contents occur in the northern and central eastern regions of the lake, and neither clay was detected in Tapaueharuru Bay, out of which the Waikato River flows. Both clays show a general increase in abundance towards the western side and, in particular, the southern end of the lake where the patterns become more intricate, probably because of variations in

directions of inflowing currents. Higher contents of both clays occur in the central and eastern parts of Stump Bay and on the western side of Waihi Bay. Higher kaolinite contents also occur as tongues extending out from Te Hape Bay, and around the Hinemaiaia Stream area. Both clays show an increase towards the southern end of Western Bay and close to the Waihaha River delta.

The pattern for montmorillonite (Fig. 6.10) is weaker than for kaolinite and illite. It shows similar trends on a broad scale, but differs in that the greatest abundance of montmorillonite in the clay fraction occurs near Waihi, followed by an area immediately to the north as far as Pukawa, Stump Bay, Te Hape Bay, sample sites 76 and 87, an area to the south of Whakaipo and Mine Bays, and in Tapaueharuru Bay. The highest montmorillonite contents as a fraction of the total sediment (i.e. 15Å XRD peak height x sediment clay content) occurs near Waihi, where a rapid increase in content occurs towards Waihi village, and on a topographic high in the centre of the lake (site 76).

Sources of clay minerals

The interpretation of possible sources of crystalline clay minerals in the lake sediments from patterns of relative abundance in the clay fraction requires consideration of several aspects.

1. Hydraulic equivalence of different crystalline clay mineral particles must be assumed, so that changes in relative abundance between them are not due to differential settling.
2. The trends shown by each crystalline clay mineral on the maps (Figs. 6.8-6.10) are relative to the sum of the other clay-sized minerals present, so actual trends for each of the crystalline clay minerals are shown only if all the crystalline clay

minerals co-vary in a similar way, and a reciprocal relationship exists between total crystalline-clay content and a clay-sized amorphous component (Fig. 7.11a and b).

3. Estimations of individual crystalline clay-mineral abundance in the total sediment and absolute sedimentation rates are complicated by the reciprocal relationships within the clay fraction and the rest of the sediment (Fig. 7.11c).

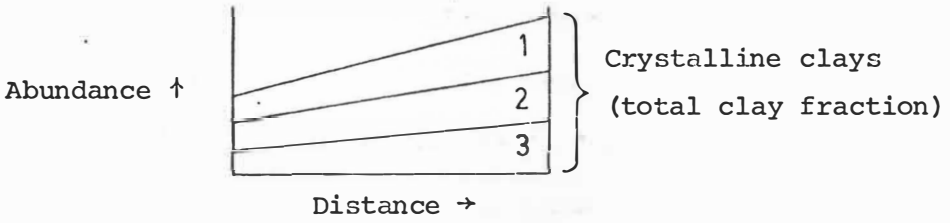
4. Clay sedimentation rates increase away from lake shore and inflow areas, under a decreasing energy gradient, then decrease with further distance as the suspended clay load decreases (Fig. 7.12).

The clay fraction in Lake Taupo contains a large amorphous component that is predominantly of an intra-lake origin (i.e. diatomaceous silica), and the input is approximately uniform over the whole lake, so it may be assumed that any crystalline clay mineral will generally increase as a proportion of the total clay fraction towards its source.

The patterns for kaolinite and illite indicate that these clays are almost certainly delivered to the lake by major streams and rivers. All three clays show a lower content in broad belts joining the Tongariro delta, Kuratau-Pukawa coast and Motuoapa headland areas, indicating a higher amorphous content in the clay-sized material there. This suggests that the currents in these areas are of sufficient strength, or variable enough in strength, to produce some differentiation of coarser and finer clay fractions, regardless of whether or not the coarser clay fraction has an intra- or extra-lake origin. The largest

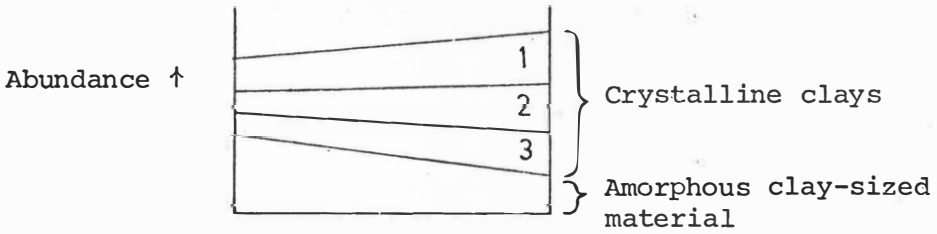
Fig. 7.11. Relationships between absolute and relative clay mineral contents in the clay fraction (a and b) and in total sediment (c).

(a) No reciprocal relationship exists between total crystalline clay content and an amorphous clay-sized component.



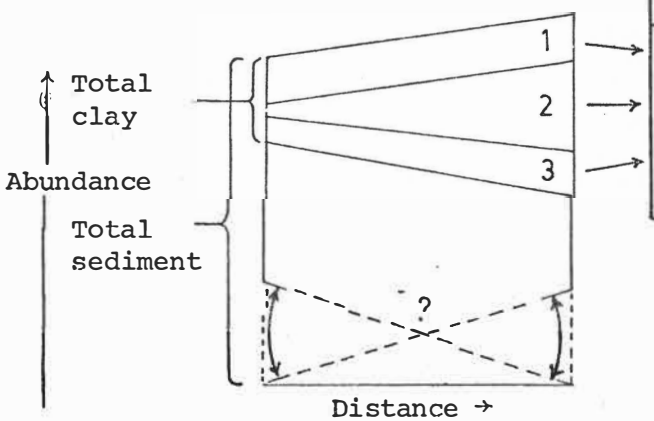
Absolute abundance increases but relative abundance remains constant with distance.

(b) A reciprocal relationship exists between total crystalline clay content and an amorphous clay-sized content.



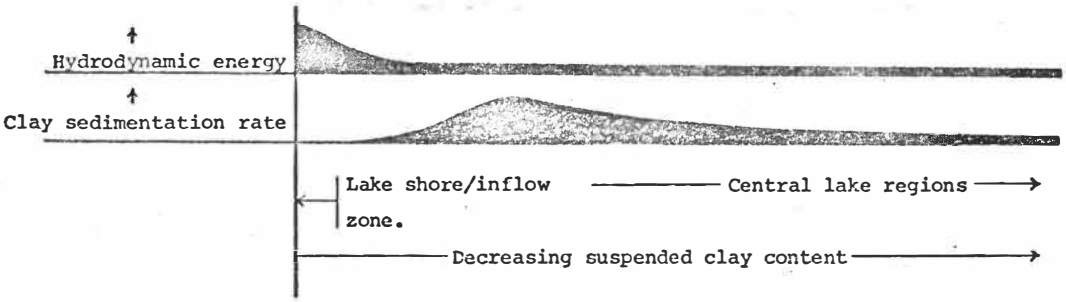
Both absolute and relative abundance of each crystalline clay mineral increase with distance.

(c)



Abundance and implied sedimentation rate with distance		
ABSOLUTE	OF TOTAL CLAY FRACTION	OF TOTAL SEDIMENT
same	decreases	?
increases	increases	?
increases	decreases	?

Fig. 7.12. Rates of clay deposition with distance from lake-shore source area.



suspended sediment loads occur when rivers are in flood (Fig. 7.13) and these flows persist within the lake until ponding occurs ultimately and the finer clays are deposited.

Clay concentration patterns suggest that the rivers transporting kaolinite and illite to the lake include the Waihaha, Kuratau, Tongariro, Waiotaka, Waimarino, Tauranga-Taupo Rivers, the Hinemaiaia Stream, and possibly the Waitahanui River. Significantly, with the exception of the Kuratau River, the headwaters of all of these rivers flow through greywacke terrains. The most readily weathered minerals in greywacke include mica and chlorite. With moderate weathering these degrade to micaceous clay minerals (weakly hydrated micas, illite, interlayered hydrous micas), clay vermiculites and montmorillonites. With strong weathering the micaceous clay minerals degrade to kaolinite (Fieldes, 1968). Greywackes within the Taupo catchment are not strongly weathered; however, they are sufficiently weathered to be a likely source for the small amounts of kaolinite observed in the sediments of Lake Taupo (H. Gibbs, 1978; pers. comm.). As illite is a precursor of kaolinite, greywackes are also a likely source for this clay mineral. Parts of the headwaters of the Kuratau River drain small areas of central yellow-brown earths and central yellow-brown loams (Fig. 2.18) formed on Miocene siltstone and sandstone. The clays of these soils include illite, montmorillonite, vermiculite and, in the central yellow-brown loams, possibly also kaolinite (Fieldes, 1968). Kaolinite does not occur as a weathering product in yellow-brown pumice soils or recent soils from volcanic ash formed entirely from

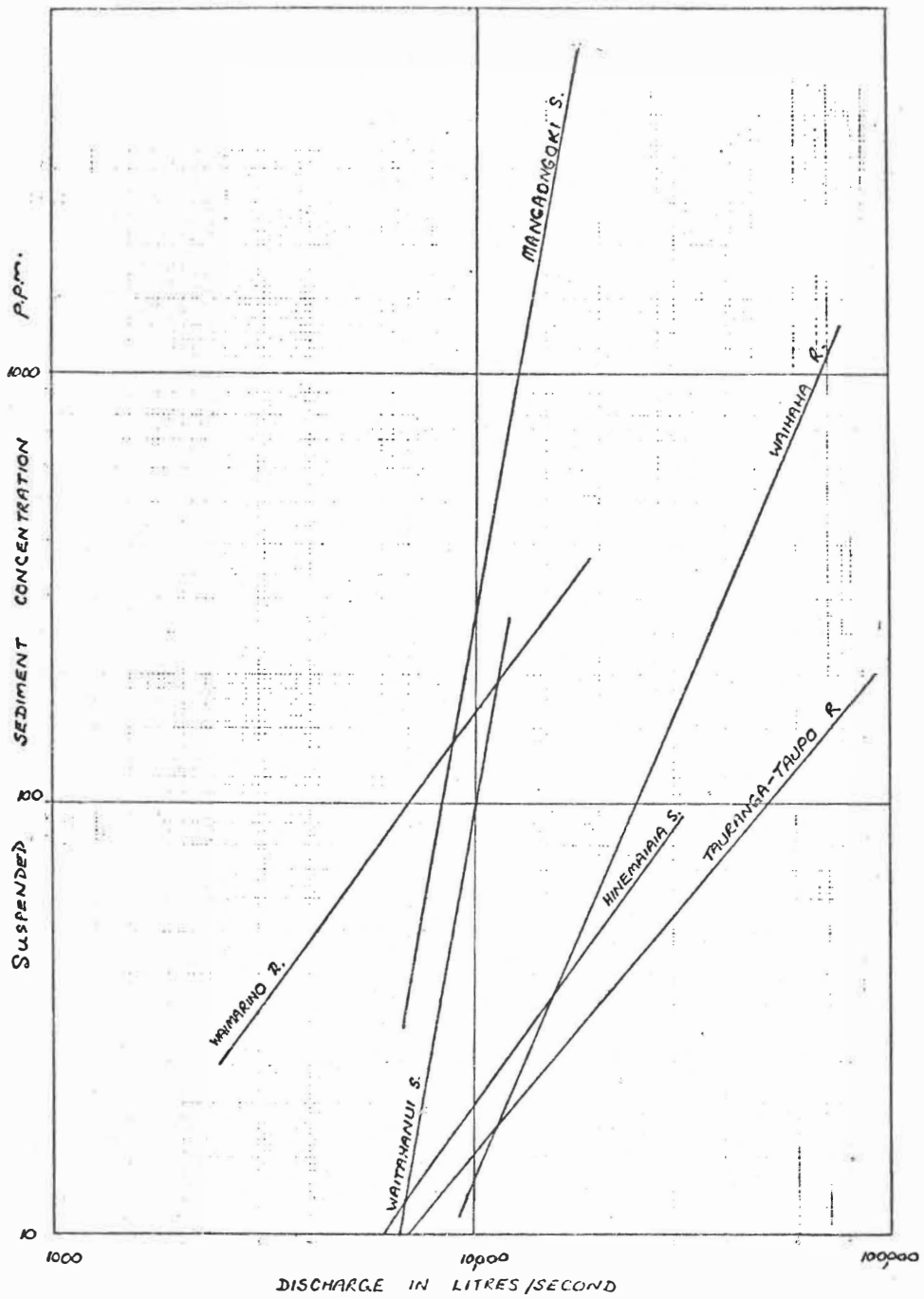


Fig. 7.13. Suspended sediment loads vs.discharge (logarithmic scales) for some rivers and streams flowing into Lake Taupo (R. Pittams, M.W.D. Water and Soil Division, Hamilton, 1978, pers. comm.).
The amount of suspended load transported by a stream increases exponentially as flow increases.

tephra (Fieldes, 1968), but trace-small amounts of mica/illite occur in the <1μ clay fraction of Taupo Ash (Kirkman, 1975).

Another possible source of kaolinite and illite is hydrothermally altered volcanic rock. Illite, kaolinite and montmorillonite have been observed as hydrothermal alteration products in Pliocene to Pleistocene silicic volcanics at Wairakei, a few kilometres north of Taupo (Steiner, 1968). Obvious hydrothermal activity within the catchment occurs at Taupo, Waihi, Tokaanu, and on the National Park volcanoes; however, neither illite nor kaolinite occur in the sediments near Taupo (Tapaueharuru Bay), or in maximum abundance near Waihi where the most extensive lake-shore hydrothermal activity occurs.

Possible sources of montmorillonite include the weathering of mica and chlorite in greywackes (chlorite does not occur in the clay fraction of the lake sediments); from soils formed on Miocene siltstone/sandstone; the intra-lake transformation of volcanic glass (and possibly allophane) which is unstable in a sub-aquatic environment (Millot, 1970); and hydrothermal alteration of volcanic rocks (Steiner, 1968). The patterns of montmorillonite abundance in the lake sediments suggest hydrothermally altered volcanic rocks are the dominant source. The highest montmorillonite contents in the lake sediments (Fig. 6.11) occur towards the shore at Waihi where the most extensive and intense hydrothermal activity occurs, and where in 1846 and 1910, landslides entered the lake. High contents of montmorillonite also occur on an isolated topographic high in the centre of the lake (site 76) where the presence of a thin crust of siliceous sinter covering the soft sediment confirms

past hydrothermal activity. Algal slime on the sinter surface and the existence of underlying cold sediment indicate that site 76 was not hydrothermally active at the time of sampling. Despite sand and pumice gravel fractions totalling 32.3 wt.%, this site has by far the highest clay content (41%) in the lake. The clay content is about twice that of the surrounding basinal sediments suggesting that it has not been transported to the site.

Montmorillonite is the only crystalline clay mineral in Tapaueharuru Bay (Taupo). If hydrodynamic equivalence of crystalline clay particles is assumed, then the montmorillonite could not have come from further south in suspension. Neither could it have come from the north, where lake waters are moving towards the outflowing Waikato River. Three possible origins exist. The montmorillonite was formed *in situ* authigenically; it arrived at the site attached to coarser particles (pumice gravel, sand); or a source exists in, or to the east or west of, the bay. Hydrothermal activity occurs to the east around Waipahihi and in the northeastern corner of the lake, however, the very low total clay (0.2 wt.%) and silt content (0.6%) at site 99 suggests that currents in the area are too strong for deposition of clay-sized material. Gravel-sized pumice in the sediment (78.7 wt.%) appears to be relict, as it is coated with algal slime and heavily stained by iron oxides, so the associated montmorillonite is possibly a sub-aqueous alteration product of volcanic glass.

These clay minerals also occur in the sediments of Lake Rotomahana (Kirkman, 1976b). Lake Rotomahana erupted in 1886 and spread lacustrine sandy mud from the lake bed over an area of 130 km^2 between Lake Rotorua and Mt Tarawera. The bulk of this mud is

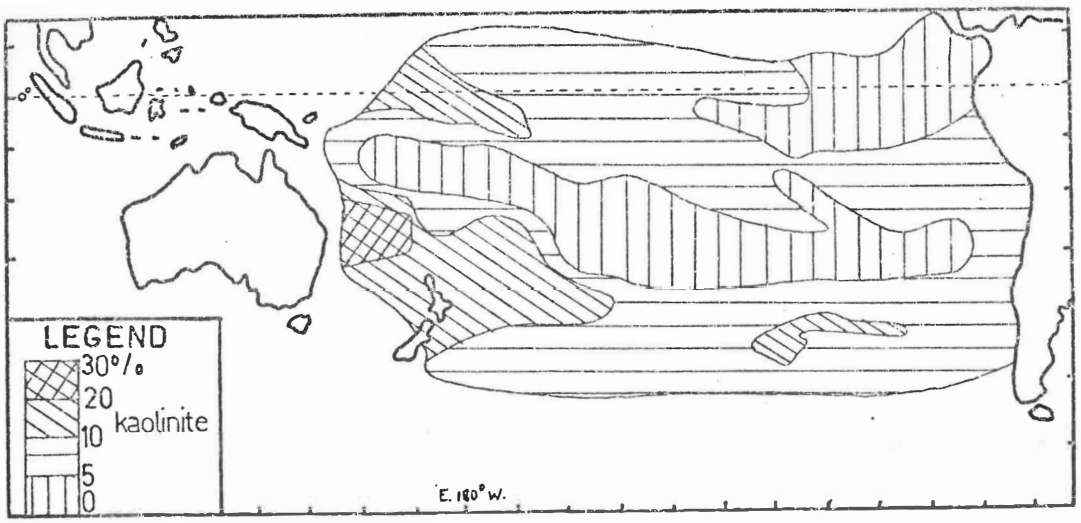
believed to have been originally derived from rhyolitic volcanics in the surrounding catchment which was hydrothermally active in places. These sediments contained a montmorillonite/mica interstratified mineral (10.5Å basal spacing), montmorillonite, mica, a kaolin mineral and traces of vermiculite. The allophane content was negligible.

Atmospheric fallout is another possible source of clay minerals to Lake Taupo. White *et al.* (1971) claimed that dry fallout of dust from the atmosphere may make a more important contribution to natural waters than is generally supposed, and that rainfall, particularly after dry periods, may wash large amounts of dust out of the atmosphere. These mechanisms may deliver material to the lake from considerable distances outside the catchment. For example, Windom (1975) has used illite, kaolinite and mica concentration patterns in South Pacific deep-marine sediments (Fig. 7.14a and b; Arrhenius, 1965; Griffin *et al.* 1968), and the mineralogical composition of dust in New Zealand snowfields (Fig. 7.14c; Windom, 1969) as evidence that the terrigenous component in South Pacific deep-marine sediments is dominated by atmospheric-fallout dust derived largely from Australian deserts. The clay-content patterns in Lake Taupo sediments suggest, however, that atmospheric fallout contributions of clay minerals to the lake are, at most, a background effect.

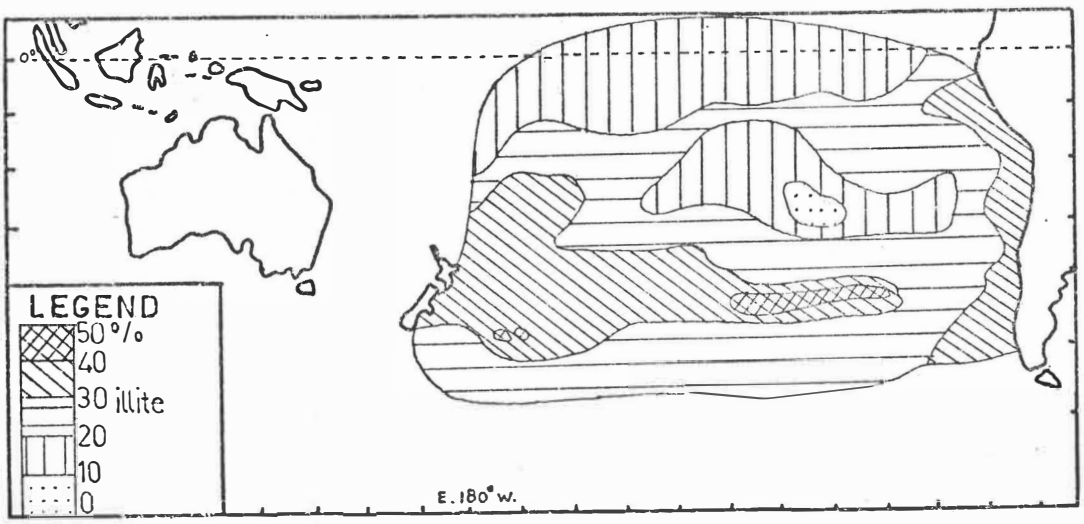
Absence of Allophane

Allophane occurs in the yellow-brown pumice soils and recent soils from volcanic ash (andesitic Ngauruhoe tephra) of the Lake Taupo catchment but not in the clay fraction of the lake sediments. Several factors probably contribute to this situation:

a)



b)



c)

Clay mineral	Wt.%
Montmorillonite	-
Illite	50
Chlorite	23
Kaolinite	27

Fig. 7.14. Distribution of (a) kaolinite and (b) illite in the clay fraction (<2 μm) of Pacific marine sediments (Griffin *et al.* 1968). (c) Composition of dust found in New Zealand snow fields (Windom, 1969).

(a) Only small amounts of allophane occur in the catchment soils (Kirkman, 1975).

(b) Only small amounts of catchment soil are eroded and transported to the lake.

(c) Allophane is rarely transported as clay-sized particles and so is rarely incorporated in the lake sediment clay fraction.

(d) Any allophane deposited in the lake sediments most probably rapidly alters to other clay minerals such as montmorillonite (Millot, 1970).

Allophane contents of up to 17% have been given for catchment topsoils, dropping to only 5% in the lower soil horizons. However, these calculations were based on the <2μm soil fraction only using Fieldes (1955) definition of allophane, which included the weathering sequence allophane B → allophane AB → allophane A. Fieldes and Furkert (1966) defined allophane B as being dominantly "hydrous" glass and "hydrous" feldspar in the coarse-clay fraction (0.2-2μm) and allophane A in the fine-clay fraction (<0.2μm). More recently Kirkman (1975), working on the clay fraction of rhyolitic tephras, and Campbell *et al.* (1977) working on the clay fraction of Taupo sandy-silt loams, concluded that allophane B was, in fact, clay-sized volcanic glass. Kirkman (1975) found that in the <1μm clay fraction alone, the volcanic glass content exceeded that of allophane ("trace or small amounts", p447) and that small amounts of mica, feldspar and imogolite occurred also. Subsequently, Kirkman (1978) proposed a weathering sequence for rhyolitic tephra in which volcanic glass and feldspar may alter to allophane in about 3,000 years and then to halloysite in another 12,000 years. The Taupo catchment soils are

formed on volcanic ash materials that are mainly younger than 2,000 years, suggesting that there has been little alteration to allophane. On this basis, the allophane content in catchment topsoils is probably no more than a few percent, and even less below the topsoil.

Most erosion in the catchment cover deposits occurs as gully or stream-bank erosion, so the soil:parent material ratio in transported sediments is probably low. Furthermore, maximum flocculation of allophane occurs at pH = 5.5-6.0 (i.e. isoelectric pH range of allophane) and appreciable dispersal in fresh water only at pH values less than 4 or greater than 10 (Fieldes, 1958), suggesting that any allophane is probably transported and deposited in the coarser sediment fractions.

7.5 ORGANIC MATTER CONTENT

Organic matter content is fairly constant over most of the lake, ranging from 6-8% (equivalent to 3.5-4.6% organic carbon) of the total sediment (Fig. 6.1). This organic matter content range is similar to those in the sediments of the oligotrophic lakes Tikitapu (3.3-4.5% organic carbon), Okaitaina (2.9-5.0% organic carbon), and Rotoma (3.9-4.9% organic carbon) reported by McColl (1977). Organic matter contents greater than 8% occur in Waihi Bay, Stump Bay, the southern part of Western Bay and around the Waihaha River delta.

Possible sources for the organic matter include vegetation, organisms, and their decomposition products of both terrestrial (allochthonous organic material) and lacustrine (autochthonous organic material) origin.

Organic material observed in Lake Taupo sediments include leaves and twigs mainly around river deltas (e.g.Frontispiece; Tongariro, Kuratau and Waihaha Rivers), aquatic macrophytes in various stages of decay on shelf weed bed areas (e.g. Waihi Bay, Stump Bay and Motuoapa Bay), chironamid larvae (ubiquitous in deep-water sediments, and occasional live or decaying freshwater mussels (*Hyridella menziesi*). Freshwater snails (*Potamopyrgus* sp.) and crayfish (*Paranethrops planifrons*) are relatively common on the lake bottom (Frontispiece A. Devcich, 1978, pers. comm.). This range of organic material contributes to the organic content of the sediments, but does not account for the uniform distribution of fine-grained organic material in deep-water muds. The uniform distribution pattern of organic matter in the lake muds suggests there is a widely distributed autochthonous source and/or an allochthonous source of fine-grained, easily dispersed organic material.

Regardless of the original source, biochemical compounds are converted to humic material relatively rapidly by microbial degradation, particularly under aerobic conditions in the water column and within the thin oxidised surface layer of sediment. Beneath this layer the production of humic material drops sharply with increasing sediment depth (Kemp and Lewis, 1968), so is influenced by rates of sedimentation and mixing. Most organic matter in lake sediments is humic material (Jackson, 1975). It is largely resistant to further microbial or chemical decomposition and tends to accumulate, particularly in the clay-sized fraction (Kemp and Lewis, 1968).

Organic matter in Lake Taupo sediments does not show distribution patterns similar to those of the clay minerals, which suggests that an autochthonous source may predominate over much of the lake. The most important source of autochthonous humic matter is algal flora (Jackson, 1975; Storch and Saunders, 1978), and humic material from algae tends to be lighter in colour than that from terrestrial sources (R. McColl, 1978, pers. comm.). Lake Taupo sediments tend to be lighter coloured in the central and northern regions, and darker coloured around the southern end of the lake, where larger inflows and higher organic contents occur (Fig. 4.14). This suggests algae are the dominant source of organic matter in the central and northern parts of the lake.

Sanger and Gorham (1970) claimed that sedimentary organic matter in distinctly oligotrophic lakes is probably dominated by allochthonous detritus. Whiteside (1965) suggested oligotrophic lake sediments contain less autochthonous organic matter than eutrophic lake sediments, and McColl (1977) showed that allochthonous organic matter inputs may obscure the relationship between autochthonous organic carbon and trophic conditions in oligotrophic lakes. Lake Taupo is oligotrophic and has a very low production of algae as indicated by the deepest secchi disc readings for any lake in New Zealand (Jolly, 1958, 1968), thus inputs of allochthonous organic matter in central and northern regions of the lake are probably negligible.

In a recent analysis of organic matter content in the top centimetre of sediment from Lakes Huron (oligotrophic), Erie (eutrophic) and Ontario (oligotrophic) in Canada, Kemp (1972) concluded that the

humic material was mainly of autochthonous origin, the precursor material being diatoms. The Lake Taupo algal assemblage is dominated by diatoms (Jolly, 1959; Hill, 1975), and the basinal sediments consist predominantly of diatom tests, particularly in the central and northern region. Diatom-derived organic material probably dominates the organic fraction of the central and northern deep-water sediments. In all three lakes studied by Kemp (1972) the organic matter consisted of three types of material in approximately similar proportions from lake to lake. Humins (stable complexes of humic acid and clay) formed 60-71%, humic and fulvic acids formed 21-36%, and bitumens (aliphatic and aromatic hydrocarbons, O-N-S compounds, pigments, lipids, fatty acids and ashphaltenes) formed 6-10%. They were produced by microbial degradation (mineralisation) of the diatomaceous organic matter, which Kemp concluded was more than 95% complete in the water column prior to deposition.

Catchment runoff undoubtedly contributes humic material to the sediments around the Waihaha River mouth and towards the southern end of Lake Taupo, where organic matter contents equal or exceed those of the central and northern regions, despite the higher terrigenous silt:diatomaceous silt ratio. The exact geographic sources of the higher organic contents in Waihi and Stump Bays are unclear from the pattern. Both of these areas are adjacent to extensive swamp regions, and show organic-matter concentration trends that are broadly similar to those of the crystalline clay minerals (Figs. 6.8-6.10), offering the possibility that at least part of the organic material is complexed with clay minerals, forming humins.

Areas of high organic matter content (8.0-9.1%) off the Waiotaka, Waimarino and Tauranga-Taupo River mouths and in Waihi Bay correspond with areas of darker coloured sediment (Fig. 4.14) but similarly high values do not occur to the northwest of the Tongariro delta where a large area of darker coloured sediment also occurs. This may be due to the coarser nature of the sediment in this area and/or a higher content of darker coloured inorganic material than in the sediment elsewhere in the lake. The highest sediment organic matter contents (10.5%) occur off the Waihaha River mouth, however, the sediment is not darker coloured, suggesting that the organic matter occurs mainly as macro-particles.

There is little correspondence between the patterns of organic-matter content (Fig. 6.1) and redox potential (Fig. 4.9a) in the sediment. The nature and amount of organic material in Lake Taupo sediments suggests that eroded catchment soil material (yellow-brown pumice soils have up to 10.1% organic carbon and recent soil from Ngauruhoe ashes up to 4.9% organic carbon; Blakemore *et al.* 1968) is an insignificant component in the sediments over most of the lake.

CHAPTER 8

STRATIGRAPHY OF SEDIMENTS DEPOSITED IN LAKE TAUPO SINCE THE 131 A.D. TAUPO PUMICE ERUPTIONS

Eleven shallow sub-bottom seismic profiles and six sediment cores were obtained from Lake Taupo to investigate the stratigraphy of the top few metres of lake sediments, determine historical sedimentation rates, and to relate these back to contemporary sedimentation processes.

8.1 SEISMIC-PROFILE CHART REFERENCING AND METHODOLOGY

Eleven seismic profile transects (Runs 1-11) for Lake Taupo, covering a total distance of 98 km, are located on Map 3 (in Map pocket). Photo strips of the profiles, reproduced at 1/3 original chart size, are presented in this chapter.

Consecutive photo strips for each seismic profile are referenced in the figures by capital letters in alphabetical order following the run number. Positions along a profile may be located on the bathymetric map (Map 3 in map pocket) by interpolating between position fix times shown on both the profile charts and Map 3 (in Map pocket), using the consecutive numbers beginning at the start of each profile run (a constant run velocity over the lake bed is assumed between each pair of position fixes). In the following interpretations a given profile position is referred to by its run number followed by the horizontal reference printed on the profile chart (e.g. R1.4).

Depth scales are printed on the chart paper as vertical columns of numbers. Numbers 0-16 refer to depth scale 'x1', 15-31 to 'x2', 30-46 to 'x3', and 45-61 to 'x4'. The depth-scale number is doubled to obtain actual depth in metres. Changes to higher depth scales are accompanied by trace shifts from the bottom to the top of the chart. Operation of a 'centre-key' function (marked on the chart when used) shifts the trace down to the centre of the chart and the depth scale must be similarly adjusted in these cases.

Profiles show vertical cross-sections of lake bottom and sub-bottom sediment structure. Reflector horizons (i.e. sound reflecting surfaces) show on the charts as thin, darkened, sub-horizontal traces, produced either by contrasting physical properties (e.g. sediment composition, compaction) at sediment layer interfaces, or by relatively thin (less than about 10 cm) layers of sediment contained within a thicker sediment layer. The lake surface shows as a reflector at zero depth on depth-scale 'x1' only. On shelf areas artificial reflectors frequently occur at integral multiples of the water depth as a result of the signal bouncing between the sediment and water surfaces. Reflectors along and across the lake are correlated through transect intersections.

The vertical axis of a profile represents the product of the sound-signal velocity and the distance travelled by the signal. As sound velocity is a function of the medium, use of the vertical axis on the chart as a depth scale assumes the physical properties of the medium are constant along the path of the signal. Sediment layer thicknesses have been determined directly from the chart depth scale on the assumption that sound velocity in the top few metres of

sediment is similar to that in the overlying water column. This assumption is based on several considerations:

(a) The sound wave velocity within these sediments (which have water contents up to about 80%) is unknown.

(b) Sediment thicknesses of only a few metres are penetrated (sound wave velocity generally increases with sediment depth; Turekian, 1968).

(c) An increase of 10% or so in sound wave velocity within these sediments, relative to that in the overlying water, might be expected (based on Turekian, 1968). However, the limit of trace resolution frequently prevents sediment layer thickness estimations with an error of less than 10%).

8.2 BASIS OF PROFILE INTERPRETATION

Interpretation of the composition, provenance, and mode of deposition for the sediment layer underlying or represented by, each reflector is based on several considerations:

(a) Surficial sediment character and sources, as determined by surficial grab sample analyses.

(b) Description of five sediment cores (presented in this Chapter), each up to 1.7 m long, four of which were collected along the 'Run 6' transect (Map 3 in Map pocket; Fig. 8.2).

(c) Volcanic events and catchment erosion affecting Lake Taupo over the last 2000 years.

(d) Present lake condition and catchment stability.

(e) Relationship between sediment units (e.g. position in chrono-stratigraphic sequence, interface topography, and thickness trends).

(f) Sound reflection properties illustrated by relative reflector strengths and sharpness on the charts (e.g. sand reflects more strongly than soft mud).

The undulating basal reflector observed in most deep-water parts of the lake is interpreted as the upper surface of an extensive deposit of pumice, hereafter referred to as the basal pumice surface, which was emplaced during and/or soon after the 131 A.D. Taupo Pumice eruptions (Healy, 1964). This interpretation is based on the following evidence and considerations:

(a) Sediment Cores 3 and 4 (Figs. 8.5 and 8.4), which penetrated only the overlying sediments, contain muds whereas Core 5 (Fig. 8.1), which penetrated the basal pumice surface, contains pumice fragments in a subordinate mud matrix over all but about the top 10 cm of its length. The pumice is subangular-rounded gravel, suggesting that it has been transported from the catchment rather than deposited directly on to the lake.

(b) Eruption of Taupo pumice was the last catastrophic volcanic event to affect the lake and catchment. Vast quantities of pumice were deposited directly on to and washed into the lake during and after the eruptions (Healy, 1967; Pullar *et al.* 1973). Detrital pumice was undoubtedly the dominant sediment type deposited in the lake for tens, and possibly hundreds of years after the eruptions.

(c) Lake sediments dominated by pumice fragments would be expected to exhibit a more rugged surface topography than do muds. This is because of the extremely wide range of clast sizes available and the unique behaviour of pumice in water (see

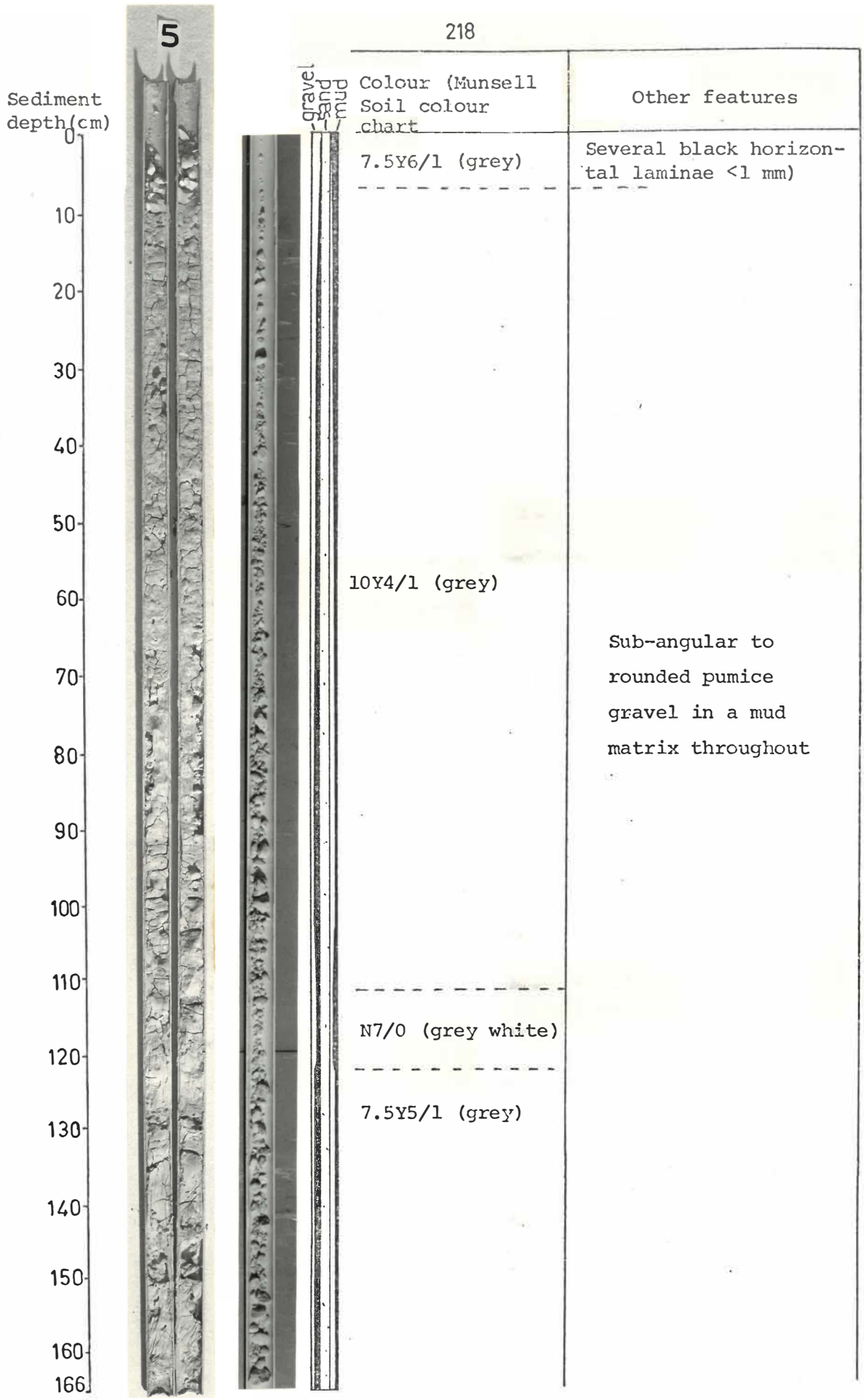


Fig. 8.1(a). Core 5 from 70 m depth on sub-lacustrine hill in the central lake region (Map 3 in map pocket). Pumice gravel in a mud matrix. (b) A core-half with the mud fraction removed.

section 7.2). Moreover, during and immediately after the Taupo Pumice eruptions, the surface of Lake Taupo was undoubtedly choked with pumice. Seismic shocks associated with the eruptions, possible volcanic vents within the lake (Healy, 1964), phenomenal sedimentation rates of very poorly sorted material, consequent redepositional processes, and fluctuating lake levels would have produced a much less placid lake environment than exists today. Post-depositional adjustment of the sediments probably continued for some time after deposition.

On this basis, and allowing an arbitrary 50 years after the Taupo Pumice eruptions for pumice deposition rates to drop to background levels in basinal regions of the lake, sediments above the basal pumice surface have accumulated in about the last 1800 years.

8.3 SEISMIC PROFILE DESCRIPTIONS AND INTERPRETATIONS

General features of profiles

In basinal and rise regions of the lake a number of reflectors are common down to sediment depths of several metres. Generally the basal pumice surface reflector is the deepest. It undulates over a vertical distance of less than a metre in southern and western basinal parts of the lake, to many metres in central lake regions, where it frequently emerges through overlying sediment layers or is covered by only a thin veneer (to tens of centimetres) of sediment. A variable number of overlying sediment layers partly or completely infill topographic lows in the undulating basal surface so as to produce a generally smooth lake floor.

The following seismic profile descriptions and interpretations are presented in an approximately south to north order.

Run 6 from Waihi towards Taupo (Fig. 8.2)

To the west and southwest of the Tongariro delta, the basal pumice surface cannot be detected in the profile, despite seismic penetration to a depth of several metres. This suggests that sedimentation rates in Waihi Bay have been high over the last 1800 years. High sedimentation rates may have resulted from landslides (e.g. geothermally promoted landslides from the Hipaua Ridge to the southwest of Waihi in 1834, 1846 and 1910) or deltaic progradation at pre-existing Tongariro River mouths. Rise sediments (R6.4-R6.18) below the 30-40 cm thick surficial layer, contain numerous sub-parallel to slightly chaotic layers, each of which is about 30-40 cm thick. The exact number of layers present, and to what sediment depth they occur cannot be accurately determined because of increasing signal attenuation with sediment depth. Undulating topography, and the more irregular nature of some sub-surface reflectors, particularly near the foot of the slope (R6.4), suggest some slumping or post-depositional movement of sediments may have occurred prior to deposition of the 30-40 cm thick surficial layer.

Core 2 (Fig. 3.3) from a 43 m deep slope/rise site (R6.4) consists mainly of massive andesitic/rhyolitic sand, with some rounded pebbles and isolated totara leaves towards the bottom, and occasional mud clasts. The sands fine upwards and are capped by a 12 cm thick mud unit. As a whole the core is vaguely reminiscent of a turbidite unit (Bouma, 1962) and may be related to landslides from Hipaua Ridge to the south. The 30-40 cm thick surficial mud

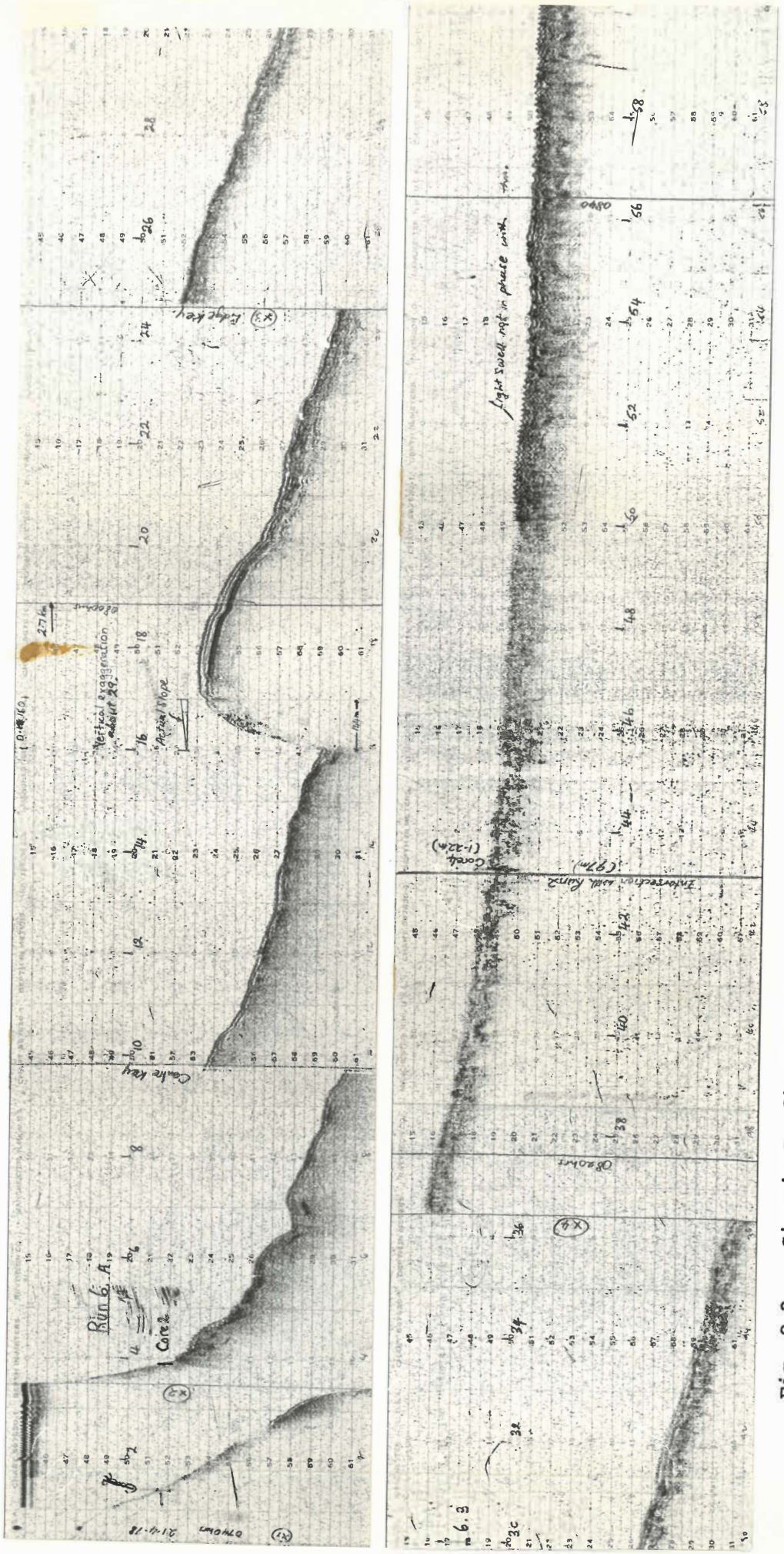


Fig. 8.2. Siesmic Profile Run 6 (Waihi to lake centre; page 1 of three pages)

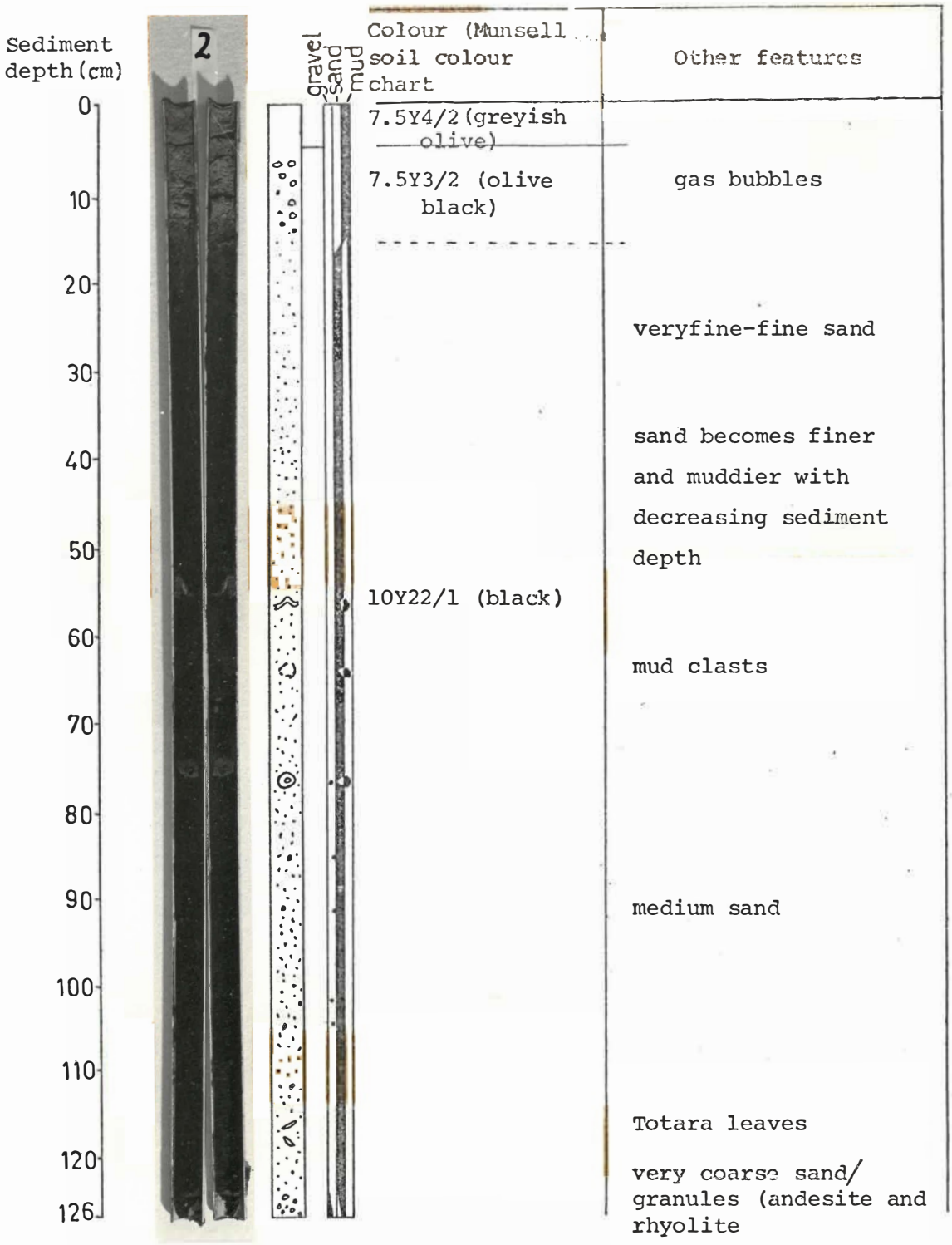


Fig. 8.3. Core 2 from 43 m depth (slope/rise) in Waihi Bay, Lake Taupo. (Map 3 in map pocket). Sand with mud capping and several mud clasts. Sediment texture coarsens with depth.

layer continues downslope at least as far as the foot of a low mound to the west of the Tongariro delta (R6.16) indicating that the most recent cycle of mud sedimentation has occurred at a more or less uniform rate over this part of Waihi Bay. The regular thickness of this mud layer over both topographic highs and lows indicates that pelagic sedimentation has characterised this part of the lake most recently, with an absence of significant bottom or near-bottom currents.

To the northwest of the Tongariro delta a distinct mound rises some 12 m above the surrounding lake floor (R6.16-R6.24). A surficial sediment layer up to 40 cm thick unconformably overlies a number of truncated sediment layers near the top of the steeper south-facing side of the mound. The processes responsible for truncation of the subsurface layers are unclear. At the bottom of the south side of the mound a topographic low has been partly infilled by up to five layers of sediment having a total thickness of about 2 m. These layers slope upwards to the south and terminate against the foot of the mound suggesting they have not been formed by redeposition of sediment from the mound. The position of the mound with respect to the Tongariro delta and the occurrence of at least five strong, parallel to sub-parallel reflectors over its top suggest that it is a sub-lacustrine extension of the Tongariro delta, the top 2 m at least of which probably contain several layers of high sand content. These layers may have been formed by material redeposited from further up the delta slope or jetted into the lake during exceptional flooding of the Tongariro River. The structure immediately below these layers (R6.17-R6.20) is difficult to discern but faint

reflectors suggest that further sub-parallel layers of approximately the same thickness (about 40 cm) occur to a sediment depth of 4 m or more. Five or six equally spaced (about 40 cm) reflectors continue down the northern slope of the mound and across the southern-lake basinal region.

Core 4 (Fig. 8.4), from a depth of 104 m near the southern rise/basin boundary (R6.43), penetrated 126 cm into the sediment layers overlying the pumice reflector. On the basis of seismic reflector depths, changes in sediment character are expected at sediment depths equal to about 40 cm multiples. Core 4 shows pumiceous clasts at sediment depths of 2-4 cm, 32-51 cm and 122-126 cm. No clasts occur at 80 cm, although a 10-15 cm thick layer of relatively more fluid sediment containing abundant gas bubbles occurs at about 60-70 cm sediment depth. The firm, compact nature and outline of the pumiceous clasts indicates they were probably originally rounded pumice fragments which have subsequently partly 'decomposed' in the sub-sediment environment. The occurrence of a pumiceous clast at 2-4 cm sediment depth indicates that such 'softening' of pumice can occur soon after burial. These pumice fragments appear to have a 'long-axis-vertical' attitude in the sediment. Such an attitude is consistent with other observations of pumice fragments which have settled through the water column in deep water parts of Lake Taupo (e.g. Fig. 4.6). This 'long-axis-vertical' attitude probably results from hydrodynamic efficiency requirements, and different buoyancy values within a pumice fragment, during its vertical descent in quiet water. The descent velocity probably increases with depth because of the increasingly negative buoyancy

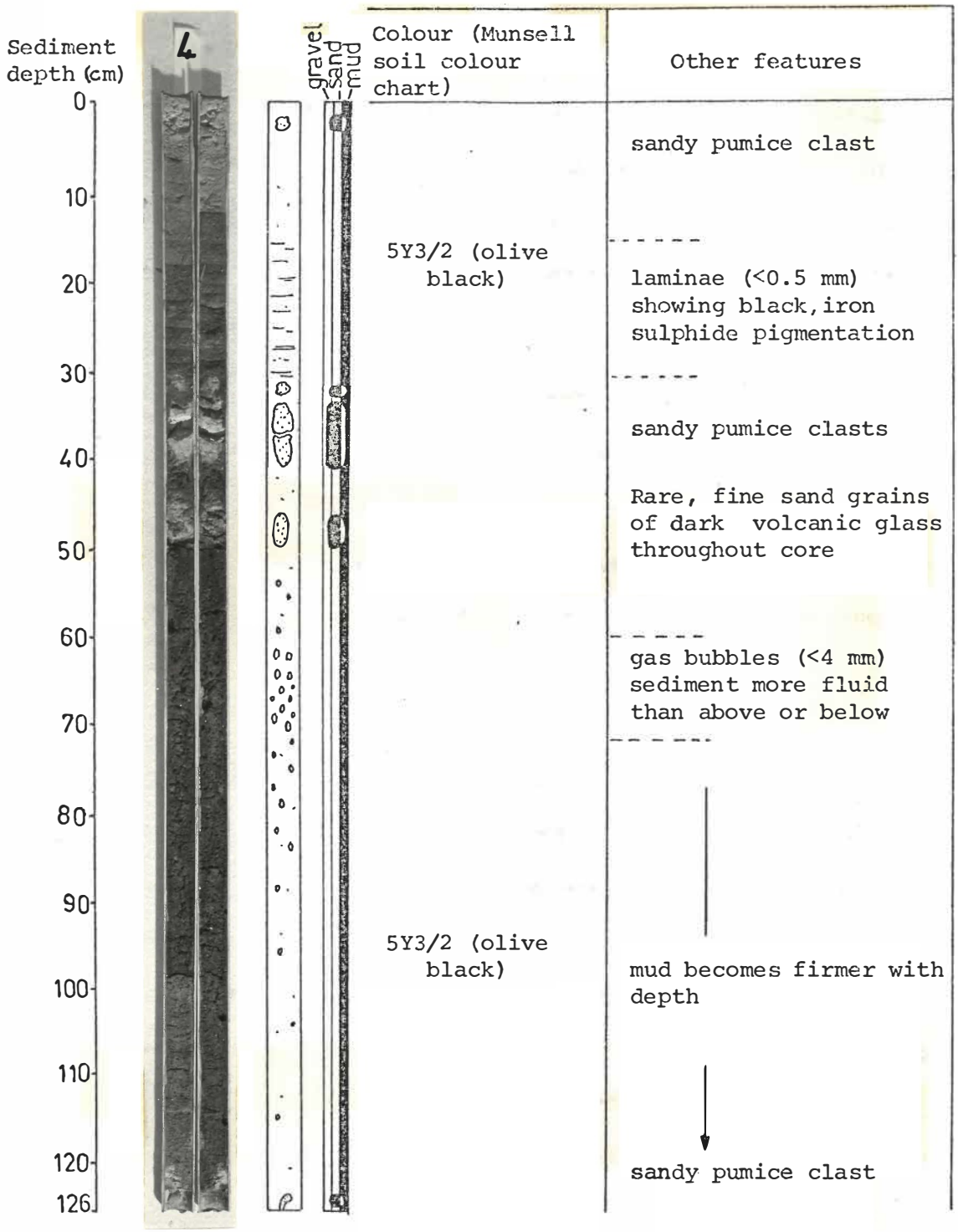


Fig. 8.4. Core 4 from 104 m depth in the Kuratau Basin (Map 3 in map pocket). Mud containing several sandy pumice clasts and gas bubbles.

as ambient pressure increases with water depth. Impact with the bottom results in partial penetration into the soft deep-water sediment with preservation of the fragments vertical attitude. On this basis, and because of the lack of associated sandy sediments, the clasts in Core 4 were probably deposited vertically through the water column rather than by redeposition from shallower parts of the lake (e.g. as in grab-sample 115).

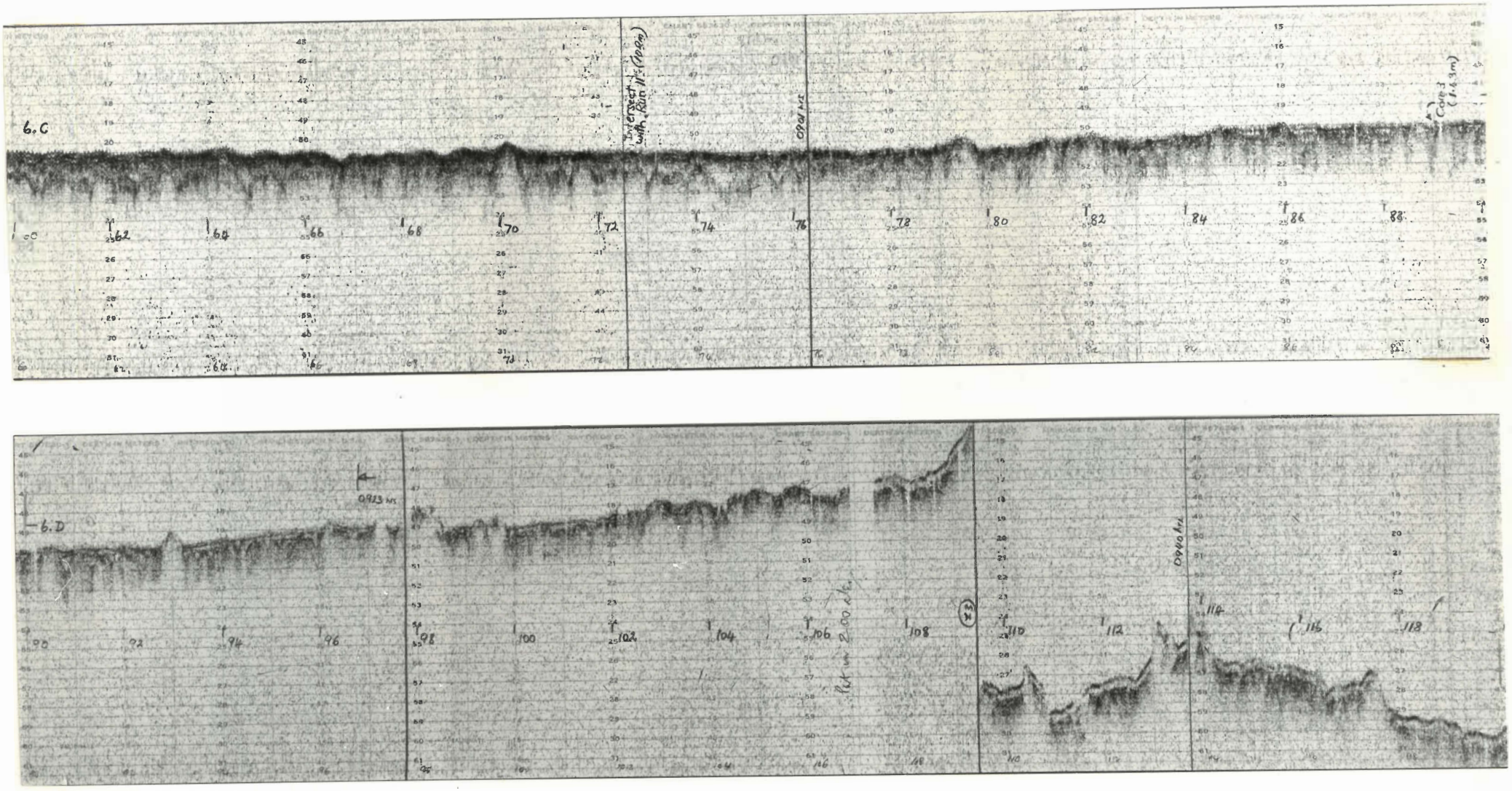
Two main questions remain unresolved by Core 4 evidence:

(a) Are the pumiceous clasts random fragments which fortuitously occur at seismic reflector depths? For example, a clast occurs in the top few centimetres of sediment yet grab-samples in this area indicate that such clasts are both random and rare. On the other hand the pumiceous fragments do occur at reflector depths and other textural differences (e.g. sandy layers) are absent.

(b) Does a layer of pumiceous clasts occur at about 80 cm sediment depth which has not been recorded in Core 4?

The occurrence of about six equally spaced reflectors above the basal pumice reflector suggests that important sedimentological events have occurred in Lake Taupo at about 300 year intervals over the last 1800 years (e.g. catastrophic storm events causing serious erosion of pumice cover deposits within the catchment).

North of about R6.64, reflectors within the bottom muds become blurred and discontinuous, or disappear (Core 3 from 102 m depth (R6.89) contains only mud throughout its length of 148 cm; Fig. 8.5). This, together with the general northward thinning of



Run 6 continued (page 2 of three pages)

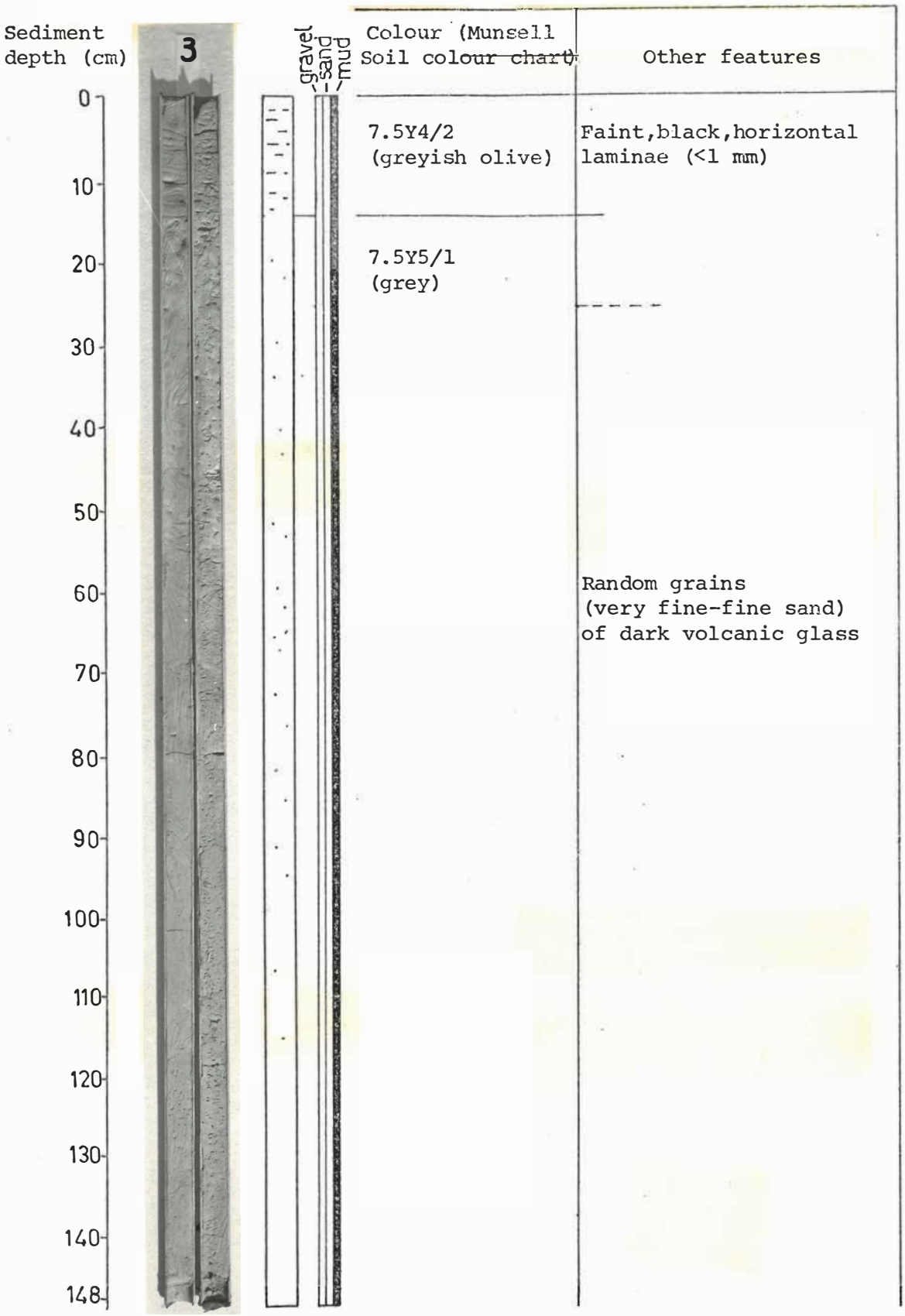


Fig. 8.5. Core 3 from 102 m depth in the southern basinal region (Map 3 in map pocket) of Lake Taupo. Mud.
N.B. Cracks and vertical striations are due to core-splitting procedures.

mud overlying the basal pumice surface, suggests the Tongariro River has been the major source of sediments in the southern half of the lake for at least the last 1800 years.

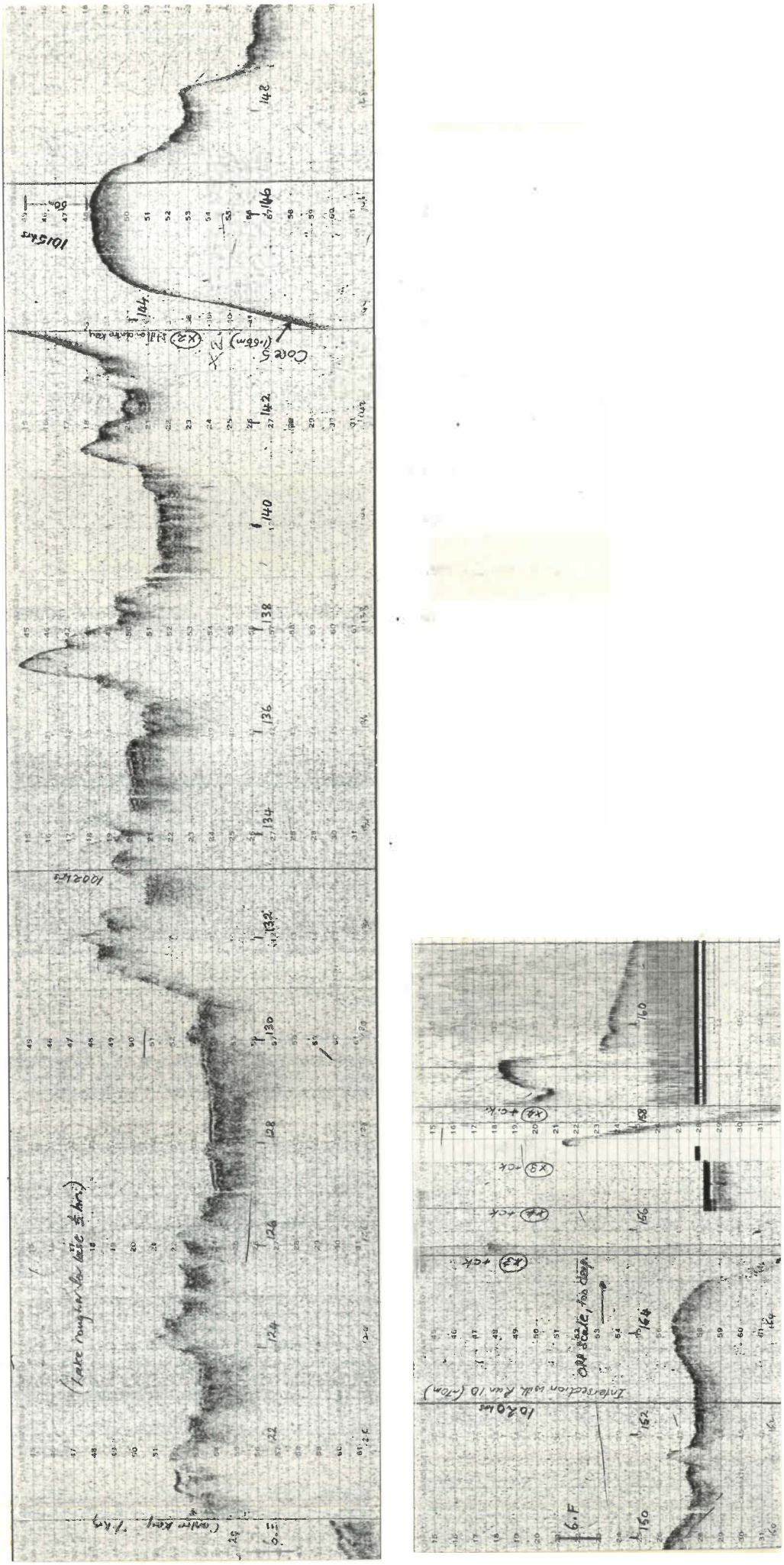
From 6.78 to R6.107 the sediment thickness above the basal pumice surface averages only about 50 cm, although thicker and thinner pockets occur locally. From R6.107 to R6.122, the water depth gradually decreases, and the lake-floor topography becomes considerably more rugged and is blanketed by a thicker (to 1 m) surficial sediment layer. The uniform thickness of this surficial layer over rugged topography indicates deposition from suspension, although a source is not indicated by thickness trends in adjacent, thinner surficial sediments. Grab-sample 77 indicates locally higher contents of montmorillonite clay, possibly produced by past sublacustrine geothermal activity (see Section 7.4), in the sediments about 4 km to the northeast of this area but it is not known whether or not the locally increased mud thickness and montmorillonite content have a common factor.

From R6.122 to the northern end of the transect (R6.161) lake floor topography is dominated by an increasingly rugged basal pumice surface and surficial mud thickness averages 50 cm or less. Deeper reflectors (2-3 m) occur below the basal pumice surface in topographic lows (e.g. R6.139-R6.143, R6.149-R6.155) suggesting redeposition of pumiceous material prior to deposition of the overlying mud cover.

mud overlying the basal pumice surface, suggests the Tongariro River has been the major source of sediments in the southern half of the lake for at least the last 1800 years.

From 6.78 to R6.107 the sediment thickness above the basal pumice surface averages only about 50 cm, although thicker and thinner pockets occur locally. From R6.107 to R6.122, the water depth gradually decreases, and the lake-floor topography becomes considerably more rugged and is blanketed by a thicker (to 1 m) surficial sediment layer. The uniform thickness of this surficial layer over rugged topography indicates deposition from suspension, although a source is not indicated by thickness trends in adjacent, thinner surficial sediments. Grab-sample 77 indicates locally higher contents of montmorillonite clay, possibly produced by past sublacustrine geothermal activity (see Section 7.4), in the sediments about 4 km to the northeast of this area but it is not known whether or not the locally increased mud thickness and montmorillonite content have a common factor.

From R6.122 to the northern end of the transect (R6.161) lake floor topography is dominated by an increasingly rugged basal pumice surface and surficial mud thickness averages 50 cm or less. Deeper reflectors (2-3 m) occur below the basal pumice surface in topographic lows (e.g. R6.139-R6.143, R6.149-R6.155) suggesting redeposition of pumiceous material prior to deposition of the overlying mud cover.



Run 6 continued (page 3 of three pages)

Run 1 and 2 from the Stump Bay Shelf to the Kuratau Shelf (Fig. 8.6)

Run 2 continues from the end of Run 1. The main feature shown by the seismic reflections is a large scale slump (or slide) block of sediment from the shelf-upper rise region on to the lower rise region off Stump Bay. This block of sediment averages some 3 m thick and is about 2.2 km across. The slump appears to have sheared just above the basal reflector and to have moved downslope as a coherent unit, doubling the sediment thickness above the basal reflector over the lower rise area. A 40-50 cm thick blanket of mud has been deposited subsequently, suggesting that slumping occurred several hundred years ago (Fig. 8.7).

If the basal reflector underlying the slump is indeed the 1800 B.P. basal pumice surface (it appears to be continuous with that in basinal regions) it indicates that very little lakeward progradation of the slope has occurred at this point within the last 1800 years, and therefore the probable absence of a pre-existing Tongariro River mouth at this point within the last 1800 years. This suggests the shelf may be largely a relict of the massive sediment influxes during and immediately after the Taupo Pumice eruptions, with some modifications under present lake level conditions (e.g. Fig. 8.8).

Across most of the flat basinal part of the transect (R2.40-R2.65) the sediment thickness above the basal pumice surface is fairly constant, averaging about 2 m. Towards the Kuratau side the average thickness is nearer 2.5 m (R2.59-R2.66) and up to four reflectors occur within the mud cover, suggesting a sediment contribution from the Kuratau River. These reflectors continue upslope and pinch out at about 60 m depth.

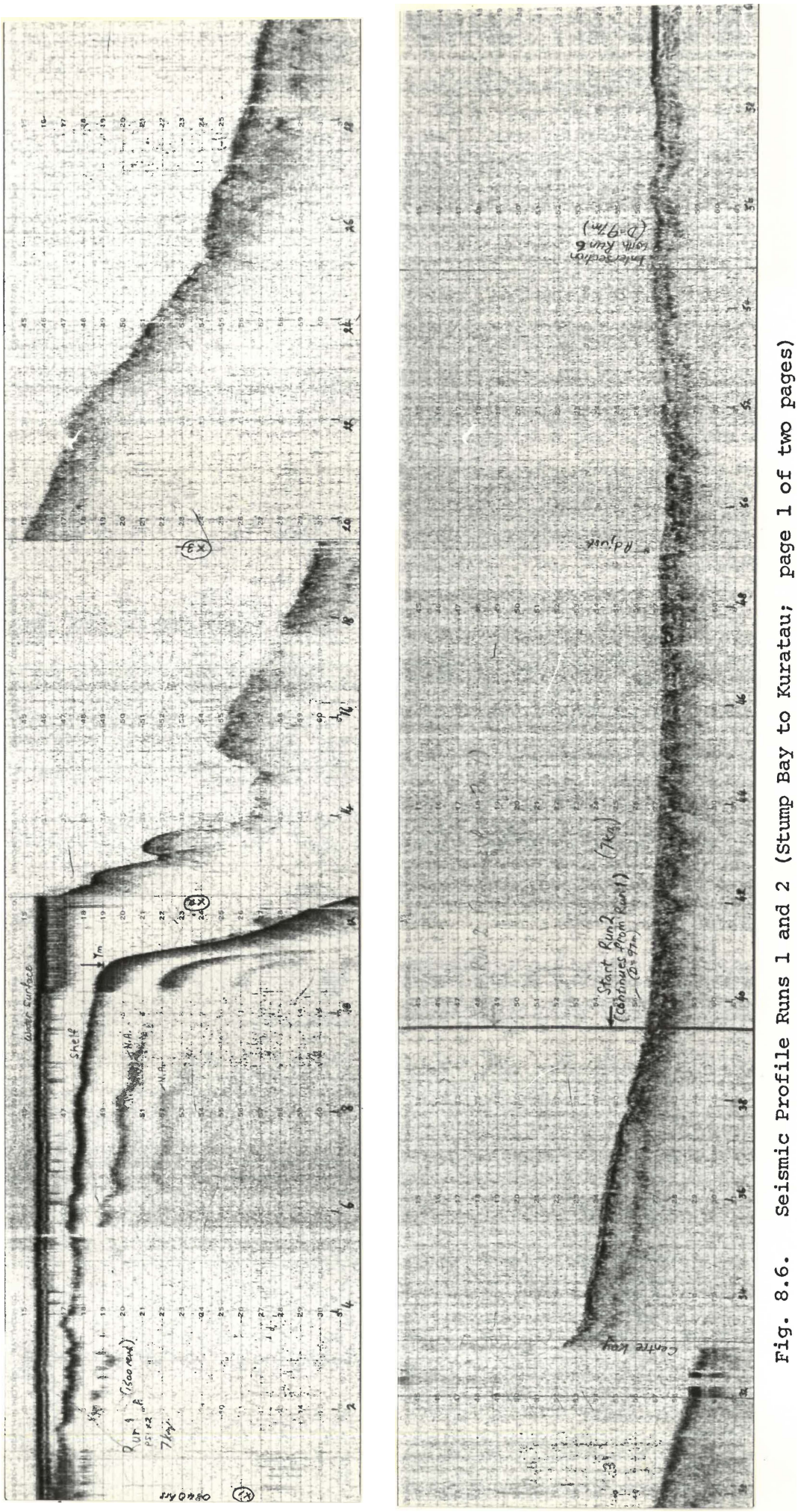
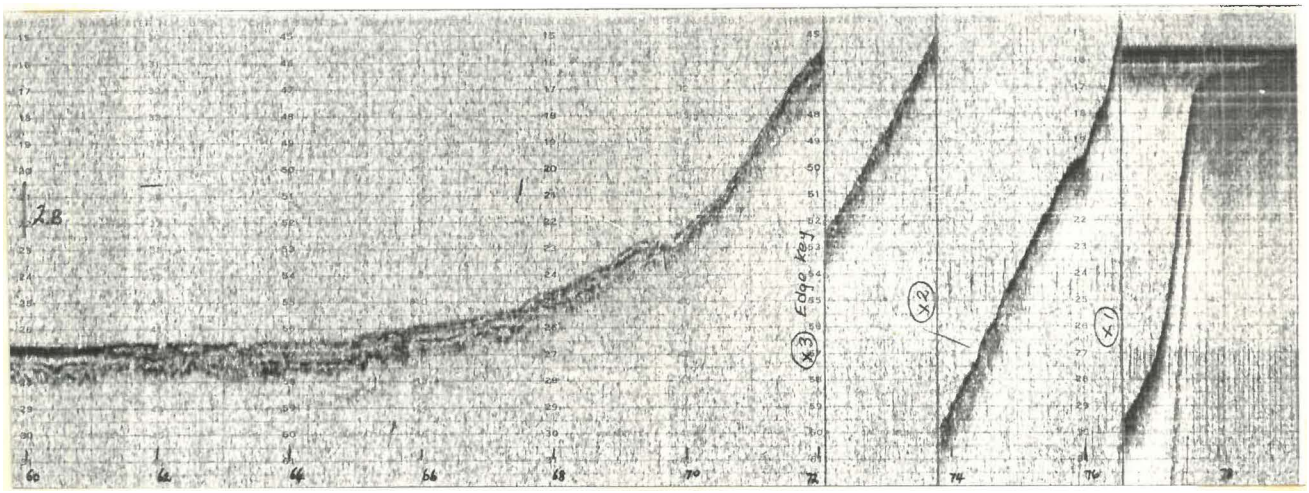


Fig. 8.6. Seismic Profile Runs 1 and 2 (Stump Bay to Kuratau; page 1 of two pages)



Run 2 continued (page 2 of two pages)

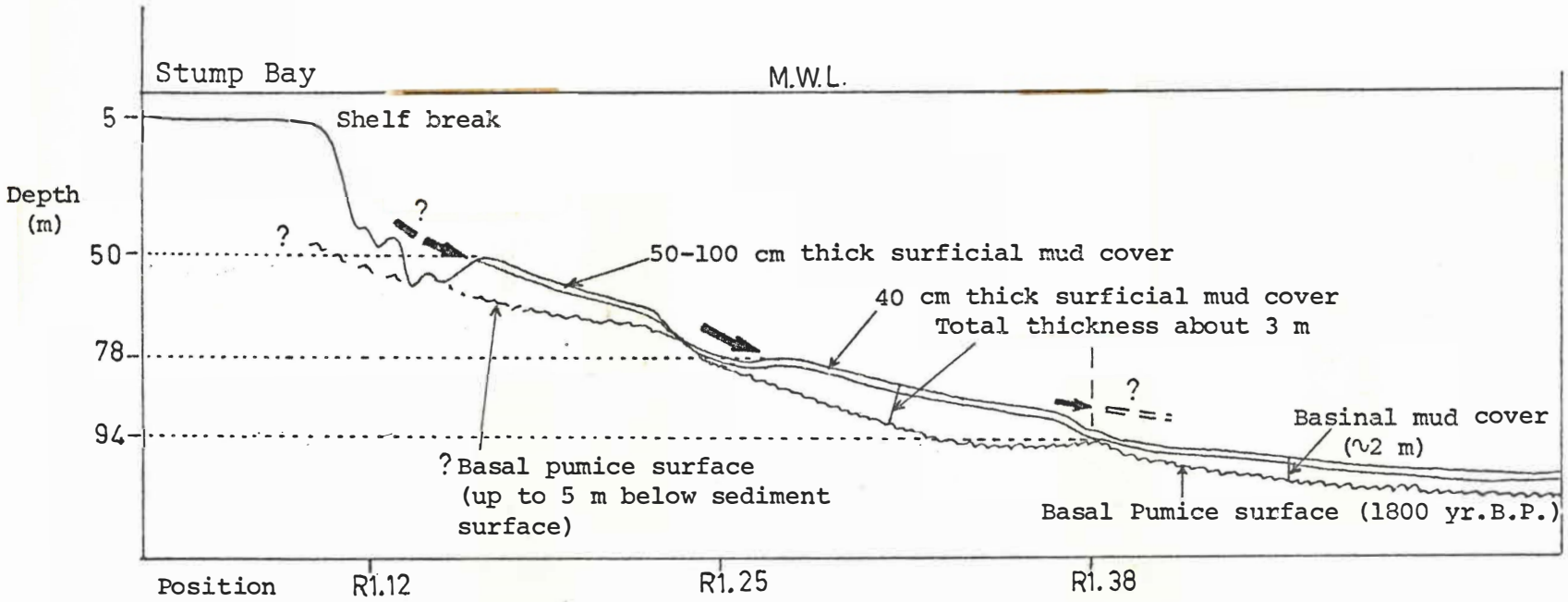


Fig. 8.7. Sediment slump movement on Stump Bay rise (based on seismic profile evidence from Run 1). Not to scale.

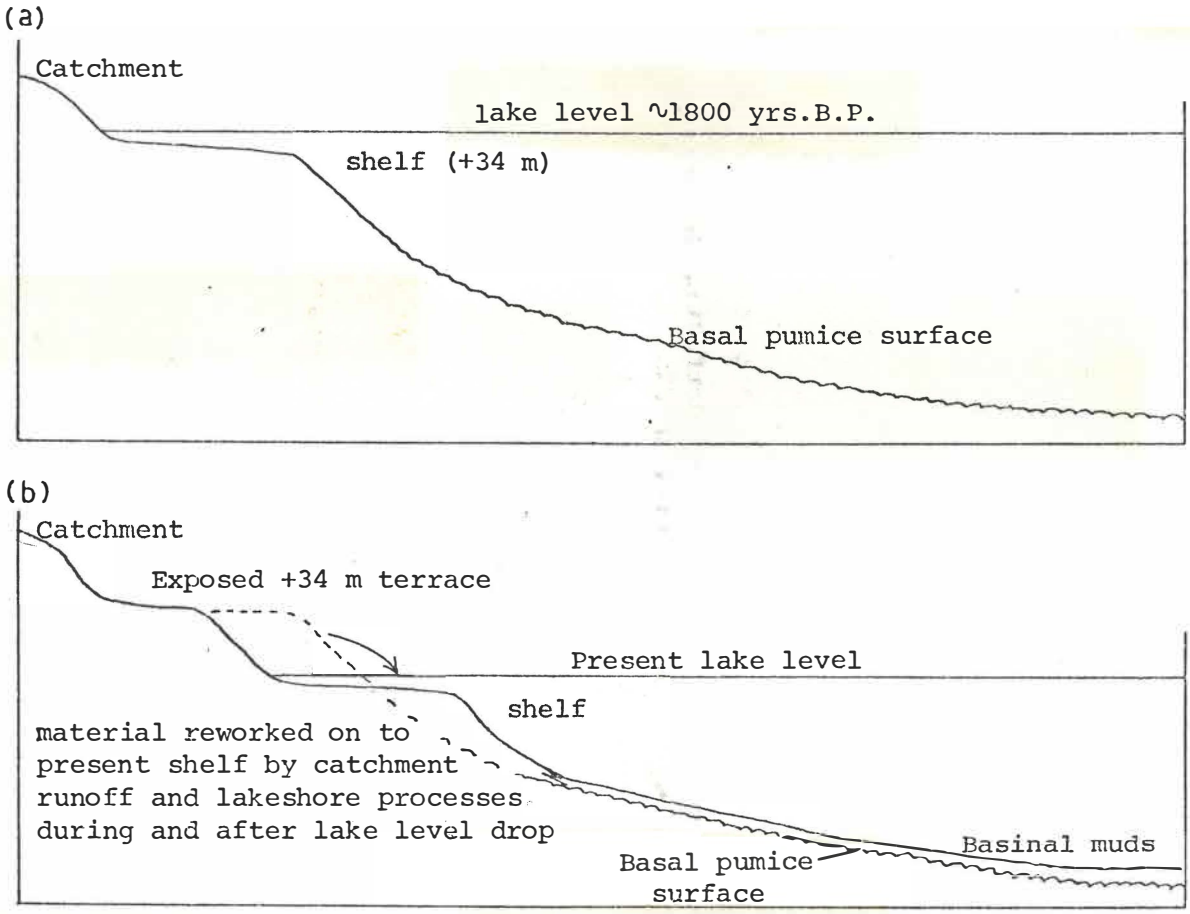


Fig. 8.8. Idealised cross-sections of a shelf region
(a) during the post-131 A.D., +34 m lake level, and
(b) today, showing shore and shelf modifications arising from a 34 m fall in lake level some 1800 years ago.

Run 11 from the Oruatua Shelf to the Poukura Shelf (Fig. 8.9)

A strong reflector occurs at about 0.6 m sediment depth and weak reflectors to nearly 2 m sediment depth on the Oruatua shelf, suggesting a finer sediment texture and/or different composition to other profiled shelf areas where no reflectors were recorded. Surficial sediments on the Oruatua shelf, except for an area of cobble lag, are generally finer than shelf sediments at similar depths from other areas (Fig. 7.3).

Below the steepest part of the Oruatua slope an area of decreased bottom gradient occurs on which four or five sediment layers have a total depth of about 1.6 m. Several metres deeper in the sediment, a weak reflector occurs which approaches the sediment/water interface as water depth increases. A surficial layer of sediment gradually thickens downslope to 0.5-0.8 m near the bottom of the rise, occasionally overlying partly infilled topographic lows in the basal reflector (e.g. R11.14, R11.16). Near the bottom of the rise (R11.24), reflectors indicate an unusually shaped body of material some 3 m thick and about 70 m across underlying the basal pumice surface.

Across basinal regions and on the lower Poukura slope, sediments overlying the basal pumice reflector are typically about 2 m thick. On the Poukura side of the basin (R11.44 on), better trace resolution clearly shows a reflector at 30-40 cm sediment depth which extends right across the basin. On the lower Poukura slope region, other weak, sub-parallel reflectors in the mud layer occur.

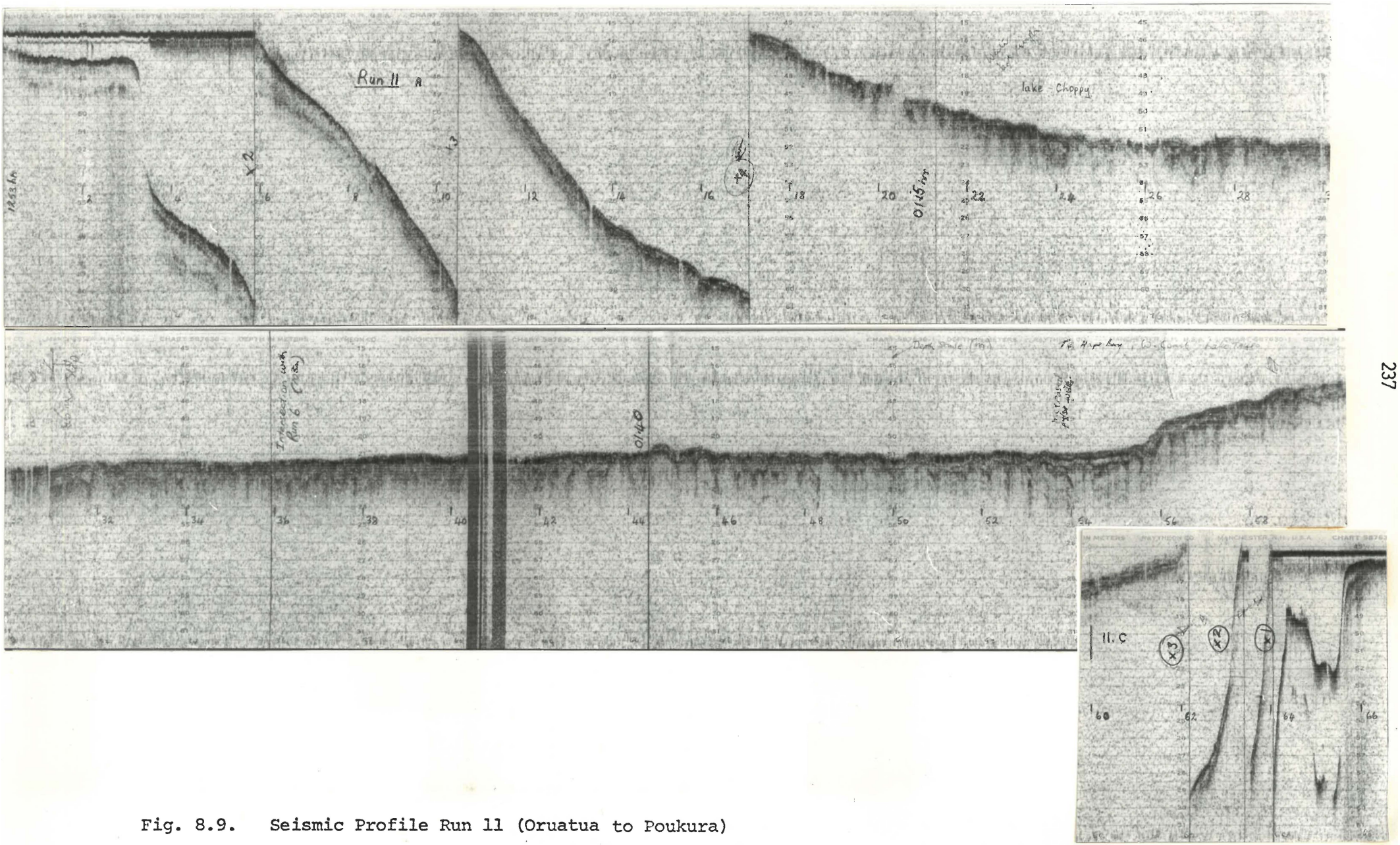


Fig. 8.9. Seismic Profile Run 11 (Oruatua to Poukura)

The approximately uniform mud thickness indicates a uniform rate of suspended-material sedimentation across this region, suggesting the absence of a dominant sediment source to either the east or the west over the last 1800 years.

Run 10 from the Waihaha Shelf to the Hatepe Shelf (Fig. 8.10)

Sediments overlying the basal pumice surface (which can be traced through from central lake regions to the east) thicken with increasing water depth off the Waihaha shelf, to about 1 m on the lower rise-basinal regions. They contain a sub-parallel reflector at about 20-30 cm sediment depth. Up to six or so reflectors, 30-50 cm apart, occur below the basal pumice surface to sediment depths of 3-4 m in central basinal regions. In places (e.g. R10.30-33, R10.53-57) these appear to be integral multiples of shallower reflectors, in which case they would not be real; however, in other places (e.g. R10.15, R10.21, R10.27, R10.48 and R10.58) the same reflectors diverge noticeably from the shallower reflectors, suggesting they are probably real. This problem requires more detailed examination.

At about R10.41 the weak surface reflector extending from the Waihaha region gives way to the first subsurface reflection, possibly as a result of decreasing Waihaha River sediment influences.

From R10.58-77 the surface mud thickness is typically 0.5-0.8 m. Two subsurface reflectors about 20-30 cm apart occur in some places (e.g. R10.66, R10.77) and it is unclear as to which of these is discontinuous and which represents the basal pumice surface. If an approximately uniform thickness of mud cover with distance is assumed then the deeper of these two reflectors is discontinuous and occurs within the basal pumice.

From R10.77 to about R10.136, water depth generally decreases to about 70 m over a central lake topographic high and bottom

topography becomes increasingly rugged due to emergence of the basal pumice surface as mounds and low hills. Overlying muds become discontinuous, being largely restricted to more level parts of the lake floor, where they are commonly 0.4-0.8 thick. Topographic lows in the basal pumice surface have been partly infilled to sediment depths of several metres, probably by redeposited pumice gravels and sands, prior to deposition of the surface mud layer.

At R1.138 a sudden increase in depth occurs down to a platform at about 115-120 m. Across the platform an indistinct surficial sediment layer 30-60 cm thick overlies numerous subparallel reflectors to sediment depths of many metres. Several unusual reflectors occur at R10.142.5 and R10.148-150.

From R10.155 towards the shelf area near Hatepe, a number of subsurface reflectors occur to sediment depths of up to 5 m or more. The basal pumice surface cannot be identified.

An unusual feature of Run 10 is the loss of reflection near R10.18 and R10.29. Near R10.29 a diffuse 'column' (60-70 m across) extends 7 m above the surrounding lake floor, against which, sediment reflectors pinch out. Emergent pumice surfaces are often poor reflectors (e.g. near R10.78); however, adjacent surficial sediments usually occur up the lower slopes of such emergent surfaces. Furthermore, position R10.29 occurs in the centre of an approximately flat basinal region of the lake. A possible cause of this phenomenon is sub-lacustrine geothermal activity. Columnar scattering of seismic signals resulting from

geothermal gas bubbling has been observed in the sea near Whale Island in the Bay of Plenty (North Island, New Zealand) by Glasby (1971), and in deep-waters towards the central eastern side of Lake Taupo by D. Northey (Ph.D. student, Victoria University, Wellington, 1977, pers. comm.) while echo-sounding deep sub-bottom structure. At the time Northey observed bubbles rising to the lake surface and a sulphurous odour. No bubbles or sulphurous odour were noticed during Run 10.

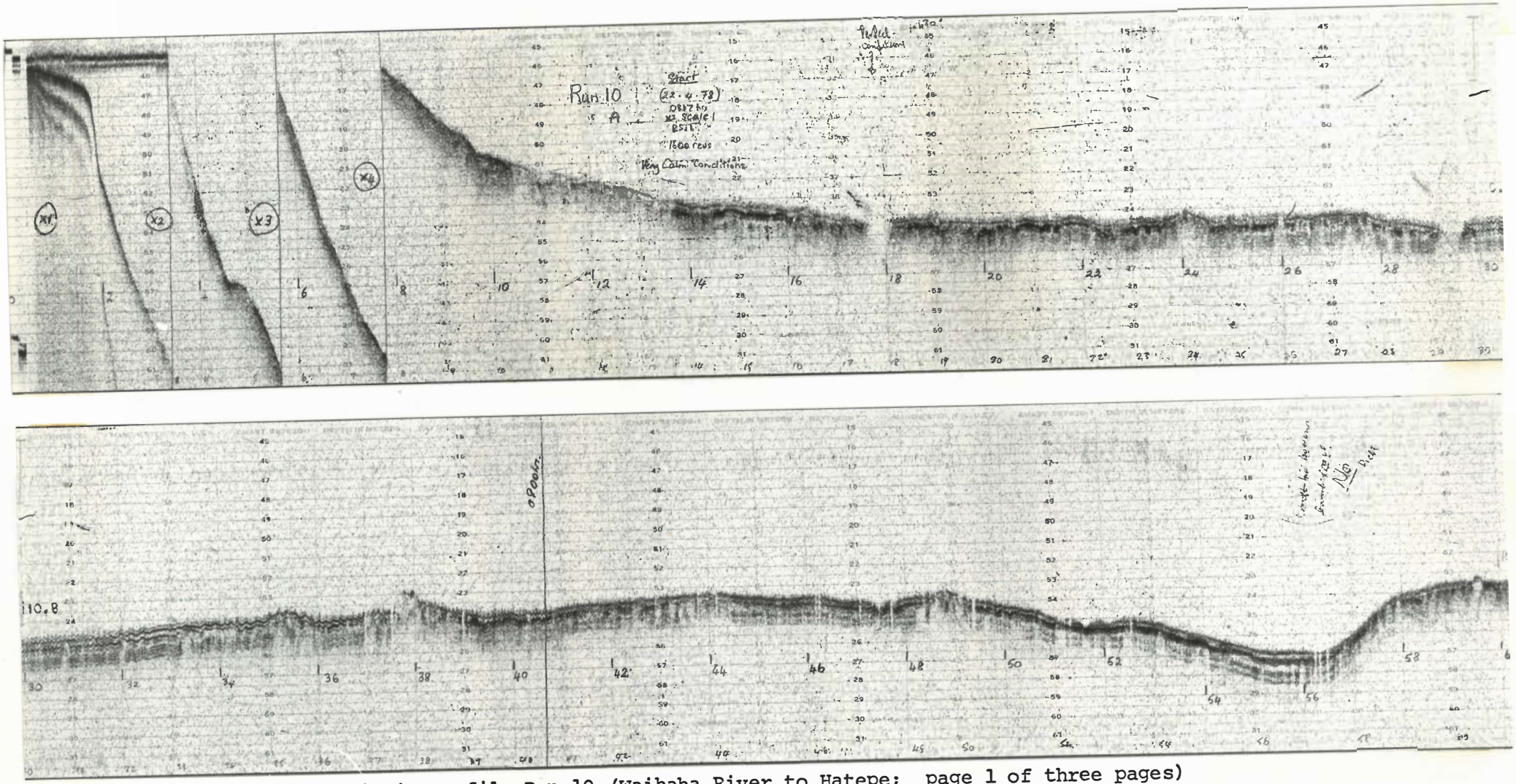
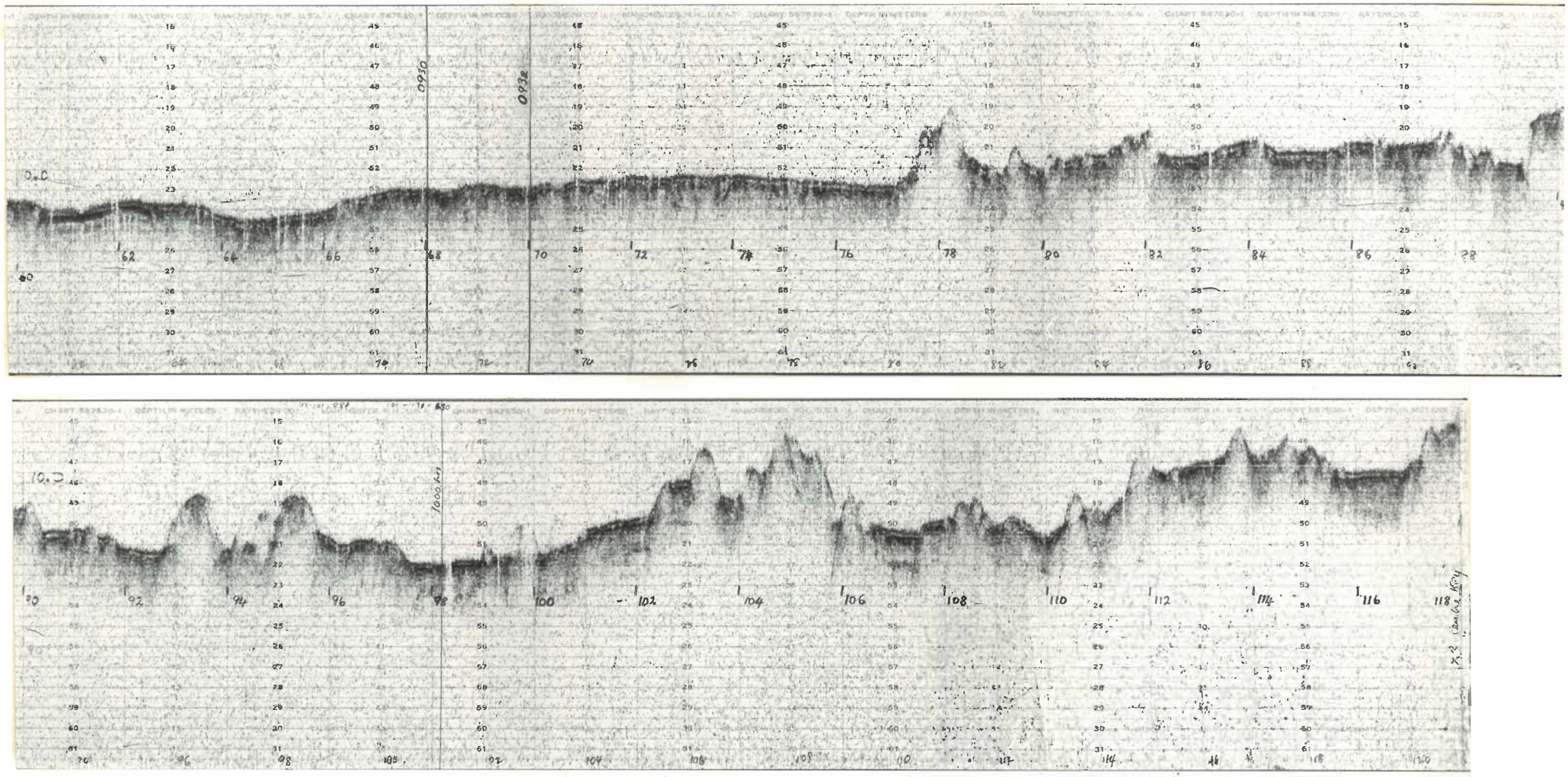
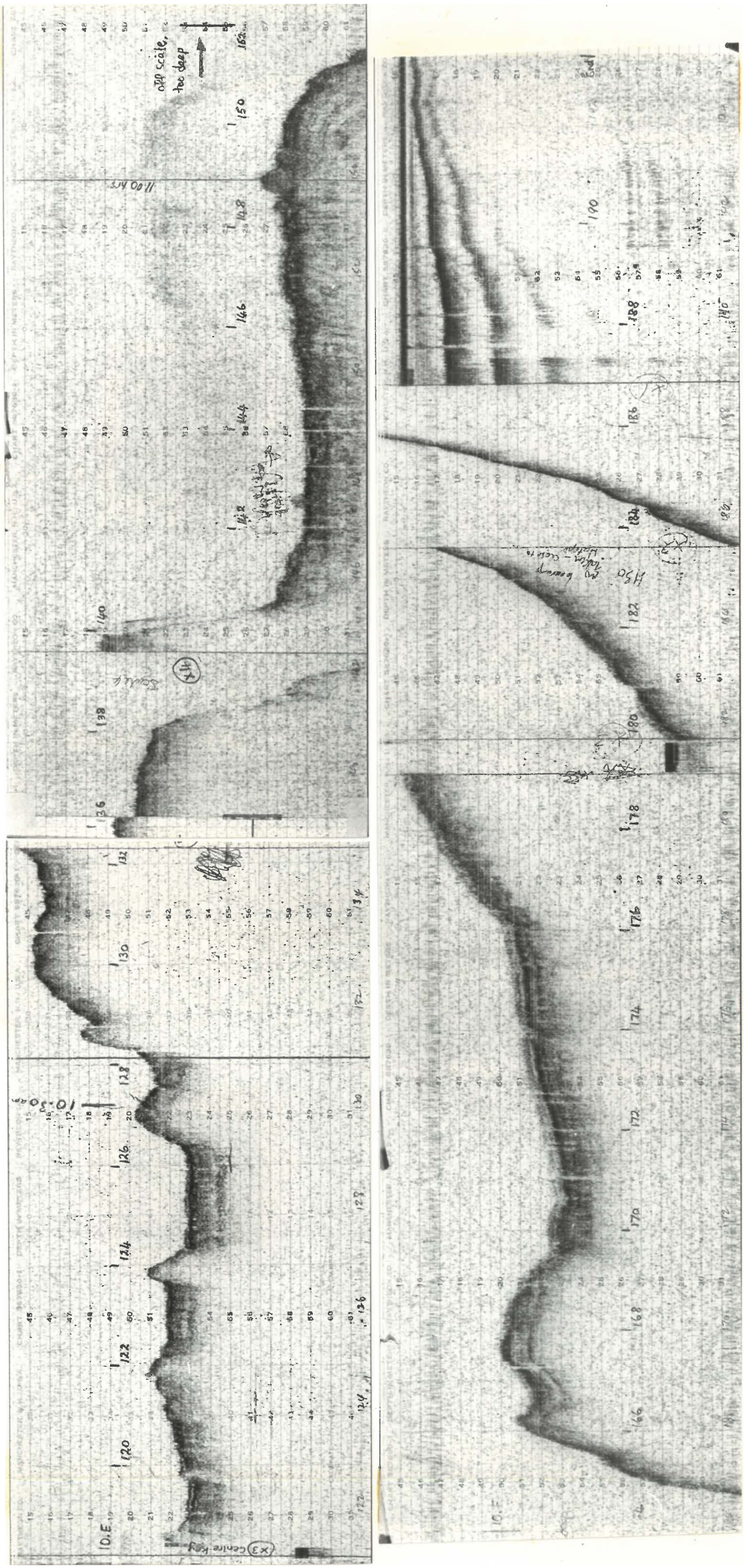


Fig. 8.10. Seismic Profile Run 10 (Waihaha River to Hatepe; page 1 of three pages)



Run 10 continued (page 2 of three pages)



Run 10 continued (page 3 of three pages)

Run 7 from Motuaiko Island to Hatepe (Fig. 8.11)

A rugged lake-bed topography occurs along the transect from Motutaiko Island to the Hatepe shelf. A thin surface layer of sediment (30-40 cm) occurs mainly over partly infilled topographic lows in the basal pumice surface.

Run 3 from Motawhara Island to Central Western Bay (Fig. 8.12)

From R3.0-R3.6 incorrect instrument adjustment prevented a trace being obtained. For the remainder of Run 3 (R3.6-R3.30) an instrumental base line trace appears at a depth of 111-112 m indicating the instrumental depth limit. Reflectors indicate a surface layer of sediment about 1 m thick above a second layer, commonly 0.5-0.8 m thick, overlying the basal reflector. At the intersection of Runs 3 and 10 (i.e. R3.18.2/R10.42) the two patterns of reflectors do not match well, mainly because of the "extra" 1 m thick surface layer in Run 3 which is not evident in Run 10. The reason for this is unclear.

Run 4 from Kawakawa Bay (Fig. 8.13)

A surface layer of sediment about 1 m thick overlies the basal reflector on the lower slope and rise regions of Kawakawa Bay.

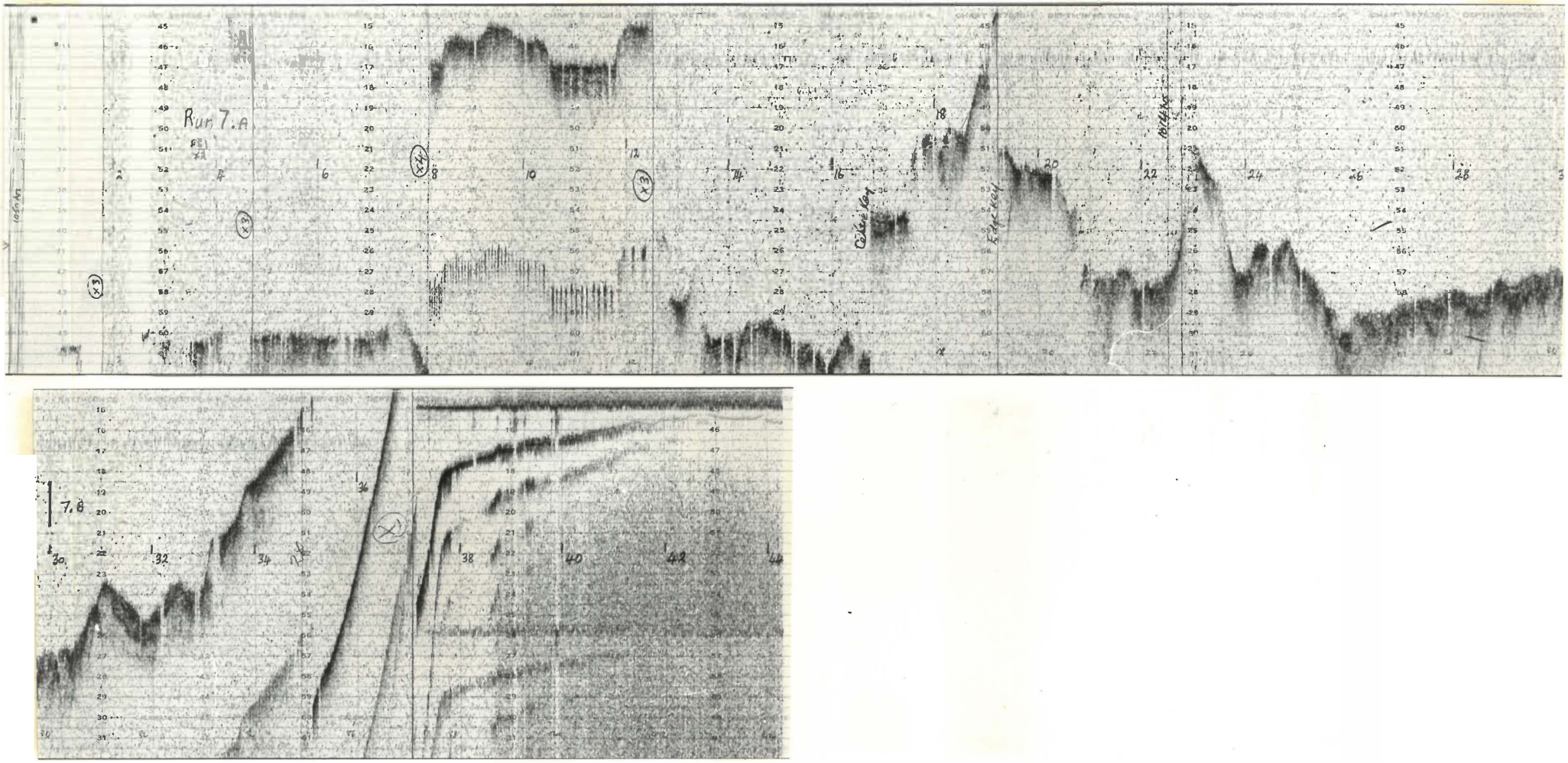


Fig. 8.11. Seismic Profile Run 7 (Motutaiko Island to Hatepe)

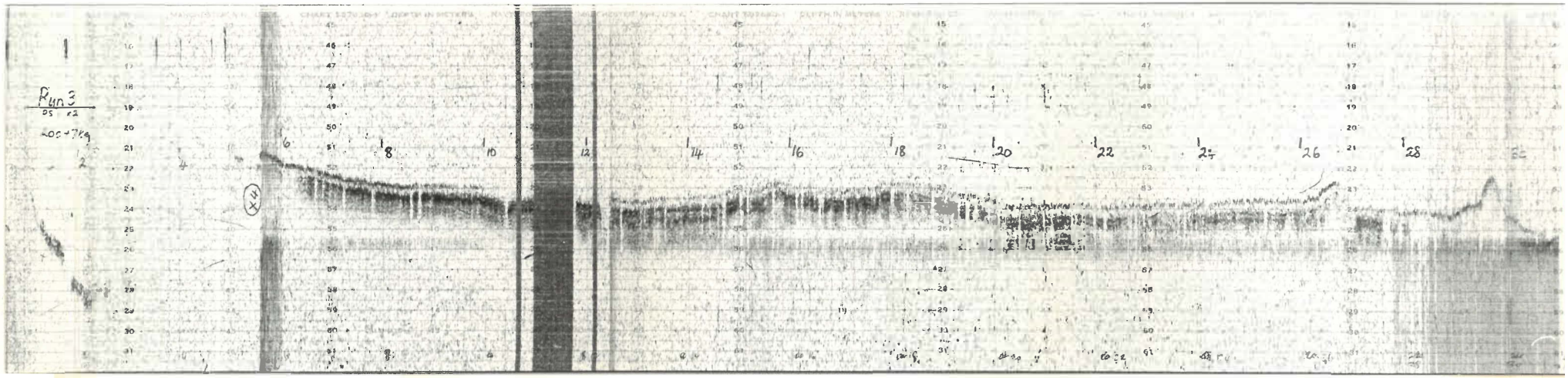


Fig. 8.12. Seismic profile Run 3 (Motawhara Island to central Western Bay)

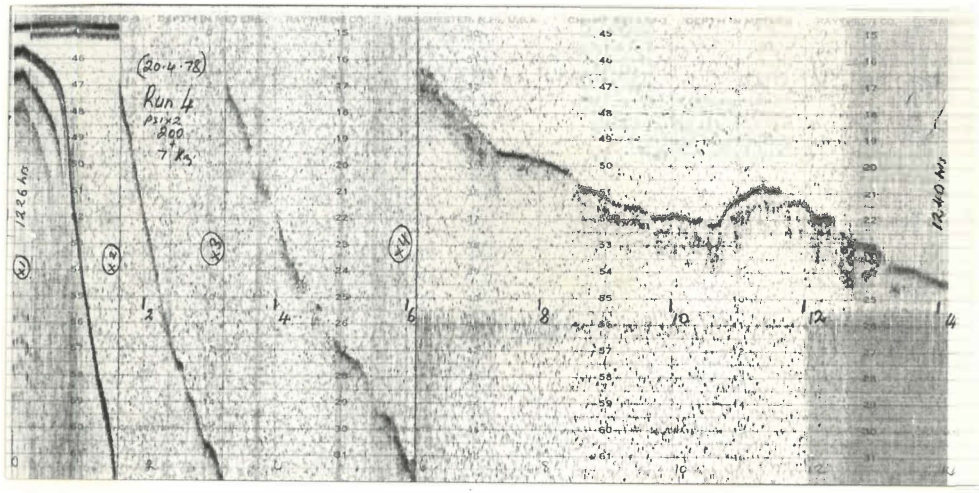


Fig. 8.13. Seismic Profile Run 4 (out of Kawakawa Bay)

Run 5 from Whangamata Bay (Fig. 8.14)

On the lower part of the slope, rise and basinal regions there are up to five subsurface reflectors, although the record is indistinct in places. A thin surficial layer about 30-40 cm thick overlies a layer commonly 0.5-1 m thick. A third, discontinuous layer about 30 cm thick occurs near the bottom of the rise (e.g. R5.14-R5.16) but appears to be absent in basinal regions. On the basis of topographic expression, sediment trends in other parts of the lake, and the absence of any major inflow into Whangamata Bay, the reflector at about 1 m sediment depth is assumed to represent the basal pumice surface. Weak deeper reflectors occur at about 3-4 m and 5 m sediment depth. The presence of a topographic 'nick' at R5.8-R5.9 and a thickened layer at the bottom of the rise (R5.19-R5.30) may indicate downslope redeposition prior to deposition of the overlying mud.

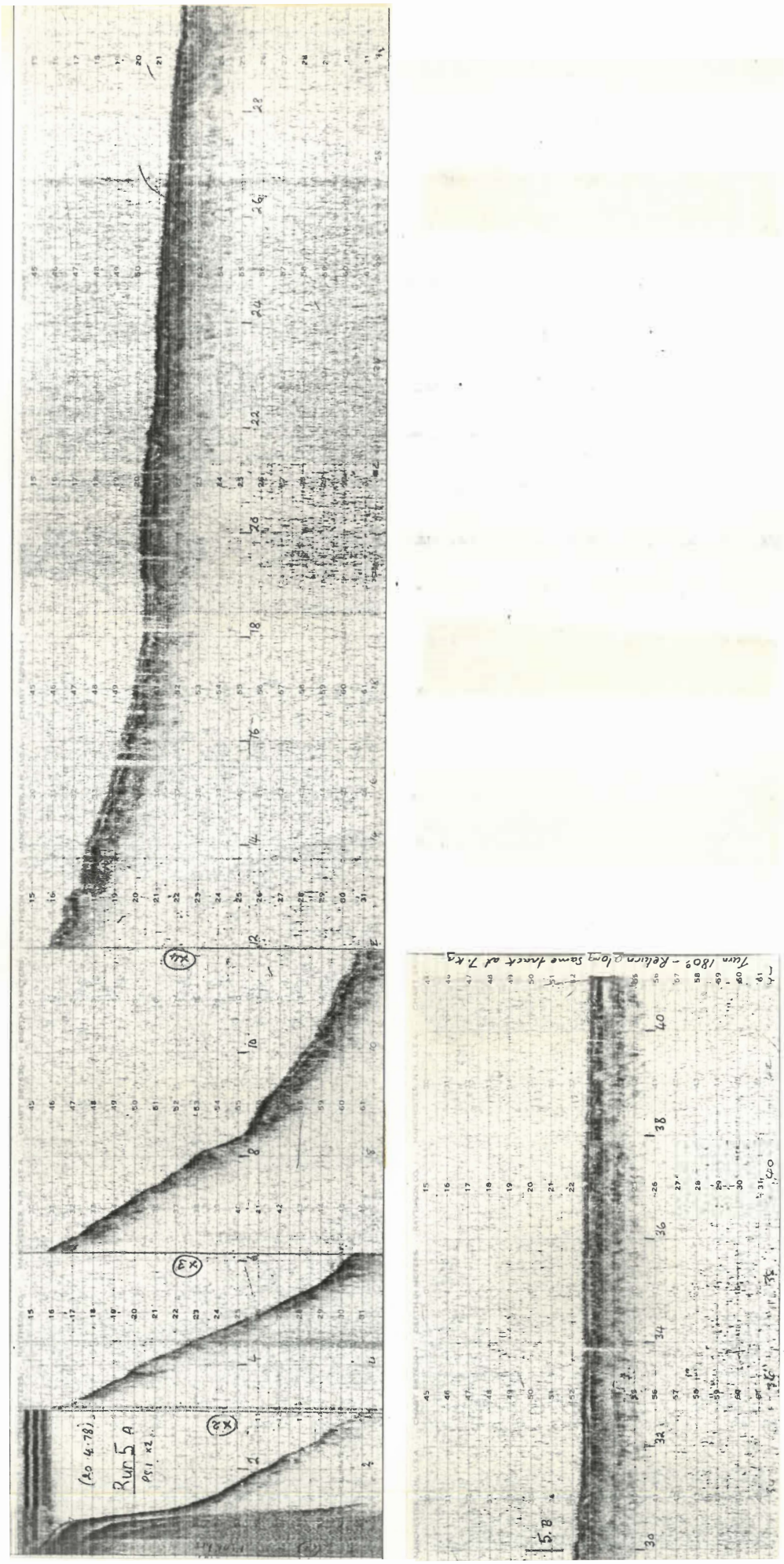


Fig. 8.14. Seismic Profile Run 5 (out of Whangamata Bay)

Run 8 from Tapaueharuru Bay (Fig. 8.15)

This transect begins in shallow water near the mouth of the Waikato River outlet. Reflectors indicate probable redeposition of sediments overlying the basal pumice surface, to a water depth of 42 m. These sediments generally thicken downslope to R8.5 and again to R8.16, terminating at R8.17.5. From 42 m to about 100 m water depth (R8.17.5-R8.36) the basal pumice surface is covered in places by a layer of sediment up to about 30 cm thick (Grab-sample 99, from 43 m water depth contained 79% pumice gravel and 21% sand indicating a paucity of mud at this depth) and lake-bed topography becomes increasingly rugged with depth. Some infilling of topographic lows occurs locally (e.g. R8.42-44), probably by redeposited basal pumice material prior to deposition of the mud layer (Grab-sample 98, from 72 m water depth, contained no gravel, 14% sand and 86% mud). Beyond 112 m water depth (R8.48) a mud layer up to 1 m thick overlies the basal pumice surface (Grab-sample 97, from 124 m contained 3% sand and 97% mud).

The general lack of mud cover at all but the deepest water depths of this transect suggests that the redeposited sediments to 42 m water depth are predominantly pumice gravel and sand.

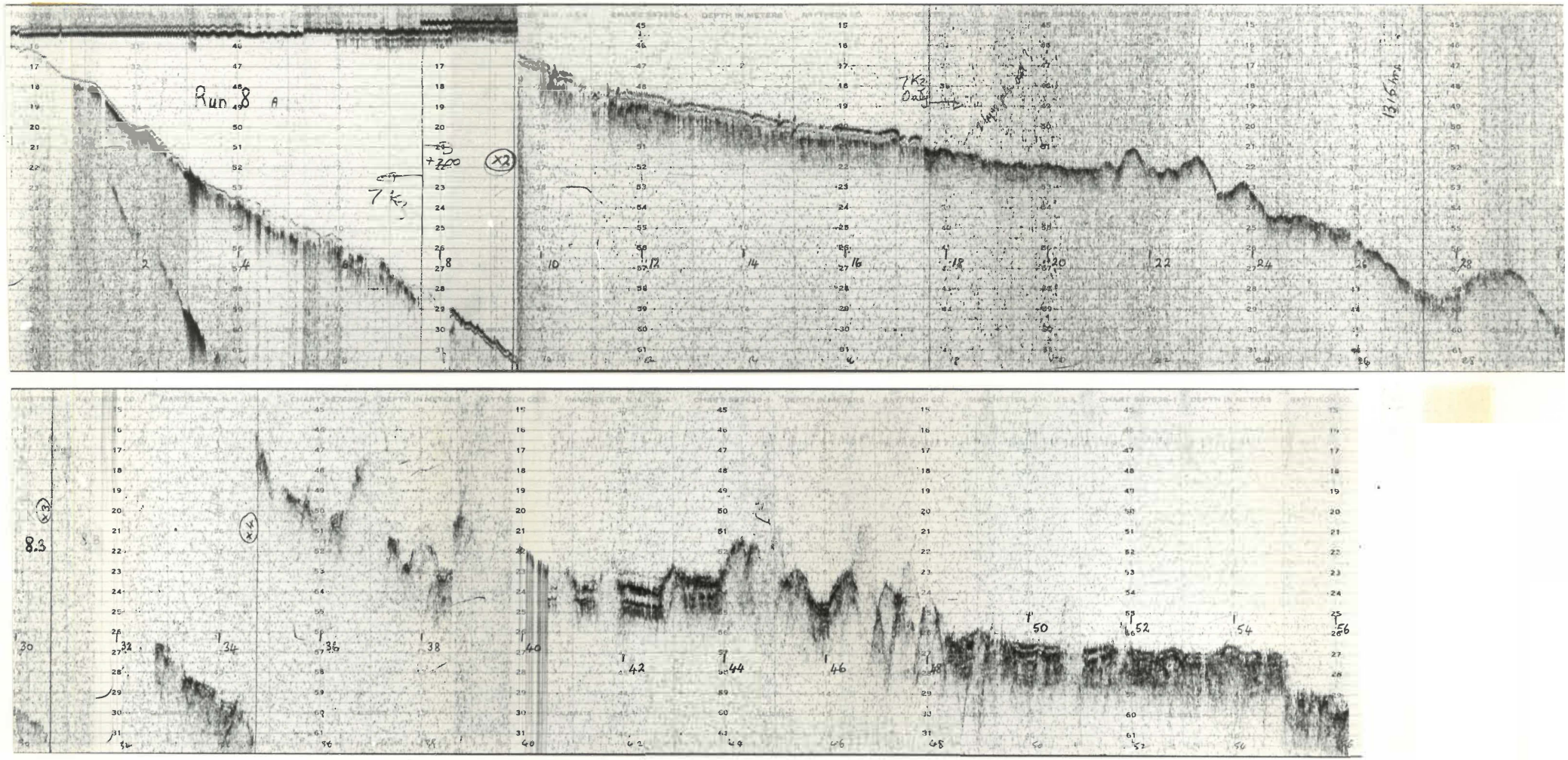


Fig. 8.15. Seismic Profile Run 8 (out of Tapaueharuru Bay)

Run 9 into Rotongaio Bay (Fig. 8.16)

This transect continues from Run 8 to the shelf area near Waitahanui. A sediment layer some 1 m thick overlies the basal pumice surface, which can be traced through from Run 8. This layer contains an internal discontinuous reflector (e.g. R9.7, R9.15); however, its uniform thickness over underlying topographic highs and lows indicates that it has been deposited primarily from suspension rather than by downslope redeposition. A number of step- or terrace-like features occur at water depths of 90-100 m (R9.12-16) which may have been caused by past contour-current erosion. The surface sediment layer gradually thins upslope, pinching out at 40-50 m water depth (R9.23-24).

Instrument depth limitations prevented seismic profiling within the 120 m isobath in the northern part of the lake. However, Core 6 (Fig. 8.17) was obtained from a water depth of 148 m in the Waitahanui Basin (Map 3 in Map pocket). This core contains mud throughout its length of 66 cm, the top 25 cm of which contains numerous bands in which dark coloured fine sand grains are dispersed. Immediately below these bands there is a disturbed mud layer some 2-3 cm thick, which in turn overlies mud without sandy bands. The dark sand grains are predominantly dark glass with some feldspar inclusions and probably represent wind-transported Ngauruhoe Ash.

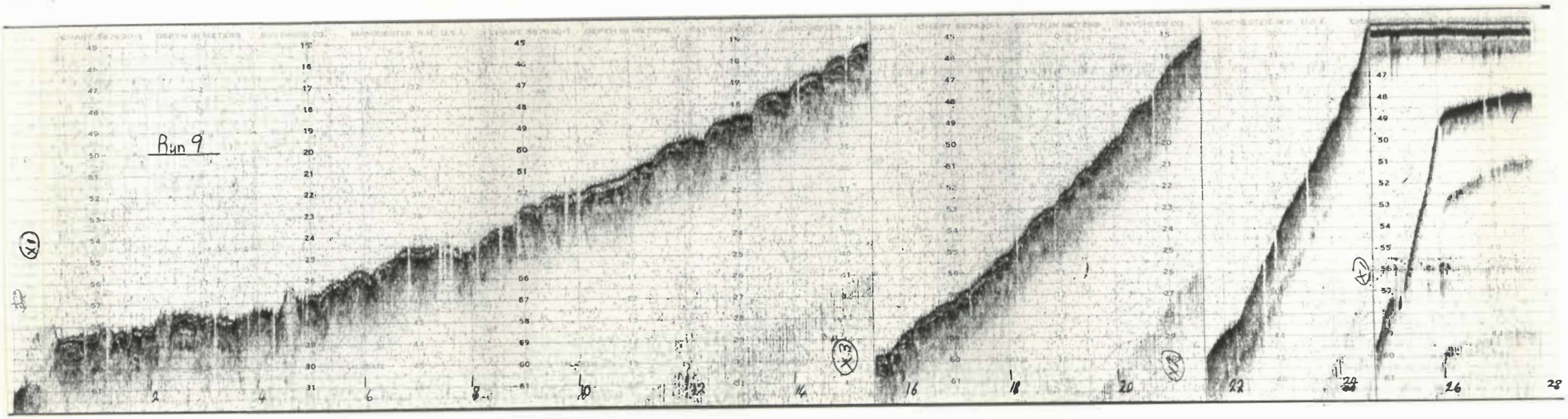


Fig. 8.16. Seismic Profile Run 9 (Into Rotongaio Bay)

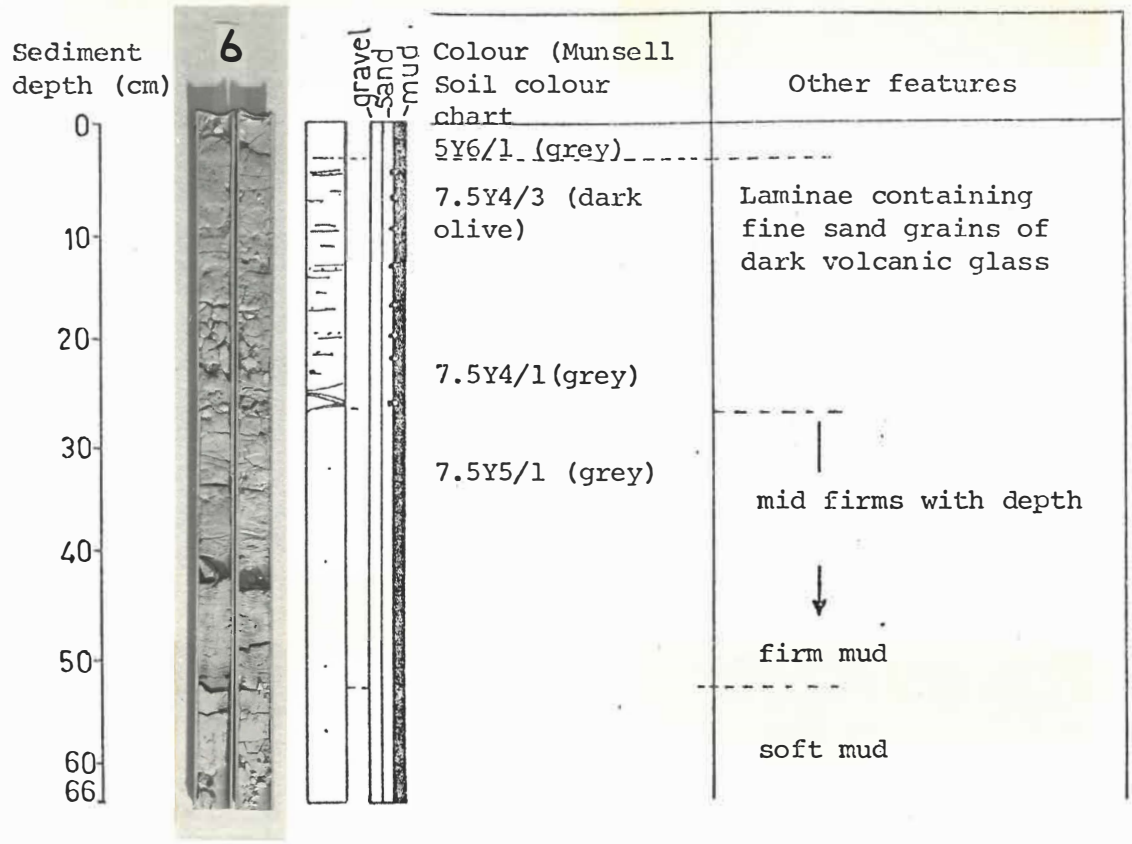


Fig. 8.17. Core 6 from 148 m depth in Waitahanui Basin (map 3 in map pocket). Mud with laminae containing sand grains.

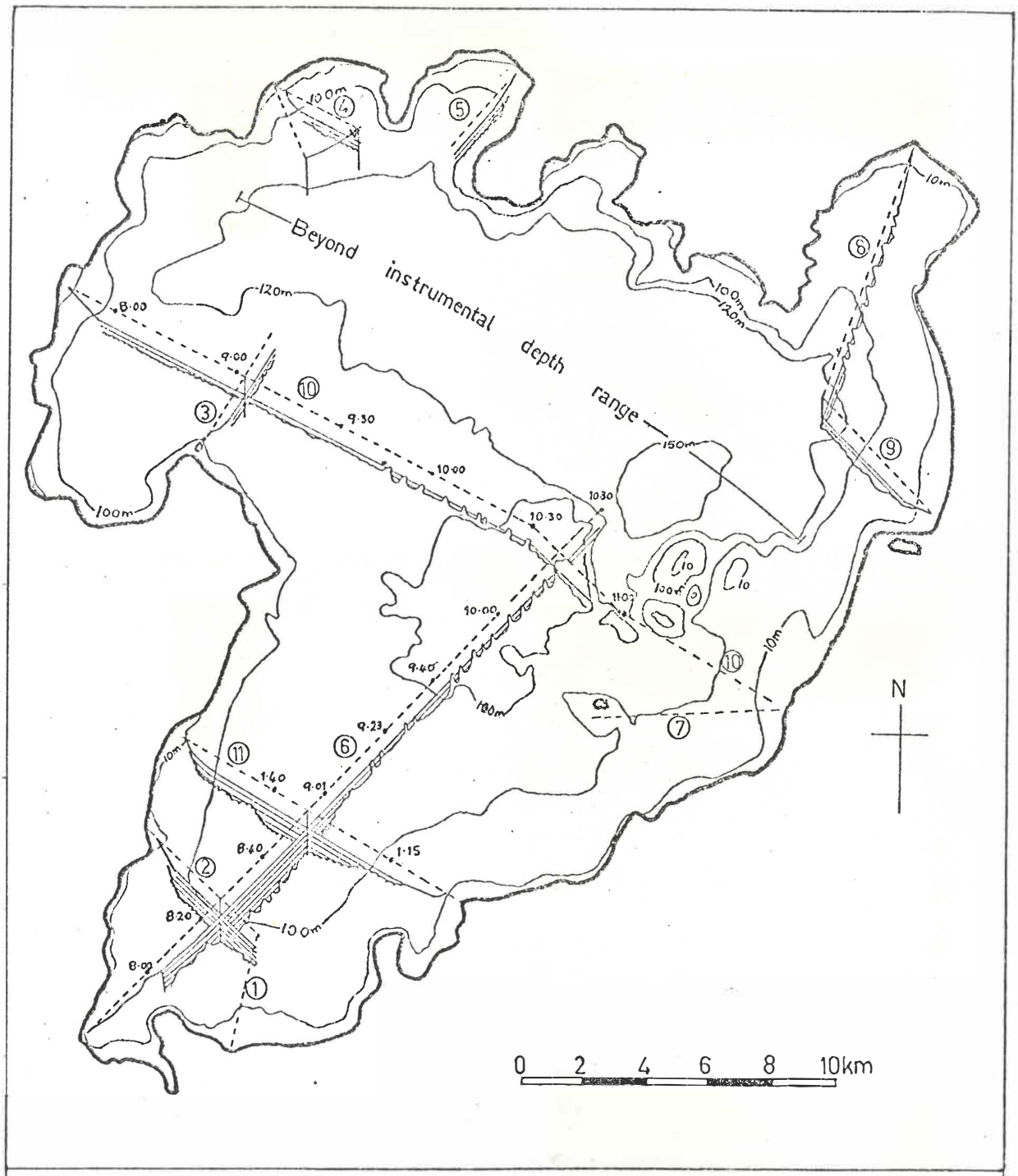
8.4 SEDIMENTATION RATES

The thickness of sediments deposited in deep-water regions of Lake Taupo over the last 1800 years (Fig. 8.18) varies spatially in response to several interdependent factors, including distance from sediment sources at the lake shore, general lake floor topography, and basal pumice surface topography.

The average sedimentation rate over the last 1800 years at any point along a seismic profile transect can be determined from the fence diagram of sediment thickness (Fig. 8.18). The sediment thickness is marked in 50 cm depth increments each of which is equal to a sedimentation rate of 1 mm/3.6 years or 28 mm/100 years.

The highest average rates of sedimentation (about 140 mm/100 years) have occurred in the deeper basinal region towards the southern end of the lake, where the highest input of river borne sediment occurs. The lowest average deep-water sedimentation rates (on approximately horizontal surfaces about 28 mm/100 years) generally occur in the central lake area where distances from lake-edge sources are greatest, lake depths are shallower than in surrounding basinal regions, and the basal surface is most rugged. Slightly higher average sedimentation rates (commonly 50 mm/100 years) occur in basinal regions towards Kuratau, and on the rise regions around Western Bay. In Tapaueharuru Bay, from which the Waikato River flows, a general lack of mud cover indicates very low sedimentation rates (commonly only 17 mm/100 years at 50-100 m water depth).

The sedimentation trends shown by seismic profiles generally agree well with the trends in the terrigenous silt content of



LEGEND

③ Seismic profile run number

8·20 Approximate course, position fix, and time of fix

Idealised sediment surface (present lake floor)
Sediment depth in 0.5 m increments (equal to an average sedimentation rate of 1 mm/3.6 yr or 28 mm/100 yrs.

Basal pumice surface (∿1800 yr.B.P.)

Fig. 8.18. Shallow, sub-bottom stratigraphy in Lake Taupo, and average sedimentation rates for the last ∿1800 years

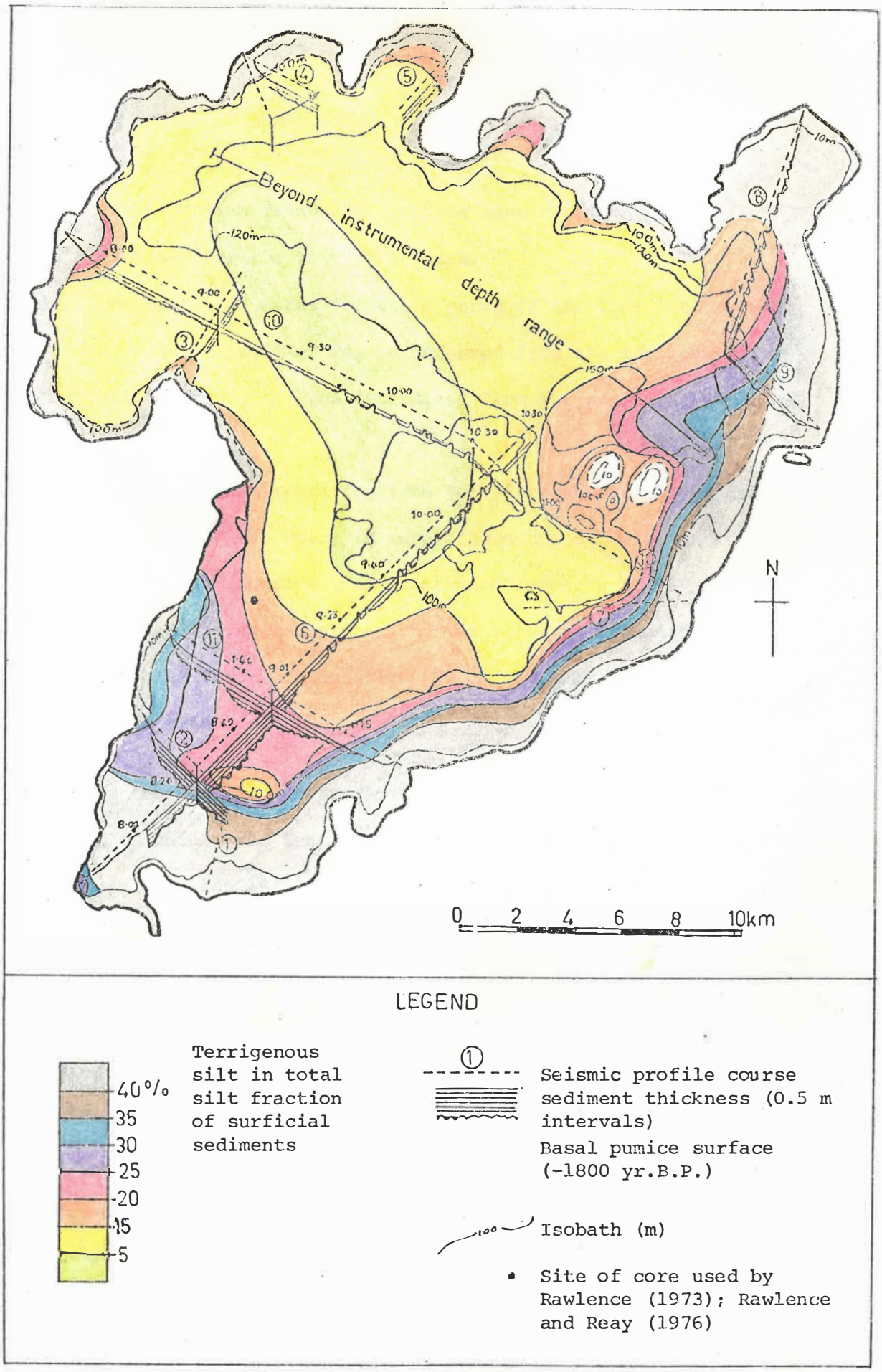


Fig. 8.19 . Average thickness of mud cover accumulated in deep-water regions during the last 1800 yrs. (oblique view) and terrigenous silt as a percentage of the total silt content in the top 20 cm of deep-water sediments.

surficial sediments (Fig. 8.19). This agreement has several implications:

(a) Sedimentation trends in the lake have remained broadly similar over the last 1800 years.

(b) Sedimentation rates for those parts of the lake not covered by seismic profiles may be inferred from the terrigenous silt content patterns determined from the surficial 15-20 cm of sediment.

(c) An average sedimentation rate for diatomaceous silica can be established, which in turn allows the calculation of terrigenous-component sedimentation rates.

(d) Local differences between the two lines of evidence may indicate recent changes (top 20 cm sediment) in local sedimentation trends.

In the central lake region, where the mud cover is typically about 50 cm thick, the terrigenous silt content in the total silt fraction of the top 15-20 cm of sediment is less than 5% (Fig. 8.19). The total silt content generally accounts for 85-90% of the total sediment in this area. Assuming the average mud component ratio is constant throughout the mud column, diatomaceous silica accounts for 40-45 cm of the mud thickness in this region. Further, assuming that the average sedimentation rate of diatomaceous silica has been much the same in all deep-water parts of the lake, subtraction of 40-45 cm from the mud thickness, at any point in the lake, leaves a net thickness of terrigenous sediment.

To compare terrigenous silt deposition rates implied by the surficial terrigenous silt-content pattern and mud-cover thickness

at a given point, the terrigenous silt percentage of the total silt fraction, a, is obtained from the total mud thickness, b, at that point, as follows:

$$a = \frac{[(b \times c) - d]100}{b}$$

where c = silt fraction of total sediment

d = thickness of diatomaceous silt

In the basinal region at the southern end of the lake a total mud thickness of 2.5 m is common and total silt accounts for about 75% of total sediment in the top 15-20 cm of sediment. Assuming a constant sediment-component ratio throughout the mud column, terrigenous silt forms 79% of the total silt content. This value indicates a considerably higher sedimentation rate for terrigenous silt than that indicated by the 20-25% in the top 20 cm of sediment, because of the non-linear relationship between terrigenous silt as a percentage of total silt, a, and total sediment thickness, b, as shown by the above equation. If the terrigenous silt value of 20-25% was constant throughout the mud column, a total mud thickness of only 70 m would have accumulated in the last 1800 years, giving an average sedimentation rate of 39 mm/100 years. This rate agrees reasonably well with a rate of 42 mm/100 years obtained through lead-210 determinations by Rawlence and Reay (1976) for the top 4-5 cm of sediment in a core from the southwestern part of Lake Taupo (Fig. 8.19). Although this indicates considerably higher rates of terrigenous sedimentation below the top 15-20 cm of sediment it is unclear whether the higher rates are part of a long term trend or simply represent periodic, severe storm-erosion events.

Because it is unknown how the mud components fluctuate with sediment depth below the surficial 20 cm of sediment, and because of the considerable variations in sedimentation rates with time, a detailed time scale cannot be matched with the mud column.

On the basis of general agreement between the surficial terrigenous silt content pattern and the seismic profiles on the broader sedimentation trends, the surficial terrigenous silt content pattern suggests a 0.5-1.0 m thick mud layer covers the basal pumice surface across the northern part of the lake, giving a total sedimentation rate of 28-56 mm/100 years.

Average sedimentation rates for deep-water regions of Lake Taupo over the last 1800 years are summarised in Table 8.1.

	Approximate thickness of mud over basal pumice surface (m)	Approximate total sedimentation rate (mm/100 years)	Approximate sedimentation rate of terrigenous material (mm/100 years)
Central Kuratau Basin	2.5	140	118
Central lake regions	0.5	28	6
Central Western Bay	1.0	52	31
Northern lake regions	0.7	40	17

Table 8.1. Average sedimentation rates for deep-water regions of Lake Taupo over the last 1800 years.

CHAPTER 9

SUMMARY AND CONCLUSIONS

9.1 SUMMARY

Catchment Characteristics

Lake Taupo, with an area of 616 km^2, is the largest of several lakes of volcano-tectonic origin in the Central Volcanic Region of the North Island of New Zealand. It occupies a major depression/collapse zone in natural catchment area of 286,515 ha. A further 67,110 ha. of borrowed catchment, resulting from the Tongariro hydro-electricity project to the south of the lake, increases the total catchment area to 353,625 ha. Lake Taupo is drained in the north-east by the Waikato River.

Catchment geology comprises mainly Quaternary rhyolitic/andesitic volcanics and Mesozoic greywackes. Andesites and andesitic ash occur mainly to the south of Lake Taupo around the active volcanoes of the Tongariro National Park. Greywackes occur in the Kaimanawa and Hauhungaroa Ranges which form the catchment boundaries to the southeast and west of Lake Taupo respectively. Rhyolites, rhyolitic breccias and rhyolitic ashes occur mainly in the eastern and northern parts of the cathment, and ignimbrites in the northwestern parts. Rhyolitic tephra from the Taupo Pumice eruptions of about 131 A.D. blankets much of the central and northern catchment areas. Since 131 A.D., sporadic and generally localised eruptions of andesitic lava and volcanic ash (Ngauruhoe Ash) from the Tongariro National Park volcanoes have occurred through to the present. Hydrothermal activity occurs on the

volcanoes and also at the southern end and northeastern corner of Lake Taupo.

Lake Taupo is surrounded by a belt of flat to rolling lowlands (<600 m a.s.l.), some 5-10 km wide, in which streams and rivers are often deeply entrenched. To the east and west the bounding ranges reach over 900 m a.s.l. The greatest altitudes and steepest terrain occur in the Tongariro National Park (Mt Ruapehu, 2797 m; Mt Ngauruhoe, 2258 m; Mt Tongariro, 1968 m) and southern Kaimanawas (1600+m).

Taupo catchment soils are developed almost exclusively on volcanic tephra deposits less than 2000 years old. Yellow-brown pumice soils, formed on Taupo Pumice, occur over central and northern catchment regions. Recent soils from volcanic ash, formed on Ngauruhoe Ash, occur in the southern catchment, Both soils are poorly developed, with only small amounts of allophane clay, and both are susceptible to erosion. Some of the lowland areas have been developed for pasture and forestry, some remain in scrub. Most of the steeper catchment remains undeveloped and covered in native forest, scrub and tussock. Bare rock and shingle screes occur at higher altitudes in the Kaimanawas and Tongariro National Park.

The catchment climate is generally cool and humid, with prevailing winds from the southwest. Rainfall is fairly evenly distributed throughout the year, although a summer minimum occurs. High rainfalls, often intense and of short duration, occur in the high country of the southern catchment; more than 3800 mm/year falls on the volcanoes, while over the remainder of the southern

catchment, including the high country to the east and west of Lake Taupo, falls from 2000 to 3000 mm/year are typical. Lake Taupo itself, the surrounding lowlands, and the northern catchment lie in a rain-shadow area with an average annual rainfall of less than 1500 mm/year. Permanent snowfields exist on Tongariro National Park volcanoes.

Runoff from central and northern catchment areas is retarded by the high natural absorbancy of the pumice tephra deposits and the high mass permeability of porous and/or jointed ignimbrites. The lowest average specific discharges ($<30\ell^{-1}$ km^{-2}) occur around the northeastern part of Lake Taupo. However, in southern catchment areas, the generally low permeability of greywackes and andesites, and the steep terrain and scant vegetation cover at higher altitudes lead to rapid runoff. Average specific discharges commonly exceed $100\ell^{-}$ km^{-2}.

More than 60 streams and rivers enter Lake Taupo but many of these are ephemeral. The Tongariro River, which drains a major part of the southern catchment, has the largest natural discharge into Lake Taupo and accounts for 25-30% of all inflows into the lake. Lake outflow (Waikato River) will eventually increase by about 27% as a result of runoff diverted into Lake Taupo from the borrowed catchment.

Catchment erosion is presently not serious but the potential risk is high. Pumice tephra deposits are liable to rill, sheet, streambank, slip and gully erosion, particularly when vegetation is removed, infiltration reduced and dry gullys reactivated. The most severe erosion occurs on the volcanoes in Tongariro National Park as

a result of the steep exposed terrain, high rainfall and pronounced physical weathering. For similar reasons, severe erosion also occurs in the southern Kaimanawas (largely in borrowed catchment) where it is characterised by debris avalanches and scree-creep of shattered greywacke.

Extensive areas of moderate erosion occur on the rolling terrain to the east of Lake Taupo. In the western Hauhungaroa Ranges and the northeastern catchment region, erosion is generally negligible.

Lake Charcateristics

Lake Taupo is classified as an oligotrophic (secchi depth, 13-18 m), warm monomictic (thermally stratified from December-April) lake of volcano-tectonic origin. The lake is roughly triangular in shape, 40 km long (Waihi-Taupo), has a maximum width of 27 km, an average depth of 97 m (max. depth 164.6 m), and a volume of $59.1 \times 10^6 m^3$. The lake floor is relatively flat except for a more rugged area in the central northeastern region. The western shores are characterised by steep ignimbrite, andesite and rhyolite cliffs which plunge into deep water. The northern shores are formed by a series of bays separated by raised fault blocks of rhyolite. In the lake, gently sloping shelves of sand and gravel have developed along the eastern side. The shelf break occurs at water depths of 5-10 m and depth increases rapidly down the slope (20-25°) to 40-70 m. Beyond this depth the lake bed gradient progressively decreases down the rise to basinal regions.

The present form of Lake Taupo has developed relatively recently. Its size, shape and depth have been modified by catastrophic volcanic events, the last being the Taupo Pumice eruptions of 131 A.D. Huge amounts of pumice from these eruptions blocked the lake outlet causing the lake level to rise 34 m above its present level. A well defined terrace formed around much of the lake before the present outlet was cut and the lake level subsided again. The catchment has restabilised since the Taupo Pumice eruptions, and the volume of sediment entering the lake has diminished drastically.

Sediment Characteristics

A number of depositional environments in Lake Taupo are broadly characterised on the basis of surficial sediment texture and depositional processes. These environments include: sub-lacustrine talus slope, shelf, slope, rise, basin, and sub-lacustrine topographic high (hill).

Sub-lacustrine talus slope sediments occur mainly in deep water (∿80+m) beneath coastal cliffs on the western side of the lake. The sediments are very poorly sorted gravel-sand mixtures with subordinate mud.

Surficial shelf sediments, except near river mouths and in the sheltered areas, are commonly unimodal, moderately to very well sorted sands and gravels. With increasing water depth towards outer shelf areas, sorting tends to deteriorate and mean grain size decreases. The gravels include mainly rhyolite and greywacke in shallower water and pumice in deeper water. The

sands consist of volcanic glass, rock fragments, plagioclase feldspar (>20 wt.%) and quartz (5-10 wt.%). Rivers and streams are slowly feeding catchment-derived sediments on to shelf areas, particularly during floods. Coarser material may be worked alongshore, onshore or offshore by wave action, and the finer grain sizes (very fine sand, silt and clay) are winnowed to deeper water by energy gradients resulting from swell and wave action.

Slope sediments are generally polymodal, poorly sorted silty sands and sandy silts. Although these sediments are below effective wave base, they may contain material worked off the shelf edge (e.g. pumice gravel, sand and diatom tests, especially *Synedra*, *Nitzschia* and *Surirella* species) as well as material deposited from suspension. With increasing depth and decreasing environmental energy, the mud content deposited from suspension increases and slope sediments grade into sandy silts and silts on the rise which in turn give way to silts in the basinal regions. Shelf and slope sediments are occasionally redeposited into rise and basinal regions giving poorly sorted mixtures of mud, sand and/or gravel.

Sediment textures on sub-lacustrine topographic highs are variable, ranging from sandy silts to muddy sandy gravels (pumice), but a mud content is usually dominant. The higher content of sand and gravel on topographic highs reflects two factors: concentration of coarse material by winnowing of fines and/or coarse sediments relict from the Taupo Pumice eruptions. The sediments on one topographic high in particular, near the centre of the lake, appear to be largely relict and also reflect the influence of past hydrothermal activity. They contain bedded

lenses of plagioclase-rich sand, silt, and clay overlain by a sinter crust in which pumice fragments are embedded. The clay content is the highest (41 wt.%) in the lake and is enriched in montmorillonite of probable hydrothermal origin.

Surficial basinal sediments are texturally classified as silts. They contain a few percent sand (commonly <4 wt.%) and up to 25 wt.% clay-sized material. The average basinal mud is lighter in colour in central and northern lake regions than in southern areas. Water content is commonly about 80 wt.% and organic matter content about 7.5 wt.%, although organic matter contents of 8 wt.% or more occur locally, particularly in Waihi and Stump Bays and lakeward of the Waihaha River mouth. Except for occasional macro-particles (e.g. Chironamid larvae, plant fragments) the organic matter is fine grained humic material which probably originates mainly from algae (e.g. diatoms), particularly in central and northern lake regions. Locally increased values (>8%) probably reflect an additional allochthonous component. Surficial basinal-sediment pH values are commonly 5-6; and Eh values generally exceed +100 mV.

The sand fraction in basinal regions is composed mainly of volcanic glass with plagioclase feldspar inclusions and has probably been deposited from wind-borne Ngauruhoe Ash.

The silt fraction of surficial basinal sediments contains two persistent grain-size modes (i.e. coarse-medium silt and medium-very fine silt) which display a reciprocal relationship. The coarse-medium silt mode is due to terrigenous material and the medium-very fine silt mode to siliceous diatom tests (*Melosira* sp. >> *Cyclotella* sp. ≃ *Epithemia* sp.). Diatom tests are especially prominent in the

central and central western lake regions, and form very well sorted, near-symmetrical, mesokurtic silts.

Terrigenous silt components display two broad areal trends relative to the diatomaceous component:

(a) A terrgienous silt component, consisting mainly of volcanic glass, rock fragments, plagioclase feldspar and quartz, decreases in abundance away from the southern end of the lake reflecting derivation from southern catchment rivers, particularly the Tongariro River.

(b) A terrigenous silt component, consisting mainly of volcanic glass, decreases in abundance westwards from the northeastern lake margin. Erosion of coastal cliffs of pumice breccia is probably the most important sediment source in this case.

Silt and clay contents display a reciprocal relationship with clay ranging from around 24 wt.% in southwestern parts of the lake to about 12 wt.% in some northern parts. Diatomaceous silica characteristically forms about half of the clay fraction; the remainder consists of three types of approximately spherical authigenic particles (siliceous, bladed microspherulites; biogenic capsules; and colloidal sulphur) and clay minerals.

Crystalline clays, which together form less than about 5% of basinal sediments, include illite, kaolinite and montmorillonite. Illite and kaolinite contents in the clay fraction show broadly similar areal trends, decreasing in a northeasterly direction away from the southern end of the lake, and increasing over a short distance towards the Waihaha River mouth; these clay minerals

are detrital from weathered greywackes in the Kaimanawa and Hauhungaroa Ranges. Montmorillonite, however, is most abundant in the southwestern corner in Waihi Bay and on a sub-lacustrine topographic high in the centre of the lake; in both areas it has probably formed from hydrothermal alteration of siliceous volcanic material.

Sedimentation Trends

The distribution patterns for terrigenous silt and clay suggest the major source of mud-sized material in the lake is the Tongariro River, and the major direction of suspended-sediment laden currents is from the southern end of the lake towards the out-flowing Waikato River in the northeast. These trends appear to have been followed for at least the last 1800 years.

An extensive surface of sedimentary pumice, deposited in the lake during and soon after the Taupo Pumice eruptions, has been identified in basinal-rise regions at sediment depths of less than 3 m. Most of this surface has subsequently been buried under a mud cover ranging in thickness from less than 0.5 m in central and northern parts of the lake to more than 2.5 m in southern parts of the lake. Corresponding average sedimentation rates have ranged from less than 30 mm/100 years to more than 140 mm/100 years over the last 1800 years.

9.2 CONCLUSIONS

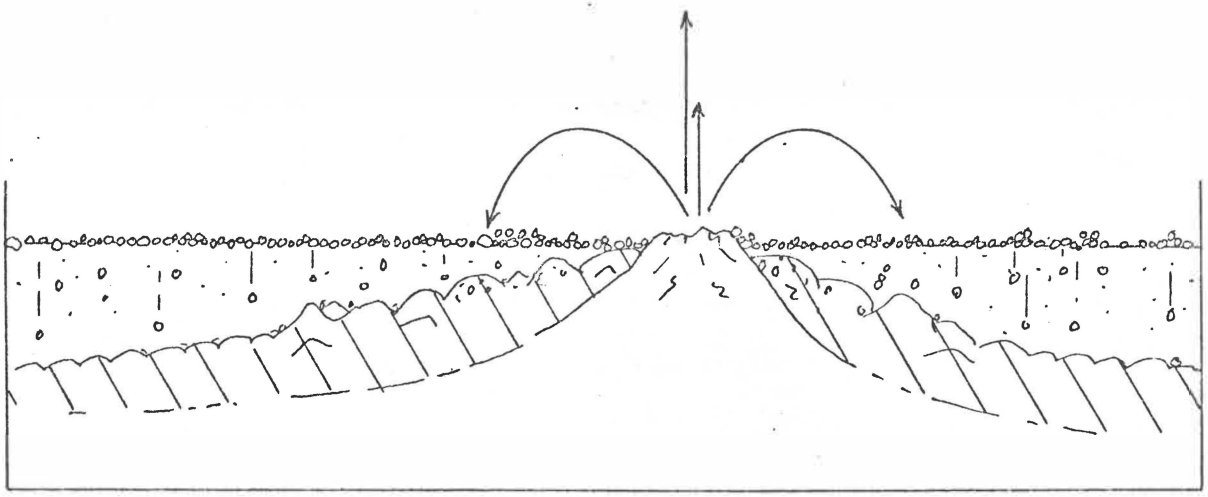
Lake Taupo has been affected in the past by catastrophic volcanic events, the last being the Taupo Pumice eruptions of about 131 A.D. During and soon after these eruptions a thick bed of pumice was deposited on the bottom of Lake Taupo. Since then the

catchment has restabilised and sedimentation in deep-water regions of the lake has diminished to a background fallout of predominantly mud-sized material from suspension. The bulk of the sediments forming shelves along the eastern side of the lake were deposited at the same time as the basinal pumice bed some 1800 years ago. These sediments were probably reworked during the 34 m fall in lake level to produce the present shelf morphology. Some shelf modifications, and growth of the Tongariro delta have occurred in the last 1800 years, particularly during flood events.

The topography of the 1800 year old pumice surface becomes increasingly rugged towards central and central eastern regions of the lake, suggesting a source vent nearby. Eruptions from such a vent, and post-eruption events may have followed the sequence illustrated in Fig. 9.1.

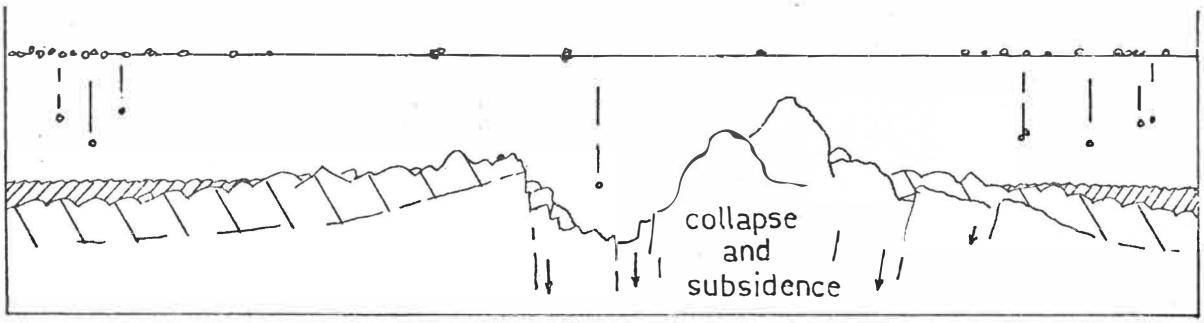
Sedimentation model

Sediment composition and texture, and sedimentation rates over the last 1800 years, indicate that the most important inputs of sediment have occurred at the southern end of Lake Taupo, particularly from the Tongariro River. This results from a number of interrelated catchment characteristics which reach their maximum values in the southern catchment (Fig. 9.2). These characteristics diminish in "intensity" towards the northern end of the catchment so that terrigenous sedimentation rates in central, northern and north-western regions of the lake are typically very low. However, in the northeastern region of the lake, relatively severe erosion of coastal cliffs of pumice breccia by wave-undercutting and slip has enhanced the terrigenous component in offshore deep-water sediments in that area.



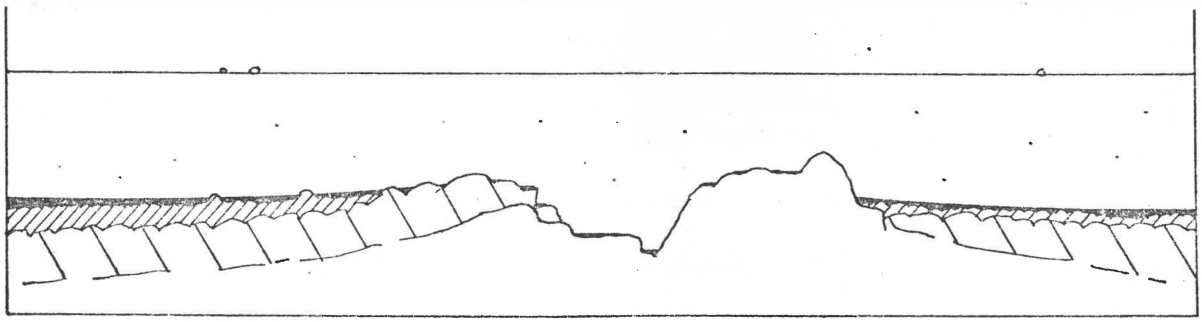
(a) ∿131 A.D. ?A Taupo Pumice vent in Lake Taupo

Taupo Pumice tephra deposited directly on to the lake



(b) ∿1800 yrs.B.P. Basal pumice surface formation complete

Pumice eroded from the catchment

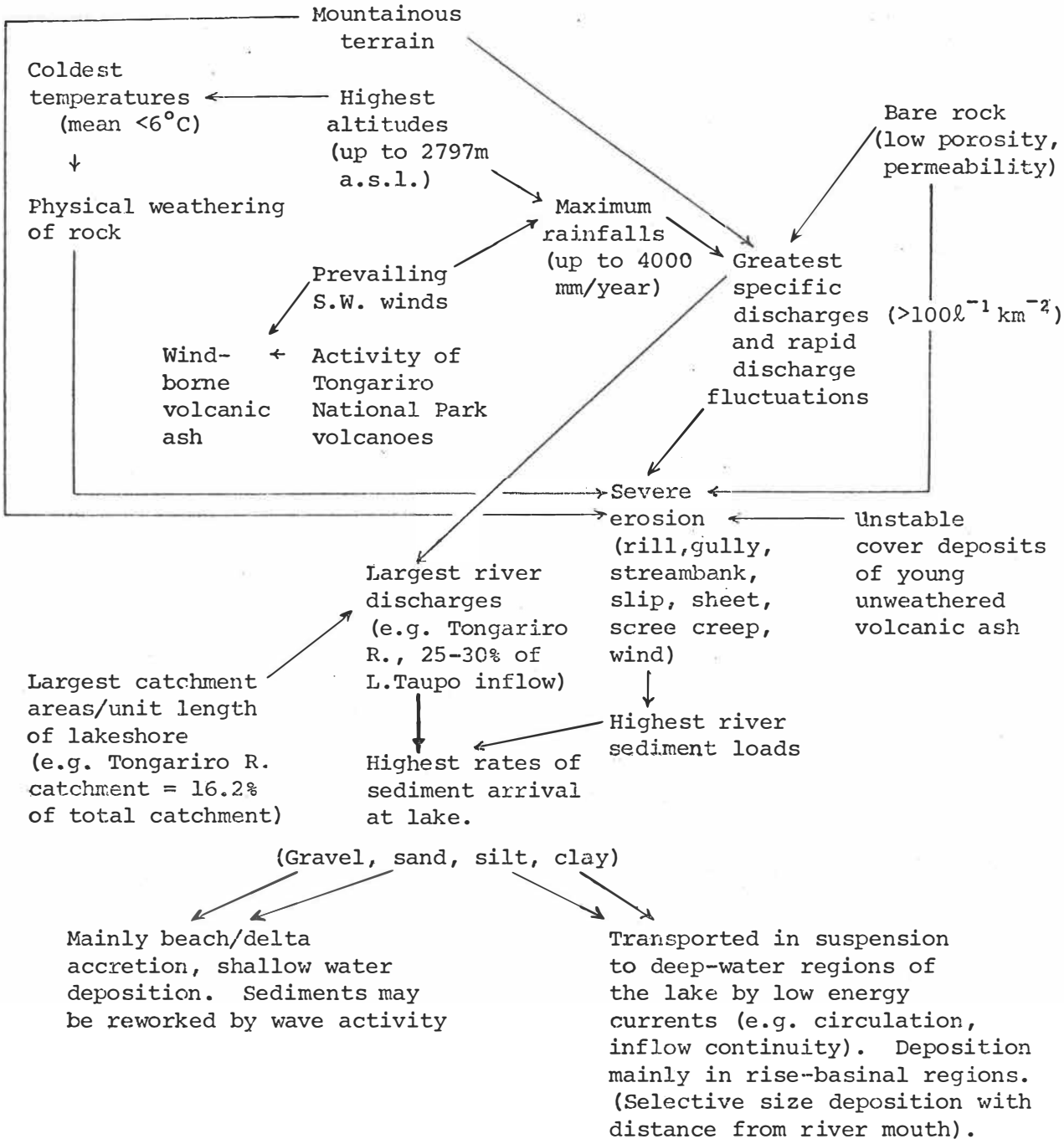


(c) Today: ∿ Stable catchment conditions

Mud accumulated in the last ∿1800 years

Fig. 9.1. Idealised cross-section of central and basinal regions of Lake Taupo showing a possible sequence of events since ∿130 A.D.

Fig. 9.2. Interrelated catchment characteristics which reach their maximum values to the south of Lake Taupo and are thus responsible for the major sediment influxes into the southern end of Lake Taupo.



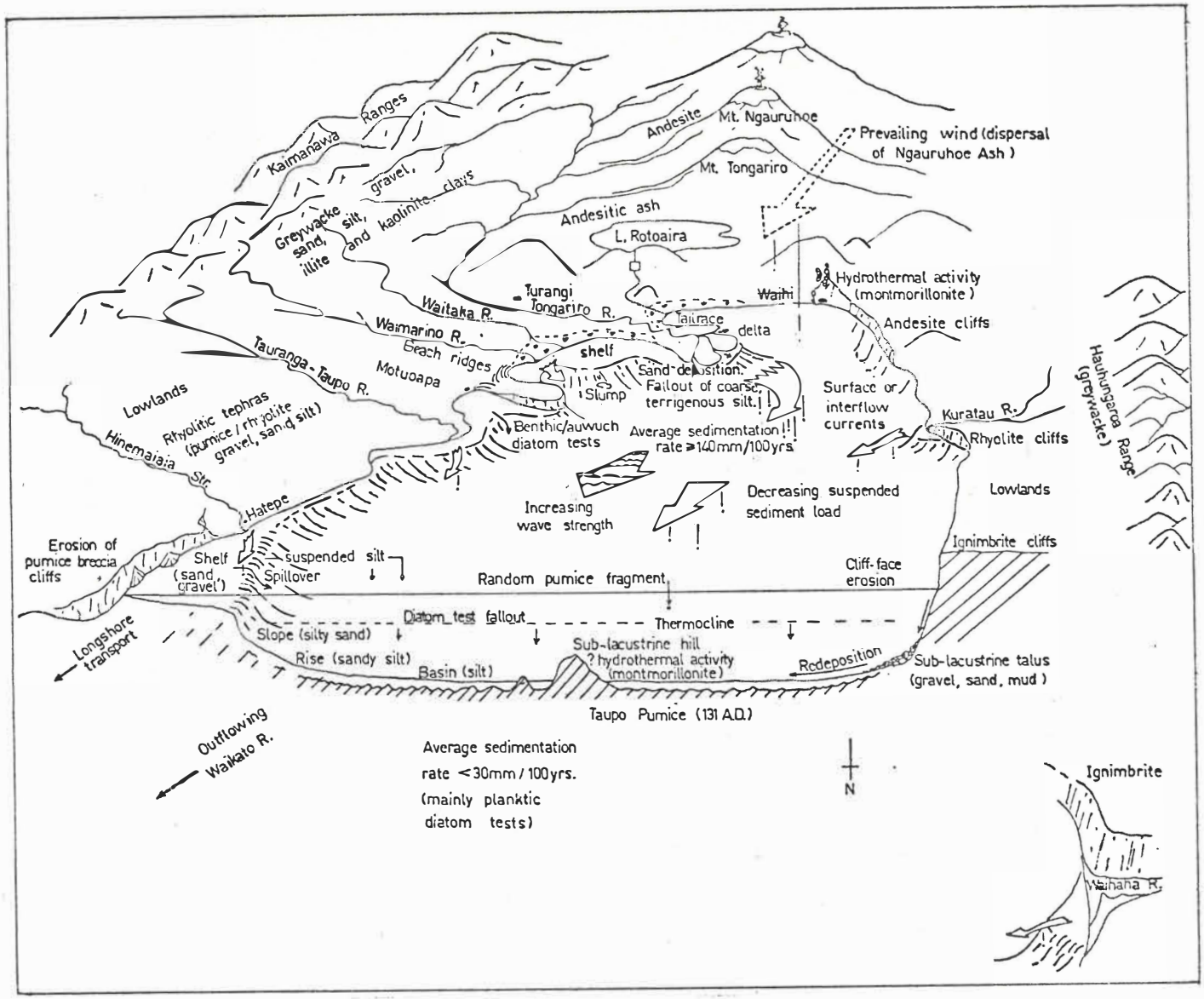


Fig. 9.3. Sedimentation model for Lake Taupo over the last 1800 years, showing main sediment provenances, transport mechanisms, depositional environments, and sediment texture and composition.

On the basis of the above conclusions, a sedimentation model may be proposed for Lake Taupo, and is diagrammatically summarised in Fig. 9.3.

Several sediment-related factors have contributed to the water clarity and oligotrophic status of Lake Taupo:

(a) Taupo catchment soils are young, poorly developed and lack a substantial clay content. Thus most of the sediment entering Lake Taupo is primary rock and mineral material, which is largely inert with respect to chemical exchange processes in an aquatic environment.

(b) Terrigenous sediment particles are mostly of a medium silt size or larger, and so are deposited relatively rapidly from the water column and do not reach all parts of the lake.

(c) Most of the lake is deep, so sediments are effectively removed from the photic zone where they could be utilised as a biological nutrient source. The depth also prevents resuspension of sediments by current action.

(d) Diatoms, which dominate the plankton in Lake Taupo, effectively remove dissolved nutrients from the photic zone waters to the sediments.

(e) Permanently oxygenated bottom waters and the oxidised microzone at the sediment/water interface help prevent the migration of dissolved species back into the water column.

Thus Lake Taupo acts as an effective sink for sediments and nutrients fed from the catchment into the lake.

APPENDIX 1. SUB-CATCHMENT AREAS

	1. Major Catchments	Hectares	% of total catchment
12	Tongariro River	58,000	16.2
9	Tauranga-Taupo River	22,910	6.4
19	Kuratau River	20,220	5.7
5	Waitahanui River	20,125	5.6
7	Hinemaiaia Stream	16,725	4.7
25	Waihaha River	15,655	4.4
13	Waipakihi River	11,715	3.3
17	Lake Rotoaira	11,370	3.2
2	Waioratene Stream	10,650	3.0
10	Waimarino River	8,275	2.3
11	Waiotaka River	7,425	2.1
27	Waihora River	6,570	1.8
23	Whanganui/Waitakahi/Mangakaruru Streams	6,330	1.8
21	Whareroa Stream	5,940	1.7
	Subtotal	221,910 ha.	63.0%
	2. Smaller Combined Catchments		
18	Omori/Pukawa/Waihi/Tokaanu area	10,340	2.9
29	Whangamata Bay	9,475	2.7
6	Motutere and Mission/Halletts Bays	7,920	2.2
1	Tapuaeharuru Bay	7,245	2.0
28	Kawakawa Bay	5,725	1.6
24	Otaunga/Oruapuraho/Waikino Streams	5,200	1.5
22	Te Hapua Plains/Karangahape	4,800	1.4
26	Te Awaroa/Otupotu/Tutaewaeroa/ Kotukutuku Streams	4,215	1.2
30	Whakaipo Bay	3,970	0.9
4	Ouaha/White Cliffs/Lake Rotongaio	2,235	0.6
2	Five Mile Beach	1,465	0.4
8	Motuoapa/Motuoapa Bay/Maraetai Bay	944	0.3
31	Waikarikari Point to Rangitira Point	893	0.3
20	Rangitukua/Te Hape Bay	183	0.1
	Subtotal	64,605 ha.	18.2%

3.	Artificially Diverted Catchments		
16	Western Catchments (incl. Whakapapaiti/ Mangatepopo Streams and Wanganui River)	31,725	8.9
14	Moawhango River	28,265	7.9
15	Southern Ruapehu Catchments (incl. Waihianoa/ Makahikatoa Streams)	7,120	2.0
	Subtotal	67,110 ha.	18.8%
4.	Natural Lake Catchment Area (totals 1 and 2)	286,515	81.2
5.	Total Catchment Area (totals 1, 2 and 3)	349,425	100
6.	Lake Areas		
	Lake Taupo	62,500	
	Lake Rotoaira	1,560	

APPENDIX 2

pH, Eh (mV) measurements and water depth (m) for Lake Taupo sediments

No.	pH	Eh	Depth (m)	No.	pH	Eh (mV)	Depth (m)	No.	pH	Eh (mV)	Depth (m)
1	6.8	80	9	44	6.3	120	77	87	-	-	132
2	6.5	120	20	45	6.3	120	97	88	-	-	3
3	6.6	130	20	46	4.5	110	110	89	6.4	240	35
4	4.0	100	57	47	5.4	195	100	90	4.8	150	44
5	7.0	310	29	48	5.2	310	100	91	-	-	4
6	6.4	90	42	49	-	-	2	92	5.4	210	78
7	7.0	430	12	50	-	-	2	93	4.8	130	70
8	6.6	390	29	51	-	-	.3	94	-	-	4
9	5.0	170	84	52	5.0	150	86	95	-	-	4
10	6.9	70	68	53	5.2	140	102	96	5.0	190	133
11	6.5	100	13	54	5.5	170	111	97	5.1	165	124
12	6.8	90	26	55	5.4	230	100	98	5.0	140	72
13	6.4	290	1	56	6.0	240	42	99	-	-	43
14	-	-	1	57	5.8	110	87	100	5.2	190	42
15	-	-	1	58	-	-	4	101	5.5	120	148
16	-	-	2	59	-	-	4	102	5.3	150	118
17	6.7	120	16	60	5.4	140	47	103	5.2	170	111
18	6.7	170	22	61	5.5	120	72	104	5.2	135	117
19	6.6	270	47	62	5.7	120	94	105	-	-	92
20	-	-	4	63	5.5	120	16	106	-	-	112
21	-	-	3	64	-	-	2	107	5.2	160	106
22	6.5	70	15	65	-	-	94	108	5.7	120	118
23	6.7	180	47	66	5.7	120	95	109	5.4	120	100
24	7.0	140	76	67	5.7	130	92	110	-	-	71
25	4.8	140	89	68	5.7	100	100	111	-	-	39
26	5.0	170	59	69	5.8	130	70	112	-	-	3
27	6.8	70	82	70	5.9	120	50	113	5.3	210	115
28	6.5	340	82	71	-	-	4	114	6.0	190	100
29	6.7	140	30	72	5.3	70	14	115	5.3	145	107
30	-	-	2	73	-	-	2	116	6.0	190	100
31	7.0	40	23	74	3.5	150	121	117	5.8	100	99
32	6.5	300	3	75	5.7	160	105	118	5.2	160	129
33	6.6	110	43	76	-	-	60	119	-	-	96
34	6.8	40	95	77	-	-	60	120	5.9	160	116
35	7.1	70	102	78	5.2	135	104	121	6.0	200	102
36	7.1	100	101	79	5.2	140	86				
37	5.9	110	14	80	5.5	160	26				
38	6.1	150	6	81	5.6	180	30				
39	-	-	3	82	-	-	59				
40	5.8	110	4	83	5.2	140	96				
41	5.4	90	30	84	5.2	190	140				
42	5.8	130	50	85	5.2	160	15				
43	5.3	100	67	86	7.0	340	132				

APPENDIX 3

TEXTURAL CHARACTER OF LAKE TAUPO SEDIMENTS (see end of Appendix 1 for expansion of abbreviations)

Sample number	Water depth (m)	wt.% gravel	wt.% sand	wt.% silt	wt.% clay	Sand/mud	Clay/silt	Mean grain (ϕ)	Median grain (ϕ)	C Statistic (ϕ)	Phi (ϕ) values of modes present	Sorting	Skewness	Kurtosis	Textural Term	Position on lake bed
1	9	7.5	30.4	38.9	23.2	0.49	0.60	4.5	5.1	-2.8	7.5,6.0,4.0,3.0,2.0,-0.5,-2.5	vps	scs	pk	gM	Sl
2	20	-	27.5	49.8	22.7	0.38	0.46	5.7	6.1	3.5	7.0,4.0	ps	cs	vpk	sZ	Sl
3	20	-	64.3	33.0	2.7	1.60	0.08	4.0	3.7	1.9	7.5,5.0,4.0	ps	sfs	lk	zS	Sl
4	57	-	3.7	81.3	15.0	0.04	0.18	6.1	6.0	3.3	7.0,5.5,4.0	ms	ns	pk	Z	Ri
5	29	66.6	28.5	3.7	1.2	5.79	0.32	-1.7	-2.2	-4.5	7.5,5.5,3.0,2.0,-1.0,-2.0,-3.5	vps	sfs	mk	msG	Ta
6	42	-	48.2	46.9	4.9	0.93	0.10	4.4	4.0	2.5	7.0,5.0,4.0	ps	sfs	mk	sZ	Sl
7	12	71.4	23.5	3.9	1.2	4.55	0.32	-1.9	-3.0	-4.5	7.5,5.5,4.5,3.0,2.0,-1.5,-3.0,-4.0	vps	sfs	mk	msG	Ta
8	29	40.8	57.6	1.3	0.3	35.44	0.25	-0.6	0.6	-5.0	3.0,2.0,0.0,-3.5	vps	scs	vpk	sG	Ta
9	84	-	11.9	76.4	11.8	0.13	0.15	5.7	5.7	2.0	7.0,6.0,3.5,2.0	ps	cs	mk	sZ	Ri
10	68	-	5.3	78.5	16.2	0.06	0.21	6.2	6.2	3.2	7.5,6.0,5.0,4.0	ps	cs	mk	Z	Ri
11	13	10.8	87.2	1.9	0.1	43.24	0.07	1.0	0.8	-2.7	4.0,3.0,1.0,-0.5,-2.5	ps	ns	mk	gS	Sl
12	26	-	61.6	29.6	8.7	1.61	0.29	4.7	3.9	3.5	7.0,6.0,4.0	ps	sfs	vpk	zS	Sl
13	1	16.5	83.2	0.3	0.1	240.37	0.17	-0.1	-0.2	-2.0	3.0,0.0	ps	ns	lk	gS	Sh
14	1	38.6	60.4	1.0	0.1	55.98	0.13	-0.6	-0.7	-2.9	4.0,-0.5	ps	ns	lk	sG	Sh
15	1	16.6	83.3	0.1	-	744.22	-	0.6	1.2	-3.0	1.5,-2.5	ps	scs	vlk	gS	Sh
16	2	-	100.0	-	-	-	-	1.8	1.8	0.5	2.0	mws	ns	lk	S	Sh
17	16	-	9.8	80.0	10.2	0.11	0.13	5.5	5.4	2.7	7.0,5.5,4.0,3.0	ps	ns	mk	Z	Sl
18	22	28.5	47.4	19.9	4.1	1.97	0.21	1.2	0.6	-3.7	7.5,6.5,4.0,3.0,2.0,-0.5,-1.5,-3.0	vps	ns	pk	gmS	Sl
19	47	-	6.1	81.1	12.8	0.07	0.16	6.0	6.1	2.9	7.0,6.0,4.0,3.0	ps	cs	mk	Z	Sl
20	4	0.5	99.5	-	-	-	-	2.8	2.9	0.0	3.0	ms	cs	lk	(g)S	Sh
21	3	95.8	4.2	-	-	-	-	-2.7	-2.8	-4.4	-2.5	ms	ns	mk	G	Ta
22	15	0.6	63.5	30.7	5.2	1.77	0.17	4.2	3.8	2.1	7.5,6.0,5.0,4.0,-3.5	ps	sfs	lk	(g)mS	Sl
23	47	1.0	34.1	54.1	10.8	0.53	0.20	5.2	5.2	-2.2	7.5,5.5,4.0	ps	ns	vpk	(g)M	Sl
24	76	-	13.9	68.2	17.9	0.16	0.26	6.0	6.7	2.6	7.5,6.0,4.0	ps	scs	lk	sZ	Ri
25	89	-	4.7	75.3	20.0	0.05	0.27	6.5	6.7	2.6	7.0,6.0,4.0	ps	scs	lk	Z	Ri
26	59	-	3.0	77.2	19,8	0.03	0.26	6.6	6.6	2.8	7.0,6.0,4.0,3.0	ms	cs	mk	Z	Ri
27	82	-	4.0	75.9	20.1	0.04	0.26	6.6	6.7	3.6	7.5,6.0,4.0	ps	cs	lk	Z	Ri
28	82	-	3.4	83.2	13.5	0.03	0.16	6.5	6.7	3.6	7.5,6.0,4.5	ps	scs	mk	Z	Ri
29	30	84.5	6.2	8.1	1.2	0.68	0.14	-2.6	-2.7	-4.9	5.0,3.5,0.5,-2.5	vps	sfs	vlk	G	Sl
30	2	5.1	94.9	-	-	-	-	0.5	0.4	-3.2	3.0,0.5,-3.0	mws	n.s.	lk	gS	Sh
31	23	-	14.1	58.8	27.2	0.16	0.46	5.9	6.6	1.6	7.5,4.0,2.0,1.5	ps	scs	lk	sZ	Sl
32	2	0.9	99.1	-	-	-	-	1.5	1.6	-1.0	2.0,-1.0	ms	cs	mk	(g)S	Sh
33	43	-	63.4	32.1	4.4	1.73	0.14	4.1	3.7	1.8	7.5,5.5,4.0	ps	sfs	lk	zS	Sl
34	95	-	8.5	74.1	17.3	0.09	0.23	6.4	6.6	2.5	7.0,6.0,4.0	ps	scs	vlk	Z	Ri
35	102	-	2.3	74.6	23.1	0.02	0.31	6.9	6.9	3.7	7.0,6.0,4.0	mws	cs	lk	Z	Ba
36	101	-	4.7	69.9	25.4	0.05	0.36	6.9	7.0	3.6	7.0,4.0	ms	scs	vlk	Z	Ba
37	14	-	36.9	47.7	15.4	0.58	0.32	4.8	4.3	2.1	7.0,4.5,3.5	ps	sfs	vpk	sZ	Sl
38	6	93.5	6.2	0.3	0.1	16.83	0.31	-2.7	-2.7	-4.4	3.5,-2.5	ms	ns	lk	G	Ta
39	3	0.8	99.2	-	-	-	-	1.8	1.9	-0.9	2.0,-0.5	ms	cs	lk	(g)S	Sh
40	4	-	96.3	3.0	0.7	26.13	0.22	3.4	3.5	1.6	4.0	vws	cs	mk	S	Sh
41	30	-	7.9	69.2	23.0	0.09	0.33	6.4	6.8	3.6	7.5,6.0,5.0,4.0	ps	scs	lk	Z	Sl
42	50	-	7.0	79.5	13.5	0.08	0.17	6.3	6.5	2.8	7.5,6.0,4.0	ps	scs	mk	Z	Sl
43	67	-	9.4	73.5	17.0	0.10	0.23	6.5	6.7	2.8	7.5,6.0,4.0	ps	scs	lk	Z	Ri
44	77	-	4.8	77.8	17.4	0.05	0.22	6.6	6.8	3.6	7.0,5.5,4.0	ps	scs	lk	Z	Ri
45	97	-	6.0	79.9	14.1	0.06	0.18	6.6	6.8	3.6	7.0,6.0,5.0,4.0	ms	scs	vlk	Z	Ba

46	110	-	7.6	73.2	19.3	0.08	0.26	6.6	6.7	2.3	7.0,6.0,4.0,3.0	ps	scs	vlk	Z	Ba
47	100	-	1.1	74.9	24.0	0.01	0.32	6.7	6.8	3.8	7.0,6.0,4.0	ms	cs	mk	Z	Ba
48	100	-	2.3	73.9	23.8	0.02	0.32	6.7	6.8	1.7	7.5,6.0,4.0,2.0	ms	scs	pk	Z	Ba
49	2	-	100	-	-	-	-	1.7	1.7	0.1	3.0,2.0	ms	ns	mk	S	Sh
50	2	23.4	76.6	-	-	-	-	-0.4	-0.2	-3.8	0.5,-2.0,-3.5	ms	scs	mk	gS	Sh
51	3	12.7	87.3	-	-	-	-	1.1	1.6	-2.6	2.0,-1.5	ps	scs	mk	gS	Sh
52	86	-	11.2	68.4	20.5	0.13	0.30	6.2	6.5	1.8	7.0,5.5,4.0,2.0	ps	scs	mk	sZ	Ri
53	102	-	2.3	75.7	22.1	0.02	0.29	6.9	6.9	3.7	7.0,6.0,4.0	mws	cs	lk	Z	Ba
54	111	-	2.4	79.3	18.3	0.02	0.23	6.8	6.9	3.7	7.0,6.0,4.0	mws	cs	vlk	Z	Ba
55	100	-	3.8	78.4	17.8	0.04	0.23	6.8	7.0	3.6	7.5,5.5,4.0	ms	scs	lk	Z	Ba
56	42	0.1	76.5	21.7	1.8	3.26	0.08	3.7	3.5	1.9	7.5,5.0,3.5	ps	sfs	vlk	(g)mS	Hi
57	87	-	6.2	80.9	12.9	0.07	0.15	6.4	6.6	2.8	7.5,5.5,4.0	ps	scs	mk	Z	Hi
58	4	-	100	-	-	-	-	1.9	1.9	0.6	2.0	mws	ns	mk	S	Sh
59	4	10.6	88.9	0.5	0.0	176.9	-	1.7	2.2	-3.3	3.0,2.0,0.5,-0.5,-1.5,-2.0	ps	scs	mk	gS	Sh
60	47	-	23.0	66.4	10.6	0.30	0.16	5.6	6.0	2.1	7.5,6.0,3.5	ps	scs	vpk	sZ	Sl
61	72	-	7.9	79.9	12.3	0.09	0.15	6.2	6.6	2.8	7.0,6.0,5.0,3.5	ps	scs	mk	Z	Ri
62	94	-	5.1	80.0	14.9	0.05	0.19	6.6	6.8	3.6	7.0,5.0,4.0	ms	scs	vlk	Z	Ba
63	16	33.2	34.6	27.1	5.1	1.08	0.19	1.5	2.9	-4.5	7.5,6.0,5.0,3.5,-1.5,-2.5,-4.0	eps	scs	vpk	msG	Sl
64	2	0.2	99.8	-	-	-	-	1.5	1.5	-0.4	2.0	mws	ns	mk	(g)S	Sh
65	94	-	6.7	78.4	14.9	0.07	0.19	6.7	6.8	3.6	7.5,4.0	ms	scs	vlk	Z	Ba
66	95	-	4.2	77.8	18.1	0.04	0.23	7.0	7.0	3.6	7.0,6.0,4.0	ms	cs	vlk	Z	Ba
67	92	0.3	54.2	37.4	8.0	1.19	0.21	3.9	3.2	-0.4	7.0,3.0,2.0,-0.5	vps	sfs	vpk	(g)mS	Re
68	100	-	5.1	80.9	14.0	0.05	0.17	6.8	6.8	3.6	7.0,5.5,4.0	ms	scs	vlk	Z	Ba
69	70	-	7.6	79.0	13.4	0.08	0.17	6.6	6.7	2.9	7.5,6.0,4.0	ps	scs	lk	Z	Ri
70	50	1.7	78.1	18.0	2.2	3.87	0.12	2.2	1.0	-1.4	7.5,5.5,1.0	vps	sfs	elk	(g)mS	Sl
71	4	23.6	76.4	-	-	-	-	-0.2	0.3	-3.2	1.0,-1.5,-2.5	ps	scs	mk	(g)S	Sh
72	14	-	31.2	61.8	7.1	0.45	0.11	5.1	5.3	2.4	7.0,5.5,4.5,3.5	ps	cs	vpk	sZ	Sl
73	2	28.5	71.5	-	-	-	-	-0.3	-0.2	-3.8	0.0,-2.5	ps	cs	mk	gS	Sh
74	121	-	7.4	73.3	19.3	0.08	0.26	6.6	6.8	1.5	7.0,5.5,4.0,3.0	ps	scs	vlk	Z	Ba
75	105	-	4.8	78.4	16.8	0.05	0.21	6.7	6.8	3.6	7.0,5.5,4.0	ms	scs	vlk	Z	Ba
76	60	7.5	24.8	26.3	41.4	0.37	1.57	3.6	3.1	-3.4	7.0,3.0,2.0,-1.5,-3.0	vps	ns	pk	gM	Hi
77	60	-	-	-	-	-	-	-	-	-	- - - - -	-	-	-	-	Hi
78	104	-	2.3	74.1	23.6	0.02	0.32	7.0	7.0	3.7	7.5,4.0	vws	ns	mk	Z	Ba
79	86	-	8.0	65.8	26.2	0.09	0.40	6.5	6.7	2.6	7.0,6.0,4.0,3.0	ps	scs	lk	Z	Ri
80	26	1.6	79.8	12.4	6.3	4.26	0.51	3.2	3.2	-1.7	7.5,5.5,3.5,2.0,1.0,-1.5	ps	ns	vlk	(g)mS	Ta
81	30	40.6	39.5	13.0	6.8	1.99	0.52	-0.2	-0.1	-4.5	7.5,6.0,4.0,3.0,2.0,0.5,-1.0, -2.0,-3.0,-4.0	vps	ns	pk	msG	Sl
82	59	80.4	19.6	-	-	-	-	-	-	-	2.0,0.5,-0.5,-2.5,-4.0	-	-	-	G	Ta
83	96	-	10.1	63.9	26.1	0.11	0.41	6.5	6.8	1.6	7.5,6.0,4.0,2.0	ps	scs	vlk	sZ	Re
84	140	-	6.9	76.6	16.5	0.07	0.22	6.8	6.9	2.6	7.5,6.0,4.0	ms	scs	vlk	Z	Ba
85	15	27.9	40.6	27.3	4.3	1.29	0.16	2.0	3.3	-3.9	6.0,5.0,4.0,1.5,-1.5,-2.5	vps	scs	vpk	gmS	Hi
86	132	1.5	62.4	18.6	17.5	1.73	0.94	3.6	2.5	-2.0	7.5,5.5,4.0,3.0,2.0	vps	sfs	lk	(g)mS	Re
87	132	19.6	28.7	31.2	20.5	0.55	0.66	2.5	2.2	-3.3	7.5,4.0,2.0,-1.5,-2.5	vps	ns	vpk	gM	Re
88	3	58.7	41.3	-	-	-	-	-1.6	-1.6	-4.4	-0.5,-1.5,-2.5,-3.5	ps	ns	pk	sG	Hi
89	35	-	44.9	45.4	9.6	0.82	0.21	4.9	5.0	1.5	7.0,6.0,3.5,2.0	ps	ns	vpk	sZ	Sl
90	44	-	13.8	74.0	12.2	0.16	0.17	6.1	6.2	2.7	7.0,6.0,4.0	ps	cs	mk	sZ	Sl
91	4	1.1	98.9	-	-	-	-	0.9	0.9	-1.2	1.0	vws	ns	mk	(g)S	Sh
92	78	3.1	46.7	41.2	9.0	0.93	0.22	3.7	2.9	-2.7	7.5,6.0,4.0,2.0,-0.5,-1.5,-2.5	vps	ns	vpk	(g)M	Ri
93	70	-	6.0	79.6	14.4	0.06	0.18	6.4	6.6	3.0	7.0,6.0,4.0	ps	scs	lk	Z	Ri
94	4	2.2	97.8	-	-	-	-	0.2	0.3	-1.4	0.5	mws	cs	lk	(g)S	Sh
95	4	0.1	99.9	-	-	-	-	2.4	2.4	0.5	3.0,-0.5	mws	ns	mk	(g)S	Sh
96	133	-	3.9	78.9	17.3	0.04	0.22	6.6	6.8	3.4	7.5,6.0,4.0	ms	cs	mk	Z	Ba
97	124	-	3.2	86.5	10.4	0.03	0.12	6.8	6.9	3.6	7.0,6.0,4.0	mws	cs	lk	Z	Ba
98	72	-	13.9	74.3	11.8	0.16	0.16	6.3	6.7	2.2	7.0,5.5,3.5	ps	scs	lk	sZ	Ri
99	43	78.7	20.6	0.5	0.2	29.27	0.49	-2.0	-3.1	-5.0	2.0,0.0,-2.5,-4.0	vps	sfs	lk	sG	Sl

100	142	-	1.8	80.8	17.4	0.02	0.22	7.0	7.0	3.7	7.5,6.5,5.0,4.0	mws	scs	vlk	Z	Ba
101	148	-	3.2	87.9	8.9	0.03	0.10	6.8	6.9	3.6	7.5,5.5,4.0	mws	scs	vlk	Z	Ba
102	118	-	1.7	83.9	14.4	0.02	0.17	7.0	6.9	3.8	7.0,6.0,4.0	vws	ns	mk	Z	Ba
103	111	-	1.4	83.7	14.9	0.01	0.18	7.0	6.9	3.8	7.0,4.0	vws	ns	mk	Z	Ba
104	117	-	1.7	82.6	15.7	0.02	0.19	6.9	6.9	3.8	7.0,5.5,4.0	mws	ns	lk	Z	Ba
105	92	46.6	40.8	8.7	3.9	3.23	0.45	-0.6	-0.5	-5.4	7.0,6.0,5.0,4.0,2.0,-0.5,-3.0	vps	ns	mk	msG	Ta
106	112	1.7	33.6	48.7	16.0	0.52	0.33	5.2	6.4	-3.8	7.0,6.0,4.0,2.0	vps	scs	vpk	(g)M	Re
107	106	-	2.1	84.2	13.7	0.02	0.16	6.9	6.9	3.7	7.0,6.0,4.0	vws	cs	lk	Z	Ba
108	118	-	1.5	84.1	14.4	0.02	0.17	7.0	6.9	3.8	7.0,6.0,4.0	vws	ns	lk	Z	Ba
109	100	-	15.1	74.6	10.3	0.18	0.14	6.0	6.6	2.7	7.0,6.0,5.0,4.0	ps	scs	mk	sZ	Ri
110	71	0.1	18.0	68.1	13.8	0.22	0.02	5.7	5.9	2.6	7.5,6.0,4.0,3.0	ps	cs	pk	(g)M	Ri
111	39	-	32.6	61.6	5.8	0.48	0.09	4.9	4.9	2.2	7.0,5.5,4.0	ps	ns	pk	sZ	Si
112	3	0.1	99.9	-	-	-	-	1.7	1.7	0.0	2.0,1.0	ms	cs	pk	(g)S	Sh
113	115	-	2.0	85.1	12.9	0.02	0.15	7.0	6.9	3.7	7.0,4.0	vws	ns	mk	Z	Ba
114	116	-	1.6	87.1	11.3	0.02	0.13	6.8	6.8	3.8	7.0,5.5,4.0	mws	cs	lk	Z	Ba
115	107	18.5	40.4	29.7	11.5	0.98	0.39	2.9	3.5	-3.3	7.5,6.0,3.5,2.0,-2.0	vps	cs	pk	gM	Re
116	100	-	9.4	78.0	12.6	0.10	0.16	6.7	6.8	2.9	7.0,5.5,4.0	ms	scs	vlk	Z	Fi
117	99	-	4.5	81.1	14.5	0.05	0.18	6.8	6.9	2.7	7.5,6.0,3.5	ms	scs	vlk	Z	Ri
118	129	-	0.6	89.4	10.0	0.01	0.11	6.9	6.9	5.1	7.0,5.5,4.0	vws	ns	mk	Z	Ba
119	96	-	4.7	83.1	12.3	0.05	0.15	6.1	6.6	3.1	7.5,6.0,4.5	ps	scs	pk	Z	Ri
120	116	-	15.5	69.0	15.5	0.18	0.22	5.9	6.8	1.3	7.0,4.0,2.0	ps	scs	vlk	sZ	Hi
121	102	0.1	24.0	58.5	17.4	0.32	0.30	5.4	6.9	1.2	7.0,5.5,4.0,2.0	vps	scs	pk	(g)M	Hi

ABBREVIATIONS

1. Textural terminology (Folk *et al.* 1970)

Gravel-bearing sediments		Gravel-free sediments	
G	gravel	S	sand
sG	sandy gravel	zS	silty sand
msG	muddy sandy gravel	mS	muddy sand
mG	muddy gravel	cS	clayey sand
gS	gravelly sand	sZ	sandy silt
gmS	gravelly muddy sand	sM	sandy mud
gM	gravelly mud	sC	sandy clay
(g)S	slightly gravelly sand	Z	silt
(g)mS	slightly gravelly muddy sand	M	mud
(g)M	slightly gravelly mud	C	clay
S	sand		
mS	muddy sand		
sM	sandy mud		
M	mud		

2. Verbal classification of inclusive graphic standard deviation

vws	very well sorted
ws	well sorted
mws	moderately well sorted
ms	moderately sorted
ps	poorly sorted
vps	very poorly sorted
eps	extremely poorly sorted

3. Verbal classification of inclusive graphic skewness

sfs	strongly fine-skewed
fs	fine-skewed
ns	near-symmetrical
cs	coarse-skewed
scs	strongly coarse-skewed

4. Verbal classification of graphic kurtosis

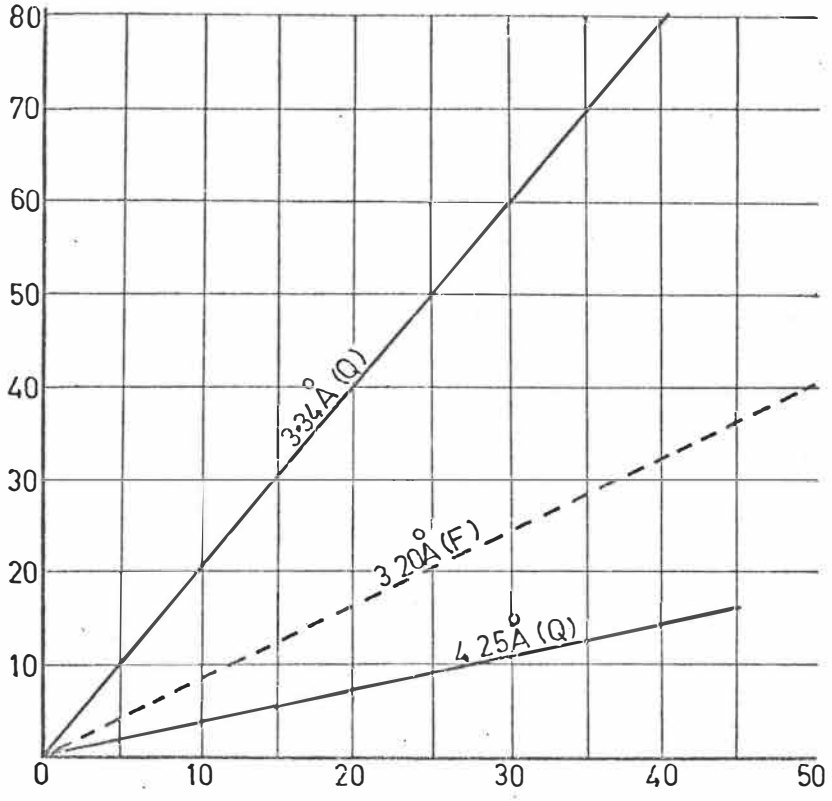
vpk	very platykurtic
pk	platykurtic
mk	mesokurtic
lk	leptokurtic
vlk	very leptokurtic
elk	extremely leptokurtic

5. Position on lake bed

Sh	Shelf
Sl	Slope
Ri	Rise
Ba	Basin
Ta	Sub-lacustrine talus slope at foot of cliffed shoreline
Hi	Top of sub-lacustrine topographic high
Re	Sediment contains redeposited material

Appendix 4

Quartz (Q) and plagioclase feldspar (F) X.R.D. intensity-concentration curves.



The quartz curve was produced using a series of quartz (<30 μm) and pumice (<30 μm) standards with the components mixed in weight percent ratios from 0.45% quartz at approximately 5% intervals. The plagioclase feldspar curve was modified from that given by Nelson and Cochrane (1970, p.158).

APPENDIX 5

BULK SAMPLE X-RAY DIFFRACTION ANALYSIS

Weight percentages of plagioclase feldspar and quartz (to nearest 1%) and plagioclase:quartz ratios in Lake Taupo sediments

(N.B. "0" = <0.5 wt.%, "-" = undetected).

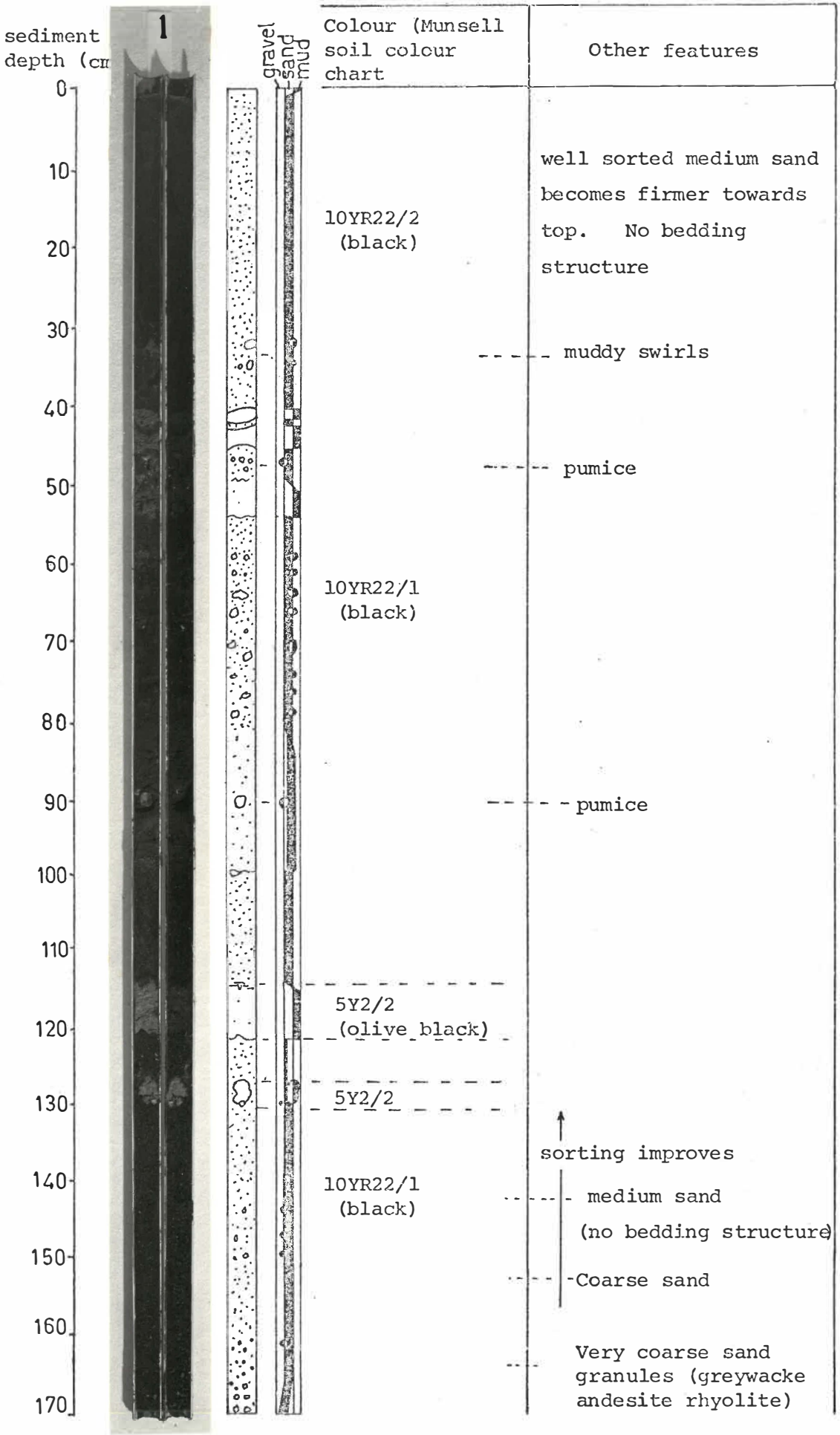
Sample number	Depth (m)	wt.% plagioclase	wt.% quartz	Plagioclase quartz	Sample Number	Depth (m)	wt.% plagioclase	wt.% quartz	Plagioclase quartz
1	9	8	3	3	39	3	36	15	2
2	20	8	2	4	40	4	18	8	2
3	20	21	3	7	41	30	6	3	2
4	57	17	5	3	42	50	4	4	1
5	29	35	0	-	43	67	3	4	1
6	42	20	4	5	44	77	6	4	2
7	12	7	3	2	45	97	1	2	1
8	29	31	1	31	46	110	7	3	2
9	84	14	5	3	47	100	7	5	1
10	68	17	5	3	48	100	7	5	2
11	13	28	4	7	49	2	56	11	5
12	26	14	4	4	50	2	35	21	2
13	1	6	2	3	51	3	24	9	3
14	1	8	2	4	52	86	10	6	2
15	1	25	15	2	53	102	6	2	2
16	2	25	16	2	54	111	4	2	2
17	16	11	9	1	55	100	4	2	2
18	22	4	1	4	56	42	17	9	2
19	47	7	5	1	57	87	3	3	1
20	4	13	4	3	58	4	45	11	4
21	3	31	0	-	59	4	25	7	4
22	15	25	10	3	60	47	4	4	1
23	47	7	5	1	61	72	6	2	3
24	76	7	4	2	62	94	1	2	1
25	89	3	4	1	63	16	13	2	7
26	59	10	5	2	64	2	31	8	4
27	82	22	5	4	65	94	3	1	3
28	82	8	4	2	66	95	1	2	1
29	30	32	2	16	67	92	13	2	7
30	2	45	14	3	68	100	1	1	1
31	23	-	-	-	69	70	1	1	1
32	2	56	17	3	70	50	6	1	6
33	43	67	6	11	71	4	35	7	5
34	95	10	4	3	72	14	4	1	4
35	102	8	3	3	73	2	38	6	7
36	101	8	4	2	74	121	3	1	3
37	14	4	2	2	75	105	3	1	3
38	6	11	2	6	76	60	-	-	-
77	60	28	0	-	100	142	1	1	1
78	104	4	2	2	101	148	0	0	-
79	86	7	3	2	102	118	1	1	1
80	26	21	2	11	103	111	1	1	1
81	30	11	1	11	104	117	3	2	2
82	59	-	-	-	105	92	-	-	-
83	96	8	3	3	106	112	14	1	14
84	140	4	1	4	107	106	1	1	1
85	15	22	0	-	108	118	3	1	3
86	132	11	0	-	109	100	4	2	2
87	132	28	0	-	110	71	6	2	3
88	3	13	1	13	111	39	7	3	2
89	35	14	1	14	112	3	35	6	7
90	44	1	0	-	113	115	4	1	4
91	4	56	11	5	114	116	0	1	-
92	78	20	3	7	115	107	6	1	6
93	70	3	1	3	116	100	1	1	1
94	4	31	9	3	117	99	1	1	1
95	4	28	3	9	118	129	1	1	1
96	133	1	1	1	119	96	1	1	1
97	124	0	0	-	120	116	6	1	6
98	72	1	1	1	121	102	1	1	1
99	43	3	0	-					

APPENDIX 6

X-RAY DIFFRACTION OF CRYSTALLINE CLAY MINERALS IN LAKE TAUPO SEDIMENTS. RELATIVE DIAGNOSTIC PEAK HEIGHTS.

Sample number	Illite (10Å)	Kaolinite (7Å)	Montmorillonite (15Å)	Sample number	Illite (10Å)	Kaolinite (7Å)	Montmorillonite (15Å)
1	12	11	17	62	8	4	3
2	7	8	13	63	2	2	2
3	9	4	2	64	sand		
4	19	9	4	65	5	2	3
5	13	8	5	66	4	1	1
6	10	5	4	67	8	5	0
7	3	2	1	68	7	2	1
8	12	9	8	69	5	3	0
9	15	7	6	70	6	3	2
10	11	3	2	71	sand		
11	6	5	3	72	3	2	2
12	8	5	0	73	sand		
13	5	5	0	74	6	7	3
14	0	0	1	75	6	5	2
15	4	3	1	76	4	1	5
16	sand			77	6	1	6
17	19	13	7	78	8	7	4
18	9	5	3	79	8	5	4
19	10	7	1	80	9	4	2
20	sand			81	4	2	2
21	sand			82	-	-	-
22	7	5	3	83	8	6	4
23	12	8	4	84	2	3	0
24	10	5	2	85	1	0	0
25	18	8	4	86	7	3	5
26	14	9	5	87	5	1	7
27	9	5	3	88	sand		
28	7	5	1	89	7	7	3
29	6	5	1	90	7	5	3
30	sand			91	sand		
31	7	4	3	92	-	-	-
32	sand			93	8	5	2
33	7	5	3	94	sand		
34	12	4	0	95	sand		
35	8	6	2	96	5	3	0
36	9	4	2	97	1	0	1
37	5	4	2	98	0	0	0
38	4	1	3	99	0	0	7
39	sand			100	7	5	4
40	sand			101	3	1	0
41	9	5	3	102	6	2	2
42	7	6	2	103	6	3	3
43	8	3	2	104	12	4	1
44	9	6	1	105	6	3	1
45	0	0	0	106	10	5	3
46	9	6	3	107	6	5	2
47	10	8	3	108	6	5	3
48	13	7	2	109	6	2	0
49	sand			110	9	4	2
50	sand			111	5	3	3
51	sand			112	sand		
52	14	8	5	113	5	4	2
53	13	4	1	114	5	4	0
54	10	9	2	115	7	3	0
55	3	0	0	116	2	3	0
56	5	3	0	117	4	3	3
57	9	3	1	118	4	3	1
58	sand			119	2	2	3
59	1	0	1	120	6	6	4
60	5	4	1	121	8	4	3
61	6	4	3				

APPENDIX 7



Core 1 from 13 m depth on the southern side of the Tongariro delta (Map 3 in map pocket). Sand containing mud clasts layers.

APPENDIX 8 Lake Taupo sediment sample Grid References (cf. map 3) and samples/subsamples stored at the University of Waikato

Sample number	Sample site grid reference	University of Waikato ref.number	Sample number	Sample site grid reference	University of Waikato ref.number
1	2330 0600	13101	62	4073 1386	13162
2	2350 0605	13102	63	4355 1365	13163
3	2543 0673	13103	64	4470 1436	13164
4	2412 0690	13104	65	4218 1550	13165
5	2416 0782	13105	66	4200 1680	13166
6	2562 0718	13106	67	4202 1782	13167
7	2435 0960	13107	68	4496 1728	13168
8	2442 0947	13108	69	4584 1610	13169
9	2505 0880	13109	70	4656 1662	13170
10	2656 0790	13110	71	4724 1490	13171
11	2676 0700	13111	72	4700 1512	13172
12	2770 0646	13112	73	4813 1867	13173
13	2871 0590	13113	74	4415 2029	13174
14	2871 0590	13114	75	4346 1941	13175
15	2958 0580	13115	76	3963 2000	13176
16	3025 0582	13116	77	3963 2000	13177
17	3115 0647	13117	78	3478 2000	13178
18	3276 0725	13118	79	2900 1865	13179
19	3243 0760	13119	80	2948 1984	13180
20	3350 0838	13120	81	2960 2188	13181
21	3342 0870	13121	82	3124 2290	13182
22	3345 0912	13122	83	3135 2281	13183
23	3349 0952	13123	84	4406 2310	13184
24	3262 0970	13124	85	4490 2195	13185
25	3180 0850	13125	86	4567 2139	13186
26	2862 0877	13126	87	4567 2139	13187
27	2815 0938	13127	88	4720 2260	13188
28	2815 0938	13128	89	4862 2078	13189
29	2460 1010	13129	90	5027 2230	13190
30	2437 1017	13130	91	5117 2261	13191

31	2522 1135	13131	92	4995 2305	13192
32	2510 1180	13132	93	5080 2416	13193
33	2600 1225	13133	94	5200 2390	13194
34	2700 1190	13134	95	5234 2364	13195
35	2875 1048	13135	96	4684 2443	13196
36	3072 0990	13136	97	4995 2870	13197
37	3408 0970	13137	98	5187 3280	13198
38	3420 0960	13138	99	5300 3500	13199
39	3670 1073	13139	100	4580 2945	13200
40	3600 0916	13140	101	4008 2842	13201
41	3548 0986	13141	102	3757 2780	13202
42	3474 1076	13142	103	3445 2662	13203
43	3458 1121	13143	104	3084 2567	13204
44	3461 1170	13144	105	2800 2747	13205
45	3468 1297	13145	106	2842 2765	13206
46	3042 1200	13146	107	2395 2684	13207
47	2853 1240	13147	108	2724 3071	13208
48	2853 1240	13148	109	2485 3250	13209
49	2608 1312	13149	110	2458 3270	13210
50	2640 1600	13150	111	2424 3290	13211
51	2703 1680	13151	112	2382 3328	13212
52	2776 1608	13152	113	3142 3317	13213
53	3028 1641	13153	114	2856 3640	13214
54	3273 1456	13154	115	3293 3724	13215
55	3707 1608	13155	116	3280 3962	13216
56	3780 1190	13156	117	4853 4007	13217
57	3930 1308	13157	118	3562 3350	13218
58	3920 1104	13158	119	4274 3665	13219
59	4200 1180	13159	120	4190 3370	13220
60	4124 1182	13160	121	4418 3269	13221
61	4100 1270	13161			

BIBLIOGRAPHY

Allen, J.R.L. 1970: "Physical Processes of Sedimentation". Allen and Unwin, London. 248p.

Anonymous 1975: Proposals for a standard of diatom terminology and diagnoses. Pp. 323-354 *in* R. Simonsen (ed.) *Proceedings of 3rd Symposium on Recent and Fossil Diatoms.*

Arrhenius, G. 1965: Sedimentary records of long period phenomena. Pp. 155-174 *in* P.M. Harley (ed.) "Advances in Earth Sciences". MIT Press.

Bates, C.C. 1953: Rational theory of delta formation. *Bull. Am. Ass. Petrol. Geol.* 37, 2119-62.

Bates, C.C.; Freeman, J.C. 1953: Interrelations between jet behaviour and hydraulic processes observed at deltaic river mouths and tidal inlets. *Proc. 3rd Conf. Coastal Eng. Berkely, Calif. Council on Wave Research.*

Baumgart, I.L. 1954: Some ash showers of central North Island, New Zealand. *Jl. Sci. Tech. 35*, 456-467.

Baumgart, I.L.; Healy, J. 1956: Recent volcanicity at Taupo, New Zealand. *Proceedings 8th Pacific Science Congress 2*, 113-125.

Bennett, J.R. 1974: On the dynamics of wind driven lake currents. *Jl. Phys. Oceanogr.* 4, 400-414.

Berner, R.A. 1971: "Principles of chemical sedimentology". McGraw-Hill, New York, 240p.

Beutelspacher, H.; Van der Marel, H.W. 1968: "Atlas of electron microscopy of clay minerals". Elsevier, Amsterdam.

Blakemore, L.C.; Miller, R.B. 1968: Organic Matter. Pp.55-56 *in* Soils of New Zealand. Part 2. *N.Z. Soil Bur. Bull.* 26.

Blakemore, L.C.; Miller, R.B. 1968: Organic Matter. PP. 55-56 *in* Soils of New Zealand. Part 2. *N.S. Soil Bur. Bull.* 26.

Blatt, H.; Middleton, G.; Murray, R. 1972: "Origin of sedimentary rocks". Prentice-Hall, New Jersey, 634p.

Bouma, A.H. 1962: "Sedimentology of some flysch deposits". Elsevier, Amsterdam, 168p.

Briggs, N.D. 1976: Welding and crystallisation zonation in Whakamaru Ignimbrite, central North Island, New Zealand. *N.Z. Jl. Geol. Geophys.* 19(2), 189-212.

Brock, T.D. 1974: "Biology of microorganisms", 2nd edition. Prentice-Hall, Englewood, Cliffs, N.J.

Brodie, J.W.; Irwin, J. 1970: Morphology and sedimentation in Lake Wakatipu, New Zealand. *N.Z. Jl. Mar. Freshwat. Res.* 4(4), 479-496.

Brown, J.M.A. 1975: Ecology of macrophytes in New Zealand lakes. Pp. 244-262 *in* V.H. Jolly and J.M.A. Brown (eds.) "New Zealand Lakes". Auckland University Press/Oxford University Press, 388p.

Brown, J.M.A.; Dromgoole, F.I.; Coffey, B.T.; Clayton, J. 1973: Aquatic macrophytes in the Nelson National Park lakes. Nelson National Park Board Report.

Burton, G.B. 1970: An Environmental Study of the Lake Taupo Catchment. Unpublished report to Taupo County Council.

Campbell, A.S.; Young, A.W.; Livingstone, L.G.; Wilson, M.A.; Walker, T.W. 1977: Characterisation of poorly-ordered alumino-silicates in a Vitric Andosol from New Zealand. *Soil Sci.* 123, 362-368.

Campbell, G.H. 1977: Lake Taupo suspended sediment study: A preliminary statement. 4p. Unpublished report. Auckland University Geography Department.

Carroll, D. 1970: Clay minerals: a guide to their X-ray diffraction identification. *Geol. Soc. Am. Spec. Paper* 126. Boulder, Colorado, 80p.

Cassie, V. 1974: Algal Flora of some North Island, New Zealand, Lakes, including Rotorua and Rotoiti. *Pacific Science* 28(4), 467-504.

Chapman, V.J. 1970: A history of the lake weed infestation of the Rotorua lakes and the lakes of the Waikato hydroelectric system. *N.Z. D.S.I.R. Information Series* 78, 52p.

Chapman, V.J.; Brown, J.MA.; Dromgoole, F.I.; Coffey, B.T. 1971: Submerged vegetation of the Rotorua and Waikato lakes. *N.Z. Jl. Mar. Freshwat. Res.* 5, 259-279.

Chittenden, E.T.; Childs, C.W.; Smidt, R.E. 1976: Sediments of Lakes Rotoroa and Rotoiti, South Island, New Zealand. *N.Z. Jl. Mar. Freshwat. Res.* 10(1), 61-76.

Coffey, B.T. 1970: Submerged vegetation of Rotorua lakes. *N.Z. Limnological Soc. Newsletter* 6.

Coffey, B.T. 1975: Macrophytes of the Waikato hydroelectric system. Pp. 263-270 *in* V.H. Jolly and J.M.A. Brown (eds.) New Zealand Lakes. Auckland University Press/Oxford University Press, 388p.

de Lisle, J.F.; Kerr, I.S. 1963: The Climate and weather of the Bay of Plenty Region. *N.Z. Met Service Misc. Pub.* 115(1).

de Lisle, J.F.; Tomlinson, A.I. 1975: The structure of the wind over New Zealand. *N.Z. Met. Service Tech. Info. Circular* No.147.

Emery, K.O.; Csandy, G.T. 1973: Surface circulation of lakes and nearby land locked seas. *Proc. Natl. Acad. Sci. U.S.* 70, 93-97.

Emery, K.O.; Rittenberg, S.C. 1952: Early diagenesis of California Basin sediments in relation to oil. *Bull. Am. Ass. Petrol. Geol.* 36, 735-806.

Ewart, A. 1963: Petrology and Petrogenesis of the Quaternary Pumice Ash in the Taupo Area, New Zealand. *Jl. Petrol.* 4(3), 392-431.

Ewart, A. 1968: The Petrography of the Central North Island rhyolitic lavas. Part 2. Regional petrography including notes on associated ash-flow pumice deposits. *N.Z. Jl. Geol. Geophys.* 11(2), 478-545.

Ewart, A.; Stipp, J.J. 1968: Petrogenesis of the volcanic rocks of the Central North Island, New Zealand, as indicated by a study of Sr^{87}/Sr^{86} ratios, and Sr, Rb, K, U and Th abundances. *Geochim. et Cosmochim. Acta* 32, 699-735.

Fairbridge, R.W. 1967: Phases of diagenesis and authigenesis. Pp. 19-89 *in* G. Larsen and C.V. Chilingar (eds.) "Diagenesis in sediments". Elsevier, Amsterdam.

Farmer, V.C.; Palmieri, F. 1975: The characterization of soil minerals by Infra-red spectroscopy. Pp. 573-670 *in* J.E. Gieseking (ed.) "Soil Components, Volume 2, Inorganic Components". Springer-Verlag, Berlin.

Fieldes, M. 1955: Clay mineralogy of New Zealand Soils. 2. Allophane and related mineral colloids. *N.Z. Jl. Sci. Tech.* 37, 336-350.

Fieldes, M. 1958: The role of clays in soil fertility. *Proc. N.Z. Inst. Agric. Sci.*, 84-108.

Fieldes, M. 1968: Clay mineralogy. Pp. 22-39 *in* N.Z. Soil Bureau 1968: Soils of New Zealand. Part 2. *N.Z. Soil Bur. Bull.* 26(2).

Fieldes, M.; Furkert, R.J. 1966: Confirmed weathering sequence in clays of New Zealand Volcanic Soils. *N.Z. Jl. Sci.* 9, p.608.

Fieldes, M.; Furkert, R.J.; Wells, N. 1972: Rapid determination of constituents of whole soils using infra-red absorption. *N.Z. Jl. Sci.* 15, 615-627.

Fieldes, M.; Perrott, K.W. 1966: Nature of allophane in soils. III. Rapid field and laboratory test for allophane. *N.Z. Jl. Sci.* 9, 623-629.

Fieldes, M.; Weatherhead, A.V. 1968: Mineralogy of sand fractions. Pp. 8-21 *in* N.Z. Soil Bureau 1968: Soils of New Zealand. Part 2. *N.Z. Soil Bur. Bull.* 26(2).

Flint, E.A. 1970: Phytoplankton in some New Zealand surface waters. *Proc. N.Z. Water Conf. 1970* 1, 7.1-7.15.

Florin, Maj-Britt 1970: The Fine Structure of some Pelagic Fresh water Diatom species under the S.E.M. *Särtryck ur: Svensk Botanisk Tidshrift Bd 64, H.1. Uppsala.*

Folk, R.L.; Andrews, P.B.; Lewis, D.W. 1970: Detrital sedimentary rock classification and nomenclature for use in New Zealand. *N.Z. Jl. Geol. Geophys.* 13, 937-968.

Folk, R.L.; Ward, W.C. 1957: Brazos River Bar: A study in the significance of Grain size parameters. *Jl. Sed. Petrol.* 27, 3-27.

Garnier, B.J. 1958: "The Climate of New Zealand - a survey". Arnold, London.

Gibbs, H.S.: Cowie, J.D.; Pullar, W.A. 1968: Soils of the North Island. Pp. 48-52 *in* N.Z. Soil Bureau 1968: Soils of New Zealand. Part 1. *N.Z. Soil Bur. Bull.* 26(1).

Gibbs, H.S.; Wells, N. 1965: Volcanic Ash Soils in New Zealand. *International Sympsoium on Volcanology N.Z. Paper* 40.

Glasby, G.P. 1971: Direct observations of columnar scattering associated with geothermal gas bubbling in the Bay of Plenty, New Zealand. *N.Z. Jl. Mar. Freshwat. Res.* 5(3 and 4), 483-496.

Glasby, G.P. 1972: Interstitial waters in Marine and Lacustrine Sediments: A Review. *Jl. Roy. Soc. N.Z.* 3(1), 43-59.

Glasby, G.P. 1975: Geochemistry of superficial lake sediments from the South Island, New Zealand. *N.Z. Oceanogr. Inst. Records* 2, 77-82.

Gorham, E.; Swaine, D.J. 1965: The influence of oxidising and reducing conditions upon the distribution of some elements in lake sediments. *Limnol. Oceanogr.* 10, 268-279.

Green. J.D. 1975: Heat budgets. Pp 106-110 *in* V.H. Jolly and J.M.A. Brown (eds.) "New Zealand Lakes" Auckland University Press/Oxford University Press, 388p.

Gregg, D.R. 1960: The Geology of the Tongariro subdivision. *N.Z. Geol. Surv. Bull.* 40, 9-152.

Gregg, J.M.; Goldstein, S.T.; Walters, L.J. 1977: Occurrence of strained quartz in the siliceous frustules of cultured freshwater diatoms. *Jl. Sed. Petrol.* 47(4), 1623-1629.

Griffin, J.J.; Windom, H.L.; Goldberg, E.D. 1968: The distribution of clay minerals in the World Ocean. *Deep-Sea Research* 15, 433-459.

Grindley, G.W. 1960: Geological map of New Zealand. Sheet 8. Taupo. 1:250,000. D.S.I.R., Wellington.

Grindley, G.W.; Mathews, W.H. 1965: Geological map of National Park Volcanoes *in* "New Zealand Volcanology, Central Volcanic Region, New Zealand". *D.S.I.R. Information Series* 50.

Grover, N.C.; Howard, C.S. 1938: The passage of turbid water through Lake Mead. *Proc. Am. Soc. Civ. Engrs.* 103, 720-732.

Healy, J. 1962: Structure and volcanism in the Taupo Volcanic Zone, New Zealand. *Amer. Geophys. Un. Geophys. Monogr.* 6, 151-7.

Healy, J. 1964: Dating of the younger volcanic eruptions of the Taupo Region. Part 1, pp.7-42 *in* Stratigraphy and Chronology of Late Quaternary volcanic ash in Taupo, Rotorua and Gisborne districts. *N.Z. Geol. Surv.* 73, 88p.

Healy, J. 1967: Recent Erosion in Taupo Pumice, Central North Island, New Zealand. *N.Z. Jl. Geol. Geophys.* 10(3), 839-854.

Healy, J. 1975: Volcanic Lakes. Pp. 70-83 *in* V.H. Jolly and J.M.A. Brown (eds.) "New Zealand Lakes". Auckland University Press/Oxford University Press, 388p.

Healy, J.; Vucetich, C.G.; Pullar, W.A. 1964: Stratigraphy and Chronology of Late Quaternary volcanic ash in Taupo, Rotorua and Gisborne districts. *N.Z. Geol. Surv. Bull.* 73.

Heinrich, E.W. 1965: "Microscopic Identification of minerals". McGraw-Hill, London.

Hill, C.F. 1975: Impounded lakes of the Waikato River. Pp. 140-150 *in* V.H. Jolly and J.M.A. Brown (eds.) "New Zealand Lakes" Auckland University Press/Oxford University Press, 388p.

Huber-Pestalozzi, G. 1942: Das phytoplankton Des Süsswassers. Pp. 367-549 *in* A. Thienemann (ed.) *Die Binnengewässer* 16: 2:2, Stuttgart.

Hughes, H.R. 1976: Research into Aquatic Weeds in New Zealand Waterways: A Review. *N.Z. D.S.I.R., Information Series* 116.

Hutchinson, G.E. 1957: A Treatise on Limnology. Vol. 1, Geography, physics and chemistry. Wiley and Sons, New York.

Irwin, J. 1972: Lake Taupo, Bathymetry, 1:50,000, N.Z. Oceanogr. Inst. Chart, Lake Series.

Irwin, J. 1974: Water Clarity records from twentytwo New Zealand lakes. *N.Z. Jl. Mar. Freshwat. Res.* 8(1(, 223-7.

Irwin, J. 1975: Morphology and Classification. Pp. 25-56 *in* V.H. Jolly and J.M.A. Brown (eds.) "New Zealand Lakes". Auckland University Press/Oxford University Press, 388p.

Jackson, T.A. 1975: Humic matter in natural waters and sediments. *Soil Science* 119, 56-64.

Jolly, V.H. 1957: Thermal stratification in some New Zealand lakes. *Proc. N.Z. Ecol. Soc.* 4, 43-44.

Jolly, V.H. 1958: A preliminary study of some New Zealand lakes. *Ver. int. Verein. theor. angew Limnol.* 13, 436-8.

Jolly, V.H. 1959: A limnological study of some New Zealand lakes. Unpublished Ph.D. thesis, University of Otago.

Jolly, V.H. 1968: The comparative limnology of some New Zealand lakes. Part 1: Physical and chemical. *N.Z. Jl. Mar. Freshwat. Res.* 2, 214-59.

Jolly, V.H.; Irwin, J. 1975: Thermal conditions. Pp. 90-105 *in* V.H. Jolly and J.M.A. Brown (eds.) "New Zealand Lakes" Auckland University Press/Oxford University Press, 388p.

Jordan, C.F.; Fryer, G.E.; Hemmen, E.H. 1971: Size analysis of silt and clay by hydrophotometer. *Jl. Sed. Pet.* 41(2), 489-96.

Kamp, P.J.J. 1978: Stratigraphy and sedimentology of conglomerates in the Kidnappers Group, Hawke's Bay. Unpublished M.Sc. thesis, University of Waikato.

Kemp, A.L.W.; Lewis, C.F.M. 1968: A preliminary investigation of chlorophyll degradation products in the sediments of Lakes Erie and Ontario. *Proc. 11th Conf. Great Lakes Res. 1968*, 206-229. Internat. Assoc. Great Lakes Res.

Kemp, A.L.W. 1972: Preliminary information on the nature of organic matter in the surface sediments of Lakes Huron, Erie and Ontario. Unpublished manuscript.

King, C.A.M. 1972: "Beaches and Coasts", Arnold, London, 570p.

Kirkman, J.H. 1975a: Clay mineralogy of some tephra beds of Rotorua Area, North Island, New Zealand. *Clay Minerals* 10, 437-449.

Kirkman, J.H. 1976a: Clay mineralogy of thirteen paleosols developed in Holocene and Late Pleistocene tephras of Central North Island, New Zealand. *N.Z. Jl. Geol. Geophys.* 19(2), 179-187.

Kirkman, J.H. 1976b: Clay mineralogy of Rotomahana Sandy Loam Soil, North Island, New Zealand. *N.Z. Jl. Geol. Geophys.* 19(1), 35-41.

Kirkman, J.H. 1978: Clay mineralogy of New Zealand Volcanic Ash Soils and Tephras. *N.Z. Soil News* 26(1), 12-18.

Kohn, B.P. 1973: Some studies of New Zealand Quaternary pyroclastic rocks. Unpublished Ph.D. thesis, Victoria University of Wellington.

Lambert, A.M.; Lüthi, S.M. 1977: Lake circulation induced by density currents: an experimental approach. *Sedimentology* 24, 735-741.

Lewin, J.C. 1962: Silicification. Pp.445-455 *in* R.A. Lewis (ed.) "Physiology and biochemistry in algae". Academic Press, New York.

Lien, S.L.; Hoopes, J.A. 1978: Wind-driven steady flows in Lake Superior. *Limnol. Oceanogr.* 23(1), 91-103.

Lund, J.W.S. 1965: The ecology of the freshwater phytoplankton. *Biol. Rev.* 40, 231-293.

Mackenzie, R.C. and Caillère, S. 1975: The thermal characteristics of soil minerals and the use of these characteristics in the qualitative and quantitative determination of clay minerals in soils. Pp. 529-572 *in* J.E. Gieseking (ed.) "Soil Components, 2, Inorganic Components". Springer-Verlag, Berlin.

McCammon, R.B. 1975: On the efficiency of systematic point-sampling in mapping facies. *Jl. Sed. Petrol.* 45(1), 217-229.

McColl, R.H.S. 1972: Chemistry and trophic status of seven New Zealand lakes. *N.Z. Jl. Mar. Freshwat. Res.* 6, 399-447.

McColl, R.H.S. 1977: Chemistry of sediments in relation to trophic condition of eight Rotorua lakes. *N.Z. Jl. Mar. Freshwat. Res.* 11(3), 509-523.

Mathews, W.H. 1967: A contribution to the geology of the Mount Tongariro massif, North Island, New Zealand. *N.Z. Jl. Geol. Geophys.* 10(4), 1027-1038.

Maunder, W.J. 1974: Climate and climatic Resources of the Waikato-Coromandel-King Country region. *N.Z. Met. Service Misc. Pub.* 115(7).

Maunder, W.J.; Browne, M.L. 1972: The climate and weather of Wanganui Region. *N.Z. Met. Service Misc. Pub.* 115(6).

Millot, G. 1970: "Geology of Clays". Chapman and Hall, London, 429p.

Mitchell, B.D. 1975: Oxides and hydrous oxides of silicon. Pp. 393-432 *in* J.E. Gieseking (ed.) "Soil Components, 2, Inorganic Components". Springer-Verlag, Berlin.

Mortimer, C.H. 1942: The exchange of dissolved substances between mud and water in lakes. *Jl. Ecol.* 30, 147-201.

Murley, R.D. 1965: An improved method of calculating particle size distribution from centrifugal sedimentation experiments. *Nature* 207, 1089-1090.

National Water and Soil Conservation Organisation, 1976: Research and Survey Annual Report - 1976.

Nelson, C.S. and Cochrane, R.H.A. 1970: A rapid X-ray method for the quantitative determination of selected minerals in fine grained and altered rocks. *Tane* 16, 151-162.

Normark, W.R.; Dickson, F.H. 1976: Manmade turbidity currents in Lake Superior. *Sedimentology* 23(6), 815-832.

N.Z. Lands and Survey, 1975b: Topography. N.M.S. 18, sheet 8, Taupo, 1:250,000.

N.Z. Lands and Survey, 1975b: Surface Water Resources, Taupō. N.M.S. 128, North Island, 1:000,000 (Hand-coloured base map, Earth Sciences Department, University of Waikato, Hamilton).

N.Z. Meteorological Service, 1973: Summaries of Climatological Observations to 1970. *Misc. Pub.* 143.

N.Z. Soil Bureau, 1962: Soil Map of the North Island of New Zealand. Scale 1:1000,000. To accompany *Soil Bureau Bulletin* No. 26 "Soils of New Zealand".

N.Z. Soil Bureau, 1964: Soil Classes for Potential Pastoral Use, North Island, New Zealand. 1:1000,000. To accompany *Soil Bureau Bulletin* No. 26 "Soils of New Zealand".

N.Z. Soil Bureau, 1973: Parent rocks of New Zealand Soils: North Island. 1:1000,000. New Zealand Soil Bureau Map 106/1 to accompany *N.Z. Soil Survey Report* 28.

Paerl, H.W. 1977: Ultraphytoplankton biomass and production in some New Zealand lakes. *N.Z. Jl. Mar. Freshwat. Res.* 11(2), 297-305.

Patrick, P.R.; Reimer, A.D. 1966: Diatoms of the United States Volume 1, Monographs of the Academy of Natural Sciences of Philadelphia 13. Philadelphia, 688p.

Pickrill, R.A. 1978: Beach and nearshore morphology of Lakes Manapouri and Te Anau, New Zealand: natural models of the continental shelf. *N.Z. Jl. Geol. Geophys.* 21(2), 229-242.

Pullar, W.A.; Birrell, K.S. 1973: Age and distribution of Late Quaternary pyroclastic and associated cover deposits of the Rotorua and Taupo area, North Island, New Zealand. *N.Z. Soil Survey Reports 1 and 2.*

Pullar, W.A.; Birrell, K.S.; Heine, J.C. 1973: Named tephras and tephra formations occurring in the Central North Island, with notes on derived soils and buried paleosols. *N.Z. Jl. Geol. Geophys.* 16, 497-518.

Rawlence, D.J. 1973: Problems associated with tracing algological changes in lake sediment. Pp. 457-468 *in* "Proceedings of the Pollution Research Conference, Wairakei, N.Z. 1973".

Rawlence, D.J.; Reay, P.F. 1976: Diatom numbers and phosphorous levels in deep water sediment from Lake Taupo, New Zealand. *N.Z. Jl. Mar. Freshwat. Res.* 10(4), 589-596.

Reeves, C.C. 1968: Introduction to Paleolimnology *in* "Developments in Sedimentology" 11. Elsevier, 228p.

Sanger, J.E.; Gorham, E. 1970: The diversity of pigments in Lake Sediments and its ecological significance. *Limnol. Oceanogr.* 15(1), 59-69.

Selby, M.J. 1967: Infiltration characteristics of some Pumice Land Soils. N.Z. Hydrological Soc. Symposium, 1967.

Selby, M.J. 1973: An investigation into causes of runoff from a catchment of pumice lithology in New Zealand. *Hydrol. Sci. Bull.* 18, 255-80.

Selby, M.J. 1974: Rates of creep in pumiceous soils and deposits, Central North Island, New Zealand. *N.Z. Jl. Sci.* 17, 47-48.

Steiner, A. 1968: Clay minerals in hydrothermally altered rocks at Wairakei, New Zealand. *N.Z. Jl. Geo. Geophys.* 19, 683-706.

Storch, T.A.; Saunders, G.W. 1978: Phytoplankton extracellular release and its relation to the seasonal cycle of dissolved organic carbon in a eutrophic lake. *Limnol. Oceanogr.* 23(1), 112-119.

Stout, V.M. 1973: The freshwater environment. Pp. 229-250 *in* G.R. Williams (ed.) "The Natural History of New Zealand", Reed, Wellington.

Stout, V.M. 1975: The limnology. Pp. 405-458 *in* G. Kuschel (ed.) "Biogeography and Ecology in New Zealand".

Sundaram, T.R.; Rehm, R.G. 1973: The seasonal thermal structure of deep temperate lakes. *Tellus* 25, 157-167.

Syers, J.K.; Harris, R.F.; Armstrong, D.E. 1973: Phosphate chemistry in Lake sediments. *Jl. Environ. Qual.* 2, 1-14.

Tanner, C.B.; Jackson, M.L. 1947: Nomographs of sedimentation times for soil particles under gravity or centrifugal acceleration. *Soil Sci. Soc. Proc.* 1947, 60-65.

Thomasson, K. 1960: Some planktic *Staurastra* from New Zealand. *Bot. Notiser* 113, 225-245.

Toohill, T.E.; Fletcher, J.R. 1971: Land use capability survey of Lake Taupo catchment. Unpublished report (manuscript and seven inventory map sheets).

Turekian, K.K. 1968: "Oceans" *in* A.L. McAlester (ed.) Foundations of Earth Science Series. Prentice-Hall, Englewood, New Jersey, 120p.

Vucetich, C.G. 1960: Yellow-brown Pumice Soils *in* Miller, R.B. (ed.) "Soil Groups of New Zealand". A restricted publication, 499p.

Vucetich, C.G.; Pullar, W.A. 1964: Stratigraphy of Holocene ash in the Rotorua and Gisborne districts. Part 2, pp. 43-63 *in* "Stratigraphy and Chronology of Late Quaternary volcanic ash in Taupo, Rotorua and Gisborne districts". *N.Z. Geol. Surv. Bull.* 73, 88p.

Vucetich, C.G.; Pullar, W.A. 1969: Stratigraphy and chronology of Late Pleistocene volcanic ash beds in the Central North Island, New Zealand. *N.Z. Jl. Geol. Geophys.* 12: 784-837.

Vucetich, C.G.; Pullar, W.A. 1973: Holocene tephra formations erupted in the Taupo area, and interbedded tephras from other volcanic sources. *N.Z. Jl. Geol. Geophys.* 16, 745-780.

Ward, R.H. 1922: Significance of the recent subsidence of the shore of Lake Taupo. *N.Z. Jl. Sci. Tech.* 5, 280-281.

Weaver, F.M.; Wise, S.W. 1973: Opaline sediments of the south-eastern Coastal Plain and Horizon A: Biogenic origin. *Science* 184, 899-901.

White, E.; Downes, M.T. 1977: Preliminary assessment of nutrient loads on Lake Taupo, New Zealand. *N.Z. Jl. Mar. Freshwat. Res.* 11(2), 341-356.

White, E.; Starkey, R.S.; Saunders, M.J. 1971: An assessment of the relative importance of several chemical sources to the waters of a small upland catchment. *Jl. Appl. Ecol.* 8, 743-749.

Whiteside, M.C. 1965: Paleoecological studies of Potato Lake and environs. *Ecology* 46, 807-816.

Wilson, M.; Turner, A.S. 1977: Water plant survey Waikato hydro lakes, March 1977. Unpublished report, 14p.

Windom, H.L. 1969: Atmospheric dust records in permanent snowfields: Implications to marine sedimentation. *Geol. Soc. Am. Bull.* 80, 761-782.

Windom, H.L. 1975: Eolian contributions to marine sediments. *Jl. Sed. Petrol.* 45(2), 520-529.

Waikato Valley Authority, 1973: Lake Taupo catchment control scheme final report, 130p. Unpublished.

Zobell, C.E. 1942: Changes produced by micro-organisms in sediments after deposition. *Jl. Sed. Petrol.* 12(3), 127-136.

"You should have seen

the size of that trout!"

